Mechanisms governing extra- and intra-islet communication in human pancreatic health and disease

By

Tiffany M. Richardson

Dissertation

Submitted to the Faculty of the

Graduate School of Vanderbilt University

in partial fulfillment of the requirements

for the degree of

DOCTOR OF PHILOSOPHY

in

Molecular Physiology and Biophysics

May 12, 2023

Nashville, Tennessee

Approved:

David Jacobson, Ph.D., Chair

Sheila Collins, Ph.D.

Jin Chen, Ph.D.

Richard Simerly, M.D.

To Abba

We have this hope as an anchor for the soul, firm and secure.

Luke 1:79

ACKNOWLEDGEMENTS

It has been a dream of mine for quite some time now to obtain my doctorate. Words could never fully capture the gratitude I have for the people that have helped me along the way. The following is a tribute to the many individuals who guided me along this journey and encouraged me to become the scientist I am today.

Dr. Brangwynne Laboratory at Princeton University

Before coming to Vanderbilt, I was a part of the Soft Living Matter Group at Princeton University led by Dr. Clifford Brangywnne. After being enthralled by Dr. Brangywnne's seminar during a summer internship at the MBL, I spent the next three years performing research in his laboratory. There, I was given the freedom to rigorously study non-membrane-bound organelle dynamics and developed my love for microscopy. Dr. Brangwynne's drive to pursue new and exciting topics in groundbreaking and innovative ways shaped how I think about complex biological problems. His interdisciplinary work exposed me to a wide variety of fields that I still find so incredibly intriguing. Dr. Marina Feric and Dr. Lian Zhu were two outstanding graduate students that walked me thru my early days of benchwork and scientific investigation. Their patience, ingenuity, and organization are hallmarks of how I approached the research in this Dissertation and will stay with me beyond the bench.

Vanderbilt community

There have been many influential people that have crossed my path while I was at Vanderbilt University. A few of which I would like to acknowledge. First are Dr. Elizabeth Bowman and Dr. Jim Patton the former leaders of Vanderbilt's Interdisciplinary Graduate Program (IGP). Drs. Bowman and Patton provided guidance even before I joined Vanderbilt and have always been tremendous supporters of mine. Additionally, Dr. Linda Sealy, Dr. Christina Keeton, and Dr. Roger Chalkley of Vanderbilt's Initiative for Maximizing Student Development (IMSD) are champions for underrepresented minorities in science and their efforts created a safe haven that fostered the growth of IMSD participants. The new leadership for IMSD Dr. Digna R. Velez Edwards, Dr. Julie Rhoades, Dr. Henrique Serezani, and Dr. Kafond Wilder are continuing this great work for future underrepresented minorities pursuing biomedical degrees at Vanderbilt and I appreciate their efforts as well.

Next, I would like to pay tribute to all of the organizations I was a part of to be of service to my community such as the Vanderbilt University Women in Science & Engineering (VU-WiSE), Vanderbilt University Program for Talented Youth, the Vanderbilt NSF GRFP

Grant Application Workshop team, Vanderbilt University Career Development Symposium Planning Committee, Vanderbilt Program in Molecular Medicine & Dr. Justin Gregory, the JDRF One Walk, the Endocrine Society Advocacy Group, and the(sugar)science. In particular, Dr. Monica Westley, Founder of the(sugar)science, has served as a mentor and cheerleader for me while also being a role model as a strong leader and patient advocate. Each of these activities taught me new skills and introduced me to people within and outside of Vanderbilt. We were able to make a real impact in the many events we organized and furthered the mission of spreading science throughout our communities.

Lastly, I would like to thank the students, faculty, and staff from the Department of Molecular Physiology & Biophysics for providing an academic home for my training and research. I am grateful to Dr. Nancy Carrasco for serving as our departmental chair, Dr. Richard O'Brien for orchestrating graduate training efforts such as the Molecular Endocrinology Training Program (METP), and our program administrators thru the years Karen Gieg, Kandi Granberry, and Bobbi Stidham for organizing the behind the curtain activities of earning a Ph.D. Thank you to my thesis committee composed of Dr. David Jacobson, Dr. Sheila Collins, Dr. Richard Simerly, and Dr. Jin Chen. This group of incredible scientists provided invaluable advice at pivotal parts of my doctoral journey that aided in the completion of this Dissertation and rounding out of my career and personal development toolbox. Finally, being a member of the MPB Graduate Student Association was transformational. We left a mark on our department (a poster of Black Physiologists) that I and other underrepresented students cherish walking the halls of the ivory tower.

Powers & Brissova Research Group and collaborators

I am incredibly grateful to have been a part of the Powers & Brissova Research group during my doctoral degree. Dr. Alvin Powers and Dr. Marcela Brissova provided me with ample resources, a training environment, and career development opportunities that honed my research, writing, and critical thinking skillsets. Dr. Powers' constant support, words of wisdom, and relentless commitment to my training propelled me thru my time in his laboratory. His enthusiasm for science and dedication to helping those with diabetes is commendable. Even though his schedule was packed to the brim, he would always serve as a sounding board and mentor for my doctoral journey's many twists and turns. I hope to be as great a mentor to others as he is to the individuals he takes under his wing. Dr. Marcela Brissova was a great help with reviewing my work, critically evaluating my science, and brainstorming the next steps to tease apart the questions addressed in this Dissertation. Thank you both for devoting countless hours to my training and setting a high bar for my scientific achievements.

The work detailed in this Dissertation is an extension and product of the impeccable scientific environment within the Powers & Brissova Research Group. I learned from Dr. Brangwynne's laboratory that I thrive within a large team of dedicated scientists and the Powers & Brissova Research Group exemplifies this exquisitely. Each person in our laboratory is always willing to lend a helping hand or brainstorm with one another which I truly appreciate. For the work done in this Dissertation, I would like to thank the lab members for their help and kindness.

I would like to extend a special thank you to Radhika Aramandla. Thank you for answering every question under the sun that I had on an almost daily basis since I joined the lab. Radhika knows exactly where to find any antibody that I need or how to perform a particular technique. Radhika was also always willing to lend a jovial break to the craziness that is a Ph.D.

Furthermore, thank you Chunhua Dai, Regina Jenkins, Anastasia Coldren, Corey Davis, Heather Durai, Danielle Gibson, Conrad Reihsmann, Amber Bradley, Jill Linder, Dr. Shaojun Mei, Dr. Adel Eskaros, Dr. Ajay Kumar Singh, Alex Hopkirk, Greg Poffenberger, Dr. Rachana Haliyur, Dr. Diane Saunders, Dr. Shristi Shrestha, Dr. Erick Spears, Dr. Heather Nelson, and Dr. Jean-Philippe Cartailler for helping me with parts of my experiments particularly running macroperfusions, many hormone assays, cutting countless pancreatic tissue slides, managing our human tissue repository, collating RNA sequencing data, and being thoughtful contributors to my many presentations. Thank you to Dr. Katie Coate, Dr. Jordan Wright, Dr. Jeeyeon Cha, and Dr. Xin Tong for being magnificent researchers and helpful hands. I look forward to seeing the success of your laboratories one day.

I also want to thank the work of current and past trainees in our laboratory. Thank you, Dr. Rachel Reinert, Dr. Rachana Haliyur, Dr. Kristie Aamodt, and Dr. Diane Saunders whose work directly contributed to the scientific questions addressed in this Dissertation. Yasminye Pettway, Dr. Nathaniel Hart, and Dr. Jack Walker were great trainees to work alongside throughout my Ph.D.

Many collaborators were also instrumental to the work done in this Dissertation: Dr. Rita Bottino, Dr. Alejandro Caicedo, Dr. Simon Robson, Dr. Jean Sévigny, Dr. Matthew Ishahak, and Dr. Ashutosh Agarwal were contributors to my projects and their teamwork propelled the impact of the work described in this Dissertation. The Stein Lab and Dean Lab were also helpful in brainstorming and shaping my scientific pursuits so thank you. Additionally, the Vanderbilt Cell Imaging Shared Resource (CISR) and Islet Procurement & Analysis (IPA) core were very helpful in providing expertise, assay analysis, and equipment for my experiments.

Lastly, to the administrative glue that keeps our laboratory together. Thank you to Al's administrative assistants, Meg Heaberlin and Laia Jones, for wrangling Al's hectic schedule to ensure that I had regular check-ins with him. Thank you, Suzzane Starr, Jan Botts Hicks, and Jessica Kimber of the Diabetes Center who was also a tremendous help during my Ph.D.

I will surely miss the Powers & Brissova Research Group, but I look forward to the many personal and scientific accomplishments that are to come from this laboratory.

Funding sources and human donors

Thankfully, the United States devotes some of the most money in the world to scientific research. I was grateful to be a recipient of funding from a multitude of grants and fellowships throughout my training and Dissertation work. These groups include but are not limited to: the National Science Foundation (NSF), the National Institute of Diabetes and Digestive and Kidney Disease (NIDDK), the U.S. Department of Veterans Affairs, the Endocrine Society, the American Diabetes Association, the Juvenile Diabetes Research Foundation (JDRF), and the Leona M. and Harry B. Helmsley Charitable Trust. The NSF has funded me throughout my scientific career starting with a Research Experience for Undergraduates (REU) at the renowned Marine Biological Laboratory in Woods Hole to an NSF BIO-REU Student Scholarship and finally an NSF Graduate Research Fellowship. These funding entities gave me the financial and intellectual independence to pursue graduate work at a top university.

I am especially grateful to the organ donors and their families for their sacrifice in contributing to my work and the work of many others. I was honored to study pancreatic tissue and islets from **67** individuals whose memory lives on to inform the scientific community indefinitely. Their selfless gift was instrumental in the discoveries detailed in this Dissertation. I urge readers of this Dissertation to become organ donors through your local mechanisms to save lives and contribute to the advancement of science.

Family and friends

Last but certainly not least I would like to thank my family and friends who walked hand in hand with me through these last 5 ½ years. Thank you to my friends in Nashville and beyond who cheered me on during the highs, commiserated with me during the lows, and laughed with me in between. You all gave me the fuel to keep going. Thank you to my friends at Trevecca Community Church for being a source to grow my faith and volunteer as well. I want to extend a special thank you to the current and soon-to-be doctors that

encompass my amazing friend group. What a strong and intelligent group of women I call friends and I am honored to be a part of your journeys as well.

Thank you to my mom, Catherine Richardson, and sister, Dr. Crystal Richardson. You both have been my greatest support system thru every trial and tribulation. Getting a Ph.D. in a global pandemic, social unrest, and honestly at any point is incredibly challenging. When I thought I couldn't go on any longer you were right there to brush me off and give me the kick to keep going. Crystal, you have been a great older sister and inspired me to get my Ph.D. in the first place. It has been so reassuring to have someone so close to me to talk about the doctoral journey and get advice along the way. You've shown me that there are so many facets to scientific discovery and that I have so much to add to our ever-growing knowledge base. Mom, you have been the strength, love, and glue that has held our family together. You taught me how to persevere with grace, kindness, and fortitude. You were the one to cart me around to the million activities I insisted on doing and supported me in whatever I wanted to pursue. You did the work of two parents and raised children that are forever in debt to your sacrifices. You have had a child in a Ph.D. program for the past 13 years and your endless support has resulted in two Black women with doctoral degrees which is sadly incredibly rare. Just five generations ago, our relatives were owned by others and forced to work the land. And now, look how far we have come. We are a family of loving, selfless, driven, accomplished, and faithful women. I truly stand on the shoulders of giants!

Thank you to my amazing husband, Andrew Walther. You are my best friend, biggest supporter, and example of selfless love. Thank you for listening to all my failed and successful experiments, my complaints about the marathon of a Ph.D., and supporting me thru everything these past 5 years. Meeting you just 5 months into my Ph.D. was the greatest stroke of luck I could have ever encountered. We have been thru the gambit of long-distance relationship experiences ranging from two combat zone deployments, multiple moves, FaceTime move date nights, you name it. You have been the best listener when it comes to my venting and bad moods brought on by 5 ½ years of doctoral training. You also share in my excitement and accomplishments being sure to celebrate the small and large achievements. You also are a package deal with your loving family, the Walther / Olsen / Walther-Muno clan, who are the kindest group of people I know. You all were supporters throughout my Ph.D. and were genuinely interested in the research (check out the mouse experiments in Chapter V). I look forward to our next steps in life.

To my Ph.D., thank you for the most challenging and growth-inducing experience.
I traversed new heights and made novel discoveries to hopefully advance my fields.

Tighten up and anchor down! Go, Commodores!

TABLE OF CONTENTS

LIST OF FIGURES

LIST OF TABLES

LIST OF ABBREVIATIONS

3D	Three-dimensional
A2A	Adenosine receptor 2A
AA#	Amino acid reference
AAb+	Autoantibody-positive
AC	Adenylyl cyclase
ACR	Apyrase conserved region
ADA	Adenosine deaminase
ADI	Alberta Diabetes Institute
ADORA	Adenosine receptor
ADP	Adenosine diphosphate
AMP	Adenosine monophosphate
ANS	Autonomic nervous system
APCs	Antigen-presenting cells
ARL67156	Ecto-ATPase inhibitor
ARX	Aristaless-related homeobox
ATP	Adenosine triphosphate
AUC	Area under the curve
BB	BioBreeder
BMI	Body mass index
Ca^{2+}	Calcium
cADDis	cAMP Difference Detector in situ
cAMP	Cyclic adenosine monophosphate
CAV1	Caveolin-1
CG	Celiac ganglia
CNS	Central nervous system
CPEP	C-peptide
cpGFP	Circularly permuted green fluorescent protein
CODEX	Co-detection by indexing
COLIV	Collagen IV
CRISPR	Clustered regularly interspaced short palindromic repeats
Cx36	Connexin36
DAPI	4′,6-diamidino-2-phenylindole
DMV	Dorsal motor nucleus of the vagus
DRG	Dorsal root ganglia
E#	Embryonic day #
ECM	Extracellular matrix

Ecto-5'-NT	Ecto-5'-nucleotidase
ELISA	Enzyme-linked immunoassay
E-NPP	Ecto-nucleotide pyrophosphatase/phosphodiesterase
EPAC2	Exchange protein directly activated by cAMP 2
Epi	Epinephrine
ENTPD3	Ecotnucleoside triphosphate diphosphohydrolase-3
E-NTPDase	Ecotnucleoside triphosphate diphosphohydrolase
ER	Endoplasmic reticulum
FBS	Fetal bovine serum
G6P	Glucose-6-phosphate
GABA	Gamma-aminobutyric acid
GAD	Glutamic acid decarboxylase (bacterial)
GAD65	Glutamic acid decarboxylase 65
GCaMP6f or GCaMP	Calmodulin-binding peptide M13 calcium biosensor
GCG	Glucagon
GCPR	G protein coupled receptor
GFP	Green fluorescent protein
GK	Glucokinase
GLP-1	Glucagon-like peptide 1
GLUT	Glucose transporter
GSIS	Glucose-stimulated insulin secretion
GTT	Glucose tolerance test
GWAS	Genome-wide association studies
HbA1C	Hemoglobin A1C
HBSS	Hank's balanced salt solution
hGH	Human growth hormone
HLA	Human leukocyte antigen
HPAP	Human Pancreas Analysis Program
HRSA	Health Resources and Services Administration
IA2	Protein tyrosine phosphatase
IBMX	Isobutylmethylxanthine
IEQ	Islet equivalent
IIAM	International Institute for Advancement of Medicine
IIDP	Integrated Islet Distribution Program
INS	Insulin
INS-1	Rat insulinoma-1
K_{ATP}	Potassium-ATP channel
KCl	Potassium chloride
MAFB	V-maf musculoaponeurotic fibrosarcoma oncogene homolog B
MODY	Maturity-onset diabetes of the young

MRS2500	P2Y1 antagonist
Na^+	Sodium
ND	Nodose ganglia
NDRI	National Disease Research Interchange
NF200	Neurofilament 200
NGF	Nerve growth factor
NKX6.1	NK6 homeobox 1
NOD	Nonobese diabetic mice
nPOD	Network for Pancreatic Organ Donors with Diabetes
NPP#	Ectonucleotide pyrophosphatase/phosphodiesterase-1
NTPDase#	Ectonucleoside triphosphate diphosphohydrolase
OCT	Optimal cutting temperature compound
OGTT	Oral glucose tolerance test
OPTN	Organ Procurement and Transplantation Network
ORAI	ORI calcium release-activated calcium modulator 1
P#	Postnatal day #
P1Y	Adenosine purinergic receptor
P2X	Purinergic receptor “X” subtype (ion channel)
P2Y	Purinergic receptor “Y” subtype (metabotropic)
PBS	Phosphate-buffered saline
PDD	Pyridoxal-dependent decarboxylase
PDE3B	Phosphodiesterase 3B
PDX1	Pancreatic and duodenal homeobox 1
PECAM-1	Platelet endothelial cell adhesion molecule 1
PGP9.5	Protein gene product 9.5
PLC	Phospholipase C
PLP	Pyridoxal 5'-phosphate
PNP	Purine nucleoside phosphorylase
PTF1A	Pancreas transcription factor 1 complex 1A
qPCR	Quantitative polymerase chain reaction
RFP	Red fluorescent protein
RIA	Radioimmunoassay
RNA	Ribonucleic acid
ROUT	Robust regression and Outlier removal
scRNA-seq	Single-cell RNA sequencing
SEM	Standard error of the mean
shScramble	Scramble control shRNA-treated pseudoislets
shENTPD3	ENTPD3 shRNA-treated pseudoislets
shRNA	Short hairpin RNA interference
siRNA	Small interfering RNA

SMG	Superior mesenteric ganglia
SST	Somatostatin
STIM	Sensor stromal interaction module
SYN	Synapsin-1, -2
T1D	Type 1 diabetes
T2D	Type 2 diabetes
TBE	Tris/Borate/EDTA
TH	Tyrosine hydroxylase
TMX	Tamoxifen
TUBB3	Tubulin β 3
UMAP	Uniform manifold alignment projection
UCHL1	Ubiquitin carboxyl-terminal hydrolase isozyme
U.S.	United States of America
VEGF-A	Vascular endothelial growth factor-a
VEGFR2	Vascular endothelial growth factor receptor 2
VNUT	Vesicular nucleotide transporter

CHAPTER I: BACKGROUND AND SIGNIFICANCE

Glucose homeostasis

Glucose homeostasis is the result of integrated physiological processes that maintain blood glucose levels in a narrow range (80-140 mg/dL; **Figure 1**). The pancreatic islet of Langerhans is central to glucose homeostasis. Endocrine cells within the islet sense nutrient states (e.g., glucose and amino acids) and integrate signals from hormones and local neurotransmitters from islet autonomic nerve fibers to regulate secretion of islet hormones such as insulin, glucagon, and somatostatin.

In response to a rise in blood glucose after a meal, beta (β) cells secrete insulin which signals peripheral tissues such as skeletal muscle, liver, and adipose to uptake glucose for utilization and to store glucose as glycogen or fat. Hypoglycemia elicits glucagon secretion from alpha (α) cells to increase hepatic glucose production via glycogenolysis or gluconeogenesis. The role of somatostatin in islet secretion is incompletely defined but somatostatin from delta (δ) cells is a negative regulator of hormone secretion from α and β cells[1]. The brain is a major utilizer of glucose and is also intricately connected to these other tissues through autonomic and somatosensory nerve fibers (**Figure 1**)[2]. Multiple forms of diabetes mellitus are the result of absolute or relative hormone secretion defects or signaling deficiencies, leading to abnormal glucose levels[3]. Diabetes mellitus will be referred to as diabetes for the remainder of this Dissertation.

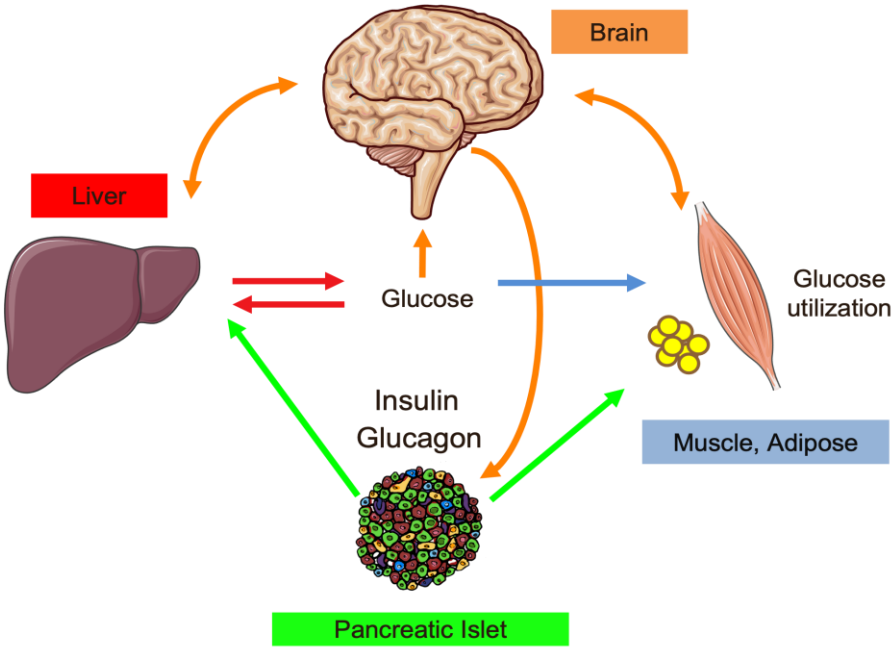

Figure 1. Pancreatic islets are vital in the maintenance of glucose homeostasis. Glucose homeostatic mechanisms are coordinated by a variety of organ systems. These organs and their mechanisms are depicted with corresponding colors: islet (green), liver (red), muscle and adipose (blue), and brain (orange). Dysfunction of these mechanisms leads to multiple types of diabetes.

The pancreas

Anatomy

The pancreas is an elongated glandular organ located in the retroperitoneal cavity behind the stomach. Anatomically, the pancreas contains three main regions: head, body, and tail[4,5]. The head rests on the descending and horizontal parts of the C-shaped duodenum of the small intestine, the body is on the inferior part of the stomach, and the tail is close to the hilum of the spleen[4,5].

Pancreatic composition and function

The pancreas is a bifunctional organ comprised of exocrine and endocrine compartments (**Figure 2**). The exocrine compartment is ~98% of the total pancreatic mass and is composed of acinar cells arranged in rosettes and ductal cells that line the extensive ductal system[6]. Acinar cells secrete digestive enzymes such as pancreatic amylase, trypsin, and lipase into an extensive branching network of ducts. These exocrine enzymes are secreted as inactive enzyme precursors that are later activated by proteolytic enzymes[7]. Subsidiary ducts drain into the main pancreatic duct, the duct of Wirsung, before flowing into the duodenum[8]. Secreted exocrine enzymes participate in the digestion of proteins, fats, and carbohydrates. The ductal epithelium within the exocrine compartment secretes bicarbonate and mucin to neutralize acids from the stomach in the small intestine[5,9].

The endocrine portion of the pancreas composes only 1-2% of the total pancreatic mass, but its action is central in maintaining glucose homeostasis[10]. Cellular clusters interspersed throughout the exocrine parenchyma called islets secrete hormones directly into the bloodstream. Islets can range from 50 – 500 μm in diameter and have an average of 1,500 cells per cluster. There are five types of hormone-producing endocrine cells in islets: insulin-secreting β cells, glucagon-secreting α cells, somatostatin-secreting δ cells, pancreatic polypeptide (PP) cells, gamma (γ) cells, and ghrelin (ε) cells. β cells are the most abundant with α and δ cells being the second and third most abundant cell types, respectively[5,11–16]. PP and ε cells are rarer cell types within the islet[5,11–16]. Endocrine cell ratios and β cell mass levels are heterogeneous between individuals but the distribution of endocrine cells between pancreatic regions is similar except for the uncinate process which has a higher proportion of γ cells[17–19]. Other nonendocrine cell types within the islet such as capillaries, nerve fibers, resident immune cells, and fibroblasts also contribute to its function.

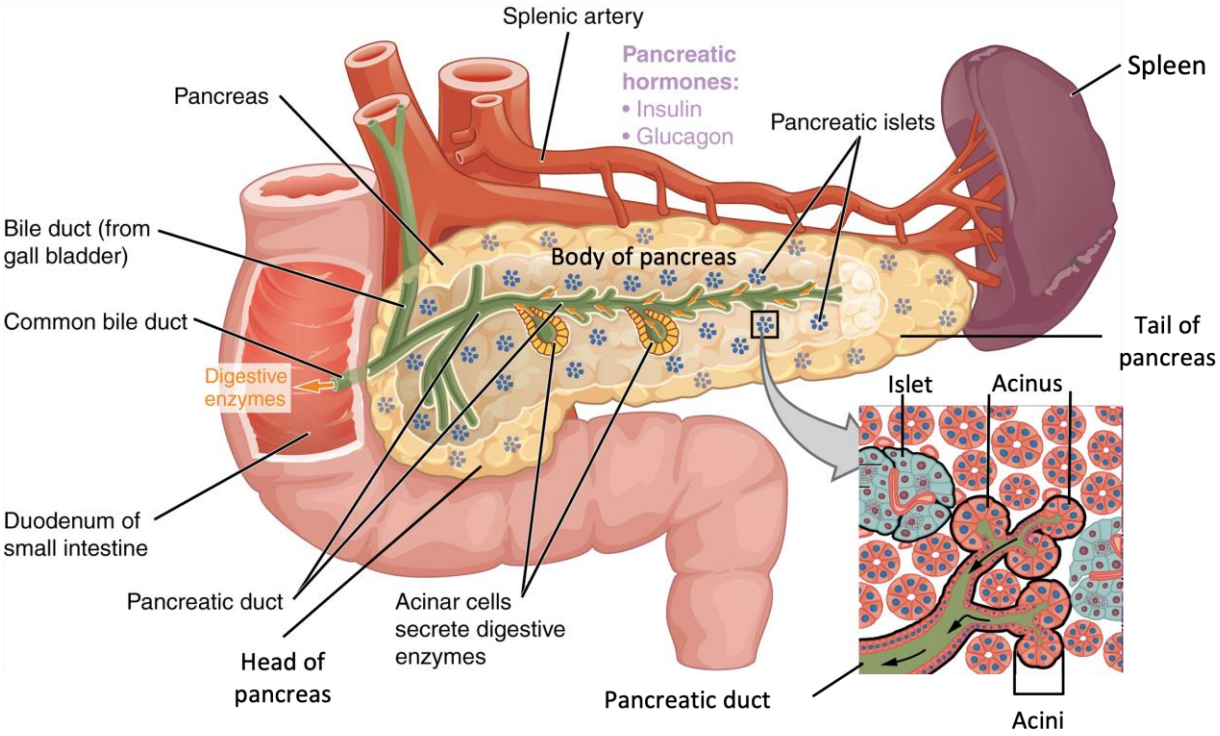

Figure 2. The pancreas is a dual endocrine and exocrine organ.
Pancreatic exocrine tissue secretes digestive enzymes into the small intestine through the pancreatic duct. Endocrine tissue comprised of Islets of Langerhans secretes hormones into the vascular system for transport throughout the body. Image adapted from OpenStax Anatomy & Physiology. Download for free at http://cnx.org/contents/e250c2d0-97c5-4ec2-88fd-20207d1acdde@12

Pancreatic development

There are two disparate functional compartments in the pancreas, but it is still a single organ system. Usually, the endocrine and exocrine portions are independently studied even though they share a common developmental lineage. The pathways dictating pancreatic organogenesis were primarily determined utilizing mouse model systems. While there have been a few recent studies of human fetal tissues, many of the generalized mechanisms summarized below are derived from mice.

Endocrine and exocrine cells arise from the embryonic foregut endoderm. Pancreatic organogenesis occurs in two distinct transitions: primary and secondary. During the primary transition, the pre-pancreatic endoderm evaginates from the foregut to create the dorsal and ventral stratified epithelial buds that first emerge around embryonic (E) day 9.5 (E9.5). Most of the pancreas originates from the dorsal bud to generate the three main pancreatic regions. Rotation of the gut tube then brings the dorsal and ventral buds together. Cellular polarization causes the pancreatic buds to expand and form a microlumen. Ductal luminal network formation and epithelium branching occur by E12.5[20].

During the secondary transition (E13.5-E16.5), the tip and trunk domains form. Tip domains contain multipotent progenitor cells that will subsequently become acinar tissue, while the trunk domain will differentiate into pancreatic ducts and endocrine cells. Insulin-positive β cells are observable by E13.5. By E15.5, after rapid acinar neogenesis has occurred, leading to an expansion of the acinar compartment. Delamination of endocrine progenitor cells from the ductal epithelial results in nascent islet clusters with various endocrine cell types (**Figure 3**). The pancreatic epithelium and islet clusters continue to expand and delaminate during late embryogenesis (E16.5-18.5)[20]. A limited investigation of human gestational pancreatic tissue shows that the general processes of bud formation, epithelial migration, and branching morphogenesis appear to be the same[21–26]. However, humans may only have a singular transition instead of two distinct transition phases[21–26].

Embryonic events detailed above lead to islet development, but these endocrine clusters are not fully structurally or functionally mature until after birth. In humans, fetal and neonatal islets resemble mouse islets with a core of β cells and α cells at the periphery. As time progresses, acinar and β cell numbers increase, leading to larger overall organ and islet sizes. Pediatric islets have an intermixed endocrine cell phenotype similar to adult islets. Additionally, hormone secretion matures postnatally such that both phases of glucose-stimulated insulin secretion (GSIS) are present in adult-isolated islets but not fetal islets[27,28]. Misexpression of or reduced expression of key regulators during

pancreatic development and postnatal functional maturation have been implicated in pancreatic diseases such as some forms of diabetes and pancreatic exocrine deficiency.

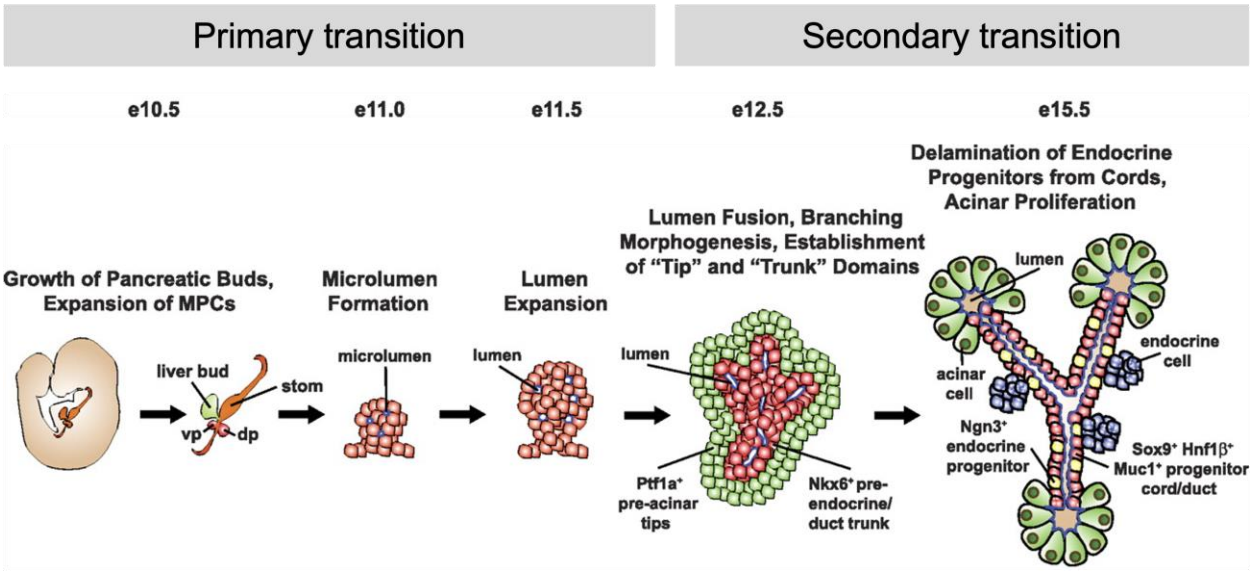

Figure 3. Major developmental milestones in pancreatic morphogenesis.
Pancreatic development includes "primary" (E9.5-E12.5) and "secondary" (E13-birth) transitions. Budding occurs early on followed by epithelial expansion and the formation of microlumens. Tubulogenesis generates "tip" and "trunk" domains that will subsequently give rise to ductal and endocrine cells. The secondary transition entails pancreatic branching, cellular differentiation, acinar cell expansion, and delamination of endocrine cells to form islet-like clusters. Figure adapted from Seymour and Sander, 2011.

Pancreatic microenvironment

Other structures and molecules within the islet also regulate islet hormone secretion. These include blood vessels, nerve fibers, immune cells, the extracellular matrix (ECM), and extracellular nucleotides (**Figure 4**). These cells and structures and substances facilitate communication between a variety of cell types by delivering nutrients and transmitting physiological cues that modulate pancreatic enzymes and hormone secretion.

The intricate microenvironment of the pancreas encompasses a diverse set of communication mechanisms that may be perturbed during disease. Direct cell-to-cell connections, electrical coupling through gap junctions, and autocrine/paracrine interactions are the three main ways that islet cells communicate. Signaling initiated by surrounding cells and the ECM in addition to non-contact signaling by the release of autocrine and paracrine substances highlight a vignette of these communication methods[29].

Various research teams utilizing intricate microfluidic devices[30–32], pancreatic slices[33,34], in vivo imaging of intraocular islet grafts[35,36], or intravital imaging to study coordinated responses in islets[37,38] have shown that islet cells collectively function as a large-scale complex of networks. Understanding the islet microenvironment is vital to understanding islet physiology and pathophysiology, whether it is through characterizing how it changes in rodent diabetes models, native human islets, and tissue samples from individuals with diabetes.

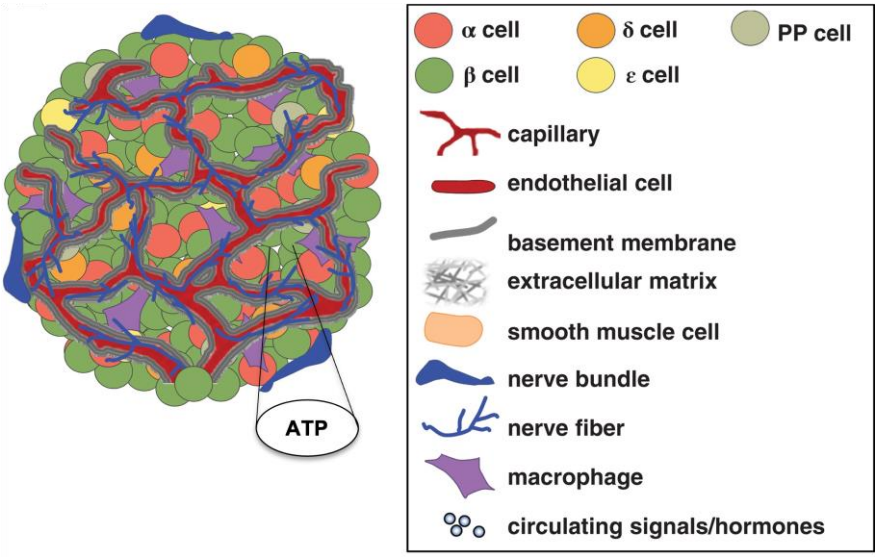

Figure 4. The pancreatic islet microenvironment. The pancreatic endocrine islet is composed of a variety of cell types. Islets are dispersed throughout the pancreas and are composed of α, β, δ, γ, ε, and PP cells. Islets also contain capillaries, endothelial cells, smooth muscle cells, nerve fibers, and resident immune cells (shown here as: macrophages). Autocrine and paracrine signaling molecules and receptors generate an intricate cell-to-cell communication system within the islet. Figure adapted from Aamodt and Powers, 2017.

Morphology and function of pancreatic vasculature

Pancreatic blood flow

Pancreatic blood flows through the superior and inferior pancreaticoduodenal arteries and branches of the splenic artery[39]. Larger arteries branch into smaller interlobular and intralobular arteries that cross through the pancreatic parenchyma to vascularize exocrine and islet tissue. Feeding arterioles within islets branch into a subset of capillaries that form a glomerulus-like structure that delivers blood throughout the islet (**Figure 5A-B**)[40]. In mice, islets are 1-2% of the overall pancreas mass but receive about 10% of total pancreatic blood flow[41]. Islets have higher capillary density with thicker and more tortuous capillaries than the exocrine compartment[42]. The islet endothelium is fenestrated to increase vessel permeability for rapid exchange between the islet and circulation[42]. Vascularization of islets is important to maintain glucose homeostasis because islets must sense dynamic changes in the blood glucose.

Controversy as to the directionality of pancreatic blood flow exists due to the reporting of many models detailing islet perfusion. Analysis of corrosion casts, intravital imaging, and tissue immunohistochemistry led to the development of multiple islet perfusion models mostly based upon rodent studies: 1) islet periphery to the center, 2) islet center to the periphery, and 3) one islet pole to the other[40,43]. The center-to-periphery model is most agreed upon in the field[34].

A new bidirectional model describes an “open” flow between the surrounding exocrine capillary network and islets[44]. This new model suggests that the exocrine tissue could affect islet function and vice versa due to the bidirectionality of blood flow[44]. Regardless of directionality, it is known that islet secretory products are carried to the liver by the portal vein[45]. The liver clears 50% of secreted insulin which suppresses gluconeogenesis and glycogenolysis[46]. The remaining secreted insulin moves through the venous circulation to the arterial circulation and then perfuses the pancreas. Understanding pancreatic blood flow directionality could elucidate the flow of hormones and other secreted factors between islet cells, exocrine tissue, and the periphery.

Vasculature and pancreatic function

The islet vasculature contains endothelial cells and pericytes that modulate vascular function (**Figure 5C**). Endothelial cells create a vessel lumen that can be constricted or dilated to alter the magnitude and rate of perfusion to the islet. Smooth muscle cells around feeding arterioles and pericytes around intra-islet capillaries have contractile properties to regulate vessel diameter[47]. Hyperglycemia increases islet perfusion and

insulin secretion[48,49]. Interestingly, if islet vascularization is reduced by genetically inactivating vascular endothelial growth factor-a (VEGF-A) in adult mouse β cells *in vivo*, there are only minimal disturbances in glucose homeostasis suggesting the contribution of other inputs to the islet such as nerve fibers and/or autocrine/paracrine mediators[50]. Most vascular function studies have been performed in rodents thus, it is important to study human pancreatic tissue and its function to better understand vascular physiology in the pancreas.

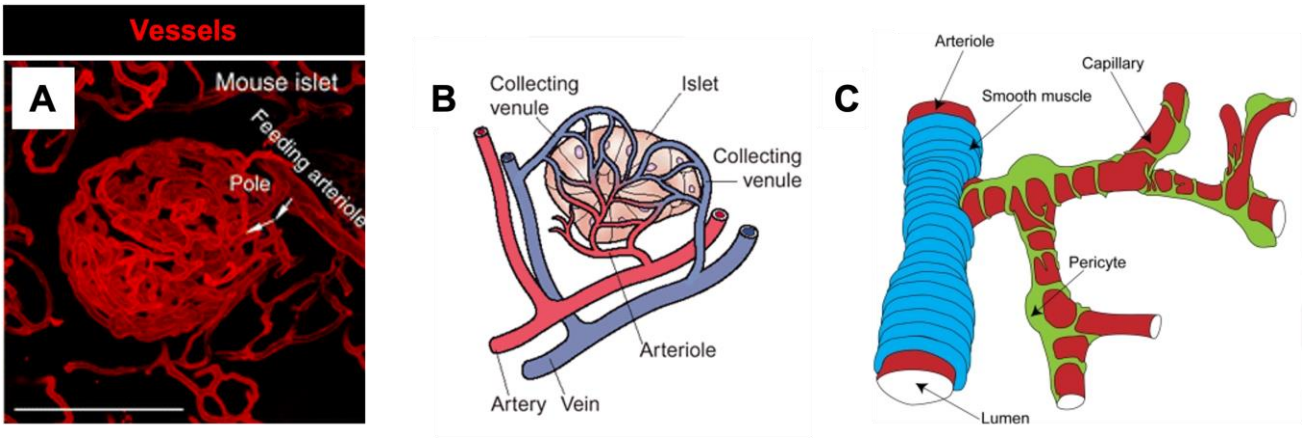

Figure 5. Islets are vascularized and composed of a variety of specialized cell types. Mouse islets receive 10 times more blood flow than acinar tissue and 5-15% of pancreatic blood flow. (A) Islet from a mouse infused with a FITC-conjugated tomato lectin to label functional vasculature (green). The islet is indicated by a dashed line. Intra-islet vessels are denser, thicker, and more tortuous than vessels in the exocrine pancreas. (B) Islets have feeding arterioles from arteries and collecting venules from veins. (C) Smooth muscle rings envelop around arterioles and pericyte processes wrap around capillaries. Figure adapted from Tang et al., 2018 (A), Cleaver and Melton, 2003 (B), and Hamilton et al., 2010 (C).

Pancreatic extracellular matrix

The islet endothelium also secretes ECM proteins that form a basement membrane. Acinar cells in the exocrine compartment produce ECM proteins as well. The ECM is composed of two matrices: the basement membrane and the interstitial matrix. The basement membrane comprises collagen, laminin, and heparan sulfate proteoglycans[51]. The interstitial matrix includes collagen, elastin, fibronectin, and polysaccharides[51]. The ECM provides structural support and a reservoir of signaling molecules that affect cell differentiation, function, and survival[52]. In rodents, islet interiors lack a basement membrane allowing for direct interaction between the vascular basement membrane around capillaries[53]. Human islets, though, have two basement membrane layers surrounding islet capillaries. The peri-islet basement membrane invaginates into islets and expresses differing laminin isoforms than the vascular basement membrane[54].

Morphology and function of pancreatic innervation

Neural anatomy of the pancreas

The pancreas receives neuronal input from multiple peripheral nervous system branches, such as the autonomic, enteric, and sensory nervous systems (**Figure 6**). These fibers enter the pancreas with the splenic artery and the superior and inferior pancreaticoduodenal arteries[55]. Autonomic axons originate in the lateral and ventromedial hypothalamus of the central nervous system (CNS)[56]. The autonomic nervous system (ANS) is composed of sympathetic and parasympathetic nerves. Sympathetic nerves originate in the spinal cord, collect at distal ganglia, and converge in intrapancreatic ganglia to then project throughout the pancreas[57,58]. Parasympathetic nerves originate in the brainstem and extend through the vagus nerve and collect at the nodose ganglion[57,58]. Parasympathetic nerves that project to the pancreas extend from the nodose ganglion into the pancreas[57,58]. Additionally, the pancreas has input from the enteric nervous system of the stomach and duodenum[59]. And lastly, sensory nerves have similar pathways as autonomic nerve fibers[60]. Because the endocrine portion of the pancreas is surrounded by exocrine tissue, nerve fibers extend into the islet from the surrounding exocrine portion of the pancreas.

Neuronal impact on pancreatic function

Neuronal inputs to the pancreas help orchestrate exocrine enzyme and islet hormone secretion necessary for digestion and maintaining healthy blood glucose levels, respectively. Pancreatic unmyelinated nerve fibers have free nerve endings that release neurotransmitters into a dispersed area instead of forming traditional synapses as seen in other tissues[61,62]. There are also neuroinsular complexes composed of nerve cell bodies close to islets that may affect islet function[63]. It is unclear how sympathetic and parasympathetic nerve fibers affect exocrine secretion due to an inability to separate the effects of vasodilation or vasoconstriction on exocrine secretion. Sympathetic activation decreases plasma insulin levels while increasing glucagon levels through the actions of noradrenaline[58]. Severing nerve inputs to the pancreas in rats increased insulin secretion in response to glucose[64] but decreased exocrine function in canines[65]. Parasympathetic activation via the vagus nerve increases insulin secretion and controls cephalic phase responses that induce gut and islet hormone release before a meal[66,67].

The role of sensory nerve fibers in pancreatic hormone secretion is not well understood. Ablation of pancreatic sensory nerves suggests conflicting conclusions of inhibitory or stimulatory impacts on exocrine and insulin secretion[68–70]. Because of the extreme pain associated with pancreatitis sensory nerve fibers are suggested to play a role in the

development of pancreatitis. This pain may be due to the inflammatory reactions of the condition[71].

Islet transplantation studies have helped to elucidate *in vivo* processes of innervation. High-resolution microscopy of islets transplanted into rodents has shown the ability of sympathetic and parasympathetic nerves to re-innervate islets at 3 weeks post-transplantation at the liver or kidney capsule[36,72]. These transplanted islets maintain insulin secretory function and direct electrical stimulation can elicit islet hormone secretion[36,72]. Interestingly, glucose homeostasis normalizes rapidly after pancreas transplantation before the pancreas and its islets would become re-innervated[73]. Therefore, the influence of innervation *in vivo* and under transplantation settings is not completely understood underscoring the necessity of defining the neurovascular architecture in human tissue in this Dissertation.

The study of human pancreatic innervation is difficult due to limited tissue availability, the necessary adaptation of traditional tools for use in fixed and live tissues, and the inability to study *in vivo* neuronal connections directly in humans. Recent studies also demonstrate major phenotypic differences between mouse and human pancreatic tissue regarding neuronal properties. For example, in **Chapter III** of this Dissertation, I show that the interior of human islets has fewer blood vessels and fewer neuronal axons compared to mouse islets which are suspected to be primarily sympathetic axons[74–76]. Furthermore, in comparison to mice, humans have a lower intra-pancreatic ganglia density in their exocrine tissue[77]. Similar autonomic effects occur in humans and mice, though, such as the cephalic phase mediated by parasympathetic nerves, autonomic control over glucagon response to insulin-induced hypoglycemia, and the relationship between sympathetic nervous system inhibition and reduced insulin secretion[58,67,78]. These inter-species differences suggest caution in extrapolating findings in mouse models to humans.

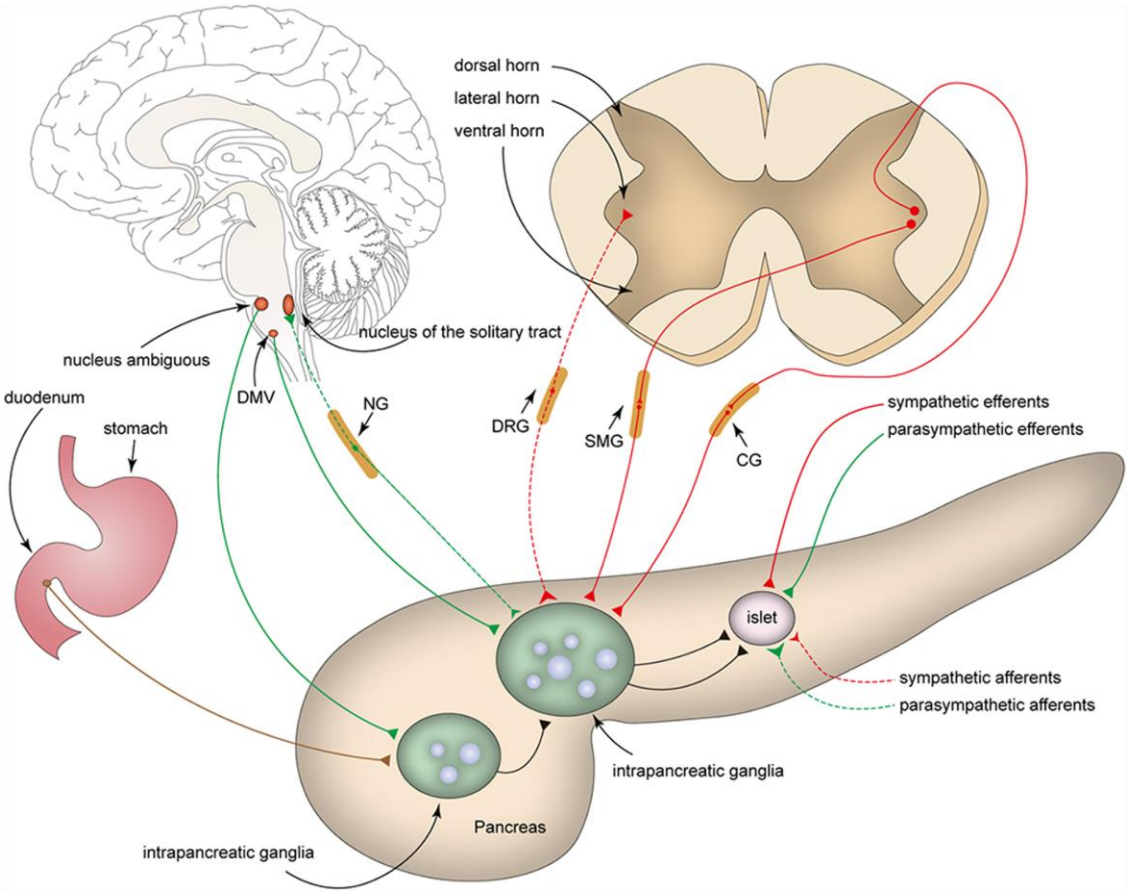

Figure 6. The pancreas receives a variety of neuronal inputs from the CNS. Sympathetic nerve fibers (red), parasympathetic nerve fibers (green), the enteric plexus (brown) synapse onto intrapancreatic ganglia. Efferent parasympathetic fibers (solid green line) project from the dorsal motor nucleus of the vagus (DMV). Efferent sympathetic nerve fibers (solid red line) project from the lateral horn of the spinal cord to the celiac ganglia (CG), superior mesenteric ganglia (SMG), or paravertebral ganglia. Afferent sympathetic and parasympathetic cell bodies are located in the nodose ganglia (NG) and dorsal root ganglia (DRG). These neuronal pathways were predominately generated from observations in rodents. Figure adapted from Li et al., 2019.

Reciprocal influences of vascular, neuronal, and extracellular matrix on islet function

The pancreatic vasculature, nervous system, and ECM contain physiological crosstalk mechanisms that impact the development and functioning of each of these components in addition to exocrine tissue and islets. Developmentally, the dorsal and ventral pancreatic buds originate near major vessels, and the aortic endothelium is required to initiate and maintain pancreatic and duodenal homeobox 1 (*PDX1*) and insulin 2 (*INS2*) expression in the pancreatic foregut endothelium[79,80]. Also, islet cell clusters are vascularized by E13.5 in mice and are essential for pancreatic growth and differentiation[42,81]. Nerve fiber extension typically occurs along arterial vessels and is reinforced by neural growth factors (NGFs) generated by target cells[82]. Neuronal cell bodies enter the pancreatic bud around E10.5[83]. In mice, islet cores become innervated postnatally while the exocrine tissue is innervated during embryonic development[84]. Reductions in sympathetic innervation during development perturb islet architecture, reduce insulin secretion, and induce glucose intolerance in mice[85]. There is new evidence for similar neurovascular developmental paradigms in human pancreata[86].

Furthermore, ECM proteins affect pancreatic and neurovascular development in addition to function. ECM proteins can increase insulin transcription, β cell survival, and β cell proliferation[54,87,88]. In culture, the addition of a collagen scaffold improves islet GSIS[89]. Neurite and vessel growth are also dependent on endocrine cell-ECM interactions to allow for proper cell migration, differentiation, and proliferation[90]. Soluble factors within the ECM, such as angiogenic and neurotrophic factors, also promote neurovascular pathfinding[90].

β cells also produce factors that influence vascularization and innervation. VEGF-A is vital for islet vascularization, revascularization, and function[42,79]. Increased VEGF-A expression in β cells leads to increased endothelial cell density, but an excess of intra-islet endothelial cell growth negatively impacts islet morphogenesis and β cell proliferation[50,91]. VEGF-A expression also directly influences intra-islet nerve fiber density suggesting a role for intra-islet vasculature in aiding intra-islet nerve fiber ingrowth and maintenance (**Figure 7**)[84]. Modulation of VEGF-A expression promotes β cell function such that VEGF-A reduction impairs insulin secretion. Withdrawal of VEGF-A normalizes β cell mass and function[92].

β cell-derived NGF may also influence islet nerve fiber ingrowth and islet function[93]. NGF is critical for the survival and differentiation of nerve axon projections in other organ systems as well. In cultured islets severed from the vascular and nervous systems, the addition of NGF improves GSIS over time compared to control islet GSIS which typically diminishes rapidly in culture[94]. An understanding of the role of these factors in human

pancreatic vascularization and innervation is needed to rationalize the neurovascular pathology seen in diabetes.

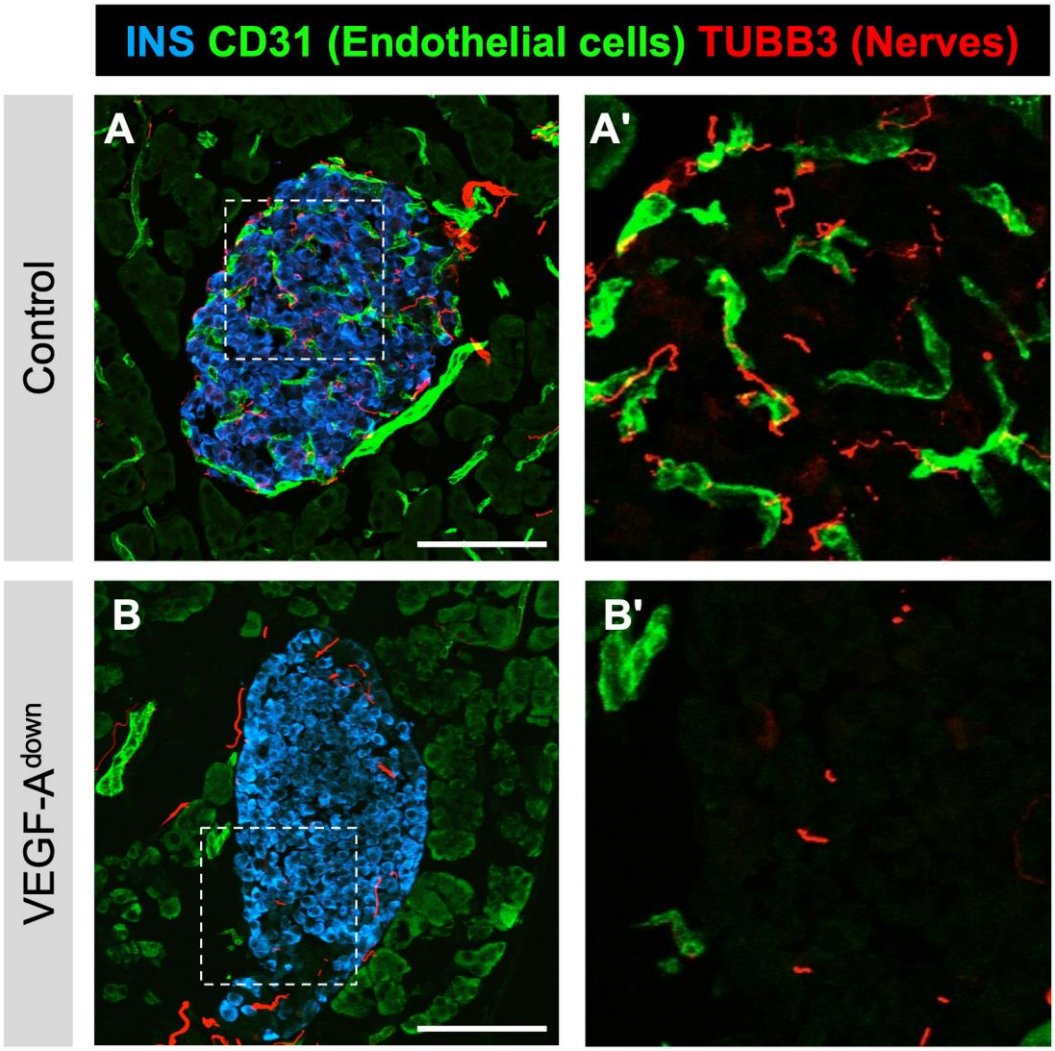

Figure 7. Intra-islet vasculature is critical for islet nerve fiber ingrowth. (A) Intra-islet endothelial cells (green) and nerves (red). (B) Reduced expression of β cell-derived VEGF results in hypovascularization and hypoinnervation in mouse islets. Figure adapted from Reinert et al., 2014.

Pancreatic β and α cell secretion mechanisms

β and α cells are the most highly studied islet endocrine cell types due to how necessary insulin and glucagon are to maintaining glucose homeostasis. Insulin and glucagon secretion are out of phase with one another such that hypoglycemia stimulates α cells to secrete glucagon and hyperglycemia stimulates β cells to secrete insulin (**Figure 8**). The mechanisms governing the hormone secretion of these two cell types are summarized below (**Figure 9**).

Islets uniquely operate as mini-organs outside of the body. Isolated islets can maintain their secretion dynamics in culture, enabling the *ex vivo* assessment of their function for phenotypic characterization and perturbation. Islet dissociation eliminates paracrine communication via a reduction of endocrine cell-derived secreted products and gap junctions that are vital for initiating and tuning hormone secretion mechanisms described above[95]. Enzymatic dissociation of islets into a single-cell suspension results in a concomitant loss of regulated function, emphasizing the importance of these cell-to-cell contacts[96,97].

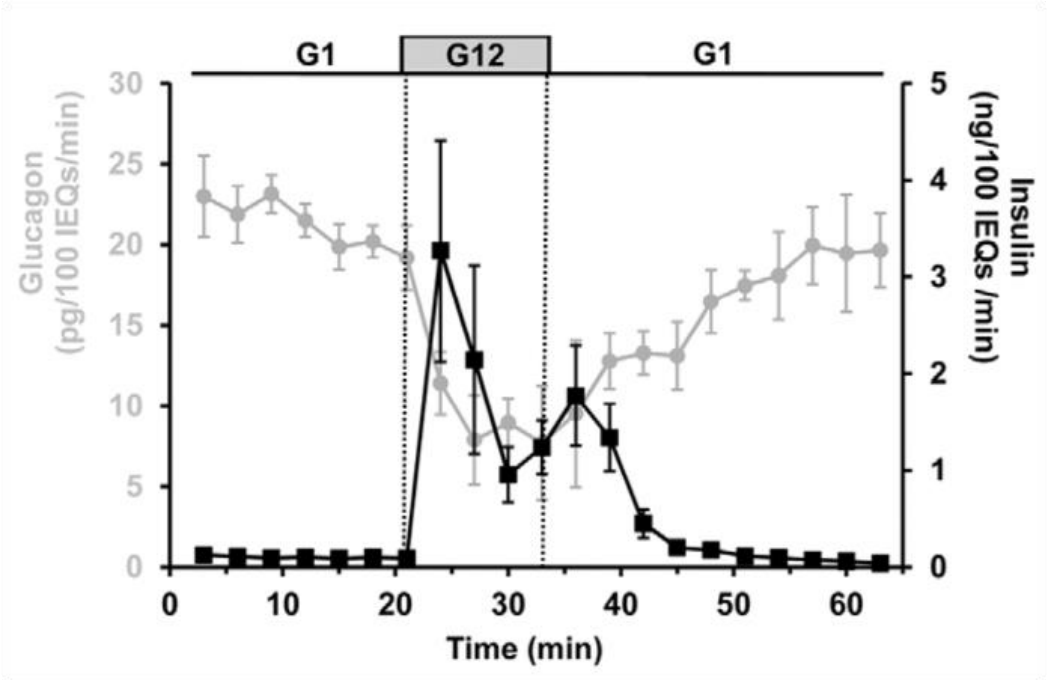

Figure 8. Insulin and glucagon secretion from perifused mouse islets are in opposite phases from one another.
Exposure of isolated islets to low glucose (1 mM; G1) for 30 minutes prior to the following experiment (N = 6 mice, 450 total islets). Insulin (black) and glucagon (grey) secretion was measured during exposure to G1, high glucose (12 mM; G12), and then G1 with normalization islet size (islet equivalent, IEQ). Mean secretion values are plotted for three replicate experiments in which errors bars represent the standard error of the mean. Figure adapted from Marchand et al., 2012.

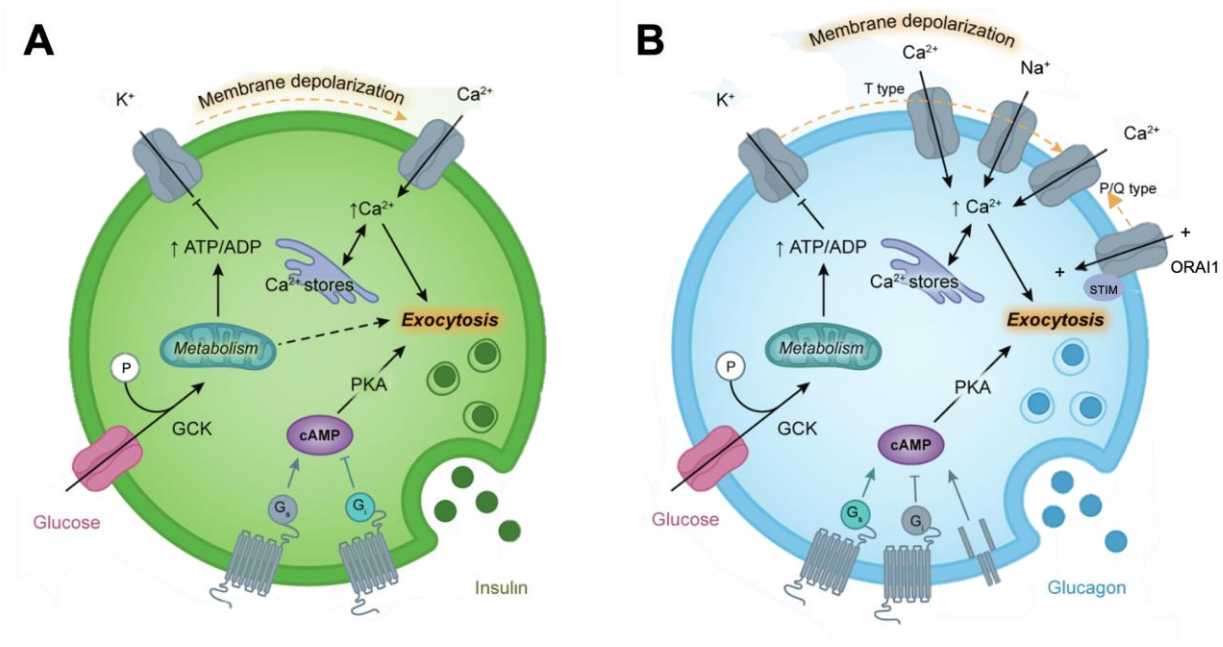

Figure 9. Intracellular signaling pathways regulate insulin and glucagon secretion from β and α cells.
Illustrations of insulin secretion from β cells (A) and glucagon secretion from α cells (B). These illustrations depict the signaling pathways behind subsequent secretion. Figure adapted from Walker, Saunders, et al., 2021.

Insulin secretion mechanisms

GSIS occurs in response to a rise in blood glucose (**Figure 9A**). Glucose is taken up by β cells through glucose transporters, GLUT2 in rodents and GLUT1 in humans[98,99]. Glucose is then phosphorylated into glucose-6-phosphate (G6P) by glucokinase (GK). Glycolysis converts G6P into pyruvate which can then enter the mitochondria via mitochondrial pyruvate carriers[100]. Oxidative metabolism in the mitochondria leads to adenosine triphosphate (ATP) generation, increasing the cytosolic ATP:ADP ratio. ATP-sensitive potassium (K_{ATP}) channels are inhibited by ATP, causing membrane depolarization mediated in part by other ion channels as well[101–103]. Membrane depolarization of about -50 mV causes the opening of voltage-gated calcium (Ca^{2+}) channels resulting in rapid and repetitive action potentials[104]. Intracellular cytosolic Ca^{2+} then interacts with exocytotic components to facilitate insulin secretory granule fusion with the plasma membrane. Ca^{2+} dynamics are coordinated across the islet resulting in oscillatory responses to high glucose[105]. These oscillations lead to pulsatile insulin secretion, which is important for maintaining peripheral insulin sensitivity[46]. Synchronized Ca^{2+} waves generated by pacemaker or “hub” β cells coordinate islet hormone secretion[106–108]. Disruption of pacemaker or “hub” β cells may underly secretory defects seen in diabetes[106–108].

Glucagon secretion mechanisms

Hypoglycemia inhibits insulin secretion but promotes glucagon secretion from α cells (**Figure 9B**)[109]. The mechanisms governing glucagon secretion are not as well understood as their β cell counterparts. There has been an attempt to superimpose insulin secretion mechanisms onto α cells, but there are important similarities and differences between the secretory machinery of β and α cells. For example, α cells express GLUT transporters to monitor blood glucose levels, but glucose-mediated mechanisms that elicit glucagon secretion are contested[110,111]. Additionally, Ca^{2+} changes in α cells are modest with non-synchronous oscillations, unlike in β cells[104]. Therefore, Ca^{2+} may play a more nuanced role in controlling glucagon secretion.

A single model for glucagon secretion is not agreed upon but two main models prevail: 1) a K_{ATP}-centric model or 2) a store-operated model[112]. The first model of glucagon secretion relies on hyperglycemia induced K_{ATP} channel membrane depolarization. High glucose conditions lead to the closure of K_{ATP} channels which leads to the inactivation of P/Q-type and sodium (Na^+) type voltage-gated channels preventing the opening of voltage-dependent Ca^{2+} and subsequent glucagon secretion[113]. Thus, once glucose levels decline, the inhibitory action of membrane depolarization on K_{ATP} channels is thought to be relieved, leading to the activation of glucagon secretion.

The second model is dependent on store-operated channels that facilitate the release of Ca^{2+} from the endoplasmic reticulum (ER) into the cytoplasm. Low glucose levels cause reduced oxidative phosphorylation and ATP levels. Decreased ATP levels deplete the ER of its Ca^{2+} stores, further causing ER-resident Ca^{2+} sensor stromal interaction module (STIM) proteins to translocate to the plasma membrane and co-cluster with ORAI calcium release-activated calcium modulator 1 (ORAI1). This interaction produces an influx of cations that depolarize the membrane and activate P/Q-type and Na+-type voltage-gated channels. Downstream membrane depolarization leads to the opening of Ca^{2+} voltage-gated channels and glucagon secretion[114,115]. α cell secretion mechanisms were determined mainly with non-human islets but given the architectural and functional differences between rodent and human islets, extrapolation to human glucagon secretory pathways remains to be determined.

Paracrine and autocrine interactions of islet hormone secretion

Other stimuli can also affect hormone secretion from β and α cells thru amplifying pathways that are downstream of intracellular Ca^{2+} increases. The secretion mechanisms discussed above fall under pathways that trigger secretion, whereas autocrine and paracrine factors contribute to the amplification or dampening of islet hormone secretion[116]. Furthermore, dissociated islet endocrine cells have different hormone secretory responses underscoring the importance of paracrine regulation by other islet cell types. Therefore, the proximity of endocrine cells to one another facilitates these autocrine and paracrine effects. It is important to consider these potential interactions when assessing the *in vivo* and *ex vivo* secretion dynamics of these islet hormones, particularly in the disease setting of diabetes.

A variety of accessory receptors are expressed on islet cells that help to modulate secretion, such as G-protein coupled receptors (GPCRs) and amino acid transporters. Under hyperglycemic conditions, somatostatin, insulin, urocortin 3, and gamma-aminobutyric acid (GABA) negatively feedback onto α cells to reduce glucagon secretion[117–120]. Insulin receptors on α cells activate phosphodiesterase 3B (PDE3B), further decreasing phosphokinase A (PKA) activity, cAMP levels, and glucagon secretion[121]. It is postulated that α cells become activated in a post-prandial state because of increased circulating amino acids such as arginine, glutamine, and alanine after a protein-rich meal[122]. α cell secretory products such as glucagon and glucagon-like peptide 1 (GLP-1) also stimulate insulin secretion through G_s-coupled receptors (**Figure 10**)[123,124]. In turn, somatostatin (SST) can activate G_i-coupled receptors on α and β cells to decrease glucagon and insulin secretion (**Figure 10**)[121,125–127]. Autocrine regulation within the islet also affects hormone secretion. For example, glucagon G_s-coupled receptors expressed on α cells can further stimulate glucagon secretion through intracellular increases of cyclic adenosine monophosphate (cAMP)[121]. α cell-derived GLP-1 can also stimulate somatostatin secretion from δ cells through activation of G_s-coupled receptors[128].

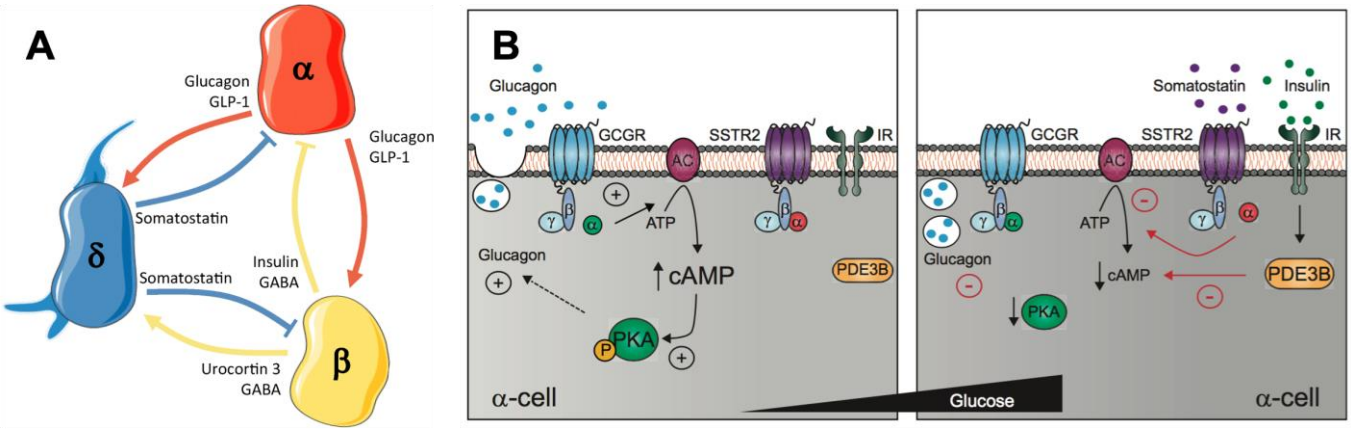

Figure 10. Intra-islet autocrine and paracrine signals in response to low and high glucose. (A) Schematic of islet α-β-δ paracrine interactions. (B) cAMP-mediated activation of glucagon secretion is controlled by paracrine regulators of glucagon secretion at low (left) and high (right) glucose concentrations. Figure adapted from Hartig and Cox 2020 (A) and Elliot et al., 2014 (B).

The purinergic system

Another important communication system within the islet is the autocrine and paracrine effects of extracellular ATP. ATP was first discovered as a potent signaling molecule in 1929 after intravenous injections of sheep heart, brain, and kidney extracts [129,130]. Then in 1962, while studying the ANS, Dr. Geoffrey Burnstock observed a neural signaling phenomenon that did not involve the traditional neurotransmitters, acetylcholine, or noradrenaline[129]. To his surprise, blockage of these latter neurotransmitters did not eliminate smooth muscle contractions. After pursuing this new neurotransmitter, he proposed the existence of "purinergic nerves" that discharge ATP from their terminals[129]. Despite much early skepticism, Dr. Burnstock is now heralded as the Father of the Purine Field as he discovered many actions of ATP and the two families of receptors in which they act through[129]. Many of these pathways are targeted for pain management, cancers, and inflammatory diseases[129,131,132].

In general, ATP is considered a neurotransmitter and affects the electrical activity of neighboring cells and inflammatory processes. The insulin granule is densely packed with insulin peptides that affect whole-body glucose homeostasis but also ATP that can act locally on neighboring islet cells[133,134]. Nucleotides can be co-secreted with other peptides, as is seen in β cells and nerve terminals[135]. Once ATP is co-secreted with insulin into the extracellular space, it can bind GPCR or ion channel purinergic receptors to modulate cellular functioning such as hormone secretion, vessel dilation, and actions of inflammatory cells[133]. Nucleotides can also be released into the extracellular space as a sign of cellular damage following hypoxia, high levels of mechanical stress, or infection[136]. Intercellular transmission of nucleotides between neighboring cells can also occur through hemichannels like connexons[136]. Connexons are implicated in synchronizing Ca^{2+} waves across the islet[137]. Therefore, the exchange and/or release of ATP may be important for islet hormone secretion dynamics, immune mechanisms underlying macrophage homeostatic roles in pancreatic development, and diabetes pathophysiology.

The purinome and pancreatic function

The purinome, which encompasses nucleotide ligands, enzymes that metabolize these nucleotides, and purinergic receptors, provides a complex signaling environment implicated in tuning islet hormone secretion[132]. Extracellular nucleotides and their derivatives affect intracellular function through purinergic signaling[138]. Purinergic receptors mediate nucleotide signaling: P1 adenosine-activated G protein-coupled receptor (GPCR) subtypes, P2X ATP-activated ion channel receptor subtypes, and P2Y ATP/ADP/AMP-activated GPCR subtypes[139].

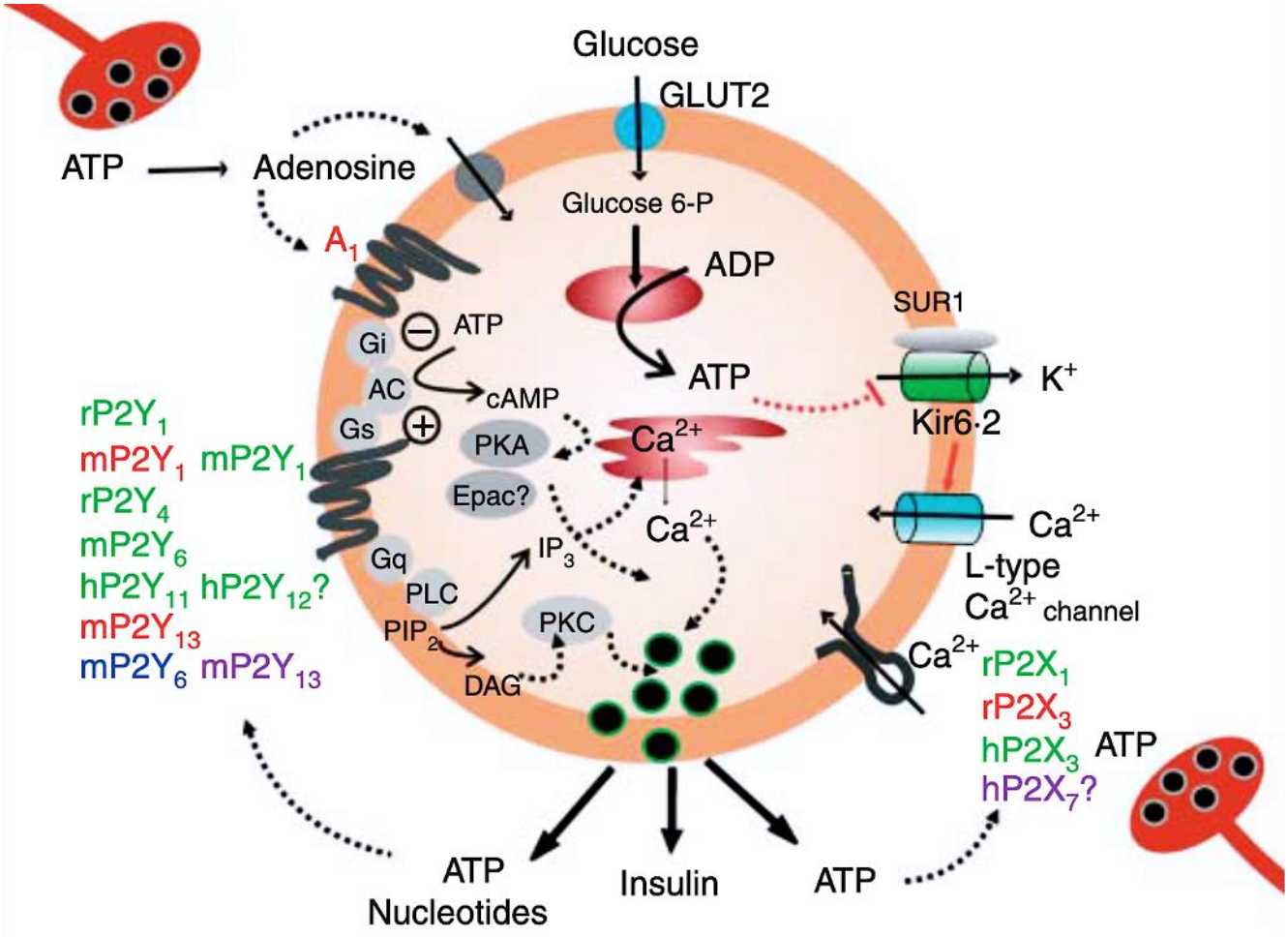

Figure 11. Purinergic receptor signaling in the regulation of β cell function and survival. Extracellular ATP can bind purinergic receptors and be metabolized by ecto-enzymes. Purinergic GPCRs or ion channels mediate purinergic intracellular signaling in beta cells is shown here. This graphic briefly summarizes key understandings from the past 40-plus years of investigation on the islet purinergic system beginning from early discoveries that ATP is released from nerves and in conjunction with insulin. Most of the characterization of the purinergic system has been performed in rodents (m, mouse; r, rat) with a handful of recent studies assessing human (h) islet dynamics. Key: green = increased insulin secretion; red = decreased insulin secretion; blue = cell proliferation, purple = apoptosis. Figure adapted from Burnstock 2014.

Many ecto-nucleosidases that face the extracellular space are major regulators of extracellular nucleotide concentrations in many tissues in the body such as the nervous system and the pancreas[140,141]. Ectonucleoside triphosphate diphosphydrolases (NTPDases) break down nucleotides into their respective derivatives and have variable affinities for ATP, ADP, and AMP[140]. These enzymes have varying affinities for different nucleotides and differential tissue expression patterns[140,142–146]. Consequently, regulation of intra-islet nucleotide levels is suggested to impact islet hormone secretion due to nucleotide-mediated autocrine and paracrine purinergic signaling (**Figure 11**)[147–150].

Ectonucleoside triphosphate diphosphohydrolase-3 (NTPDase3), which preferentially converts ATP into ADP in the extracellular space, has recently been shown to be a preeminent marker of mature β cells with expression transitioning from acinar tissue to β cells postnatally in humans[151,152]. It is also expressed in regions of the brain, digestive tract, and the bladder[142,143,153–156]. *In vitro* NTPDase3 inhibition in rodent β cell lines and isolated rodent islets potentiated or decreased GSIS leading to variable conclusions on the role of NTPDase3 on islet insulin secretion[145,156].

Compared to other tissues such as the nervous system the purinergic system is vastly understudied in the pancreatic islet. The β cell-specific expression and ability of NTPDase3 to modulate the concentration of purinergic receptor ligands suggest a role in regulating intra-islet hormone secretion and glucose homeostasis[140,157]. Additionally, the receptor subtypes that intra-islet ATP stimulates are largely unknown, with P2X and P2Y receptors being implicated in signal transduction in dispersed β cells and intact islets[147–149,158–160]. Given the understudied ATP signaling pathways present within the islet, it is important to investigate the expression patterns of ecto-enzymes and purinergic receptors and to elucidate the dominating pathways in controlling nucleotide-mediated hormone secretion. **A focus of the work in this Dissertation is the role of purinergic signaling in the pancreatic islet, particularly the function of NTPDase3 in regulating insulin secretion in mouse and human.**

Species-specific differences between rodent and human islet physiology

Rodent models and humans have many different characteristics in terms of pancreatic physiology, metabolic rate, and circadian rhythms. Rodent models were critical in laying the foundation for physiologic mechanisms for pancreatic islet function and dysfunction. Nonetheless, the differences identified between these species warrant caution for direct translation from rodents to humans.

In mice, β cells are arranged in the “core” while α and δ cells make up the “mantle” of the islet (**Figure 12A**). Adult human islets have a more interspersed endocrine cell

architecture with β and α cells at a closer ratio (**Figure 12B**)[161,162]. Mouse islets are about 75% β cells with α and δ cells making up about 19% and 6% of the endocrine cell population, respectively (**Figure 12C**). Whereas human islets have a lower proportion of β cells with a higher proportion of α cells compared to mouse islets (**Figure 12D**). Therefore, human β cells are more likely to make heterotypic contacts with other endocrine cells over the primarily homotypic contacts in mouse islets. These architectural differences have implications for the efficacy and actions of endocrine cell autocrine and paracrine feedback mechanisms as well as how the islet responds to extrinsic factors such as those from nerve fibers and the vasculature.

The insulin secretory profiles of mice and humans differ as well. Human non-fasting plasma glucose concentration is lower than mice at 5 mM glucose[163]. Human islets secrete more insulin at basal levels with a lower stimulation index during high glucose conditions compared to insulin secretion from mouse islets[163]. Human islets also do not alter their gene expression profile as robustly as mouse islets following high glucose culture over a 48–72-hour period[163,164]. Furthermore, human β cells have a lower proliferative capacity than mouse β cells in response to stress like obesity and pregnancy. These differences convolute therapeutic hypotheses for β cell regeneration to ameliorate diabetes in humans[165]. Given these inter-species differences between mice and humans, additional models are needed to understand human islet physiology. The studies assessing the neurovascular architecture (**Chapter III**) and the purinergic system (**Chapter V**) in human pancreatic tissue provide a direct understanding of human physiology and illuminate important interspecies differences between mouse and human.

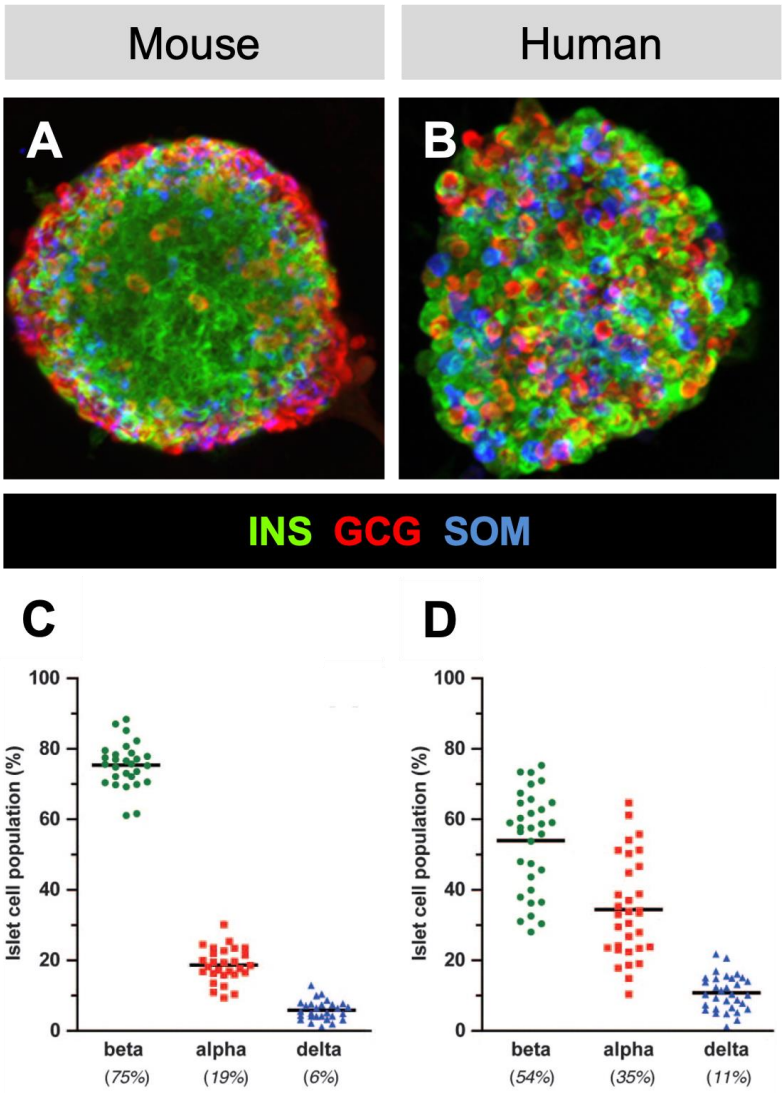

Figure 12. Islet endocrine cell proportions differ between mice and humans. (A-B) Mouse and human islets labeled for insulin (green), glucagon (red), and somatostatin (blue). (C-D) Quantification (mean) of endocrine cell composition consisting of β (green, beta), α (red, alpha), and δ (blue, delta) cells from mouse (C) and human (D) islets. Figure adapted from Brissova et al., 2005.

Diabetes

The pancreatic islet is implicated in the development of and pathology of diabetes. Diabetes is a growing global health concern with an estimated 463 million adults living with diabetes worldwide according to the United States (U.S.) Center for Disease Control[166]. In the U.S. alone, approximately 34 million adults have diabetes or about 11% of the population[166]. Additionally, an estimated 40% of the American population have pathologically elevated fasting or post-prandial blood glucose levels referred to as "prediabetes"[166]. Projections reveal that these staggering statistics will nearly double by 2030[166].

Forms of diabetes

Type 2 diabetes (T2D) is the most common form, with about 95% of all diabetes cases being diagnosed as T2D. Type 1 diabetes (T1D) cases are about 5% of total diagnoses and require lifelong exogenous insulin therapy[167]. T1D is a chronic disease that occurs following an autoimmune-mediated attack of pancreatic β cells. During the autoimmune process of T1D, autoantibodies towards β cell-specific proteins are generated and β cells are selectively destroyed. Given the essentiality of β cell insulin secretion in maintaining glucose homeostasis, this autoimmune process greatly disrupts pancreatic islet function. Rarer forms of diabetes result from genetic mutations of insulin production or secretion, such as neonatal diabetes or maturity-onset diabetes of the young (MODY)[168,169]. Secondary development of diabetes from infections, surgical procedures, or medications may also contribute to some forms of diabetes prevalence.

Diabetes diagnosis

Typically, T1D presents at a younger age compared to T2D with classical symptoms of hyperglycemia such as polyuria, polydipsia, polyphagia, and weight loss. T1D and T2D are formally diagnosed due to elevated plasma glucose levels after fasting, after an oral glucose tolerance test (GTT), or random venous levels. Additionally, a glycated hemoglobin (HbA1C) percentage ≥ 6.5% indicates atypical glucose metabolism throughout the last three months and is an indicator of diabetes[170]. There is currently no diagnostic test to distinguish between T1D or T2D, so clinicians utilize additional characteristics such as weight, age, insulin sensitivity, family history, autoantibody test, and C-peptide levels[170].

Diabetes treatment

Maintaining normoglycemia is imperative to prevent the immediate and long-term ramifications of T1D and T2D. Those with diabetes must routinely monitor their blood glucose levels through glucometers or glucose sensors. Additionally, techniques to replace β cell mass such as transplantation (of islets or pancreas) and stem cells (embryonic or induced pluripotent) are gaining traction and utility.

Treatment for T2D entails lifestyle changes such as weight and nutrition management, oral agents, and insulin injections for more severe cases[171]. Although the first course of treatment for T2D typically focuses on diet, exercise, and weight loss, many patients eventually need to add oral medications and/or exogenous insulin to effectively control their hyperglycemia. The following medications are the main categories of oral medications currently prescribed for T2D: A) metformin, which decreases hepatic glucose production, B) sulfonylureas, which directly promote insulin secretion by closing the K_{ATP} channel and causing cell depolarization, C) sodium channel blockers, which promote glucose excretion in the urine, D) PPAR receptor agonists, which increase insulin sensitivity, and E) incretin mimetics, which encourage satiety, weight loss, and protection of cells[172–174]. Insulin replacement therapy at the onset of hyperglycemia through exogenous insulin injections or pumps is the primary treatment for T1D. Immunomodulatory drugs like Teplizumab, a new monoclonal antibody treatment directed towards a T-cell receptor antigen (anti-CD3), could be utilized in the future to delay or prevent T1D for those in Stage 2 of T1D (autoantibody+ with normoglycemia and mild glucose intolerance)[175].

A limitation of diabetes treatment regimens is the risk of hypoglycemia during the course of glycemic management with some oral medications or insulin injections[176]. Hypoglycemia impairs physiological and behavioral defenses against subsequent hypoglycemic events and is occasionally fatal in those with T1D and many people with advanced T2D. Minimizing hypoglycemia in diabetes involves choosing suitable, tailored glycemic goals, and offering systematic patient education that will frequently lower the incidence of hypoglycemia for the majority of people with diabetes who are at risk for, or experiencing iatrogenic hypoglycemia. Therefore, understanding why hypoglycemia occurs and how to prevent this phenomenon is relevant to the work conducted in this Dissertation.

Type 2 diabetes (T2D)

T2D cases account for more than 90% of all diabetes cases globally. T2D is frequently linked to obesity and/or advanced age, however, its prevalence in young patients is quickly rising concomitantly with the rise in childhood obesity. T2D has a significant genetic component but lifestyle factors including weight, nutrition, and activity impact one's risk of developing T2D as well[172,177]. Clinically, T2D is a very diverse condition with several possible biochemical mechanisms and time courses leading to hyperglycemia.

Emerging concepts in the pathophysiology of T2D

In the T2D model (**Figure 13**), insulin secretion becomes progressively insufficient to meet (potentially elevated) insulin demand. Insulin resistance tends to remain consistent throughout the disease while β cell functional mass decreases, indicating initial and progressive cell failure as a crucial pathogenesis factor (**Figure 13**)[178]. Over time, insulin production is reduced requiring more therapeutics to promote glucose homeostasis[179]. An alternative theory for the progression of T2D is that insulin hypersecretion and subsequent hyperinsulinemia is the initial defect, with hyperinsulinemia leading to insulin resistance, obesity, and β cell failure[180]. Islet failure in T2D impacts multiple cell types, but research focuses mostly on β cell dysfunction. Notably, dysregulated glucagon production from α cells leads to increased hepatic glucose output and can aggravate insulin insufficiency[3,181]. Non-endocrine cells such as macrophages, endothelial cells, and pericytes that contribute to general function are also affected by T2D[53,182–185]. More research is required to determine if the metabolic environment in T2D, inherent cell abnormalities, or the lack of the proper paracrine signals from nearby islet cells negatively impacts islet dysfunction in T2D.

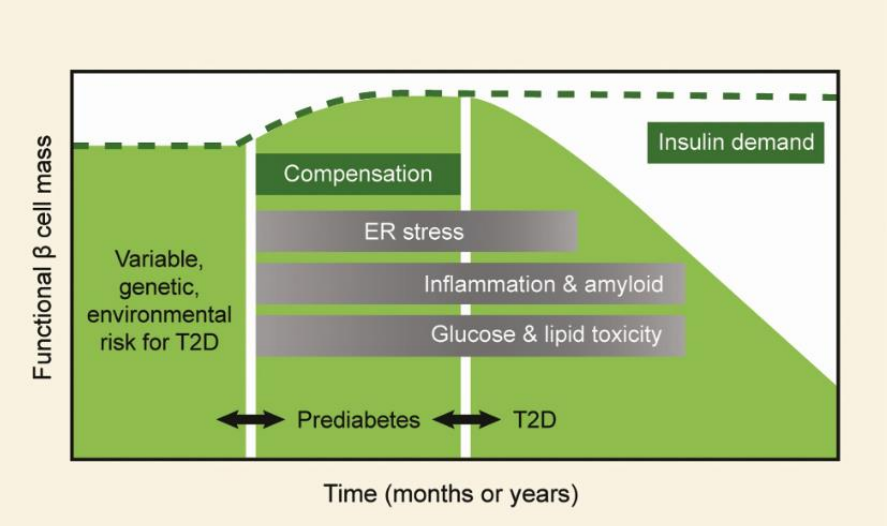

Figure 13. Model for the development of type 2 diabetes (T2D). Type 2 diabetes (T2D) is marked by increasing deficiencies in insulin production and action to meet insulin demands needed to reduce blood glucose levels. Insufficient insulin secretion may then lead to glucotoxicity, lipotoxicity, islet infiltration by macrophages, amyloid deposits, and/or alteration of islet capillaries further disrupting islet architecture and function. Figure adapted from Walker and Saunders, et al., 2021.

Type 1 diabetes (T1D)

Staging of T1D pathophysiology

Dr. George S. Eisenbarth developed a model for T1D pathophysiology that recognizes the chronic autoimmune processes of T1D as evidenced by islet-infiltrating immune cells and the emergence of islet autoantibodies (**Figure 14**)[186]. A revised paradigm with discrete stages of T1D is summarized below.

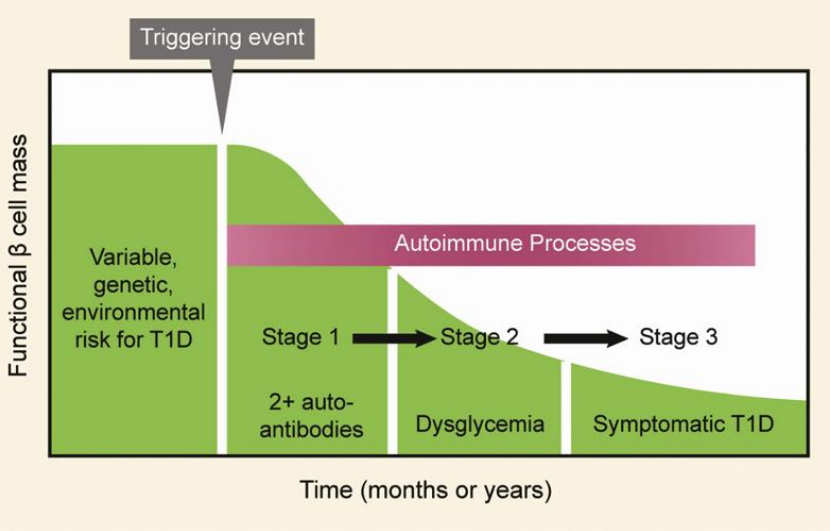

Figure 14. Model for the development of type 1 diabetes (T1D). Unknown "triggering" event(s) are postulated to lead to the initiation autoimmune process, islet autoantibodies emergence, and loss of β cell mass. The three stages of T1D are: Stage 1 – multiple autoantibodies, Stage 2 – dysglycemia, and Stage 3 –symptomatic T1D. Figure adapted from Walker and Saunders, et al., 2021.

Stage 1 is characterized by normoglycemia with positivity for two or more T1D-associated islet autoantibodies[186]. An unknown "triggering" event is proposed to initiate islet autoimmunity. Seroconversion to multiple autoantibodies within the first five years of life positively correlates with the probability of T1D development[187]. Upwards of 75% of those with T1D are positive for autoantibodies against glutamic acid decarboxylase (GAD65), a producer of gamma-aminobutyric acid (GABA) in human pancreatic β cells and bacterial populations within the gut[188]. Autoimmune linkages between the gut microbiome and islets susceptible to autoimmune attack need to be further elucidated which is explored in **Chapter VI**[189–191]. Stage 2 is characterized by two or more autoantibodies and early signs of glucose intolerance or dysglycemia[192–195]. Additionally, immune signatures are altered during this stage before β cell destruction, which may indicate that immune cells are already primed to attack pancreatic β cells[196,197].

In Stage 3, it is hypothesized that clinical symptoms of T1D present once an individual reaches about 10-30% of their original β cell mass. At this point, exogenous insulin therapy to maintain normoglycemia is needed. Stage 4 is characterized by reduced insulitis, rare insulin-positive islets, and a clinical treatment focus on maintaining glycemic control[198]. Long-term challenges of diabetes treatment such as hypoglycemic unawareness present in this stage and are discussed below. The studies discussed in **Chapter III** examine the neurovascular architecture of healthy and symptomatic T1D individuals.

T1D pathophysiology

Insights from rodent models of T1D

The non-obese diabetic (NOD) mouse and BioBreeder (BB) rat models are the predominant spontaneous T1D animal models of T1D. These models are advantageous because immune processes governing T- and B-cell pathology in T1D can be directly manipulated and studied. I have gained an understanding of immune responses in islets and pancreatic draining lymph nodes such as the importance of the lymph nodes for T-cell effector activation[199]. Animal models also serve as pre-clinical testing of newly developed pharmacological modulators.

Although these rodent models share many characteristics with human T1D pathology, there are also considerable variances. These differences include T- and B-cell signaling pathway components, the severity of insulitis in NOD mice, and the absence of predictive human islet autoantibodies in mice[200–202]. Animal models run the risk of failing to accurately reflect human disease in all of its complexity. For example, upwards of 200 immune intervention studies that showed encouraging outcomes in NOD mice did not show positive outcomes in patients[203]. Therefore, our understanding of T1D pathophysiology must be complemented by studies of the human pancreas both non-diabetic and those with T1D.

Pancreatic tissue is mainly acquired through either surgical procedures or postmortem tissue donation. I cannot safely biopsy the human pancreas or islets, which creates immense barriers to studying human islet physiology. Increased availability of human islets through private and federal mechanisms such as the Human Pancreas Analysis Program (HPAP, https://hpap.pmacs.upenn.edu/), the network for Pancreatic Organ Donors with Diabetes (nPOD, https://www.jdrfnpod.org/), and the Integrated Islet Distribution Program (IIDP, https://iidp.coh.org/) has greatly expanded scientific research[204–207]. The scarcity, though, of human pancreatic tissue, biological variability between donors, and uncontrollable physiological impact of organ isolation and transport

has led researchers to utilize animal models of diabetes to better understand T1D pathophysiology *in vivo*.

Impaired counterregulatory responses and glucagon secretion

In T1D, α cells under hypoglycemic conditions cannot appropriately initiate a counterregulatory glucagon response and have defects relating to their responses to hypo- and hyperglycemia[208]. Hypoglycemia elicits a systemic glucose counterregulatory response to return the body to normoglycemia (**Figure 15**). Rising circulating cortisol, growth hormone, and adrenal gland-derived epinephrine levels signal to the liver and islet to initiate processes that raise blood glucose levels[69,209]. Thus, liver glucose production and glucagon secretion increase as insulin secretion decreases. The ANS aids in the regulation of hypoglycemic responses by sensing low blood glucose at the level of the CNS[69]. The CNS then communicates to the body that blood glucose is low, leading to sympathetic activation such as increased heart rate, a desire to eat, and the release of norepinephrine, acetylcholine, and epinephrine[69]. These circulating modulators and sympathetic nerve fibers can act directly on the pancreatic islet to stimulate glucagon secretion[69].

Insulin-induced hypoglycemia in those with T1D ranging from 2 weeks to 42 years did not induce a glucagon response, but growth hormone and cortisol responses were still intact[210,211]. Impaired glucagon secretion responses became apparent in donors with disease durations < 5 years before impaired sympathetic epinephrine responses in donors with disease > 10 years emphasizing that loss of an appropriate glucagon response is an early pathological defect (**Figure 16**)[210,212]. These defects also did not correlate with typical autonomic neuropathy[213]. Conversely, there is a relative excess of postprandial glucagon secretion due to increased responses to amino acid stimulation (**Figure 17**). As disease duration increases, α cell hypersecretion after amino acid exposure increases, possibly due to the progressive loss of paracrine inputs from β cells[214,215].

Repeated episodes of hypoglycemia in T1D attenuate sympathetic nerve fiber activity leading to hypoglycemic unawareness or the failure to recognize autonomic such as neuroglycopenia and cognitive dysfunction[216]. This maladaptation is life-threatening[216]. Therefore, the etiology α cell dysfunction in T1D and a broader understanding of the causes underlying these secretory disturbances are needed.

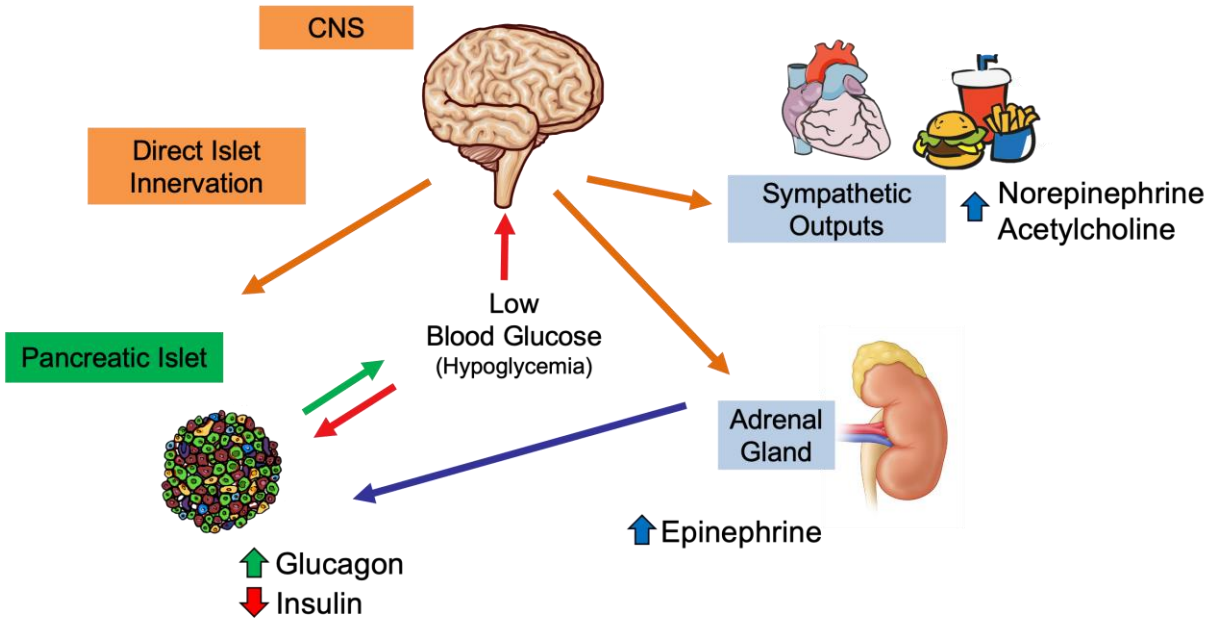

Figure 15. Systematic glucose counter-regulation to hypoglycemia.
Hypoglycemic decreases insulin secretion and increases glucagon secretion which can stimulate the liver to produce glucose. Hypoglycemia also raises circulating epinephrine, cortisol, norepinephrine, acetylcholine levels which in turn increase autonomic responses such as heart rate, hunger, and sweating.

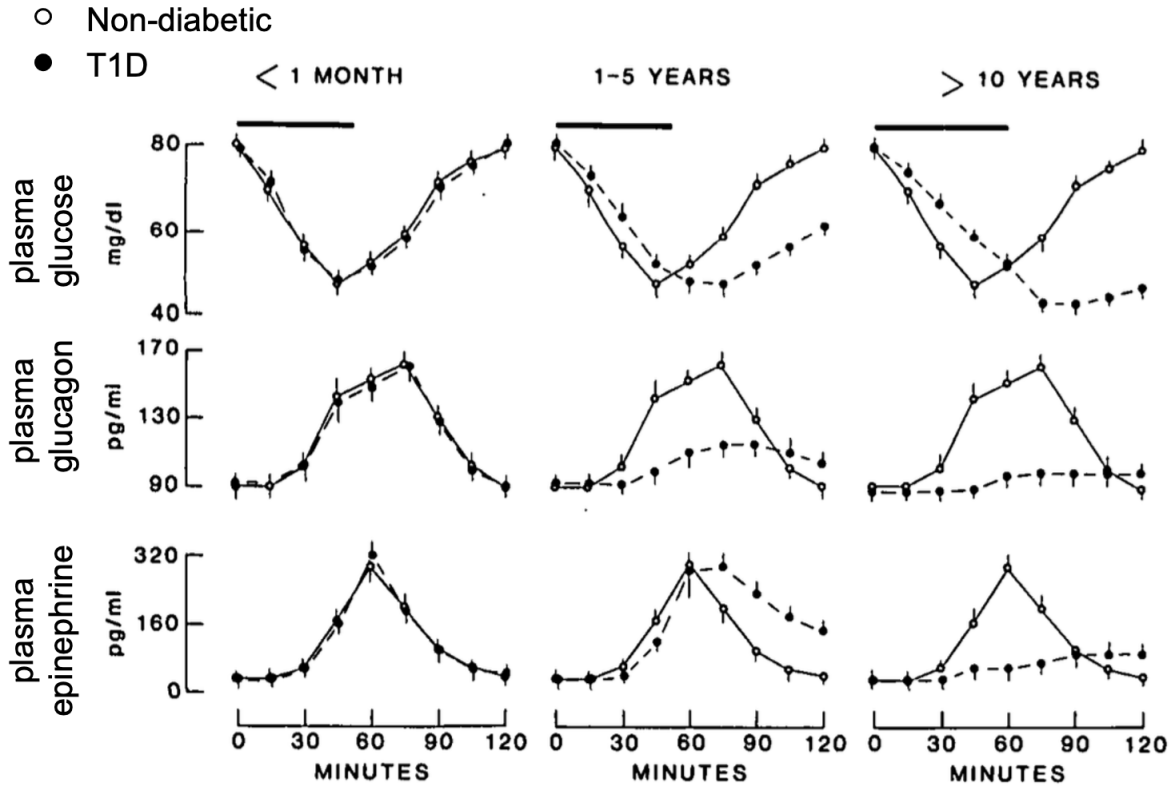

Figure 16. Impaired glucagon secretion in response to hypoglycemia occurs prior to dysregulation of epinephrine secretion.
Plasma glucose, glucagon, and epinephrine levels were assessed during insulin-induced hypoglycemia (IIH) from 1-60 minutes. Compared to non-diabetic (ND) individuals (N = 10, open circles), those diagnosed with T1D (black circles) <1 month (N = 5), 1-5 years (N = 11), and > 10 years ago (N = 5) achieved hypoglycemia similar to ND participants but impaired recovery (60-120 minutes) to normoglycemia at increasing disease duration. T1D participants with disease for 1-5 years had reduced glucagon levels during IIH but increased epinephrine levels in the recovery phase. Participants with T1D for > 10 years had a nearly absent glucagon and epinephrine responses. Figure adapted from Bolli et al., 1983.

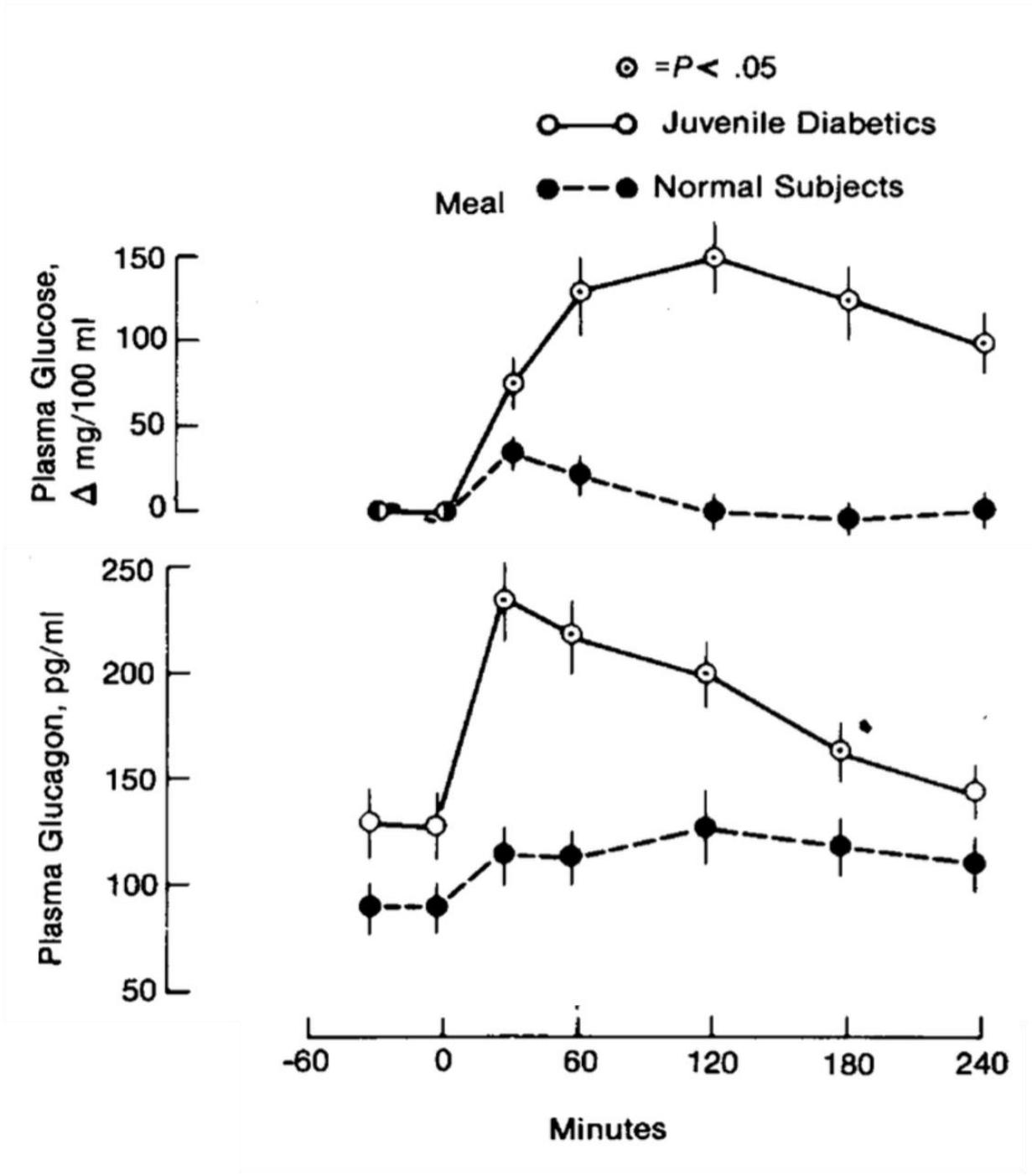

Figure 17. Individuals with T1D have abnormal post-prandial glucagon secretion. Post-prandial hyperglycemia in conjunction with abnormal glucagon release occurred in those with T1D (disease duration 1-17 years, N =12, open circles) compared to non-diabetic controls given a standard meal. Plasma glucose (top) and glucagon (bottom) levels were measured over 240 minutes. Figure adapted from Gerich et al., 1975.

Pathologic neurovascular architecture and function in diabetes

It is hypothesized that vascular and nervous system impairments contribute to the pathophysiology of T1D as a result of autoimmune processes leading to β cell destruction. In T1D islets, nerve fibers are postulated to be a target of immune cell infiltration which may underlie glucagon secretion deficiencies associated with T1D[217]. Therefore, autoimmune islet attack in T1D may negatively impact nerve fiber and vessel functioning, and there may be a conserved link between dysglycemia and neurovascular architecture. NOD mice have reduced intra-islet sympathetic nerves that are directly proportional to the degree of insulitis and a reduction in glucagon responses to insulin-induced hyperglycemia[218]. Similar to NOD mice, BB rats had a loss of islet sympathetic nerve fibers and impaired glucagon secretion[219,220]. Interestingly, if one corrects CNS defects in diabetic animals with severe β cell loss, glucagon responses are restored[218,221]. A study of T1D donors with disease duration from 0-16 years also demonstrated decreased vessel diameter and increased vessel density in T1D tissue[222].

Isolated human T1D islets have reduced glucagon secretion dynamics[223,224]. Additionally, dysregulated α cell gene expression is not corrected by returning to an *in vivo* normoglycemic murine environment[223]. α cell identity and functionally important genes are also downregulated in T1D with increased expression of stress response factors and cell-to-cell contact proteins. Thus, altered expression of transcription factors likely leads to reduced α cell glucagon production and disrupted electrical activity which works in tandem to impair glucagon secretion[223,224]. Given that the hypoglycemic glucagon response diminishes with increasing T1D disease durations and T1D heterogeneity, it is imperative to study a larger cohort with wider disease durations as was done in this Dissertation to better understand whether this hypothesis can be aptly attributed to T1D glucagon secretion deficiencies.

Proposed hypotheses for defective glucagon response in T1D

The disruptions of counterregulatory glucagon responses in T1D are hypothesized to result from these defects:

1) Loss of sympathetic nerve fiber inputs to α cells may contribute to T1D glucagon deficiencies.
2) α cell-intrinsic defects may contribute to disruptions in T1D glucagon secretion.
3) The loss of neighboring β cells leads to a reduction in paracrine signaling of insulin to α cells or δ cells.

These hypotheses are explored in **Chapters III** and **VII** of this Dissertation with a particular focus on alterations in pancreatic neurovascular architecture.

Aims and summary of Dissertation

The primary goal of the research included in this Dissertation is to advance our understanding of communication mechanisms in pancreatic islets that regulate islet physiology and pathophysiology seen in diabetes. Pancreatic islet cells have sophisticated cell-to-cell communication systems that depend on sensing activities from adjacent and distant cells to effectively carry out their homeostatic functions. The secretory activity of endocrine cells within the islet is significantly impacted by the loss of the communication pathways discussed in this Chapter and is implicated in the pathogenesis and pathophysiology of diabetes.

In this Dissertation, I explore a variety of unknowns concerning extra- and intra-islet communication networks. To accomplish these aims, I utilized and improved existing technologies while developing new experimental approaches as described in the methods section of this Dissertation (**Chapter II**).

Chapter III: Human pancreatic neurovascular architecture

- *Overarching questions*
  - What is the neurovascular architecture of human islet and acinar tissue?
  - How do nerve fibers and capillaries associate with pancreatic ECM?
  - Is the neurovascular architecture changed in the T1D pancreas?
- *Study outcomes*
  - To define morphological characteristics of capillaries and nerve fibers in islets and acinar tissue compartments, I analyzed neurovascular assembly across the largest cohort of T1D and normal individuals studied thus far. To determine if islet neurovascular arrangement is altered following beta cell loss in T1D, I compared pancreatic tissues from non-diabetic, recent-onset T1D (<10 years duration), and longstanding T1D donors (>10 years duration). Both islets and acinar tissue had greater capillary density in recent-onset T1D accompanied by overall greater islet nerve fiber density in recent-onset and longstanding T1D as visualized by a pan-neuronal marker. I did not detect changes in sympathetic axons in either T1D cohort. These results indicate that pancreatic capillaries and nerve fibers persist in T1D despite beta cell loss, suggesting that alpha cell secretory changes may be decoupled from neurovascular components.

Chapter IV: Development of a live cell imaging microperifusion platform

- *Overarching questions*
  - Can I co-register intracellular signaling dynamics with islet secretion?
  - Does islet intracellular Ca^{2+} and cAMP signaling correlate with insulin and glucagon secretion dynamics?

- *Study outcomes*
  - I report on the integrated live-cell imaging and microfluidic platform using primary human pseudoislets, which resemble native islets in morphology, composition, and function. Pseudoislets of controlled size are generated through the dispersion and reaggregation of primary human islet cells. While in a dispersed state, islet cell gene expression can be manipulated including the introduction of biosensors, cADDis, or Ca^{2+} biosensor, GCaMP6f. Once formed, pseudoislets expressing a genetically encoded biosensor in combination with confocal microscopy, and a microperifusion platform allow for synchronous assessment of fluorescent biosensor dynamics and alpha and beta cell hormone secretory profiles to provide more insight into cellular processes and function.

Chapter V: Role of NTPDase3 islet purinergic signaling and hormone secretion

- *Overarching questions*
  - What components of the purinergic system are present within islets?
  - Does β cell expressed NTPDase3 affect glucose homeostasis in mice?
  - What is the role of β cell-derived ATP in modulating insulin secretion in mice and human?
- *Study outcomes*
  - To define the cellular distribution of purinergic ecto-enzymes and nucleotide receptors in human islets, I used single-cell RNA sequencing (scRNA-seq) data. In addition to β cell NTPDase3 expression, a variety of ecto-enzymes and purinergic receptors were found to be expressed within the islet, exocrine, and accessory cells such as immune cells. To study the function of this purinergic system, I studied the effects of NTPDase3 in both mice and human. I observed diminished *in vivo* and *in vitro* insulin secretion in our tamoxifen-inducible *Entpd3* floxed mouse model (*MIP-CreER; Entpd3*$^{fl/fl}$). In human pseudoislets, shRNA knockdown of ENTPD3 resulted in the potentiation of insulin secretion mediated by the purinergic receptor P2Y1. These pseudoislet findings suggest that reducing the enzymatic breakdown of ATP by NTPDase3 in human islets results in an autocrine potentiation of insulin secretion mediated by P2Y1. Overall, these studies provide insight into how extracellular nucleotides and purinergic signaling mechanisms fine-tune human islet hormone secretion.

Chapter VI: Human GAD65 and bacterial GAD sequence homology implications for T1D pathogenesis

- *Overarching questions*
  - Do human GAD65 and bacterial GAD share sequence homology?

- Do important enzymatic motifs in bacterial GAD show similarities to human GAD65?
- Could sequence similarities between bacterial GAD and human GAD65 contribute to T1D pathogenesis?

- *Study outcomes*
  - I utilized *in silico* analyses to show that 25 GAD sequences from human gut bacterial sources show sequence and motif similarities to human β cell GAD65. Our motif analyses determined that most gut GAD sequences contain the pyroxical dependent decarboxylase (PDD) domain of human GAD65, which is important for its enzymatic activity. Additionally, I showed relevant motifs and T cell epitope overlaps with known human GAD65 T cell receptor epitopes, which may implicate the immune destruction of β cells. Thus, I propose a physiological hypothesis in which changes in the T1D gut microbiome result in a release of bacterial GAD, thus causing miseducation of the host immune system. Due to the notable similarities, I found between human and bacterial GAD, these deputized immune cells may then target human β cells leading to T1D development.

The studies in this Dissertation helped to elucidate the intricate neurovascular, purinergic, and immunological communication systems within the human pancreas. Additionally, I developed sophisticated microfluidic systems to better understand intracellular mechanisms dictating islet hormone secretion. The significance of these findings and future directions are presented in **Chapter VII**.

CHAPTER II: MATERIALS AND METHODS

Some methods in this chapter have been included in Bedi, Richardson, Jia et al., 2022[225], Richardson et al., 2023a[76], Richardson, Pettway, et al., 2023 (manuscript under review), and Richardson, et al., 2023b (manuscript in preparation).

Mouse models and human tissue

Mouse models

All animal studies described in this Dissertation were approved by the Institutional Animal Care and Use Committee at Vanderbilt University Medical Center, and animals were kept in facilities monitored by the Vanderbilt University Division of Animal Care on a 12-hour light / 12-hour dark schedule with unrestricted access to standard chow and water. Mouse models and their abbreviations are summarized in **Table 1**:

Table 1. Mouse Models

Abbreviation	MGI Nomenclature or Strain Name	References
Entpd3$^{fl/fl}$	*Entpd3*$^{fl/fl}$	Sandhu et al. (2021)[226]
MIP-CreER	Tg(Ins1-cre/ERT)1Lphi	Wicksteed et al. (2010)[227]
βΔEntpd3	MIP-CreER; *Entpd3*$^{fl/fl}$	N/A

Tamoxifen (TMX)-inducible β cell-specific *Entpd3* knockout mice (βΔEntpd3) were generated by crossing hemizygous MIP-CreER male mice and *Entpd3*$^{fl/fl}$ female mice, both on a C57BL/6 background[227]. Founder *Entpd3*$^{fl/fl}$ male mice were generously provided by Dr. Simon Robson of Beth Israel Deaconness Medical Center. In the *Entpd3*$^{fl/fl}$ mice, *loxP* sites are inserted flanking exon 3 of *Entpd*3. In this βΔEntpd3 model, the mouse *Ins1* promoter drives Cre recombinase expression specifically in pancreatic β cells. Upon exposure to TMX, the Cre recombinase translocates to the nucleus, excising *Entpd3* alleles through Cre-*loxP* recombination and subsequently preventing *Entpd3* expression in β cells.

Human specimens and pancreas procurement

The Vanderbilt University Institutional Review Board declared that studies on de-identified human pancreatic specimens do not qualify as human subject research. Additionally, all donors' families gave informed consent to use pancreatic tissue in research.

Pancreata from non-diabetic (N = 41) and T1D (N = 26) donors were obtained through partnerships with the International Institute for Advancement of Medicine (IIAM; https://iiam.org/), National Disease Research Interchange (NDRI; https://ndriresource.org/), Integrated Islet Distribution Program (IIDP; https://iidp.coh.org/), Alberta Diabetes Institute (ADI; https://www.ualberta.ca/alberta-diabetes/index.html), Human Pancreas Analysis Program (HPAP; https://hpap.pmacs.upenn.edu/) and network for Pancreatic Organ Donors with Diabetes (nPOD; **https://www.jdrfnpod.org/**), and local organ procurement organizations. Deidentified medical histories provided both information for T1D staging and clinical characteristics to correlate with generated data (**Figure 17**). See **Tables 2-4** for detailed donor characteristics.

Pancreata were processed in Pittsburgh by Dr. Rita Bottino (Allegheny Health System or Imagine Pharma) or the University of Pennsylvania HPAP program for both islet isolation and histological analysis as previously described[92,228,229]. Pancreata from non-diabetic and T1D donors were received within 18 hours from cross-clamp and maintained in cold preservation solution on ice until processing, as described previously[92]. The pancreas was then cleaned of connective tissue and fat, measured, and weighed. Multiple cross-sectional slices of the pancreas with 2-3 mm thickness were obtained from the head, body, and distal tail, further divided into quadrants, and processed into paraformaldehyde-fixed cryosections as described previously[92].

This study also used data from the Organ Procurement and Transplantation Network (OPTN) that was in part compiled from the Data Hub accessible to IIDP-affiliated investigators through the IIDP portal https://iidp.coh.org/secure/isletavail). The OPTN data system includes data on all donors, wait-listed candidates, and transplant recipients in the US, submitted by the members of the OPTN. The Health Resources and Services Administration (HRSA), U.S. Department of Health and Human Services, provides oversight to the activities of the OPTN contractor. UNOS has supplied the data reported here as the contractor for the OPTN. The interpretation and reporting of these data are the responsibility of the authors and in no way should be seen as an official policy of or interpretation by the OPTN or the U.S. Government.

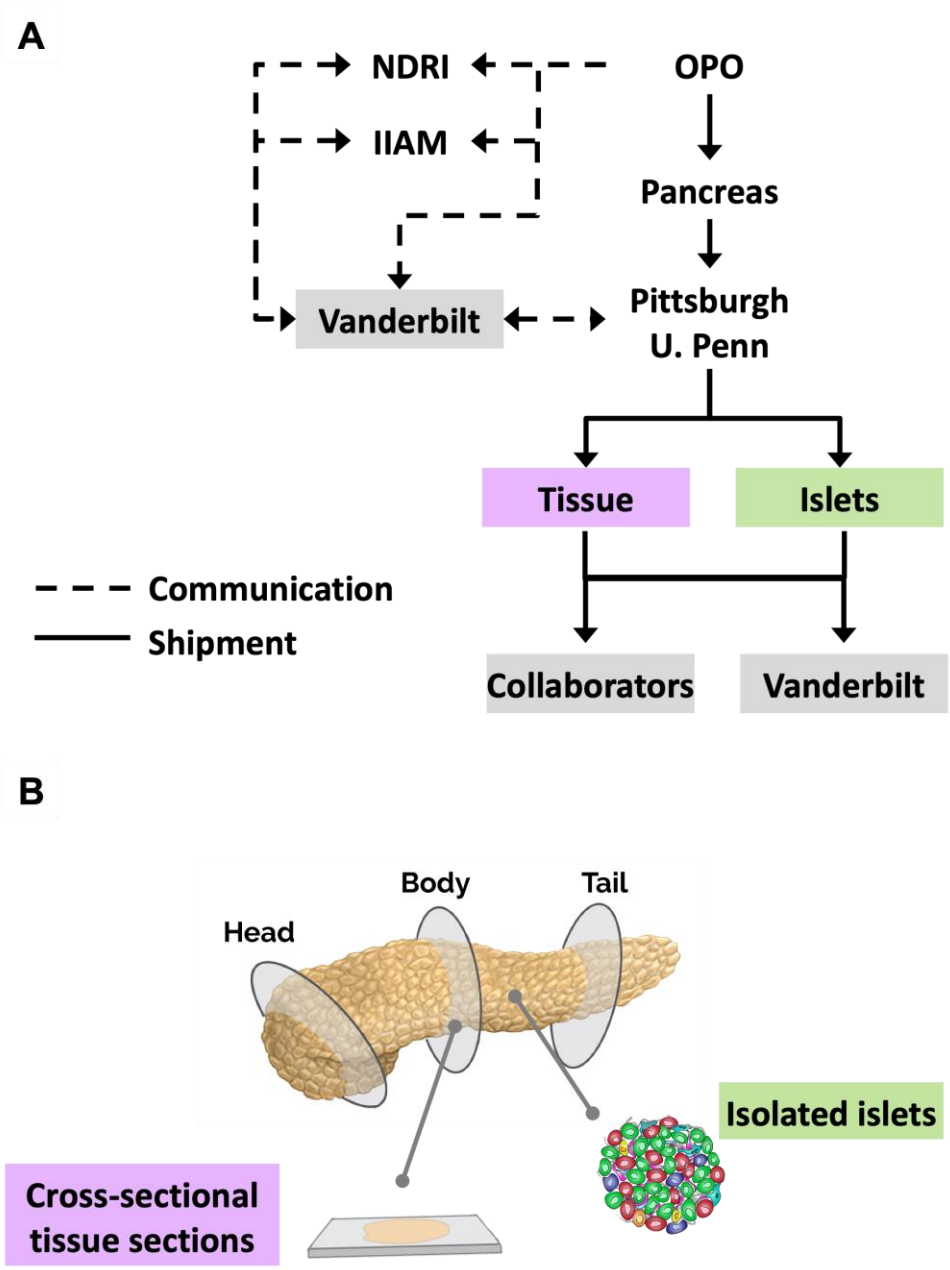

Figure 18. Infrastructure for the study of the human pancreas and islets. (A) The infrastructure established by the Powers & Brissova Research Group and colleagues to collect organ-donated quality tissue for analysis. (B) Tissue is obtained from all regions of the pancreas (Head, Body, and Tail). Isolated islets are also obtained from donor pancreata. We integrate histology and functional analyses with the clinical summary from the donor's redacted medical chart. Abbreviations: OPO – Organ Procurement Organizations; NDRI – National Disease Research Interchange; IIAM – International Institute for the Advancement of Medicine; U. Penn – University of Pennsylvania HPAP Programs.

Human islet isolation

Isolated human islets were obtained through partnerships with the IIDP (https://iidp.coh.org/), HPAP (https://hpap.pmacs.upenn.edu/), Dr. Rita Bottino's group (Alleghany Health Network & Imagine Pharma), or Prodo Laboratories. See **Tables 2-4** for detailed donor characteristics.

Human pancreata were processed for islet isolation by the above groups/organizations mentioned in the prior paragraph using an approach previously described[223]. Briefly, 18G or 22G catheters were inserted into the main pancreatic duct, and ducts were clamped to prevent leakage of collagenase solution during infusion. Collagenase solution consisting of DNase I (12000U/isolation, Worthington Biochemical Corporation), collagenase NB1 (1600 U/isolation, Crescent Chemical), neutral protease NB1 (200U/isolation, Crescent Chemical) was pre-warmed to 28°C and delivered intraductally using a Rajotte's perfusion system and then maintained at 37°C for approximately 20 minutes. The inflated tissue was then transferred to a Ricordi's chamber apparatus for combined mechanical and enzymatic digestion, which was maintained at 36°C for 5-15 minutes before warm and cold collection. The digest was incubated in cold RPMI media (Mediatech) supplemented with heat-inactivated 10% Fetal Calf Serum (Life Technologies) for 1 hour on ice. If post-digestion tissue pellet was larger than 2 mL and islets were distinguishable from exocrine tissue by dithizone staining (Sigma), a purification step consisting of density gradient (Biocoll, Cedarlane) centrifugation on a COBE 2991 Cell Processor (Gambro-Terumo) was used to separate islets from exocrine tissue. Islets were re-suspended in CMRL 1066 media (Mediatech) supplemented with 10% heat-inactivated Fetal Calf Serum (Life Technologies), 100 units/mL Penicillin/0.1mg/mL Streptomycin (Life Technologies), 2 mmol/L L-glutamine (Life Technologies). Islets were cultured for 12-24 hours and then shipped to Vanderbilt University for further analysis following shipping protocols developed by IIDP. Isolated islets were shipped overnight to Vanderbilt and plated into 15 ml of CMRL1066 media (5.5 mM glucose, 10% FBS, 1% Pen/Strep, 2 mM L-glutamine) in 5% CO2 at 37°C at a density of 10,000 –15,000 islet equivalent (IEQ) per 10-cm nontreated tissue culture dish (Corning). All human islet preparations were hand-picked in our laboratory before perifusion. Subsequent assays with isolated islets were set up within 48 hours of arrival.

Table 2. Demographic and phenotypic information of ND and T1D donors in Chapter III.

#	Donor ID	Age (years)	Disease State	T1D Duration (years)	Ethnicity/Race	Sex	BMI (kg/m²)	Cause of Death	AutoAb	C-peptide (ng/mL)	HbA1c (%)
1	DON4	10	Non-diabetic	N/A	Caucasian	M	19.3	Head Trauma	Negative	Not reported	Not reported
2	DON99	16	Non-diabetic	N/A	Caucasian	F	17.58	Head Trauma	Negative	6.55	Not reported
3	DON126	19	Non-diabetic	N/A	Caucasian	M	21.2	Anoxia	Negative	3.96	5
4	DON54	20	Non-diabetic	N/A	Hispanic or Latino	M	19.4	Head Trauma	Negative	11.73	5.6
5	DON65	24	Non-diabetic	N/A	Caucasian	M	35.54	Head Trauma	Negative	9.9	5.5
6	DON215	26	Non-diabetic	N/A	Caucasian	M	62.44	Anoxia	Negative	40.26	5.7
7	DON346	35	Non-diabetic	N/A	Caucasian	F	22.07	Head Trauma	Negative	Not reported	Not reported
8	DON246	42	Non-diabetic	N/A	Caucasian	M	32.2	Overdose	Negative	7.23	6
9	DON227	45	Non-diabetic	N/A	Caucasian	F	29.75	Anoxia	Negative	Not reported	5.6
10	DON204	52	Non-diabetic	N/A	Black	M	29.2	ICH	Negative	12.6	Not reported
11	DON61	55	Non-diabetic	N/A	Black	M	35.6	CVA/ICH	Negative	Not reported	Not reported
12	DON172	18	T1D Recent-Onset	2	Caucasian	F	25.03	Anoxia	IAA, GAD65	0.06	10.3
13	DON24	12	T1D Recent-Onset	3	Caucasian	F	26.6	Anoxia	mIAA	0.05	9.8
14	SAMN 19842600	12	T1D Recent-Onset	3	Caucasian	F	15.4	Anoxia, Asphyxiation	IAA, IA-2	0.06	9.8
15	SAMN 18741979	65	T1D Recent-Onset	4	Caucasian	F	42.62	Anoxia/Cardiovascular	Negative	N/D	5.9
16	DON71	13	T1D Recent-Onset	5	Caucasian	M	19.1	Anoxia	IA2A, mIAA	<0.02	Not reported
17	DON229	18	T1D Recent-Onset	5	Caucasian	M	21.2	Anoxia/Cardiovascular	Negative	0.09	12.4
18	SAMN 19763626	26	T1D Recent-Onset	5	Hispanic or Latino	M	16.4	Anoxia/Drug Intoxication (MVA)	Negative	N/D	9.8
19	SAMN 19776479	27	T1D Recent-Onset	6	Hispanic	M	25.03	Not reported	Negative	<0.02	10.2
20	SAMN 19776454	17	T1D Recent-Onset	7	Caucasian	F	21.35	Anoxia/DKA	IAA	<0.02	8.9
21	DON37	20	T1D Recent-Onset	7	Caucasian	M	25.5	Anoxia	IA2A	0.43	Not reported
22	SAMN 19776485	24	T1D Recent-Onset	7	Caucasian	M	28	DKA	GAD65, IA-2	N/D	10.4
23	SAMN 18741942	29	T1D Recent-Onset	7	Caucasian	M	22.04	Head Trauma	IAA	0.03	Not reported
24	SAMN 19842602	24	T1D Recent-Onset	8	Hispanic or Latino	M	25.9	Stroke	GAD65	0.17	8.2
25	DON97	19	T1D Recent-Onset	10	Caucasian	M	24.3	Anoxia	mIAA	0.02	Not reported
26	DON88	44	T1D Recent-Onset	10	Caucasian	M	24.43	Head Trauma	IAA, GAD65	<0.02	7.4
27	DON73	27	T1D Longstanding	17	Caucasian	M	18.5	Anoxia	Negative	<0.02	Not reported
28	DON131	24	T1D Longstanding	18	Caucasian	F	20.87	Anoxia/Drug Intoxication	Negative	N/D	11.3

29	DON63	30	T1D Longstanding	20	Caucasian	M	29.8	Anoxia	Negative	<0.02	Not reported
30	DON82	46	T1D Longstanding	20	Caucasian	F	29.8	CVA/ICH	Negative	1.78 *	Not reported
31	DON141	56	T1D Longstanding	25	Caucasian	M	33.34	Head Trauma	IAA	<0.02	7.6
32	DON19	58	T1D Longstanding	31	Caucasian	M	21.7	Anoxia	Negative	N/D	8.8
33	DON125	33	T1D Longstanding	32	Caucasian	M	30.8	Anoxia/Seizure	Negative	<0.02	7.9
34	DON34	42	T1D Longstanding	32	Caucasian	M	22.5	Head Trauma	Negative	N/D	Not reported
35	DON81	45	T1D Longstanding	43	Caucasian	M	25.06	Anoxia/Cardiovascular	IAA	<0.02	Not reported
36	DON58	63	T1D Longstanding	44	Caucasian	M	24.06	Anoxia/2nd Cardiovascular	IAA	<0.02	Not reported
37	DON109	57	T1D Longstanding	45	Black	M	33.35	Stroke	Negative	N/D	Not reported
38	DON23	62	T1D Longstanding	48	Caucasian	F	33.5	Stroke	IAA	<0.02	Not reported

Abbreviations: M, male; F, female; BMI, body mass index; AutoAb, Autoantibodies; mIAA, Insulin autoantibody; IA2 & IA2A, Autoantibody to the transmembrane protein of the protein tyrosine phosphatase family; GAD65, Autoantibody to Glutamic acid decarboxylase; N/D, non-detectable; HbA1c, Hemoglobin A1c. Asterisk (*) indicates a statistical outlier excluded when comparing recent-onset and longstanding T1D C-peptide levels.

Table 3. Demographic information of human pancreatic donors in Chapter IV.

#	Donor ID	Age	Ethnicity/ Race	Sex	BMI (kg/m^2)	Cause of Death	Tissue/Islet Source
1	DON470	19 years	Caucasian	M	29	Head Trauma	Imagine Pharma
2	DON486	55 years	Caucasian	M	35	Anoxia	Imagine Pharma
3	DON501	58 years	Caucasian	M	32	Anoxia	Prodo Laboratories
4	SAMN22562812	58 years	Hispanic	F	38	CVA	HPAPT2D
5	SAMN15579355	21 years	Hispanic	M	27.2	Head Trauma	IIDP
6	DON428	51 years	Caucasian	F	22	CVA	University of Pittsburgh
7	SAMN19842595	58 years	Black	F	31	CVA	HPAPT2D
8	SAMN19776477	19 years	Black	M	21	Anoxia	HPAPT2D

Abbreviations: N/A, not applicable; IIAM, International Institute for the Advancement of Medicine; CVD, Cardiovascular Disease; CVA, Cerebrovascular Accident; ICH, Intracerebral Hemorrhage; HPAPT1D or HPAPT2D, Human Phenotyping and Analysis Programs for T1D of T1D; IIDP, Integrated Islet Distribution Program.

Table 4. Demographic information of human pancreatic donors in Chapter V.

#	Donor ID	Age	Ethnicity/ Race	Sex	BMI (kg/m^2)	Cause of Death	Tissue/Islet Source
1	DON115	G18 weeks	N/A	N/A	N/A	Anencephaly	IIAM
2	DON196	2 months	Caucasian	F	19	Anoxia/CVD	IIAM
3	DON120	19 years	Caucasian	M	20	Head trauma	NDRI
4	DON61	55 years	Black	M	36	CVA/ICH	IIAM
5	SAMN22562814	49 years	Caucasian	F	36	Stroke	HPAPT2D Program
6	DON501	58 years	Caucasian	M	32	Anoxia	Prodo Laboratories
7	SAMN20923891	45 years	Caucasian	M	51	Head trauma	IIDP (Loyola)
8	SAMN22562815	4 years	Hispanic	M	21	Anoxia	HPAPT1D Program
9	SAMN25600001	51 years	Hispanic	F	28	Head trauma	HPAPT2D Program
10	SAMN26024925	31 years	Caucasian	M	36	Anoxia	HPAPT1D Program
11	DON517	49 years	Caucasian	M	34	Stroke	Imagine Pharma
12	SAMN25221445	52 years	Not reported	M	36	Not reported	Alberta
13	SAMN28088753	41 years	Hispanic	F	32	Not reported	HPAPT2D Program
14	DON470	19 years	Caucasian	M	29	Head trauma	Imagine Pharma
15	SAMN18614363	42 years	Caucasian	F	31	Stroke	IIDP (Scharp Lacy)
16	SAMN22562806	23 years	African American	F	34	Anoxia	HPAPT1D Program
17	SAMN22562808	54 years	African American	F	29	Anoxia	HPAPT2D Program
18	SAMN22562810	28 years	Hispanic	F	25	Stroke	HPAPT1D Program
19	SAMN28088755	51 years	Not reported	F	Not reported	Not reported	HPAPT2D Program
20	SAMN26419385	50 years	Not reported	F	24	Neurological	Alberta
21	DON513	26 years	Hispanic	F	30	Head trauma	Prodo Laboratories
22	DON512	40 years	Black	F	36	Head trauma	Prodo Laboratories
23	SAMN27022590	44 years	Caucasian	F	31	Stroke	Prodo Laboratories
24	SAMN31257358	19 years	Hispanic	F	18.1	Anoxia	HPAPT1D Program
25	SAMN31242270	52 years	Hispanic	M	37.5	Not reported	IIDP (SC)

Abbreviations: N/A, not applicable; IIAM, International Institute for the Advancement of Medicine; CVD, Cardiovascular Disease; CVA, Cerebrovascular Accident; ICH, Intracerebral Hemorrhage; HPAPT1D or HPAPT2D, Human Phenotyping and Analysis Programs for T1D of T1D; IIDP, Integrated Islet Distribution Program; SC, Southern California Islet Cell Resource Center.

Mouse-related methodologies

DNA extraction and genotyping

Mouse models used in our breeding schemes were maintained by genotyping using the primers and PCR conditions listed in **Table 5**. DNA was extracted, and PCR reactions were performed with tail snips from mice using the REDExtract-N-Amp Tissue PCR Kit (Sigma). Both DNA extraction and preparation of PCR reaction mixtures were performed according to the manufacturer's instructions. Primers (Jackson Laboratory & Sigma) were reconstituted in RNase/DNase-free water to 100 µM and further diluted 1:10 and then stored at -20°C for use in PCR reactions. Thermal cycler conditions listed in **Table 5** were used to amplify DNA before resolving on 2% agarose gel (E-gel EX 2% Invitrogen) in 1X Tris/Borate/EDTA (TBE) buffer.

Table 5. PCR primers and conditions for genotyping.

Mouse Model	Genotyping Primers	PCR Conditions	Expected Products
Entpd3$^{fl/fl}$	5' – CACCTCCTAAAAGCTGAGACTTATGT – 3' (foreword) 5' – GCTCCATAGTGAGACCCTGTCT – 3' (reverse)	95°C…3' 95°C…30' 60°C…60' 39 cycles 72°C…60' 72°C…X' 4°C…hold	125 bp for transgene (2% agarose)
MIP-CreER	5' – TTAATCCATATTGGCAGAACGAAAACG – 3' (foreword) 5' – CAGGCTAAGTGCCTTCTCTACA – 3' (reverse)	95°C…3' 95°C…30' 60°C…60' 39 cycles 72°C…60' 72°C…X' 4°C…hold	200 bp for transgene (2% agarose)

Compound preparation and administration

Entpd3 knockdown was induced in βΔEntpd3 mice by subcutaneous injection of 4 mg TMX (20 mg/mL; 200 µL) every 48 hours for a total of 3 doses over 5 days. TMX (20 mg/mL) was prepared fresh in filter-sterilized corn oil the day before each injection and allowed to dissolve overnight on a nurator at room temperature, protected from light. Vetbond tissue adhesive (3M) was used to seal injection sites to prevent oil leakage.

Glucose tolerance and stimulated in vivo insulin secretion

Glucose tolerance testing was performed after a 6-hour fast by administering 2 g/kg of filter-sterilized 10% D-glucose only or 500 mL intraperitoneal injection of a D-glucose (2g) + L-arginine (2g) PBS solution (16 mL)[164,230]. Blood plasma samples were drawn from the retroorbital space before injection (time 0 minutes) and 15 minutes after injection with heparinized blood collection tubes and immediately placed on ice. Blood plasma was separated as a supernatant after a 10-minute centrifugation at 13,000 rpm before being stored at -80°C. Plasma glucose was measured in whole blood from nicked tail veins before glucose injection (time 0 minutes) and at 15, 30, 60, 90, and 120 minutes after injection using an Accu-chek glucose meter (Roche Diagnostics) calibrated according to the manufacturer's instructions.

Mouse islet isolation

Mouse islets were isolated in collaboration with the Vanderbilt Islet Procurement and Isolation Core by intra-ductal infusion of 3 mL collagenase P (0.6 mg/mL; Roche Molecular Biochemicals) prepared in Hank's balanced salt solution (HBSS) as described[231,232]. Following injection, the inflated pancreas was removed and digested in 6.7 mL collagenase P (0.6 mg/mL in HBSS) for an additional 4-8 minutes on a wrist-action shaker at 37°C and 1-2 minutes by manual shaking at room temperature. Collagenase was inactivated by adding 7-8 mL cold 10% fetal bovine serum (FBS) in HBSS. Then pancreata were washed three times with 14 mL of 10% FBS/HBSS, centrifuging at 1000 rpm for 2 minutes at 4°C between washes to pellet the tissue. After the last wash, pancreatic tissue was resuspended in 10% FBS/HBSS and plated in Petri dishes on ice. Islets were hand-picked to near 100% purity in 10% FBS/HBSS with RNase-free pipette tips using an inverted microscope.

Mouse tissue collection and fixation

Mouse pancreata were collected from anesthetized mice prior to cervical dislocation. Organs were washed in ice-cold 10 mM phosphate-buffered saline (PBS), and fat and other excess tissue were removed before pancreata were in 0.1 M PBS containing 4% paraformaldehyde (Electron Microscopy Sciences) for 2-3 hours on ice with mild agitation, washed in four changes of 0.1 M PBS over 2 hours, and equilibrated in 30% sucrose/0.01 M PBS overnight. After blotting to remove excess sucrose, tissues were mounted in Tissue Tek cryomolds filled with Tissue-Plus Optimal Cutting Temperature (OCT) compound (VWR Scientific Products). Tissue molds were placed on dry ice until the OCT was set, then stored at -80°C. Tissues were sectioned from 5-10 μm thick on a Leica

CM1950 cryostat (Leica), and these cryosections were attached to Superfrost Plus Gold slides (Thermo Fisher Scientific).

Human specimen-related methodologies

Fluorescence-Activated Cell Sorting (FACS) of human β and α cells

Human β and α cell sorting was performed in collaboration with the Vanderbilt Flow Cytometry Core. Human islets were dispersed using a modified protocol as described previously[233]. Briefly, 0.025% trypsin was used to disperse cells and reaction was quenched with modified RPMI medium (10% FBS, 1% Penn/Strep, 5 mM glucose). Cells were washed in the same medium and counted on a hemocytometer, then transferred to FACS buffer (2 mM EDTA, 2% FBS, 1X PBS). Indirect antibody labeling was completed via two sequential incubation periods at 4°C, with one wash in FACS buffer following each incubation. Primary and secondary antibodies, listed in **Tables 6 and 7**, have been characterized previously and used to isolate high-quality RNA from β and α cells[151,234–236]. Appropriate single color compensation controls were run alongside samples. Prior to sorting, propidium iodide (0.05 ug/100,000 cells; BD Biosciences) was added to samples for non-viable cell exclusion. Flow analysis was performed using an LSRFortessa cell analyzer (BD Biosciences), and a FACSAria III cell sorter (BD Biosciences) was used for FACS. Sorted islet cells then underwent the pseudoislet protocol described below.

Pseudoislet formation and adenovirus transduction

Pseudoislets were formed as previously described[32]. Briefly, non-diabetic human islets were hand-picked to purity and then dispersed with 0.025% HyClone trypsin (Thermo Scientific) for 7 minutes at room temperature before counting with an automated Countess II cell counter or manually by hemacytometer. Dispersed human islets were incubated in adenovirus at a multiplicity of infection of 250 (biosensors), 500 (biosensors or shRNA), or 1000 (shRNA) for 2 hours in Vanderbilt pseudoislet media before being spun and washed. Cells were then resuspended in the appropriate volume of Vanderbilt pseudoislet media to allow for seeding into wells at 2000 cells per 200 µL each well of CellCarrier Spheroid Ultra-low attachment microplates (PerkinElmer). Pseudoislets were allowed to reaggregate for 6 days before being harvested and studied.

Viral vectors

Adenovirus containing U6-driven scramble or ENTPD3 targeted shRNA and CMV-driven mCherry or PGK-driven mKate2 red fluorescent tag were prepared, amplified, and purified by Welgen, Inc. (Worcester, MA). Viral titers were determined by Welgen, Inc. via

plaque assay. The fluorescent biosensors, Adenovirus-CMV-GCaMP6f (Catalog #1910, Malvern, PA) and Adenovirus-CMV-cADDis (Welgen, Inc.), were utilized to monitor intracellular Ca^{2+} and cAMP signaling.

RNA isolations and cDNA synthesis for quantitative RT-PCR

To assess knockdown, RNA was extracted from pseudoislets using an RNAqueous RNA isolation kit (Ambion). RNA quality control and quantity assessment (QC/QA) was performed by the Vanderbilt Technologies for Advanced Genomics (VANTAGE) using a Bioanalyzer instrument. cDNA was synthesized using High-Capacity cDNA Reverse Transcription Kit (Applied Biosystems, 4368814) according to the manufacturer's instructions. Quantitative PCR (qPCR) was performed in collaboration with Dr. Chunhua Dai using TaqMan assays and reagents from Applied Biosystems (Foster City, CA). Quantitative PCR (qPCR) was performed using TaqMan probes for ACTB (Hs99999903_m1) as endogenous control and ENTPD3 (Hs00154325_m1). Relative changes in mRNA expression were calculated by the comparative ΔCt method using Applied Biosystems Stepone Plus System.

Assessment of extracellular ATP and hormone secretion by static incubation

Primary islets or pseudoislets were loaded into well inserts (12.0 µm, Millicell), placed into a 12-well plate (Corning), and allowed to equilibrate for 30 minutes in 200 µL 1.7 mM glucose or 1 mL 5.6 mM glucose. Well inserts with primary islets or pseudoislets were transferred between wells into media containing stimuli of interest for 60 minutes per condition. Stimuli included: 1.7 mM glucose or 16.7 mM glucose + 100 µM 3-isobutyl-1-methyl-xanthine (IBMX, Sigma) with or without a non-specific NTPDase3 inhibitor, ARL67156 (Tocris). Primary islets or pseudoislets were incubated in a total of 200 µL media for ATP measurements. After each stimulus, the supernatant was collected, assessed for extracellular ATP, and stored at -80°C for subsequent hormone analyses. Extracellular ATP was measured with ENLITEN bioluminescence assays (Promega). Insulin levels and glucagon levels were assessed from the stored supernatant as previously reported[145,223]. ATP and hormone secretion were normalized per IEQ.

Islet perifusion

Assessment of mouse islet and human pseudoislet function by macroperifusion

Macroperifusions were performed either by Powers and Brissova Research Group or Vanderbilt's Islet Procurement and Analysis Core. The function of mouse islets and human pseudoislets was studied in a dynamic cell perifusion system at a perifusate flow

rate of 1 mL/min[237]. The effluent was collected at 3-minute intervals using an automatic fraction collector, and then islets were retrieved and lysed with an acid ethanol solution to extract. Insulin concentrations in each perifusion fraction and total hormone content were assessed by enzyme-linked immunosorbent assay (ELISA; Mercodia). Insulin and glucagon secretion was normalized per IEQ or hormone content. Area under the curve (AUC) above baseline hormone release was calculated with the trapezoidal method in GraphPad Prism 8.0-9.3 as previously described[32].

Assessment of pseudoislet function by live cell imaging microperifusion

The microperifusion platform is based on a previously published microfluidic device with modifications[32,238]. The microperifusion apparatus was contained in a temperature-controlled incubator (37°C) fitted to an FV3000 laser-scanning confocal microscope (Olympus). Pseudoislets (~25 IEQs/chamber) were loaded into a prewetted well, imaged with a stereomicroscope to determine loaded IEQ, and perifused at 100 µL/ min flow rate with DMEM buffer at 37°C. Perifusion fractions were collected using a fraction collector (Bio-Rad) at 2-minute intervals following a 20-minute equilibration period of 2 mM glucose and various stimuli which included: 16.7 mM glucose, 16.7 mM glucose + 100 µM 3-isobutyl-1-methyl-xanthine (IBMX, Sigma), and 1 µM P2Y1 antagonist (MRS2500; Tocris). Fractions were then analyzed for insulin and glucagon concentration. Insulin and glucagon secretion was normalized per IEQ or hormone content.

GCaMP6f or cADDis biosensors were excited at 488 nm, and fluorescence emission was detected at 493–574 nm. Images were acquired at 15 µm depth every 2 seconds using an Olympus UPLFLB 20X/0.50 objective. Image analysis was performed with cellSens software (Olympus). Pseudoislets in the field of view (3–10 pseudoislets/field) were annotated using the region-of-interest tool. The GCaMP6f or cADDis fluorescence intensity recorded for each time point was measured across annotated pseudoislet regions and normalized to the baseline fluorescence intensity acquired over the 2 mM glucose period before stimulation.

Insulin and glucagon hormone assays

Insulin and glucagon hormone assays were selected based on current protocols of the Islet Procurement and Analysis core (https://www.vumc.org/vdrc/cores-ipa). Insulin and glucagon were measured by radioimmunoassay (RIA) (human insulin, RI-13K, Millipore; glucagon, GL-32K, Millipore), enzyme-linked immunosorbent assay (ELISA) (human insulin, 10-1132-01, Mercodia or 80-ISNHU-E01.1, Alpco; mouse insulin, glucagon, 80-INSMSU-E01, Alpco; 10-1281-01, Mercodia), or Homogeneous Time Resolved Fluorescence (HTRF) assay (glucagon, 62CGLPEH, Cisbio).

Immunohistochemistry, imaging, and analyses

Islet tissue embedding

Primary islets (mouse and human) and human pseudoislets were embedded in collagen gels as previously described[162,223]. Collagen-embedded primary islets and pseudoislets were processed in PBS containing 4% paraformaldehyde (Electron Microscopy Sciences) for 1.5 hours on ice with mild agitation, washed in three changes of PBS over 2 hours, and equilibrated in 30% sucrose/PBS overnight as previously described[92]. After blotting to remove excess sucrose, tissues were mounted in Tissue Tek cryomolds filled with Tissue-Plus Optimal Cutting Temperature (OCT) compound (VWR Scientific Products). Tissue molds were placed on dry ice until the OCT was set and then stored at -80°C. Tissues were sectioned to 8 µm thick on a CM1950 cryostat (Leica) and these cryosections were attached to Superfrost Plus Gold slides (Thermo Fisher Scientific) for further immunohistochemical analyses.

Immunohistochemistry of pancreatic tissue, primary islets, and pseudoislets

Cryosections were air dried and then either post-fixed with 1% paraformaldehyde in 10 mM PBS for 10 minutes before permeabilization or immediately permeabilized in 0.2% Triton-X in 10 nM PBS. After permeabilization, sections were washed three times in 10 nM PBS for 3-5 minutes per wash. Cryosections were then blocked in 5% normal donkey serum in 10 mM PBS for 60-90 minutes in a humidified chamber at room temperature. Cryosections were incubated overnight with primary antibodies (**Table 6**) diluted in antibody buffer (0.1% Triton-X, 1% BSA in 10 nM PBS) in a humidified chamber at 4°C, then washed three times in 10mM PBS for 10 minutes per each. Cryosections were then incubated with secondary antibodies (**Table 7**) prepared in antibody buffer for 90 minutes in a humidified chamber protected from light, at room temperature. Sections were then treated with 4′,6-diamidino-2-phenylindole or DAPI to visualize nuclei (5 mg/mL stock diluted 1:50,000 in 10mM PBS) for 10 minutes and then washed three times in 10 mM PBS for 15 minutes per wash. Slides were mounted using SlowFade Gold antifade reagent (Invitrogen Molecular Probes) and sealed with fingernail polish prior to imaging.

For neurovascular architecture studies, multiple 10 µm and 30 µm serial cryosections from the pancreatic head, body, and tail regions of 27 T1D and 11 age-matched non-diabetic donors were lightly paraformaldehyde-postfixed and then labeled for immunofluorescence as described previously and above[223,239]. Primary and secondary antibodies and their working dilutions are listed in **Table 6** and **Table 7**, respectively. Acinar tissue was visualized by DAPI nuclear counterstain, and islet location was defined by hormone markers. Insulin and glucagon were visualized on the same channel.

Table 6. Primary antibodies for immunohistochemistry

Antigen	Marker	Species	Dilution	Source	Catalog #
Hormones					
Glucagon (GCG)	α cells	Mouse	1:500	Abcam	ab10988
Glucagon (GCG)	α cells	Rabbit	1:100	Cell signaling	2760s
Insulin (INS)	β cells	Guinea Pig	1:2000	Dako	A0564
Insulin (INS)	β cells	Guinea Pig	1:1000	Fitzgerald Industries International	20-IP3
C-peptide (CPEP)	β cells	Rat	1:200	DSHB	GN-ID4
Somatostatin (SST)	δ cells	Goat	1:500	Santa Cruz	Sc-7819
Somatostatin (SST)	δ cells	Rat	1:500	Abcam	Ab35788
Nerve fibers					
Tubulin beta 3 (TUBB3)	Pan-neuronal	Rabbit	1:20000	BioLegend	802001
Synapsin-1, -2 (SYN)	Pan-neuronal	Rabbit	1:2000	Synaptic Systems	106003
Tyrosine Hydroxylase (TH)	Sympathetic nerve fibers	Rabbit	1:2000	Abcam	ab6211
Capillaries					
Caveolin 1 (CAV1)	Capillaries	Rabbit	1:500	Abcam	ab2910
Platelet endothelial cell adhesion molecule (PECAM-1) – anti-human	Capillaries	Mouse	1:100	BD Biosciences	BD550389
PECAM-1 – anti-mouse	Capillaries	Rat	1:50	BD Biosciences	BD550274
Extracellular Matrix (ECM)					
Collagen IV alpha1 (COLIV)	ECM	Goat	1:1000	Novus	NBP1-26549
NTPDase3					
NTPDase3 – anti-mouse	NTPDase3	Sheep	1:5000	R & D Systems	AF4464

NTPDase3 – anti-human	NTPDase3	Mouse	1:50	http://ectonucleotidases-ab.com and Vanderbilt Antibody and Protein Resource	hN3-B3S and hN3-H10S
Biosensors					
GFP	GCaMPf or cADDis	Chicken	1:500	Abcam	ab13970
RFP	mCherry or mKate2	Goat	1:500	MyBioSource	MBS448092
FACS sorting					
HIC0-4F9 [Biotin] (HPi1)	Pan-endcrine marker	Mouse (IgG)	1:50	Novus	NBP1-18872B
HIC3-2D12 (HPa3)	α cells	Mouse (IgM)	1:100	Dr. Streeter Laboratory	N/A
NTPDase3	β cells	Mouse (IgG)	1:100	Dr. Sévigny Laboratory	N/A

Table 7. Secondary antibodies for immunohistochemistry

Host Species	Primary Ab Species	Fluorophore	Dilution	Source	Catalog #
Donkey	Chicken	Cy2	1:500	Jackson Immunoresearch	703-225-155
Donkey	Goat	Cy2	1:500	Jackson Immunoresearch	705-225-147
		Cy3	1:500	Jackson Immunoresearch	705-165-147
		Cy5	1:500	Jackson Immunoresearch	705-175-147
Donkey	Guinea Pig	Cy2	1:500	Jackson Immunoresearch	706-225-148
		Cy5	1:200	Jackson Immunoresearch	706-175-148
Donkey	Rabbit	Cy3	1:500	Jackson Immunoresearch	711-165-152
		Cy5	1:200	Jackson Immunoresearch	711-175-152
Donkey	Rat	Cy5	1:500	Jackson Immunoresearch	712-175-153
Donkey	Mouse	Cy2	1:200	Jackson Immunoresearch	715-225-151
		Cy3	1:500	Jackson Immunoresearch	715-165-151
		Cy5	1:200	Jackson Immunoresearch	715-175-151
Donkey	Sheep	Cy3	1:500	Jackson Immunoresearch	713-165-147
Goat	Mouse (IgM)	PE	1:1000	Jackson Immunoresearch	115-116-075
	Mouse (IgG)	APC	1:500	BD Pharmingen	550826
---	BV421-Strep	---	1:500	BD Pharmingen	563259

Image acquisition and processing

Digital images were acquired with a Zeiss LSM880 laser scanning confocal microscope (Carl Zeiss), FV3000 (Olympus) laser scanning confocal microscope, a Leica DMI6000B fluorescence microscope equipped with a Leica DFC360FX digital camera (Leica), a BX41 fluorescence microscope (Olympus), or Fluorescent ScanScope (Aperio).

All confocal images in **Chapter III** underwent deconvolution and were then displayed as maximum-intensity projections. Nearest neighbor-constrained iterative algorithms were employed with the cellSens v3.1 (Olympus). Z-Stack and 3D reconstruction videos were made using cellSens, Imaris v9.8 (Oxford Instruments), or ImageJ software and exported as mp4 files.

Morphometric analysis of pancreatic neurovascular architecture 2-D images

Digital images of 10 µm cryosections in **Chapter III** were acquired with a ScanScope FL (Aperio) for human tissue and a Leica DMI6000 B Microscope (Leica Biosystems) for mouse tissue. These images were then analyzed using MetaMorph v 7.10 software (Molecular Devices LLC). Analyses were run on manually annotated islets (region of interest, ROI) identified by hormone staining. Three equally sized ROIs, outside of islet annotations, were randomly selected per image for acinar measurements. Intensity thresholding was set per individual fluorescence channel to collect object data using the Integrated Morphometry Analysis function (MetaMorph).

For innervation measurements in **Chapter III**, a pixel filter was set to ≥ 0.463 µm to avoid the inclusion of single pixels as neural fibers. Large nerve fiber bundles around pancreatic ducts and pancreatic ganglia were excluded from formal analyses. A pixel filter was set to ≥ 2.000 µm for vasculature analysis to prevent the inclusion of single pixels and non-vascular structures. Islet and acinar nerve fiber length, nerve fiber density, and vascular density were calculated by dividing MetaMorph output with the total ROI area. The analyzed islet area was similar between groups (**Figure 26**). We analyzed an average of 34 ± 1 islets with a cross-sectional diameter > 50 µm / donor / condition. For a donor to be included in aggregate analyses, a minimum of 10 islets needed to be assessed. Detailed metrics can be found in respective figure legends.

Analysis of neuronal and ECM colocalization

Digital images of 30 µm sections were acquired with Zeiss LSM880 (Zeiss Microscopy Ltd) or Olympus FV3000 (Olympus) microscopes. Z-stacks were assembled to generate 3D reconstructions and max intensity projections with cellSens (Olympus) and ZEN (Zeiss) software. To quantify colocalization between the pan-neuronal marker (TUBB3) and ECM marker (COLIV), we used Mander's coefficients generated from the ImageJ plugin "Just Another Co-localization Plugin" (https://imagej.nih.gov/ij/plugins/track/jacop2.html).

Cytonuclear analysis of transduced pseudoislets

Digital images of individual primary islets and pseudoislets were acquired at 20X with 2X zoom using an FV3000 confocal laser scanning microscope (Olympus). Cytonuclear algorithms (HighPlex FL v3.2.1 or Cytonuclear v3) via HALO software (Indica Labs) were used to determine primary islet and pseudoislet endocrine cell proportion (β, α, δ), pseudoislet transduction efficiency (reporter-positive β and α cells), or NTPDase3 knockout efficiency in mouse islets (NTPDase3+ cells).

In silico **analyses**

RNA-sequencing for mouse versus human transcriptomic profile comparison

Previously published data was queried to determine general expression profiles of angiogenic, neuronal, morphogenic pathways, extracellular matrix, and purinergic components in mouse and human islet cells. Gene lists were compiled by authors based on previous publications[50,230,240,241] and HGNC-curated gene group pages[242]. Normalized count matrices were accessed from bulk RNA-seq datasets as follows: mouse β and endothelial cells, GSE163825[230]; human endothelial cells, GSE157546[243]; human β cells[244]; fetal and adult human α and β cells, GSE67543[245]. Raw single-cell (sc) datasets were accessed as follows: mouse, GSE159844 [246]; mouse embryonic and postnatal time points, GSE87375[247]; human, GSE183568[248]. See **Chapter III** for information on experimental parameters, sample sizes, and specific samples utilized.

For sc mouse dataset in **Chapter III**, wild-type samples were processed and visualized by uniform manifold alignment projection (UMAP) using 30 PCA dimensions, and KNN-based clustering was performed with a resolution of 0.5 in Seurat[249] yielding 18 clusters. A total of 6 clusters were removed based on strong expression of exocrine markers or mixed cell type assignment, then further clustering of remaining cells (30 dimensions at resolution = 1) yielded 21 clusters. Cell-type assignment was determined using canonical

markers (**Table 8**) for endocrine, endothelial, and immune cell populations, and multiple clusters expressing the same canonical markers were combined as applicable. Stellate cells could not be resolved from endothelial cells in this dataset. For sc human dataset, clustering was performed as previously described[248], with technical replicates combined and donor values averaged. In **Figure 23**, for clarity, only gene expressed in >2% of cells in cell types were kept (sc), and log2 expression >8 (bulk) was graphed. All values will be provided in a data file upon publication.

Table 8. RNA-sequencing data utilized for transcriptomic comparison

Cell type(s)	Species	Method	Cell type identification	n	Samples	Reference
Endothelial	Mouse	Bulk RNA-seq	$CD31^+$ $CD11b^-$	4	GSM: 4987986, 4987987, 4987988, 4987989	Saunders et al., 2021 (GSE163825)
β			GFP*	4	GSM: 4987982, 4987983, 4987984, 4987985	
Endothelial	Human		$CD31^+$ $CD34^+$	8	GSM: 4769751, 4769754, 4769757, 4769760, 4769763, 4769766, 4769769, 4769775	Jonsson et al., 2020 (GSE157546)
β			$HPi1^+$ $CD39L3^+$	15	Non-diabetic	Walker et al., 2021
α, β, δ, γ, endothelial, immune	Mouse	scRNA-seq	Unsupervised clustering, marker genes^	2	GSM: 484825, 4848255	Erener et al., 2021 (GSE159844)
α, β, δ, γ, endothelial, immune, stellate	Human			5	GSM: 5560782, 5560783, 5560784, 5560785, 5560786, 5560787, 5560788, 5560789, 5560790, 5560791, 5560792, 5560793, 5560794, 5560795	Shrestha et al., 2021 (GSE183568)

* Transgenic mouse line *MIP-GFP* enabled isolation of β cells by GFP.
^ Marker genes: *GCG* (α), *INS* (β), *SST* (δ), *PPY* (γ), *PECAM1* (endothelial), *HLA-DRA* or *H2-Eb1* (immune), *PDGFRB* (stellate).

GAD sequence and T cell receptor epitope curation

Twenty-five bacterial GAD proteins from species of interest, including mice, chimpanzee, and human GAD65 sequences, were curated from the NCBI genes database[250]. The bacterial species were chosen by considering their association with the gut microbiome, their significance in the gut microbiome alterations seen in T1D patients, human-related pathogen status, and non-human-related environmental species. GAD65 T cell receptor epitopes were curated from a literature review[250].

All GAD sequences in bacteria and the three mammalian species under consideration were obtained by performing a BLASTP search, with human GAD65 as the query sequence. Furthermore, only those sequences with significant e and p values were well annotated on the NCBI database and/or RefSeq and were identified as GAD proteins were considered. All other hits, including unnamed protein products, were ignored.

Multiple sequence alignment and motif identification

Multiple sequence alignment was performed using ClustalW (Ver. 1.2.2) with a gap opening penalty of 10 and a gap extension penalty of 0.2[251]. The resulting alignment is visualized and annotated with CLC Sequence Viewer (Ver. 8.0) to highlight conservation and amino acid properties. Identification of ungapped motifs was done using the MEME tool (Ver. 5.4.1) under the MEME suite tools for motif discovery and enrichment[252]. The output consisted of 10 motifs, shared by various (not necessarily all) organisms into consideration. The motifs identified for each organism were then ordered based on the phylogenetic tree constructed for the sequences under consideration, using the Simple Phylogeny Tool (https://www.ebi.ac.uk/Tools/phylogeny/simple_phylogeny/). The phylogenetic tree was re-rooted at Homo sapiens using iTol, and the resulting tree was exported locally (**https://itol.embl.de/**). Subsequently, each motif was run against protein families, using a Pfam (Ver 33.1) search. The Motifs identified by MEME were mapped against the query sequences using MAST(Ver. 5.4.1) to obtain the coordinates of motifs in each gad sequence[252].

Logo plot & T cell receptor epitopes

The multiple sequence alignment obtained was converted into a logo plot using Weblogo (Ver 2.8.2)[253]. Here, each logo consists of a stack of symbols, and each symbol's height is indicative of the amino acid conservation at a particular location. All motifs and T cell receptor epitope coordinates, obtained in the previous steps, were marked on the logo plot. The plot was then trimmed, with a special emphasis on regions with high overlap between motifs and T cell receptor epitopes.

Statistical analysis

Statistical tests are described in the figure legends and text where appropriate. Data is represented as mean ± standard error (SEM), with each mouse or donor considered as N = 1. Outliers were determined and excluded from analyses using the Robust regression and Outlier removal (ROUT) method with Q = 1%. P-values < 0.05 were considered significant and non-significant p-values are designated with “ns” or not denoted. Statistical comparisons were performed using GraphPad Prism software 8.0-9.3 and R version 4.1.2.

CHAPTER III: HUMAN PANCREATIC CAPILLARIES AND NERVE FIBERS PERSIST IN TYPE 1 DIABETES DESPITE β CELL LOSS

Text and data in this chapter have been published in Richardson et al. (2023). *American Journal of Physiology – Endocrinology and Metabolism*[76].

Introduction

Hormone secretion from pancreatic islets of Langerhans is essential to maintain blood glucose levels within a narrow physiological range. Vascular and neuronal inputs to the islet aid in the regulation of coordinated hormone secretion[2,58,67,78,254]. α cells within the islet secrete glucagon to counterbalance insulin secretion by β cells and prevent hypoglycemia. In type 1 diabetes (T1D), α cell function is dysregulated with loss of glucagon secretion in response to hypoglycemia[210,255], which interestingly precedes a secretory impairment of major α cell stimulus, epinephrine, produced by adrenal chromaffin cells[210]. Paradoxically, individuals with T1D secrete more glucagon during mixed-meal stimulation[256,257]. Recurrent hypoglycemic episodes, which correlate with progressive β cell loss in T1D, lead to an impairment of sympathoadrenal responses and the risk of a life-threatening hypoglycemia unawareness syndrome, also known as hypoglycemia-associated autonomic failure[258]. Additionally, autonomic dysfunction could be further exacerbated with disease duration, and progressive diabetic neuropathy may affect autonomic innervation of the pancreatic islet[2,210,256,259]. Thus, defining the neurovascular architecture in the pancreas of individuals with T1D is crucial to understanding the mechanisms of dysregulated glucagon secretion.

Studies from rodent and human T1D pancreatic tissues provide a spectrum of inferences on disease-associated intra-islet innervation phenotypes. Work first done in rodent models of T1D, such as the BioBreeder (BB) rat and nonobese diabetic (NOD) mouse, showed a loss of intra-islet sympathetic nerve fibers associated with insulitis and decreased glucagon secretion in response to tyramine-mediated norepinephrine release[218,220,221,260,261]. By contrast, a recent study used optically cleared tissue from NOD mice to show an increase in islet nerve fibers[262]. Other studies, however, revealed considerable inter-species differences in intra-islet nerve fiber and capillary densities, thus raising concerns about whether the data from rodent models reflect the findings about human islet neurovascular architecture in T1D[54,74,75,263]. Moreover, two recent studies of human pancreatic sympathetic innervation in short-duration T1D reached opposing conclusions as well; one study indicated an early decline in islet sympathetic nerve density in T1D[264], while the other one showed no significant differences between non-diabetic and short-duration T1D donor islets[265]. Interestingly, the latter study found that pancreata from autoantibody-positive (AAb+) human donors had lower sympathetic

nerve fiber density, specifically within pancreatic islets[265]. In addition, Lundberg et al. showed that the second arm of the autonomic nervous system, parasympathetic nerve fibers, may also be altered in human T1D[266]. Considering the developmental and functional links between vascularization and innervation[50,84,267], it is noteworthy that islet vessel density was found to be greater in short-duration T1D than in non-diabetic donors[222].

Thus, there is a need to systematically define changes in the human neurovascular architecture across a broader range of T1D duration and large cohort, including not only islet but also acinar tissue compartment, since both appear to be influenced in the disease process[268,269]. Because innervation has been studied extensively in rodent T1D models, we first compared the islet neurovascular architecture between mouse and human. We found dramatic inter-species differences that were not easily explained by transcriptomic profiles of factors guiding angiogenesis and neuronal development. Next, we performed high throughput morphometric analyses of the islet neurovascular architecture in thin human pancreatic tissue sections from a large cohort of bio-banked tissues, including 15 recent-onset and 12 longstanding T1D donors, and compared them to 11 non-diabetic controls. We found that islets and acinar tissue had greater capillary density in recent-onset T1D. This was accompanied by overall increases in islet nerve fiber densities visualized by a pan-neuronal marker in both early-onset and longstanding T1D. We did not detect changes in sympathetic axon densities in T1D tissues. Further assessment of 3D reconstructions from thicker sections (30 μm versus 10 μm) highlighted the persistence of intra-islet nerves in T1D donors and a relationship between pancreatic nerves, blood vessels, and extracellular matrix (ECM). Collectively, our data indicate that islet capillaries and nerve fibers persist in T1D, suggesting that α cell secretory changes may be decoupled from neurovascular components.

Results

Neurovascular architecture of pancreatic islets and acinar tissue differs significantly between mouse and human

To better understand prior reports of inter-species differences in neurovascular architecture, we first defined the neurovascular architecture in non-diabetic mouse pancreas, focusing on both islets and acinar tissue, and compared it to human. Blood vessels were visualized by immunofluorescence labeling for platelet endothelial cell adhesion molecule 1 (PECAM-1), nerve fibers were labeled for pan-neuronal marker tubulin beta 3 (TUBB3), and islet β and α cells were co-labeled for insulin (INS) and glucagon (GCG), respectively. To confirm TUBB3 immunolabeling of nerve fibers in human tissue, we assessed 30 laser-scanning confocal microscopy images where individual image tiles (captured at 10X magnification) were stitched to visualize the entire

pancreatic tissue sections. Additionally, we reviewed over 1,000 whole-slide images (captured at 20X magnification) that were used for our high-throughput morphometric analyses. We found many TUBB3+ inter-lobular nerve fiber bundles throughout our tissues demonstrating the utility of this neuronal marker (**Figure 19**). We then utilized morphometric analyses to measure capillary and nerve fiber structural characteristics (**Figure 20**). Using this approach, we found striking inter-species differences; capillaries were much more abundant in mouse islets compared to human (**Figure 21A-B**), with capillary density being greater in islets than acinar tissue in both species (**Figure 22A-B**). The capillary size was similar in the islet and acinar tissue compartments in mouse and human (**Figure 21E-F, Figure 22C-D**).

To investigate possible explanations for the species differences in vascularization with emerging islet bulk and single-cell RNA-sequencing data, we compared the transcriptional profile of angiogenic factors and their cognate receptors in cells from mouse and human islets using existing resources and, for the first time in this context comprehensively assessed mouse and human islet datasets side-by-side. The cell-specific expression of angiogenic ligand and receptor transcripts was similar in bulk, and single-cell (sc) RNA-sequencing (RNA-seq) datasets from mouse[230,246] and human[243,244,248] islets (**Figure 21G**), notably with high VEGFA expression in endocrine cells and associated receptor KDR highly expressed in endothelial cells. Transcripts encoding ECM components, including integrins, collagens, and laminins, were detected at high levels in pooled islet endothelial cells from both species, as well as single stellate cells from human islets (**Figure 21H**).

Nerve fiber densities were 15-fold greater, and nerve fiber lengths were 63-fold greater in mouse compared to human (**Figure 23A-B**). In contrast, human acinar tissue had a greater nerve fiber density and length when compared to mouse (**Figure 23D-F**). Expression profiles of molecules that directly provide signals for axon growth, survival, and guidance cues, such as neurotrophic factors, ephrins, and semaphorins, and their associated receptors were relatively consistent between mouse and human islets, while SLIT/ROBO pathway components were detected at higher levels in mouse β cells compared to human (**Figure 23G**). Overall, the nerve fibers in the human pancreas were surprisingly more abundant and longer in acinar tissue than in islets (**Figure 22E-H**), and there were modest differences in neuronal signaling pathways by transcriptomic analysis (**Figure 24**). Additionally, percent capillary and nerve fiber area analyses revealed similar findings as described above (**Figure 25**). Our results demonstrate that the neurovascular architecture of islets and acinar tissue differs considerably between mouse and human supporting prior findings on pancreatic inter-species differences[74,262,263]. We also showed that despite significant inter-species differences in islet neurovascular architecture, transcriptomic profiles of factors guiding angiogenesis and neuronal development in islets

were quite similar, suggesting other cross-species regulatory relationships.

Capillary density is greater in islet and acinar tissue of recent-onset T1D.

Utilizing the largest T1D cohort to date to assess neurovascular architecture, we investigated whether architectural changes are associated with or related to T1D disease duration. Because the frequency of neuropathy increases with longer diabetes duration and the heterogeneity of T1D tissues, we subdivided a T1D donor cohort of 27 donors into two groups (**Figure 26a**): 1) relatively recent-onset (< 10 years of disease) and 2) longstanding T1D (> 10 yrs of disease)[223]. Recent-onset T1D donors had low but measurable C-peptide levels, whereas the levels in longstanding T1D donors were mostly below the detection limit (**Table 9**). Additionally, 33% (6 recent-onset; 3 longstanding) of these T1D donors were previously phenotyped for endocrine composition and/or islet function[223,224,270]. The de-identified record of these donors did not specify whether the donors had autonomic or peripheral neuropathy (donor summary in **Table 2** and **Table 9**). Lastly, the analyzed islet area was similar between groups for all capillary and nerve fiber analyses (**Figure 27**).

The density of pancreatic capillaries, visualized by immunofluorescence labeling for caveolin-1 (CAV1) with 10 µm tissue sections, was greater in recent-onset T1D than in non-diabetic and longstanding T1D tissue in both pancreatic compartments (**Figure 26B-D**), with no significant difference among anatomical regions (**Figure 26E-H**). As with non-diabetic donors, T1D donors showed greater islet capillary density than in the acinar tissue (**Figure 28b, Figure 26A-B**), while area per capillary did not vary by T1D subgroup (**Figure 26I-L**) or between the islet and acinar compartments (**Figure 28D, 26C-D**). Additionally, we found a negative correlation between the capillary density of islets (**Figure 26F**) and acinar tissue (**Figure 26H**) and age and disease duration in T1D donors. Quantification of percent capillary area revealed similar findings as described above (**Figure 29**).

Pancreatic islet and acinar nerve fibers persist in T1D

To investigate whether nerve fiber density is altered in T1D, we visualized all pancreatic nerve fibers with TUBB3. Genetic ablation of intra-islet capillaries through inactivation of a major angiogenic factor produced by β cells, vascular endothelial growth factor A (VEGF-A), leads to extensive islet nerve fiber loss, thus highlighting coordinated interactions between islet innervation and vasculature and the importance of studying these two islet compartments simultaneously[50]. To our knowledge, the simultaneous comparison of nerve fibers and capillaries has not been done at this scale in human T1D tissues. Like non-diabetic pancreata, T1D nerve fibers projected from the acinar

compartment into islets but were less frequent within islets compared to acinar tissue (**Figure 30**, **Supplemental Videos 1-3**). Interestingly, fiber density in islets (**Figure 30D**), but not acinar tissue (**Figure 30F**), was greater in both recent-onset and longstanding T1D when compared to non-diabetic donor tissue. Acinar nerve fiber length did not differ among groups (**Figure 30J**). Within each group, both nerve fiber density and length were greater in acinar tissue compared to islets (**Figure 30, Figure 31A-B**). However, neither nerve fiber density nor length correlated to donor age or T1D duration in either compartment (**Figure 30E, 30I, 30G, 30K**).

Sympathetic nerve fibers are similar in T1D and non-diabetic pancreata

The autonomic nervous system is important for initiating α cell response to hypoglycemia, particularly through sympathetic fibers[2]. Early loss of rodent sympathetic nerve fibers in models of T1D has been hypothesized to lead to the dysregulation of glucagon secretion[218,220,221]. Therefore, we assessed T1D pancreatic sympathetic nerve fibers utilizing the marker tyrosine hydroxylase (TH). In contrast to findings in T1D rodent models, we did not detect a change in sympathetic islet or acinar fiber density in recent-onset or longstanding T1D (**Figure 32**)[218,221]. In line with our findings using the pan-neuronal marker TUBB3, the density and length of TH+ sympathetic nerve fibers were greater in the acinar tissue compared to islets of both ND and T1D donors (**Figure 31C**). Furthermore, sympathetic fibers predominated in the islet compartment (**Figure 33A-B**) but made up only a subset of TUBB3+ pan-neuronal fibers in the acinar compartment (**Figure 33C-D**). There was a negative correlation between TH+ islet fiber density and length versus T1D cohort age but not the disease duration (**Figure 33E, 33I**). Quantification of percent nerve fiber area revealed similar findings as described above (**Figure 34**).

Nerve fibers in islets and acinar tissue overlap with the extracellular matrix

The ECM is an essential part of the vasculature by providing structural blood vessel support and regulating vascular phenotype and function[52,90]. At the same time, it also regulates neuronal migration, the formation of axonal processes, and their function [52,90]. To understand the structural relationship between pancreatic nerve fibers, capillaries, and the ECM, we determined nerve fiber and ECM patterning in non-diabetic, recent-onset T1D, and longstanding T1D tissues. Three-dimensional (3D) reconstructions of TUBB3+ nerve fibers and ECM show that nerve fibers follow ECM within acinar tissue prior to extending into islets (**Figure 35A-F, Supplemental Videos 1-3**). By visualizing capillaries, nerve fibers, and ECM with PECAM-1, TUBB3, and collagen IV (COLIV), respectively, we found that nerve fibers associated with the ECM in the acinar and islet compartments regardless of disease state (**Figure 35A-F**). Our image analyses showed

~40% overlap of TUBB3+ nerve fiber area with COLIV+ ECM area (**Figure 35G**). These results demonstrate that there is a strong spatial association between nerve fibers and ECM (**Figure 35D', 35E', 35F'**), whereas, in acinar tissue, they follow ECM generated by acinar cells in areas devoid of capillaries (**Figure 35D", 35E", 35F"**). Overall, these data indicate that pancreatic capillaries and nerve fibers persist in longstanding T1D (**Figure 36**), contrasting with the loss of pancreatic innervation in rodent T1D models and thus emphasizing potentially distinct mechanisms of intrinsic α cell defects in dysregulated human glucagon secretion.

Discussion

Hypoglycemia is a major limitation of insulin therapy in T1D, and impaired glucagon secretion is a major contributor. Using bio-banked pancreatic tissues from T1D donors that spanned a wide range of diabetes duration, we investigated if impaired glucagon secretion could be attributed, at least in part, to the reduced islet innervation as suggested by studies in rodent models of T1D. To understand changes in the neurovascular architecture of human T1D pancreatic tissue, we systematically assessed innervation and vascularization in both islet and acinar tissue compartments of recent-onset and longstanding T1D donors and age-matched controls. As part of this study, we also analyzed the neurovascular architecture in mouse pancreas, a widely used model of human disease, and compared it to that of non-diabetic human controls. We found that human islets are much less vascularized and innervated than mouse islets (more than a 15-fold difference). In contrast to mouse islets, human islets are less innervated compared to surrounding acinar tissue. Human islets have fewer intra-islet capillaries with sparse nerve fibers, with these in close association with ECM. We also found that both nerve fibers and capillaries were present with greater capillary density in recent-onset T1D islets and acinar tissue. Surprisingly, we found that islet innervation was similar in T1D donors and controls, indicating that the islet neurovascular structures persist and are relatively unchanged in human T1D. These results, in conjunction with reports from others, suggest the need for alternative hypotheses other than reduced innervation to explain the dysregulated glucagon secretion in human T1D[74,75,263,271].

The mechanisms responsible for the marked difference in vascularization and innervation in the mouse and human pancreas are unknown. Since in islets, innervation is tightly linked to vascularization with the vascular network generating an ECM scaffold for nerve fiber migration[84], one possible explanation is that greater vascularization in the mouse islets promotes greater innervation. This could explain the difference in innervation patterns between mouse and human islets. Our comparative analysis of transcriptome data available for mouse and human islet endocrine and endothelial cells found overall similar transcriptomic profiles of factors guiding angiogenesis and neuronal development in islets suggesting other regulatory mechanisms, including possibly post-transcriptional

processes[42,50,84,90,91,272,273]. For example, the generation of different isoforms of a master regulator of islet vascularization, VEGF-A, by alternative splicing [272] across different species could lead to isoforms with varying levels of activity due to their regulation by ECM, which could further influence growth factor availability, islet vascularization, and morphogenesis[75,161,162,274–276]. Because vascularization and innervation are complex processes, it is also possible that a combinatorial difference in the ligand-receptor expression could yield different neurovascular patterning between mouse and human. Alternatively, stromal and/or immune cells could further modulate signaling in a species-specific manner during the development of neurovascular assembly[277,278]. Furthermore, the greater innervation in the human exocrine compartment compared to the mouse indicates that the degree of innervation and vascularization is not always linked[42,50,84,90,91,272,273]. The inter-species differences in islet vascularization and innervation are reminiscent of other differences, such as islet cell composition and spatial arrangement, basement membrane organization, proliferative capacity, and basal insulin secretion, but the responsible molecular mechanisms for these are also not well-defined underscoring the caution needed when translating findings from model systems to human disease[161–163,279].

Although the fundamental ability of the autonomic nervous system to activate pancreatic secretion is present in mice and humans, each species may integrate and respond to these signals differently[58,67,78]. Rodent models of T1D show an early loss of islet nerve fiber density dependent on the degree of insulitis, suggesting a role for the immune system in perturbing these structures in conjunction with targeting β cells[202,218,221] leading to an impaired sympathetic nerve fiber activation of glucagon secretion. In human T1D tissues, we did not detect a reduction or loss of sympathetic nerve fibers. Instead, we found the persistence of these nerve fibers in islets. These differences between human and rodent models may be due to inter-species differences in the islet-related T1D pathogenesis with much more profound insulitis in NOD mice compared to human[58,67,78,202,265]. Other nerve fiber type densities not assessed here due to reagent availability, such as parasympathetic or sensory nerves, may also change and influence secretion dysfunction seen in T1D[77,266]. Furthermore, a previous study found differences in the islet microvasculature between T1D insulin-positive and insulin-negative islets which we did not capture in the current study due to our immunolabeling paradigms[222]. Additionally, an upregulation in vascular gene sets such as angiogenesis and blood vessel morphogenesis found in T1D islets parallels the histological capillary changes reported in our current study[280]. Therefore, the heterogeneous nature of β cell loss across T1D islets may lead to variabilities in T1D islet microvasculature and nerve fiber densities which need to be further studied. Overall, our studies of many human tissues do not support the hypothesis that glucagon secretion defects in T1D result from decreased islet sympathetic nerve fiber density.

Some differences exist between our findings and prior reports, including tissue thickness, the number of donors assessed, and nerve fiber markers utilized. One experimental difference is that we utilized both thin (10 μm) and thick (30 μm) cryosections from human tissue that were gently fixed to maximally preserve cellular and anatomical structures. Compared to optically cleared sections, 10 μm sections do not always capture the full length of some nerve fibers or capillaries. In contrast to much thicker optically cleared tissue sections, though, 10 μm sections allowed for high throughput morphometric analysis of ~3400 islets in total from a unique bio-banked cohort of 38 non-diabetic and T1D donors. We sought to circumvent this limitation by studying a tremendous number of islets from a large cohort of donors. Our high throughput analysis also allowed us to overcome high variability in human samples, particularly in T1D donor tissues. Other differences between this and other studies may be due to donor variability, sample size, and/or technical differences during tissue handling, which may affect the downstream quantification of delicate structures such as nerve fibers. We used the pan-neuronal marker, TUBB3, while others have used neural cell adhesion molecule 1 (NCAM), neurofilament 200 (NF200), and ubiquitin carboxyl-terminal hydrolase isozyme (UCHL1 or PGP9.5)[77,262,265,281] with a similar distribution of nerve fibers in human islets and acinar tissue when compared to PGP9.5 maker, thus further underscoring the appropriate utilization of TUBB3 in this study[281]. It is important to note that TUBB3+ intrapancreatic ganglia could not be identified in either full-section confocal images or over 1,000 whole-slide images that we used for our high-throughput analyses. Therefore, nerve fiber bundles served as a positive control for TUBB3 immunolabeling of pancreatic nerve fibers in our study. Additionally, we used the sympathetic nerve fiber marker, TH, that labels throughout the axon to the nerve terminal and allows direct comparison to other studies utilizing this same marker.

The preservation of neurovascular architecture in T1D islets suggests other explanations for impaired glucagon secretion, such as intrinsic nerve fiber or capillary dysfunction and/or an intrinsic α cell defect. Recent studies using isolated islets and tissues from the same organ donors provide significant support for intrinsic α cell defect in T1D at both molecular and functional levels showing that impaired glucagon secretion was associated with reduced expression of key α cell-enriched regulators, including transcription factors *MAFB* and *ARX* and pointing to changes in metabolic pathways related to glycolysis and oxidative phosphorylation[223,224,282]. While we show that neurovascular architecture is preserved in T1D, one cannot exclude an islet nerve fiber or capillary dysfunction, which are far more difficult to elucidate in human. For example, hyperglycemia could cause neurotransmitter receptor oxidation and reduced acetylcholine receptor activity in sympathetic neurons[283]. Conversely, hypoglycemia sensed in the brain promotes counterregulatory responses from the adrenal gland and α cells. Dysfunctional CNS

hypoglycemia-sensing in T1D could disrupt sympathetic activation in islets, further impairing glucagon secretion[280]. Given prior findings that sympathetic nerve fibers preferentially innervate smooth muscle cells within the islet, disruptions in the autonomic modulation of intra-islet vascular contractile components in T1D may also contribute to diminished glucagon secretion during hypoglycemia[74]. The recent development of pancreatic slice physiology, which preserves vascular cytoarchitecture, highlighted the importance of islet pericytes in modulating local vasodilation and constriction[182,284].

Additional research is needed to determine whether the dysregulated glucagon secretion in T1D results primarily from α cell-intrinsic defect and whether it is further compounded by neuronal dysfunction. It is important that such studies examine a broad range of T1D duration since mechanisms may differ with disease stages. New technologies, approaches, and models to probe neurovascular function in islets are emerging, and these include the islet-on-a-chip platform, pancreatic slices, islet transplantation models, and new imaging approaches[33,35,36,285,286]. For example, examining in vivo the processes of both innervation and vascularization of human islets transplanted into immunodeficient mice may provide insights into the molecular mechanisms of such processes.

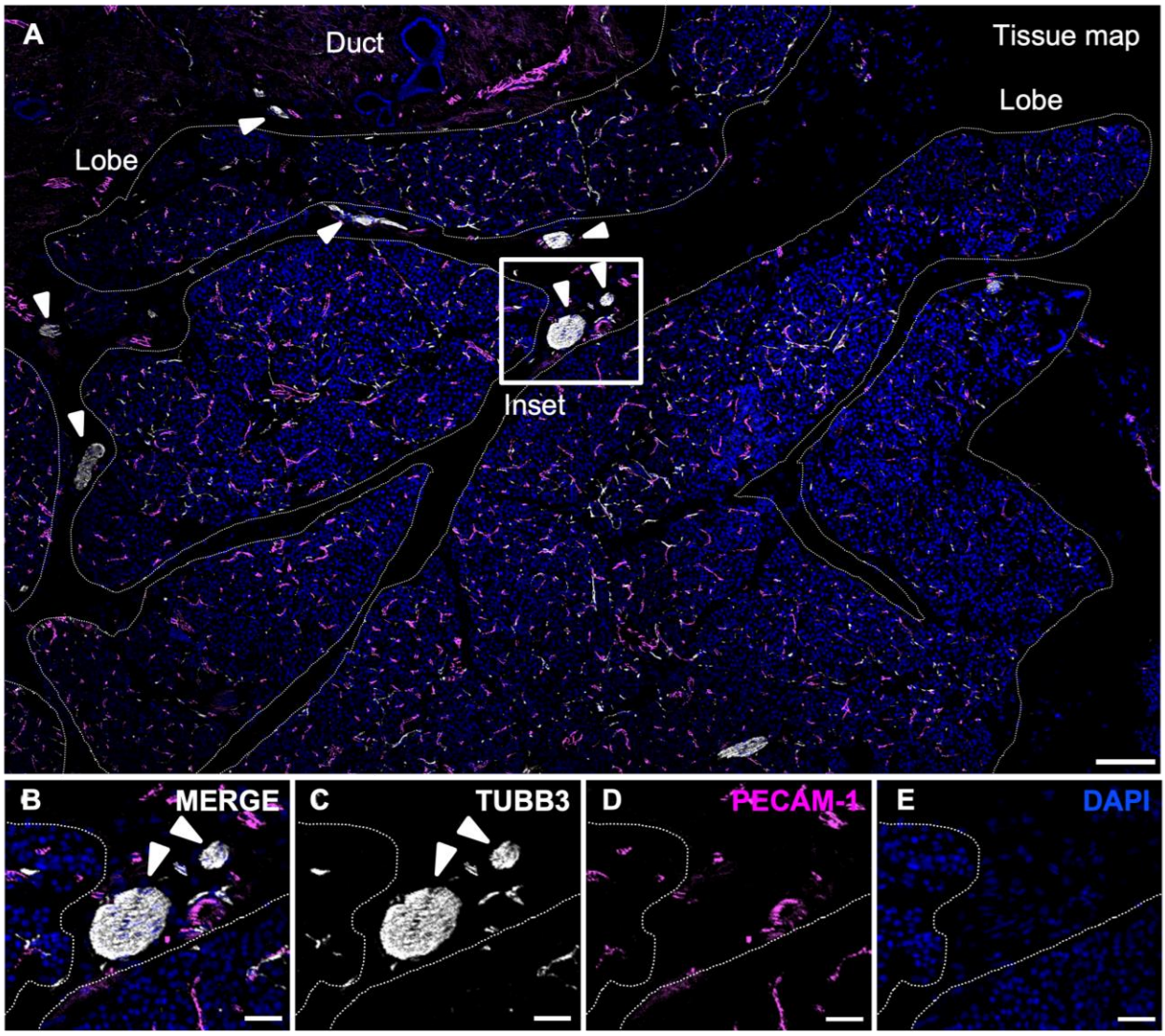

Figure 19. Human pancreatic nerve fiber bundles immunolabeled with TUBB3. (A-E) Representative immunofluorescent images of TUBB3+ nerve fiber bundles in a human pancreatic tissue section. Nerve fibers are labeled with TUBB3 (white), capillaries are labeled with PECAM-1 (magenta), and cell nuclei are denoted with DAPI (blue). Pancreatic lobes are outlined with dashed white lines. Arrowheads denote inter-lobular nerve fiber bundles. (b-e) Inset showing a magnified image of two TUBB3+ nerve fiber bundles. The tissue map scale bar is 100 μm and inset scale bars are 40 μm in length.

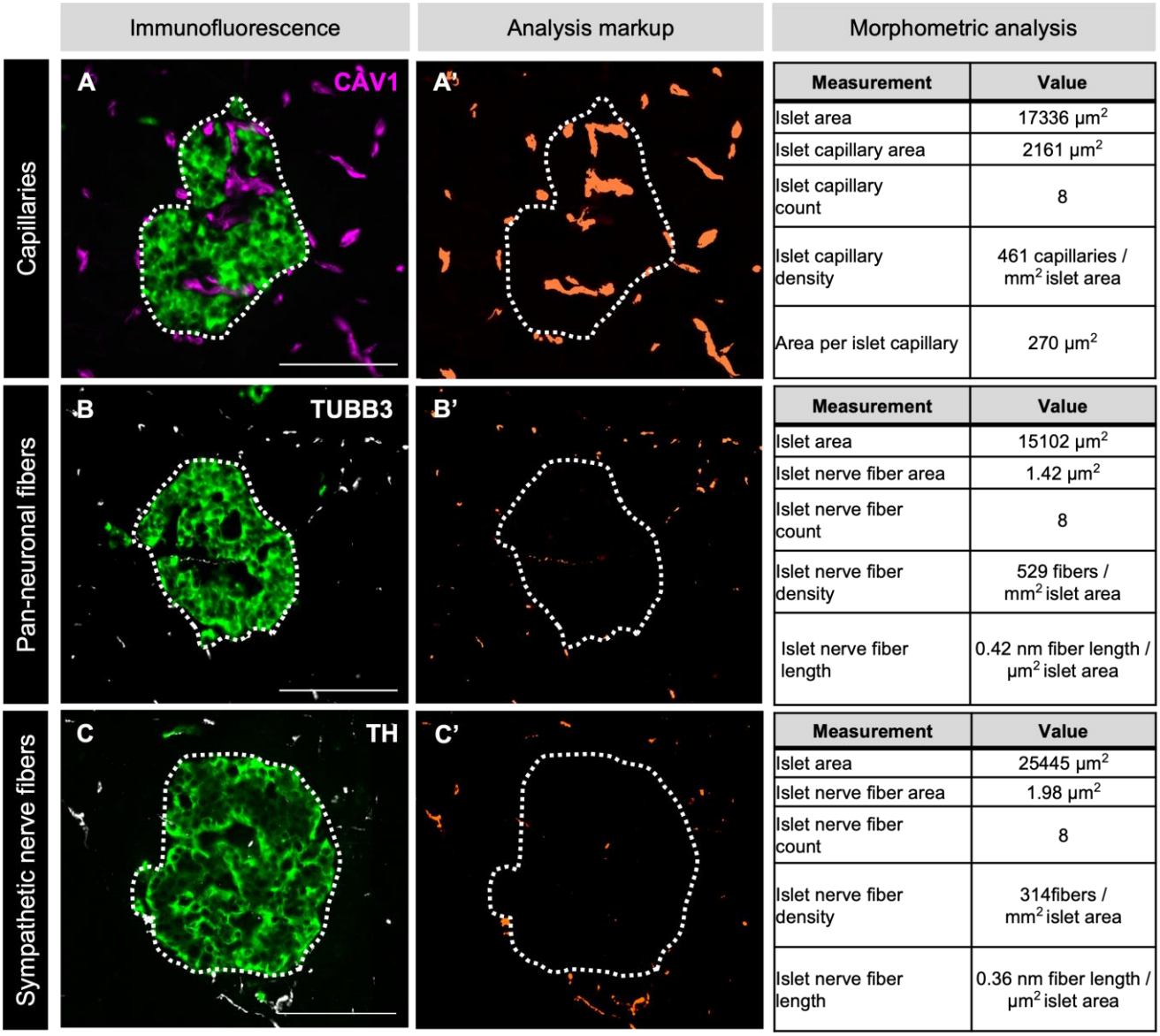

Measurement	Value
Islet area	17336 μm^2
Islet capillary area	2161 μm^2
Islet capillary count	8
Islet capillary density	461 capillaries / mm^2 islet area
Area per islet capillary	270 μm^2

Measurement	Value
Islet area	15102 μm^2
Islet nerve fiber area	1.42 μm^2
Islet nerve fiber count	8
Islet nerve fiber density	529 fibers / mm^2 islet area
Islet nerve fiber length	0.42 nm fiber length / μm^2 islet area

Measurement	Value
Islet area	25445 μm^2
Islet nerve fiber area	1.98 μm^2
Islet nerve fiber count	8
Islet nerve fiber density	314fibers / mm^2 islet area
Islet nerve fiber length	0.36 nm fiber length / μm^2 islet area

Figure 20. Representative metamorphic analysis of human pancreatic tissue sections. (A-C) Representative immunofluorescent staining of a 10 μm pancreas section from a non-diabetic donor pancreas. Adjustments of brightness and contrast were where made on each individual image manually. Islets are outlined with dashed white lines. (A-C) Merged image of islet (green) and CAV1+ capillaries (magenta), TUBB3+ nerve fibers (white), or TH+ nerve fibers (white). (A'-C') Metamorphic analysis markup. The last column details image-specific metamorphic measurements. Scale bars are 100 μm in length**.**

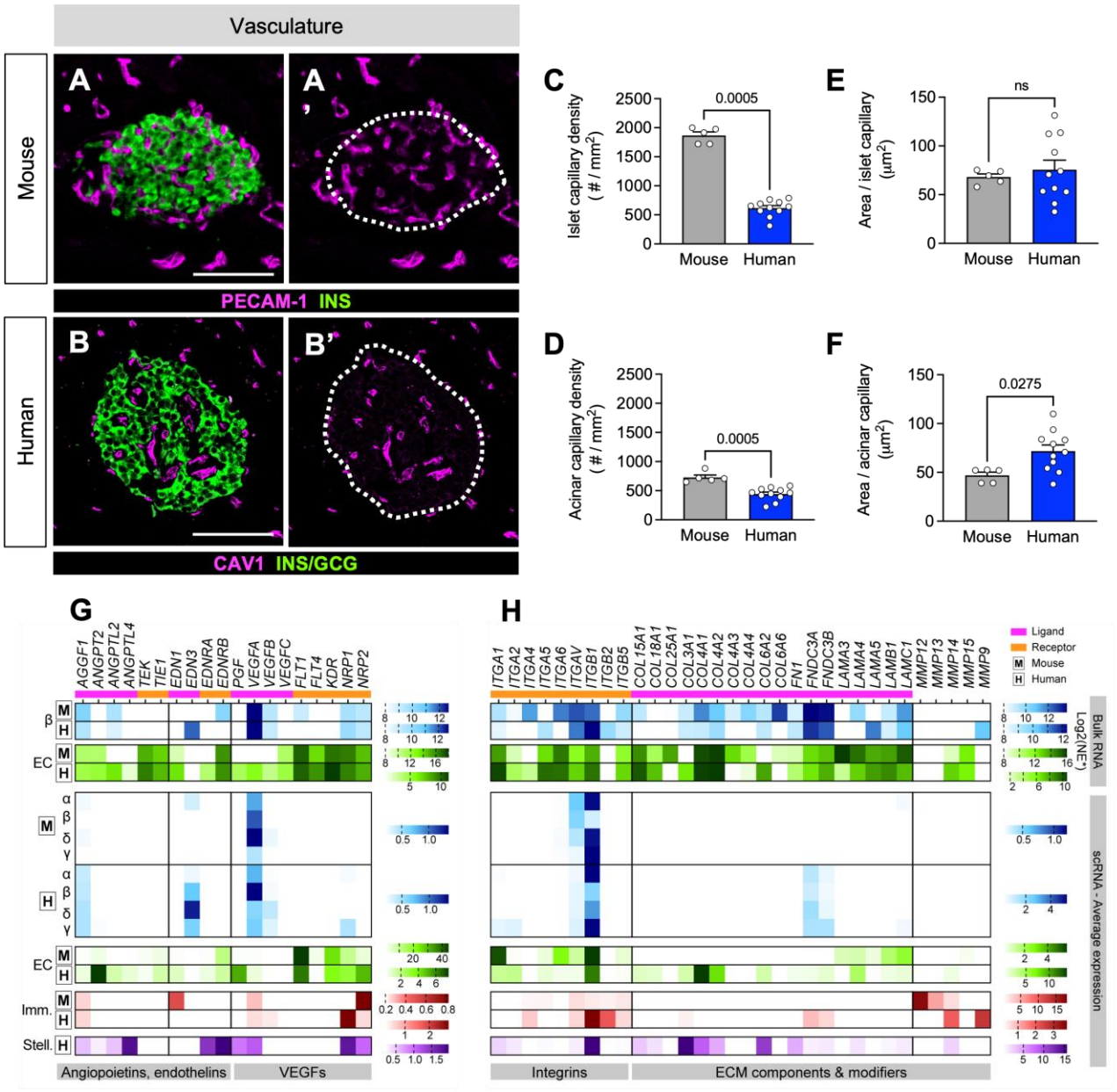

Figure 21. Human islets are less vascularized than mouse islets.
Representative immunofluorescent staining (A-A', B-B') and quantification (C-F) of vasculature, as measured by endothelial cell staining (PECAM-1 or CAV1; magenta). Islets are visualized by hormones (insulin, INS; glucagon, GCG; green) and panels A' and B' show PECAM-1 or CAV1 only with islet area outlined. Scale bars, 100 µm. Quantification (mean ± s.e.m.) includes capillary density (panels C, D; left) and area per capillary (right) in islets (E) and acinar tissue (F) from mouse (grey; N = 5; 129 total islets, 127 total acinar measurements) and human (dark blue; N = 11; 488 total islets, 1392 total acinar measurements). Symbols on bar graphs represent individual mouse or human donors. Statistically significant p-values (< 0.05) are stated for Mann-Whitney tests. (G-H) Transcript levels of select angiogenic factors and receptors (G) and extracellular matrix (ECM) molecules (H) detected in islet endocrine cells, endothelial cells, and immune cells as measured by RNA-sequencing (RNA-seq). From top to bottom: mouse bulk datasets, Saunders et al. 2021; human bulk beta, Walker et al. 2021; human bulk endothelial, Jonsson et al. 2020; single-cell (sc) datasets: mouse, Erener et al. 2021; human, Shrestha et al. 2021. Boxed 'M' and 'H' label mouse and human datasets, respectively. Only values >0.2 (sc) and log2 >8 (bulk) are graphed. Normalized expression (NE) units vary by study; see Methods. EC, endothelial cell; Imm., immune; Stell., stellate; VEGF, vascular endothelial growth factor.

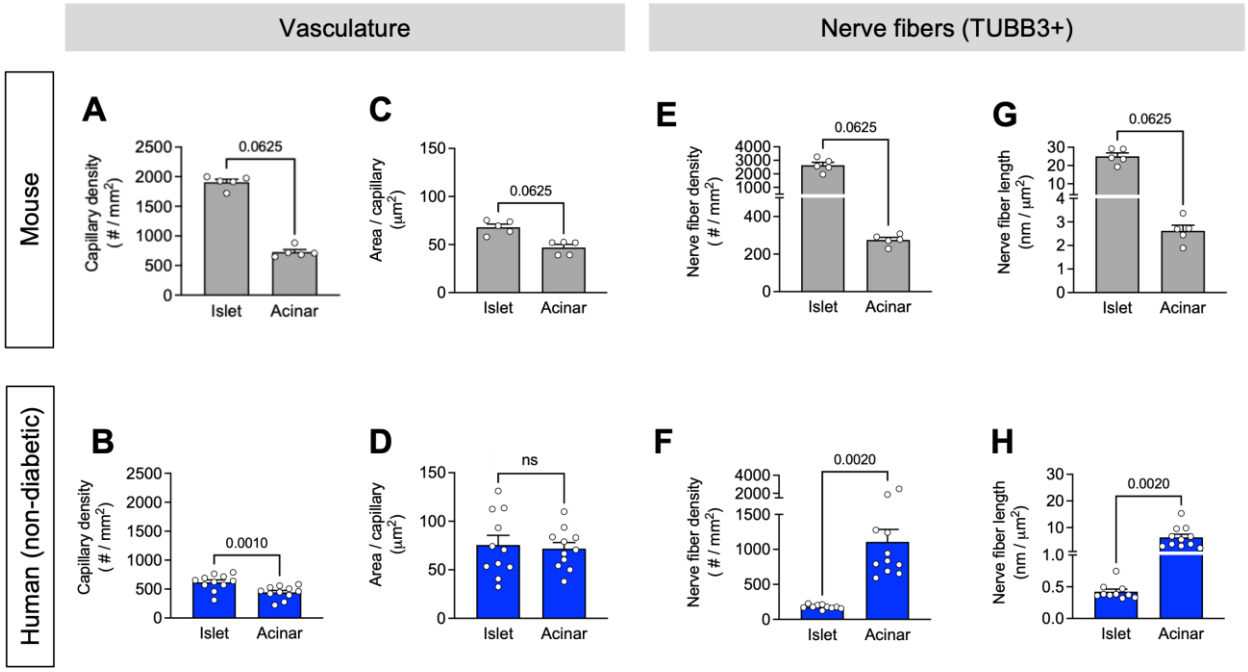

Figure 22. Mice and humans show greater capillary density in islets compared to acinar tissue, but humans have greater islet nerve fiber density compared to the acinar compartment.

Quantification (mean + s.e.m.) comparing islet and acinar capillary density (A,B), area per capillary (C,D), nerve fiber density (E,F), and nerve fiber length (G,H) for mouse (grey, n = 5) and human non-diabetic (dark blue, n = 11). P-values were calculated by paired Wilcoxon t-tests in which a $p < 0.05$ is significant.

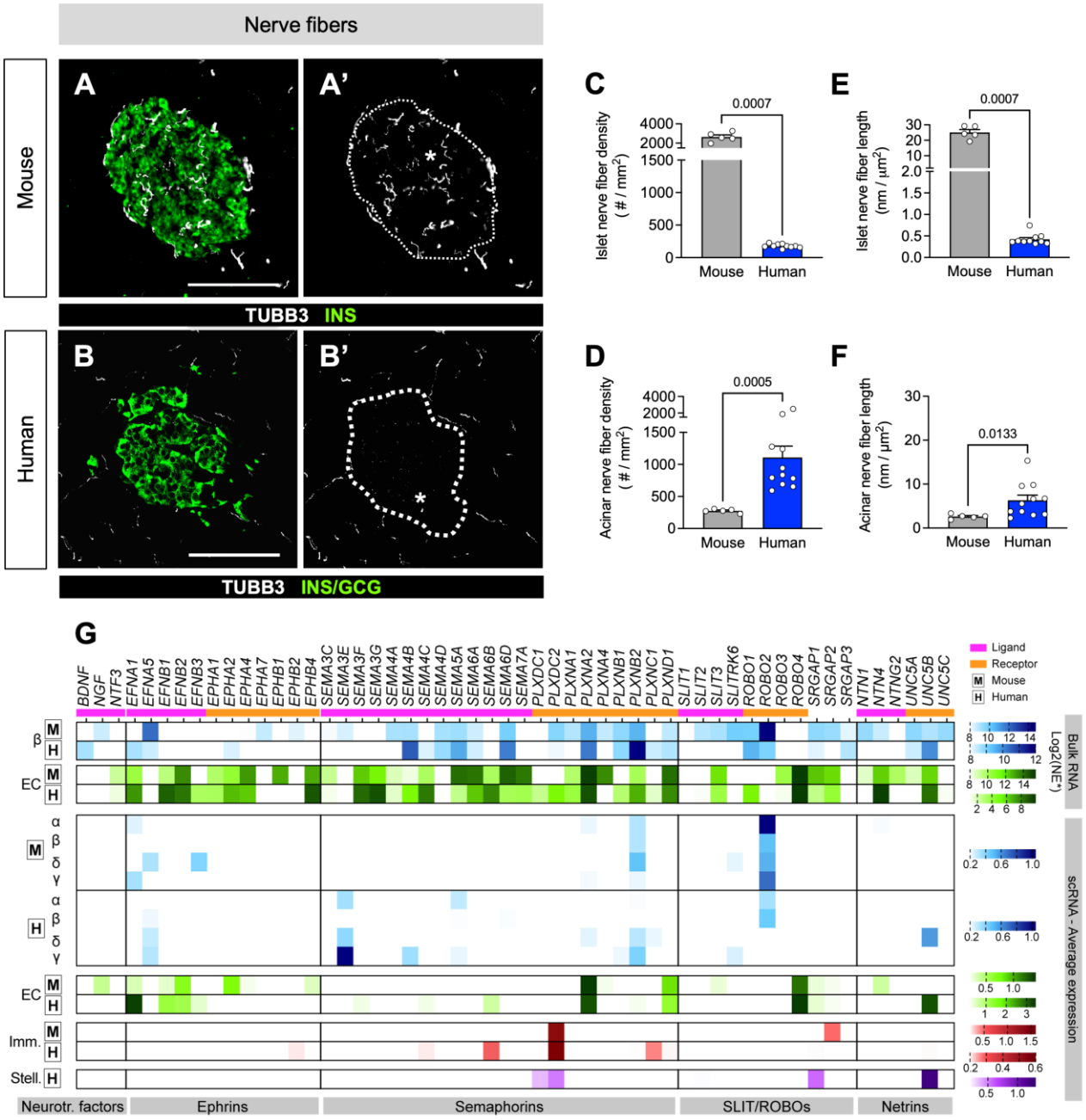

Figure 23. Human islets are less innervated than mouse islets.
Representative immunofluorescent staining (A-A', B-B') and quantification (C-F) of nerve fibers, as measured by tubulin beta 3 (TUBB3; white). Islets are visualized by hormones (insulin, INS; glucagon, GCG; green) and panels A' and B' show TUBB3 only with islet area outlined. Asterisk (*) denotes intra-islet nerve fibers. Scale bars, 100 µm. Quantification (mean ± s.e.m.) includes TUBB3+ fiber density (panels C, D; left) and length (right) in islets (E) and acinar tissue (F) from mouse (N = 5; 128 total islets, 262 total acinar measurements) and human (N = 11; 547 total islets, 1830 total acinar measurements). Symbols on bar graphs represent individual mouse or human donors. Statistically significant p-values (< 0.05) are stated for Mann-Whitney tests. (G) Transcript levels of select neuronal ligands and receptors as measured by RNA-sequencing (RNA-seq). From top to bottom: mouse bulk datasets, Saunders et al. 2021; human bulk beta (β), Walker et al. 2021; human bulk endothelial, Jonsson et al. 2020; single-cell (sc) datasets: mouse, Erener et al. 2021; human, Shrestha et al. 2021. Boxed 'M' and 'H' label mouse and human datasets, respectively. Neurotr. factors = neurotrophic factor genes. Only values >0.2 (sc) and log2 >8 (bulk) are graphed. Normalized expression (NE) units vary by study; see Methods. EC, endothelial cell; Imm., immune; Stell., stellate.

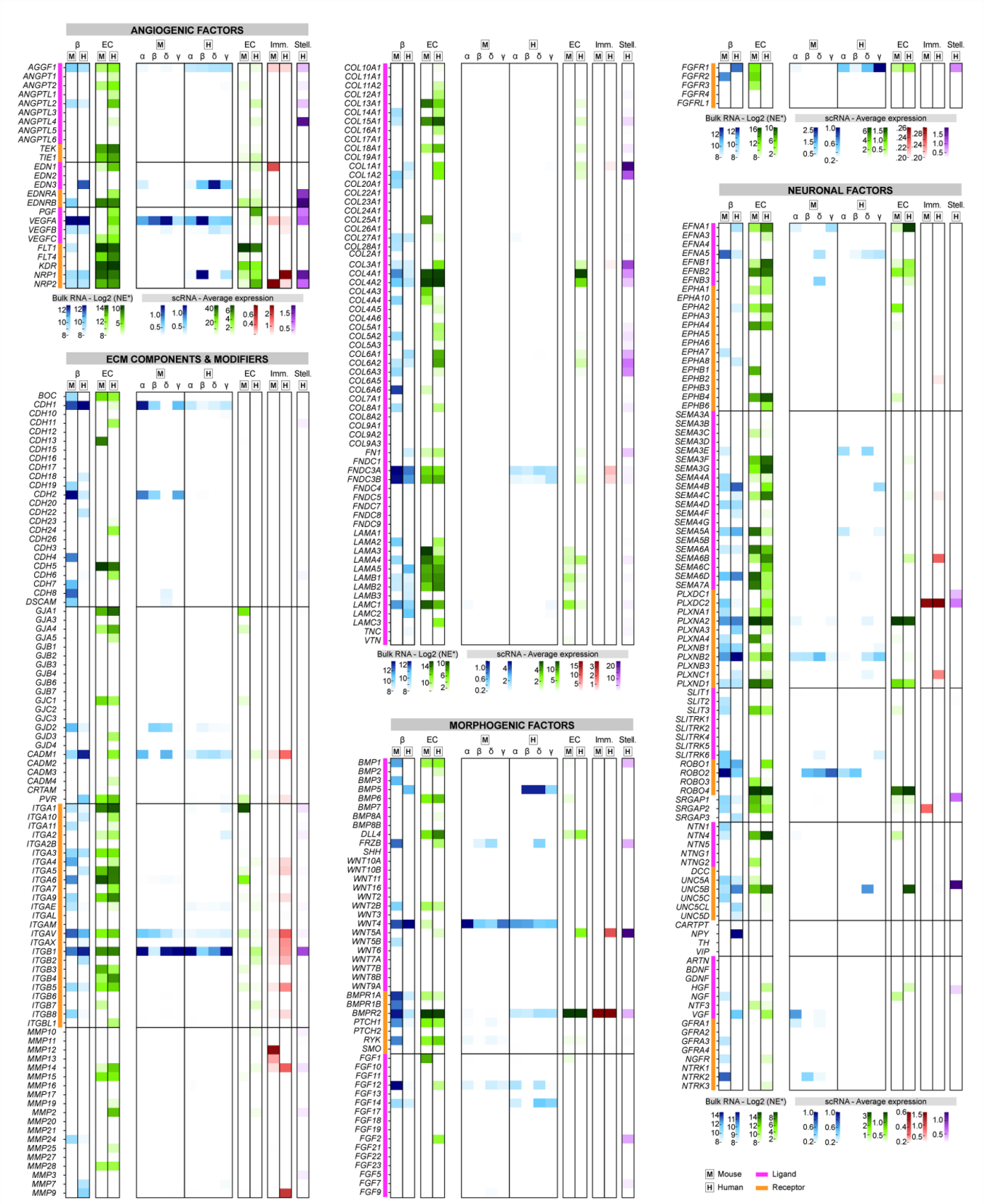

Figure 24. Endocrine cells, endothelial cells, and immune cells from mouse and human islets show different transcriptomic profiles for angiogenic, neuronal, morphogenic, and extracellular matrix-related molecules.

Figure 24. Endocrine cells, endothelial cells, and immune cells from mouse and human islets show different transcriptomic profiles for angiogenic, neuronal, morphogenic, and extracellular matrix-related molecules.
Transcript levels of ligands (magenta), receptors (orange), and other molecules detected in endocrine cells (blue color scale), endothelial cells (green), immune cells (pink), and stellate cells (purple) as measured by RNA-sequencing (RNA-seq). From left to right: mouse bulk datasets, Saunders et al. 2021; human bulk β, Walker et al. 2021; human bulk endothelial, Jonsson et al. 2020; single-cell (sc) datasets: mouse, Erener et al. 2021; human, Shrestha et al. 2021. Only values >0.2 (sc) and log2 >8 (bulk) are graphed. Normalized expression (NE) units vary by study; see Methods. EC, endothelial cell; Imm., immune; Stell., stellate**.**

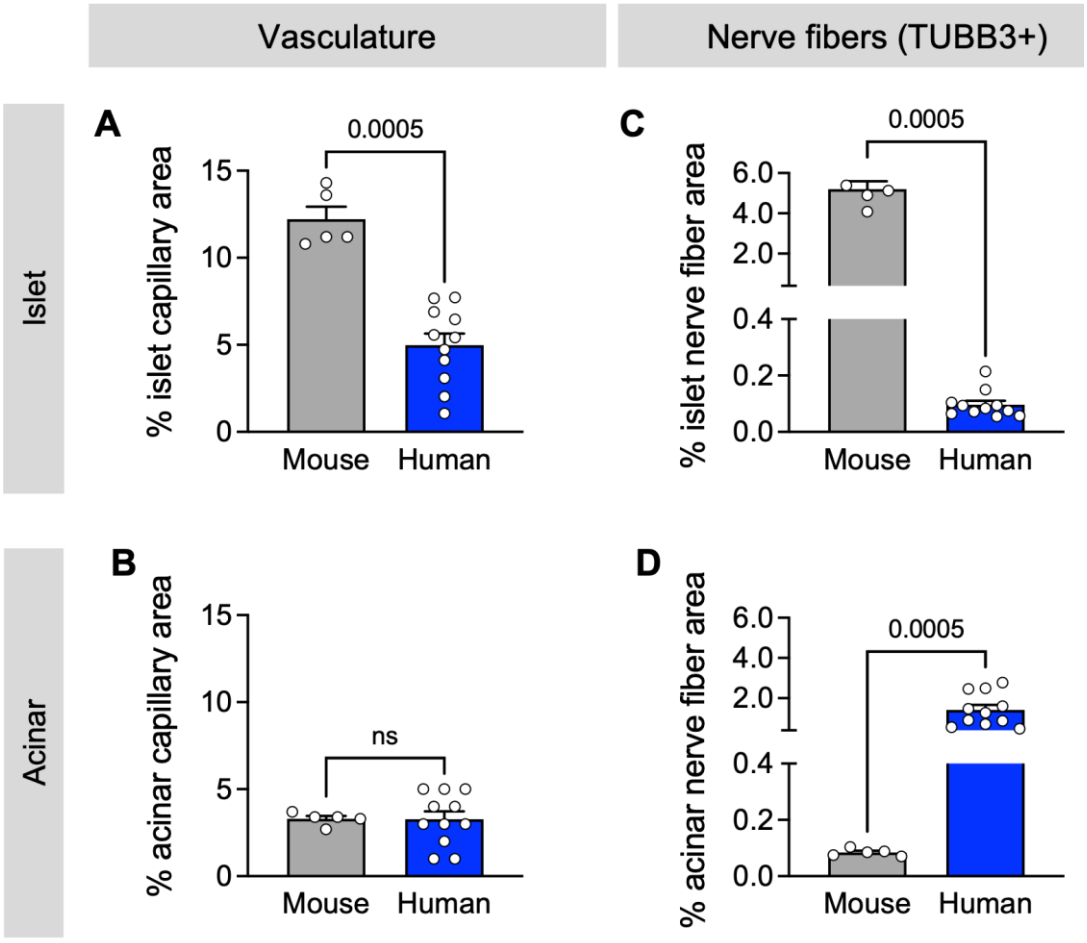

Figure 25. Percent capillary and nerve fiber area analyses show similar trends as density measurements performed in Fig 21 & 23.
Quantification (mean + s.e.m.) comparing islet (a,c) and acinar (b,d) percent capillary area (a-b) and percent nerve fiber area (c-d) for mouse (grey, N = 5) and human non-diabetic (dark blue, N = 11). See Figure 20 & 22 for islet and acinar measurement counts. P-values were calculated by paired Wilcoxon t-tests in which a $p < 0.05$ is significant.

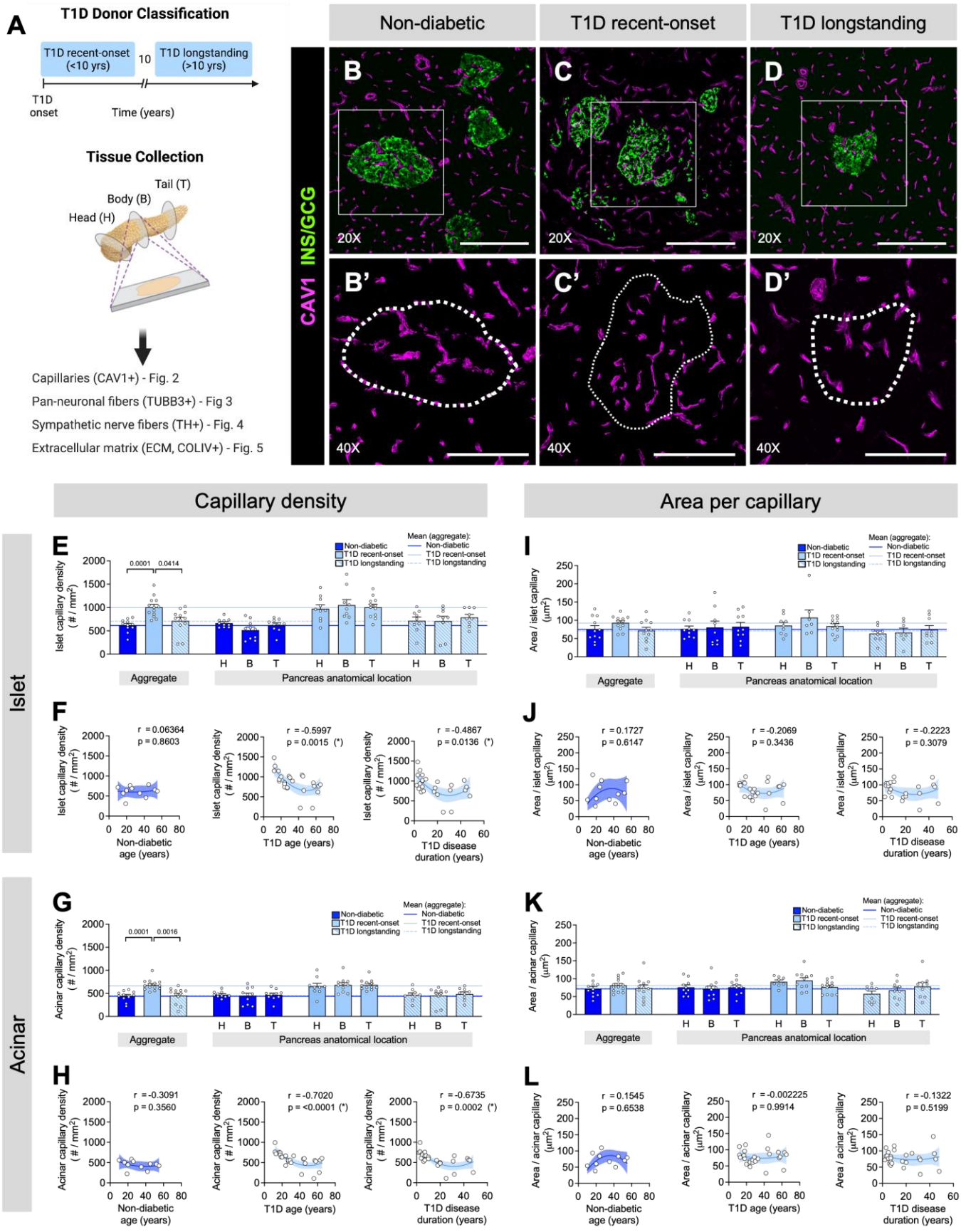

Figure 26. Islets in recent-onset T1D have greater vascular density compared to controls.

Figure 26. Islets in recent-onset T1D have greater vascular density compared to controls.
(A) Schematic illustrating donor classification and experimental approach. (B-D) Representative immunofluorescent staining of vasculature labeled with caveolin-1 (CAV1; magenta) in pancreatic tissue sections from non-diabetic (B), T1D recent-onset (C), and T1D longstanding (D) donors. Panels (B'-D') show insets of (B-D), CAV1 channel only, with islet area outlined. Asterisk (*) denotes intra-islet nerve fibers and triangles denote nerve fibers crossing from the acinar to islet compartment. A magnified image of the area denoted by a solid square is shown with an appropriate scale bar in each image. Scale bars, 100 μm. (E-L) Quantification (mean + s.e.m.) of capillary density (E-H) and area per capillary (I-L) in islet (E-J) and acinar (G-L) tissue from pancreata of non-diabetic (dark blue; N = 11; 488 total islets, 1392 total acinar measurements), T1D recent-onset (light blue; N = 14; 471 total islets, 1332 total acinar measurements), and T1D longstanding (light blue striped; N = 12; 316 total islets, 867 total acinar measurements) donors. Each symbol represents an individual donor; 'aggregate' graph values reflect the average data from all pancreas regions, which are stratified (H, Head; B, Body; T, Tail) to the right. Horizontal lines represent mean values and are colorized based on the donor group. (F) Islet and (H) acinar capillary density in ND and T1D tissue, plotted as a function of donor age and disease duration. (J) Islet and (L) acinar area per capillary in ND and T1D tissue, plotted as a function of donor age and disease duration. Statistically significant p-values (< 0.05) are stated for the following statistical tests: (E, I, G, K) aggregate, Kruskal-Wallis One-Way ANOVA with Dunn's multiple comparisons tests; anatomical location, Mixed-effects One-Way ANOVA with Holm-Sidak's multiple comparison tests; (F-J, H-I) nonlinear regression analysis with lines of best fit and Spearman correlation r values denoted on each plot.

Table 9. Overview of donor cohort characteristics.

Donor Group	N	Age (years)	Disease Duration (years)	Sex (F / M)	BMI (kg/m²)	HbA1c (%)	C-peptide (ng/mL)
Non-diabetic	11	31 ± 15	N/A	3 / 11	30 ± 13	5.57 ± 0.30	13.18 ± 11.41
T1D Recent-onset (<10 yrs)	15	25 ± 14	6 ± 2	5 / 15	24 ± 6	9.49 ± 0.168	0.11 ± 0.13 (* vs. ND & T1D >10 yrs)
T1D Longstanding (>10 yrs)	12	45 ± 14	31 ± 11	3 / 12	27 ± 5	8.9 ± 1.45	< 0.02 or UD (* vs. ND & T1D <10 yrs)

Abbreviations: N, sample size; F, female; M, male; BMI, body mass index; HbA1c, Hemoglobin A1c; T1D, type 1 diabetes; UD, undetectable. Averages are displayed with mean ± standard deviation when applicable for non-diabetic and T1D donors. Asterisk (*) represents a statistically significant p-value < 0.05 for comparisons between donor groups assessed by Mann-Whitney tests. For statistical purposes, C-peptide values < 0.02 ng/mL (the lower limit of assay detection) and undetectable C-peptide levels were set to 0. For T1D recent-onset, 4 donors had C-peptide values < 0.02 ng/mL, and 3 donors had undetectable values. For T1D longstanding, 7 donors had C-peptide levels < 0.02 ng/mL, 4 donors had undetectable values. The T1D longstanding donor with a C-peptide level of 1.78 was determined to be an outlier and excluded from analyses.

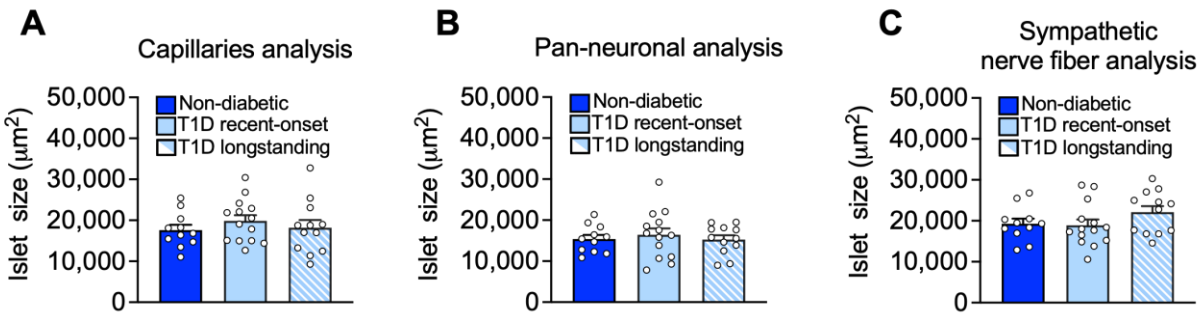

Figure 27. Analyzed average islet size for vasculature and innervation did not differ between ND and T1D donor groups.

(A-C) Average islet size analyzed with capillary marker, CAV1; pan-neuronal marker, TUBB3; and sympathetic nerve fiber marker, TH from non-diabetic (dark blue; n = 11), T1D recent-onset (light blue; n = 15), and T1D longstanding (light blue striped; n = 12). P-values were calculated by Kruskal-Wallis One-Way ANOVA with Dunn's multiple comparisons tests where no statistical significance was below a p-value < 0.05.

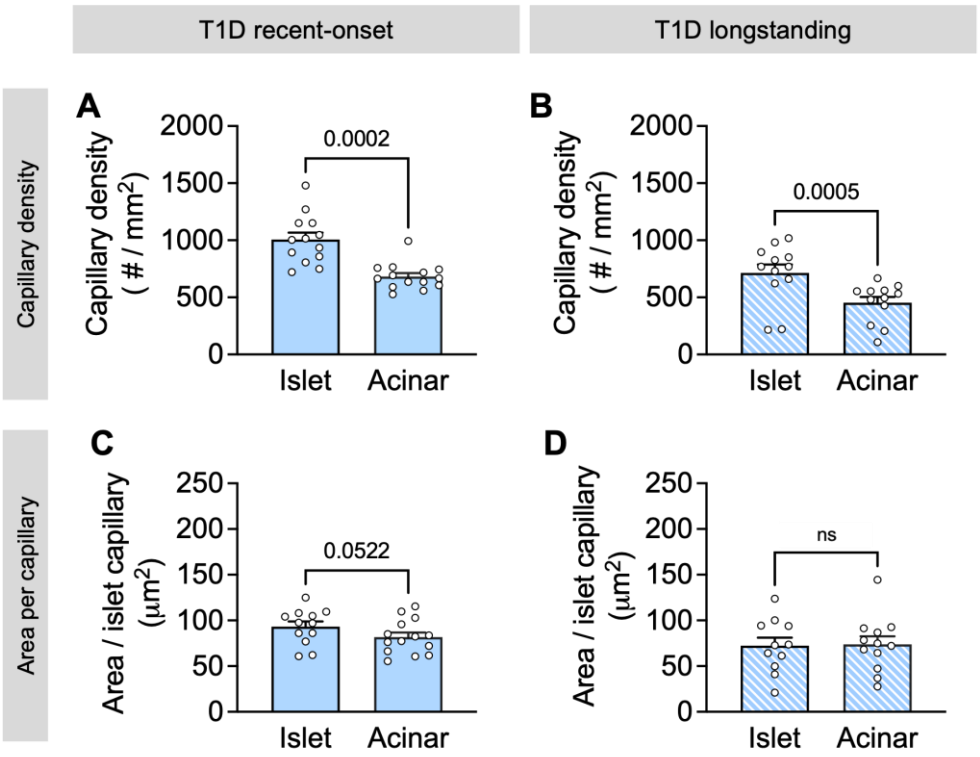

Figure 28. T1D capillary density is greater in islets than acinar tissue. Quantification (mean + s.e.m.) comparing islet and acinar capillary density (A,B) and area per capillary (C,D) for T1D recent-onset (light blue, n = 14) and T1D longstanding (light blue striped, n = 12). P-values were calculated by paired Wilcoxon t-tests in which a $p < 0.05$ is significant.

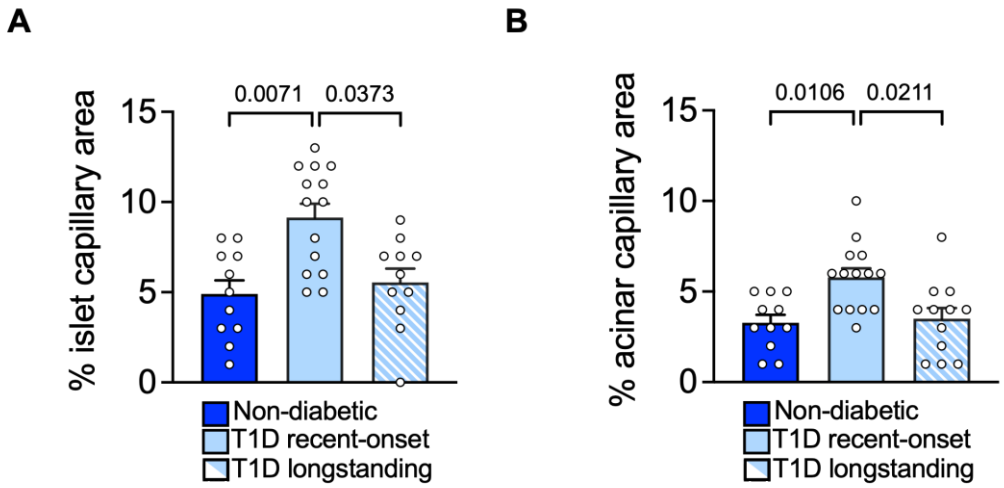

Figure 29. Percent capillary area analyses show similar trends as capillary density measurements performed in Fig 26.
Quantification (mean + s.e.m.) comparing islet (A) and acinar (B) percent capillary area for non-diabetic (dark blue; N = 11), T1D recent-onset (light blue; N = 13), and T1D longstanding (light blue striped; N = 11). See Figure 25 for islet and acinar measurement counts. P-values were calculated by Kruskal-Wallis One-Way ANOVA with Dunn's multiple comparisons tests in which a $p < 0.05$ is significant**.**

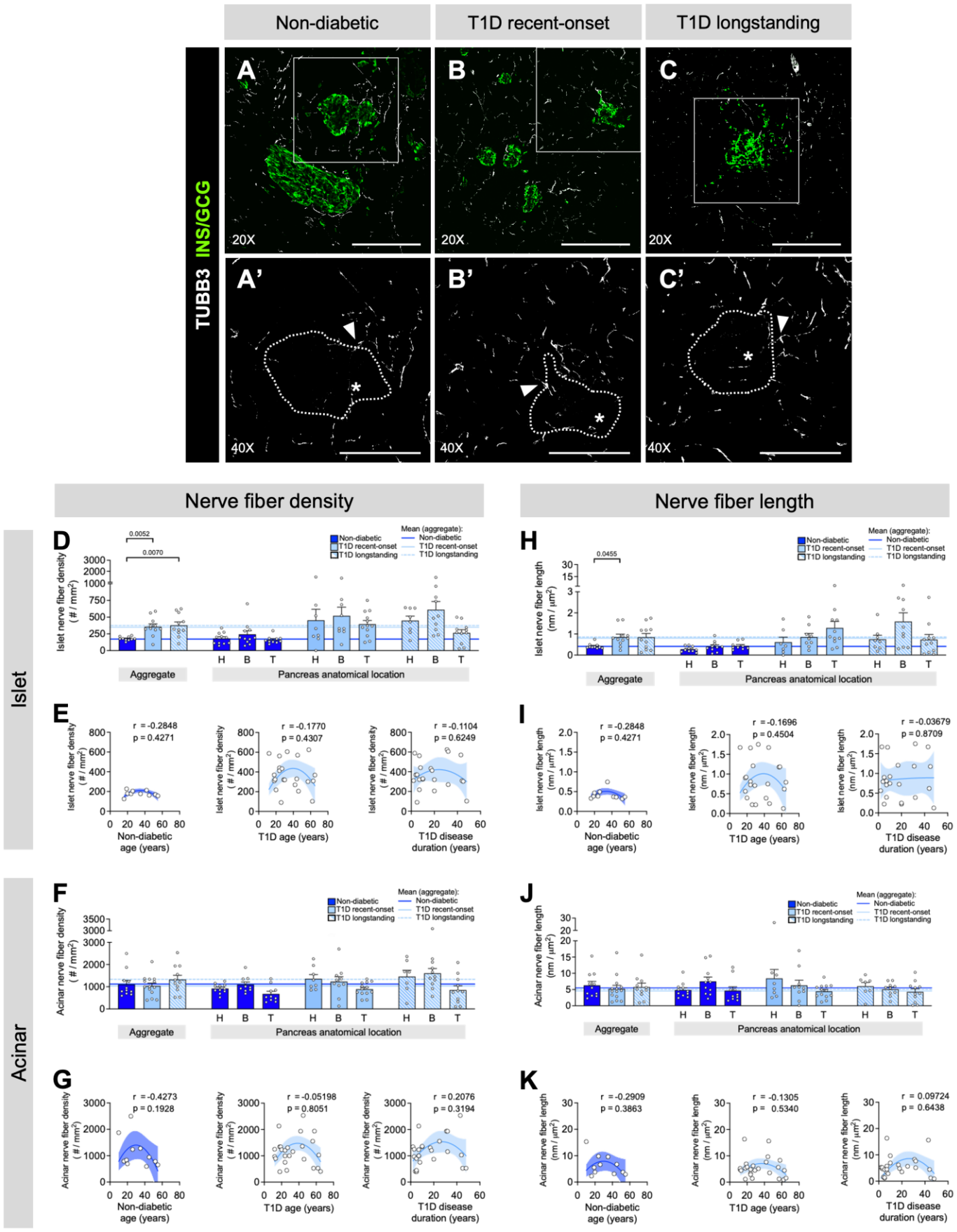

Figure 30. Islets in T1D have greater nerve fiber density compared to controls.

Figure 30. Islets in T1D have greater nerve fiber density compared to controls.
(A-C) Representative immunofluorescent staining of nerve fibers labeled with tubulin beta 3 (TUBB3; white) in pancreatic tissue sections from non-diabetic (A), T1D recent-onset (B), and T1D longstanding (D) donors. Panels (A'-C') show insets of (A-C), TUBB3 channel only, with islet area outlined. Asterisk (*) denotes intra-islet nerve fibers. A magnified image of the area denoted by a solid square is shown with an appropriate scale bar in each image. Scale bars, 100 μm. (D-K) Quantification (mean + s.e.m.) of nerve fiber density (D, E, F, G) and nerve fiber length (H, I, J, K) in islet (D-I) and acinar (F-K) tissue from pancreata of non-diabetic (dark blue; N = 11; 536 total islets, 1830 total acinar measurements), T1D recent-onset (light blue; N = 14; 417 total islets, 1258 total acinar measurements), and T1D longstanding (light blue striped; N = 11; 345 total islets, 1044 total acinar measurements) donors. Each symbol represents an individual donor; 'aggregate' graph values reflect the average data from all pancreas regions, which are stratified (H, Head; B, Body; T, Tail) to the right. Horizontal lines represent mean values and are colorized based on the donor group. (E) Islet and (G) acinar nerve fiber density in ND and T1D tissue, plotted as a function of donor age and disease duration. (I) Islet and (K) acinar nerve fiber length in ND and T1D tissue, plotted as a function of donor age and disease duration. Statistically significant p-values (< 0.05) are stated for the following statistical tests: (D, H, F, J) aggregate, Kruskal-Wallis One-Way ANOVA with Dunn's multiple comparisons tests; anatomical location, Mixed-effects One-Way ANOVA with Holm-Sidak's multiple comparison tests; (E, I, G, K) nonlinear regression analysis with lines of best fit and Spearman correlation r values denoted on each plot.

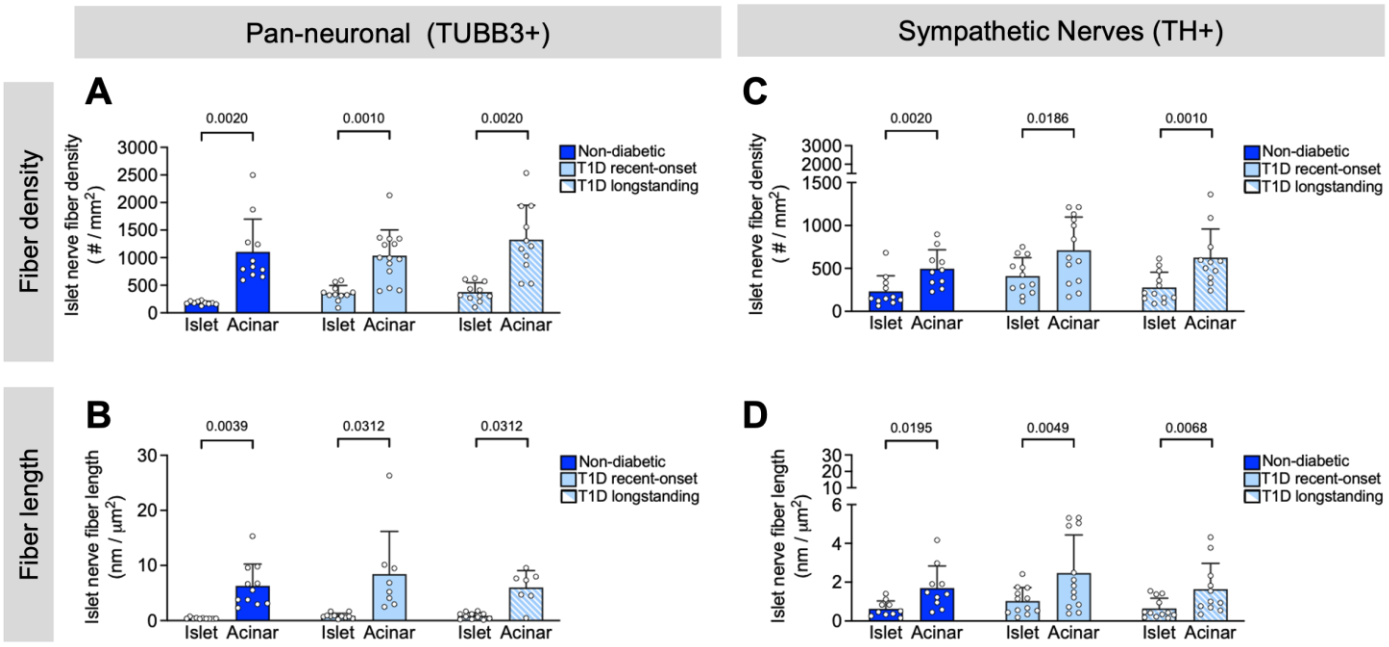

Figure 31. Pan-neuronal and sympathetic innervation are greater in acinar tissue compared to islets.

Quantification (mean + s.e.m.) comparing islet and acinar pan-neuronal (A-B) and sympathetic (C-D) nerve fiber density (A,C) and nerve fiber length (B,D) from non-diabetic (dark blue; n = 11), T1D recent-onset (light blue; n = 13), and T1D longstanding (light blue striped; n = 12). P-values were calculated by paired Wilcoxon t-tests and a $p < 0.05$ is significant.

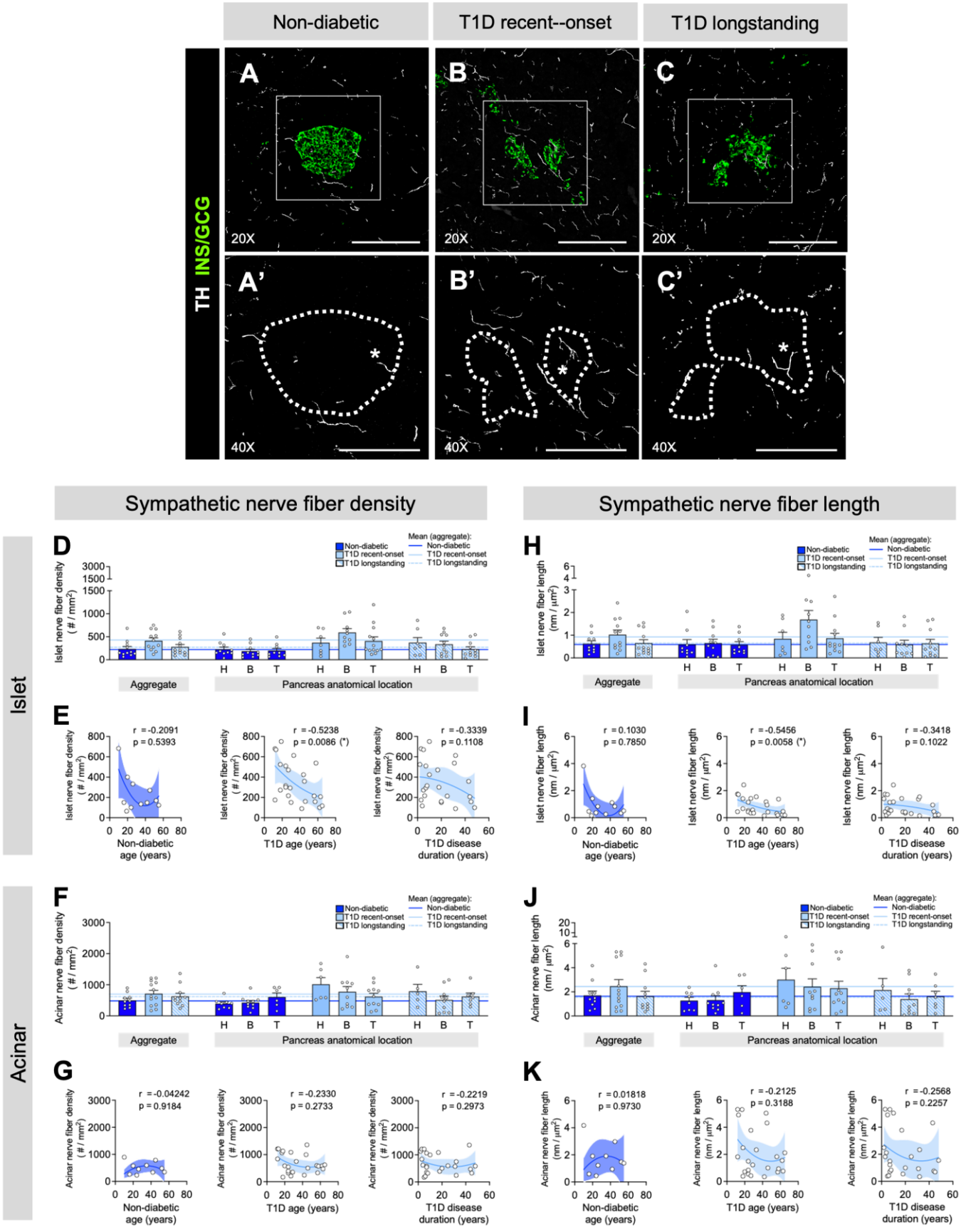

Figure 32. Sympathetic nerve fibers are not reduced in human T1D islets compared to ND.

Figure 32. Sympathetic nerve fibers are not reduced in human T1D islets compared to ND. (A-C) Representative immunofluorescent staining of sympathetic nerve fibers labeled with tyrosine hydroxylase (TH; white) in pancreatic tissue sections from non-diabetic (A), T1D recent-onset (B), and T1D longstanding (C) donors. Panels (A'-C') show insets of (A-C), TH channel only, with islet area outlined. A magnified image of the area denoted by a solid square is shown with an appropriate scale bar in each image. Scale bars, 100 μm. D-K) Quantification (mean + s.e.m.) of sympathetic nerve fiber density (D, E, F, G) and nerve fiber length (H, I, J, K) in islet (D-I) and acinar (F-K) tissue from pancreata of non-diabetic (dark blue; N = 11; 514 total islets, 789 total acinar measurements), T1D recent-onset (light blue; N = 13; 469 total islets, 864 total acinar measurements), and T1D longstanding (light blue striped; N = 12; 325 total islets, 504 total acinar measurements) donors. Each symbol represents an individual donor; 'aggregate' graph values reflect the average data from all pancreas regions, which are stratified (H, Head; B, Body; T, Tail) to the right. Horizontal lines represent mean values and are colorized based on the donor group. (E) Islet and (G) acinar sympathetic nerve fiber density in ND and T1D tissue, plotted as a function of donor age and disease duration. (I) Islet and (K) acinar sympathetic nerve fiber length in ND and T1D tissue, plotted as a: (D, H, F, J) aggregate, Kruskal-Wallis One-Way ANOVA with Dunn's multiple comparisons tests; anatomical location, Mixed-effects One-Way ANOVA with Holm-Sidak's multiple comparison tests; (E, I, G, K) nonlinear regression analysis with lines of best fit and Spearman correlation r values denoted on each plot.

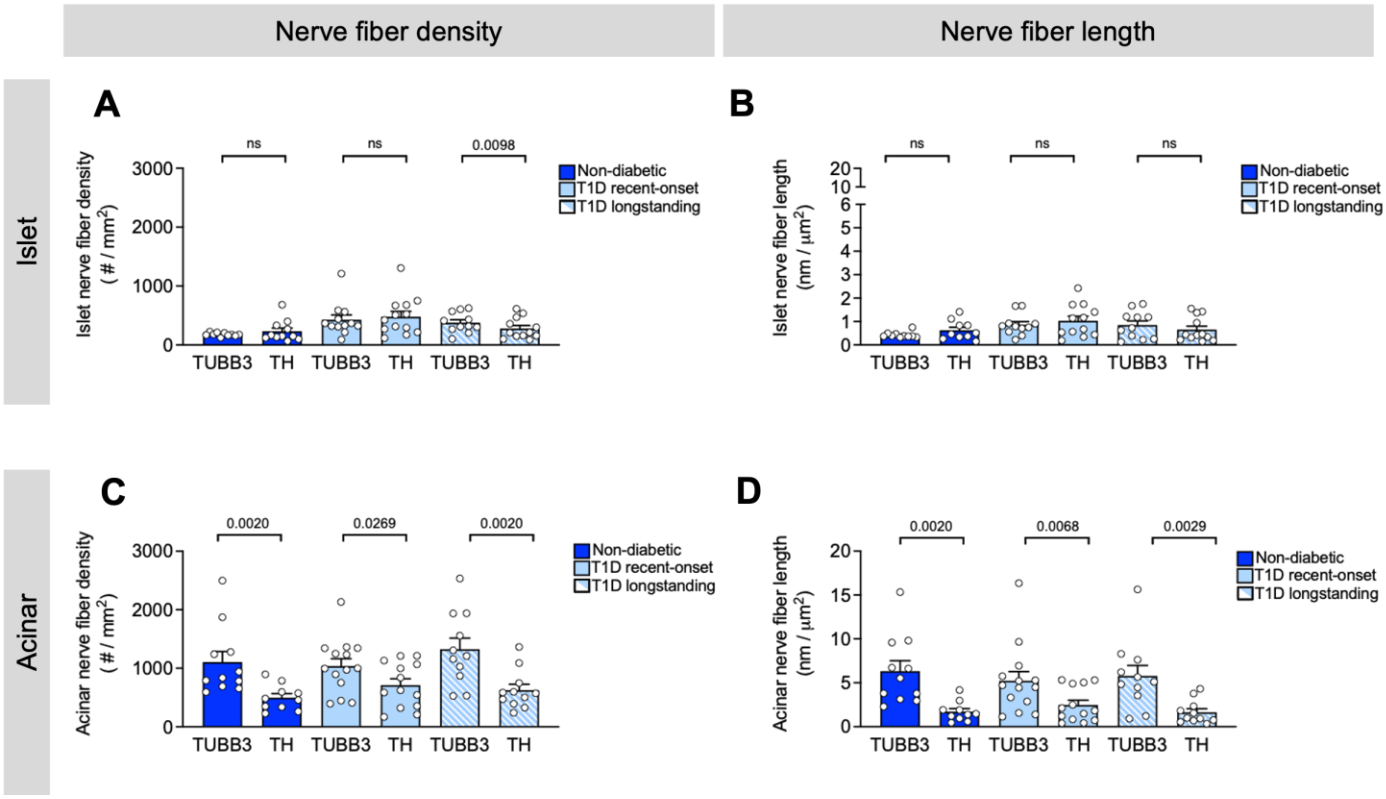

Figure 33. Sympathetic nerve fibers predominate in islets but are only a subset of acinar nerve fibers.

Quantification (mean + s.e.m.) comparing islet and acinar TUBB3+ and TH+ nerve fiber density (A, C) and nerve fiber length (B, D) from non-diabetic (dark blue; n = 11), T1D recent-onset (light blue; n = 13), and T1D longstanding (light blue striped; n = 12). P-values were calculated by paired Wilcoxon t-tests and a $p < 0.05$ is significant.

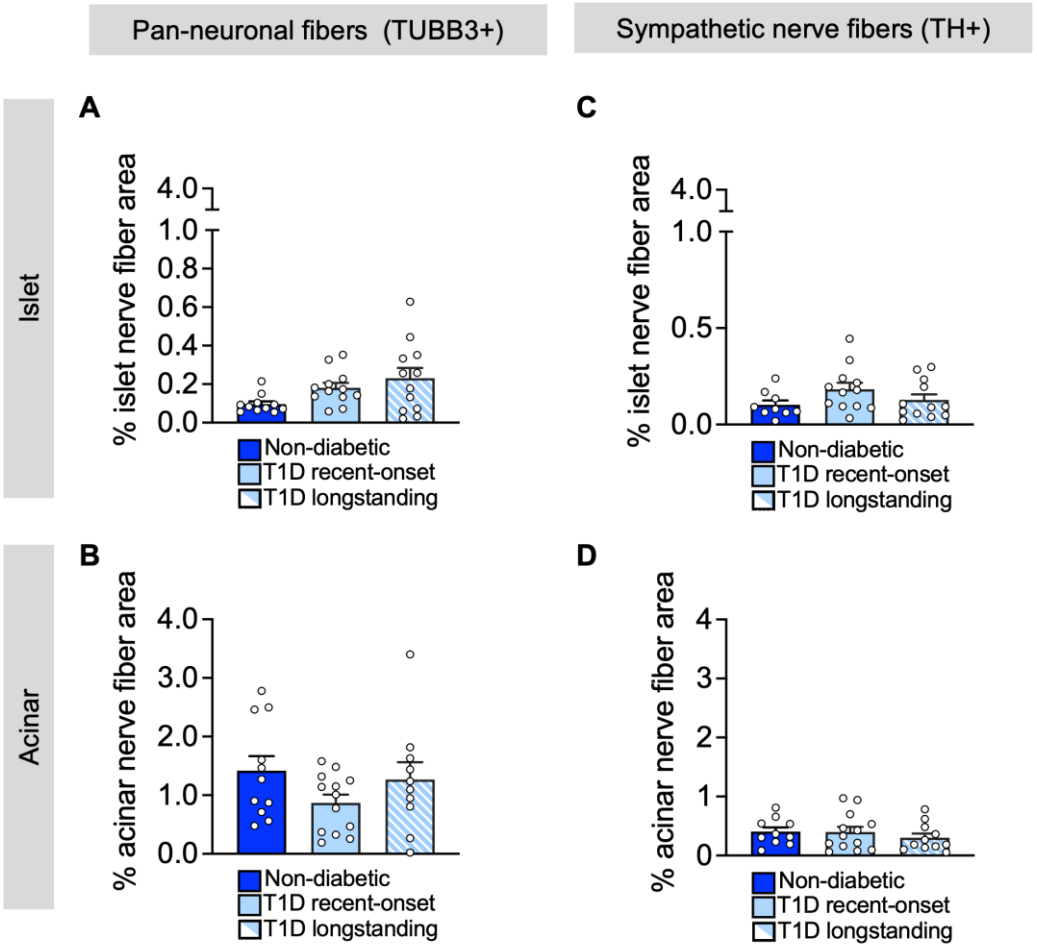

Figure 34. Nerve fiber percent area analyses show similar trends as nerve fiber density measurements performed in Fig 30 & 32.
Quantification (mean + s.e.m.) comparing islet (A,C) and acinar (B,D) percent nerve fiber area for non-diabetic (dark blue; N = 10), T1D recent-onset (light blue; N = 13), and T1D longstanding (light blue striped; N = 11). See Figure 29 & 31 for islet and acinar measurement counts. P-values were calculated by Kruskal-Wallis One-Way ANOVA with Dunn's multiple comparisons tests where no statistical significance was below a p-value < 0.05.

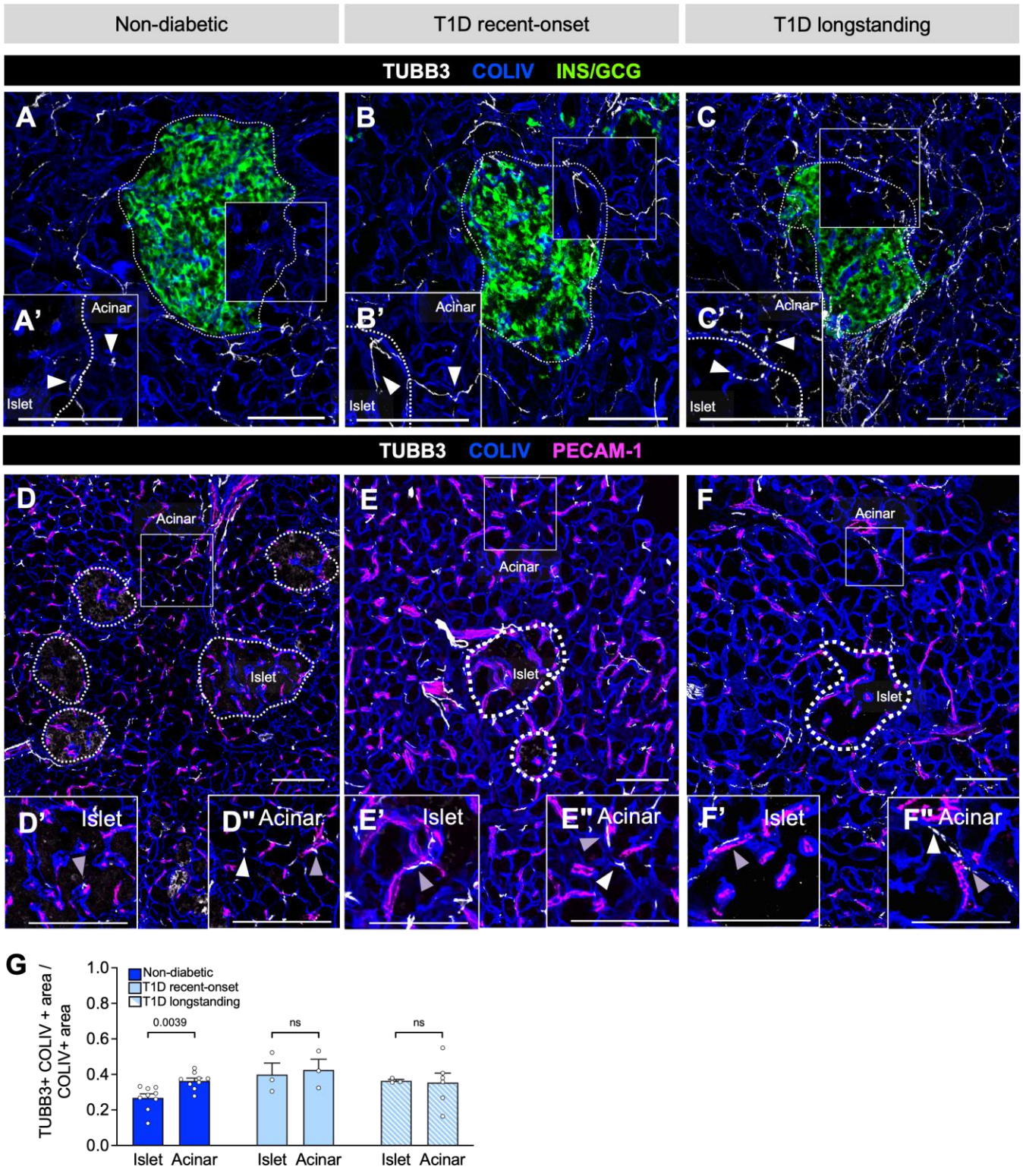

Figure 35. Pancreatic nerve fibers associate with extracellular matrix (ECM) in acinar tissue and islets in human pancreatic tissue.

Figure 35. Pancreatic nerve fibers associate with extracellular matrix (ECM) in acinar tissue and islets in human pancreatic tissue. (A-C) Representative images of pancreatic tissue from non-diabetic and T1D donors co-stained for nerves (TUBB3; white), ECM (COLIV; blue), and islets (INS/GCG; green). Insets (A'-C') show nerve fibers and ECM overlapping (white arrowheads) in both endocrine and exocrine compartments; the endocrine channel is removed for clarity. (D-F) Co-staining for nerves, ECM, and endothelial cells (PECAM-1; magenta). Insets from islet (D'-F') and acinar (D"-F") regions show nerve fibers and ECM overlapping with endothelial cells (yellow arrowheads); while white arrows distinguish regions where there is no overlap with the vasculature. Islets are outlined in white using dim TUBB3+ endocrine cell staining and differential islet and acinar COLIV+ patterns such that ECM surrounding acinar rosettes or islet capillaries. Scale bars, 100 μm. G) Quantification (mean + s.e.m.) of overlap between nerve fibers (TUBB3+) and ECM (COLIV+) of islet and acinar tissue from non-diabetic (dark blue; N = 9; 35 total islets, 46 total acinar measurements), T1D recent-onset (light blue; N = 3; 11 total islets, 13 total acinar measurements), and T1D longstanding (light blue striped N = 6; 12 total islets, 19 total acinar measurements). Manders' overlap coefficients range between 0 and 1, in which 1 indicates 100% overlap. P-values were calculated by paired Wilcoxon t-tests where ns indicates a p-value > 0.05.

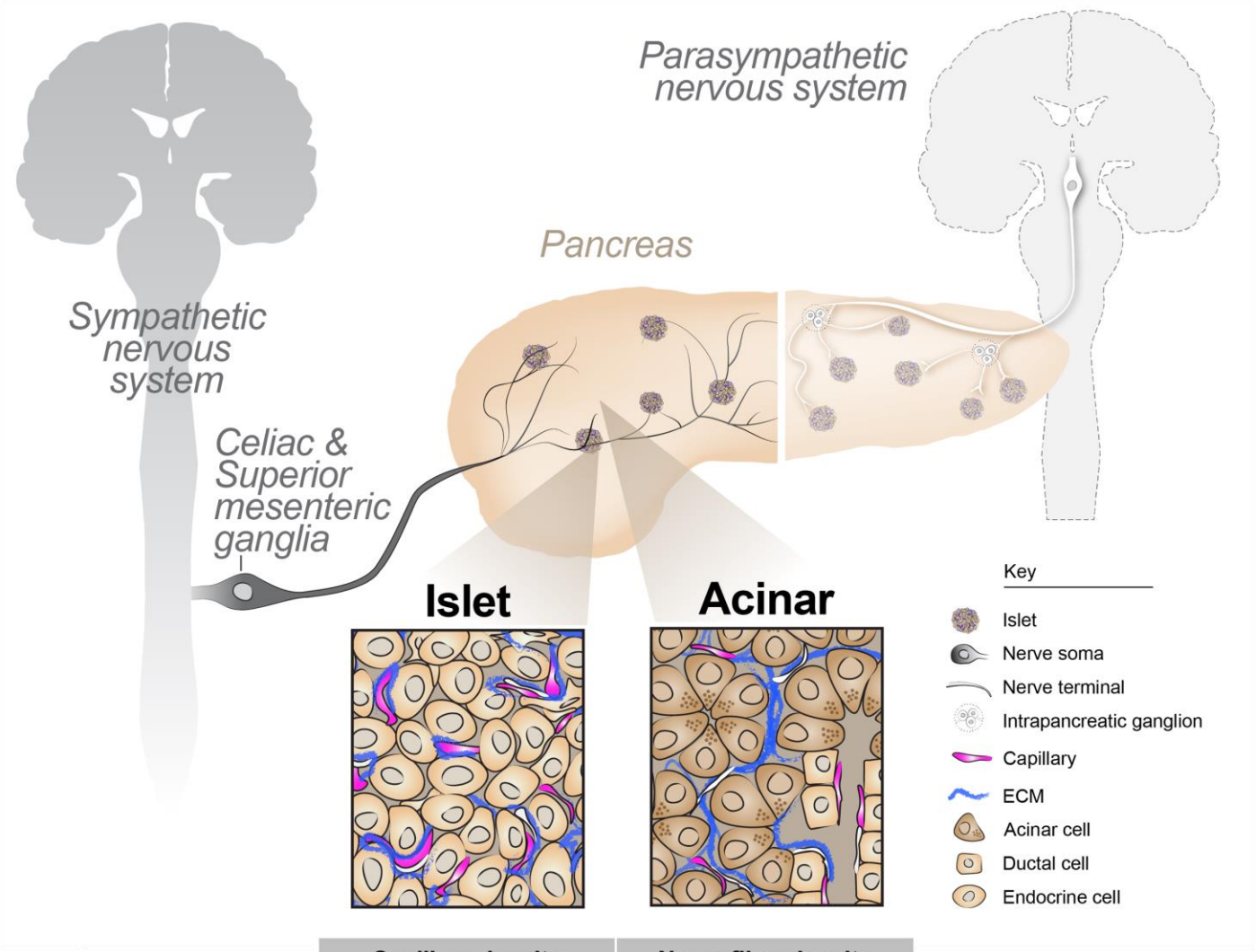

	Capillary density	Nerve fiber density
Inter-species	Mouse > Human (islet & acinar)	Mouse > Human (islet) Mouse < Human (acinar)
Non-diabetic (ND)	ND < T1D recent ND ≈ T1D longstanding	ND < T1D
T1D	T1D recent > ND, T1D longstanding	T1D recent, T1D longstanding > ND
Islet vs. acinar	Islet > acinar (Mouse, ND, & T1D)	Islet > acinar (Mouse) Acinar > islet (Human)

Figure 36. Human pancreatic neurovascular components in health and type 1 diabetes.

Figure 36. Human pancreatic neurovascular components in health and type 1 diabetes. The pancreas is intricately connected to the central nervous system and vasculature through branches of the autonomic nervous system and branching vessels. Nerve fibers and blood vessels can directly influence pancreatic function. Sympathetic projections originate in the spinal cord before extending through distal ganglia to islets. Parasympathetic nerve fibers, which were not studied here, project from intrapancreatic ganglia into islets throughout the pancreas. Islets (see inset; left) receive vascular and nerve fiber inputs that overlap with each other. Acinar tissue (see inset; right) is innervated and vascularized, with these components extending around acini. Pancreatic nerve fibers are associated with ECM within the islet and acinar tissue. There exist inter-species and disease differences in the neurovascular patterns in the pancreas, as described by the summary table. The key denotes pertinent neuronal components (nerve soma, nerve terminals, intrapancreatic ganglia), capillaries, extracellular matrix (ECM), and various pancreatic cell types (acinar, ductal, endocrine).

CHAPTER IV: HUMAN PSEUDOISLET SYSTEM ENABLES SYNCHRONOUS ASSESSMENT OF FLUORESCENT BIOSENSOR DYNAMICS AND HORMONE SECRETORY PROFILE

Text and data in this chapter is under review at the
Journal of Visualized Experimentation (Richardson*, Pettway*, et al. 2023)
* = co-first authors

Introduction

Islets of Langerhans are mini-organs scattered throughout the pancreas whose function is crucial for the maintenance of glucose homeostasis. Insulin is secreted from β cells following the metabolism of glucose, increase in ATP/ADP ratio, closure of ATP-sensitive potassium channels, depolarization of plasma membrane, and the influx of extracellular Ca^{2+} [46]. Glucagon secretion from α cells is less understood, but it has been postulated that intracellular and paracrine pathways contribute to glucagon granule exocytosis[110,287,288]. Both type 1 and type 2 diabetes are associated with islet cell dysfunction[223,289,290]. Therefore, elucidating the intracellular signaling pathways mediating islet hormone secretion is essential to understanding physiologic and pathologic mechanisms in pancreatic islets.

The spherical architecture of islets presents certain obstacles to experimentation. These challenges include islet size variation and the 3D nature of islets reducing viral transduction within the islet core among many others. To overcome these challenges, we developed a novel system in which we disperse human islets into single cells, virally transduce these cells with constructs of our choosing, and allow for their spontaneous reaggregation, forming the islet-like structures we now refer to as pseudoislets[32]. Compared to islets from the same donor that have been cultured in parallel, these pseudoislets are similar in morphology, size, endocrine cell proportions, and hormone secretion[32]. We have also validated our ability to express viral constructs throughout the pseudoiset[32], overcoming a previous barrier to uniform genetic manipulation of primary human islets[32].

Here, we combine our pseudoislet system with a microfluidic device to overcome live-cell imaging limitations with traditional cell perifusion systems. We constructed a microperifusion system that exposes pseudoislets in a microchip to a steady flow of secretagogues via a peristaltic pump[238]. The microchip has a transparent glass bottom and can be mounted on a confocal microscope to assess intracellular signaling dynamics via changes in biosensor fluorescence intensity. Simultaneously, the microperifusion effluent is collected by a fraction collector for subsequent analysis of insulin and glucagon

secretion[32]. Thus, our optimized microperifusion system allows for the monitoring of intracellular signaling and synchronous quantification of hormone secretion from pseudoislets.

To harness the utility of this system, we expressed the cyclic adenosine monophosphate (cAMP) Difference Detector in situ (cADDis) or GCaMP6f biosensors in human pseudoislets to assess cAMP dynamics and hormone secretion. The cADDis biosensor is composed of a circularly permuted green fluorescent protein (cpGFP) positioned in the hinge region of EPAC2 connecting its regulatory and catalytic regions. The binding of cAMP to the regulatory region of EPAC2 elicits a conformational change in the hinge that increases fluorescence from the cpGFP[291]. The GCaMP6f biosensor is composed of the calmodulin-binding peptide M13, a circularly permuted GFP protein fused with calmodulin[292]. Intracellular messengers such as cAMP and Ca^{2+} elicit insulin secretion after upstream activation of G-protein coupled receptors or upstream membrane depolarization[291,293]. The live-cell imaging coupled with microperifusion helps to connect intracellular cAMP dynamics with islet hormone secretion.

In this protocol, we generated cADDis or GCaMP6f-expressing pseudoislets to monitor cAMP or Ca^{2+} responses in α and β cells to various stimuli: low glucose (2 mM glucose; G 2), high glucose and isobutylmethylxanthine (IBMX), phosphodiesterase inhibition [20 mM glucose + 100 μM isobutylmethylxanthine; G 20 + IBMX], and low glucose plus epinephrine (Epi) (2 mM glucose + 1 μM Epi; G 2 + Epi). We highlight steps leading to the preparation of the microperifusion apparatus for live-cell imaging experiments, loading of pseudoislets into the microchip, synchronous live-cell imaging and microperifusion, and analysis of biosensor traces and hormone secretion by microplate-based hormone assays.

Results

Generating biosensor-expressing human pseudoislets

We applied adenoviral transduction to dissociated native human islet cells and created human pseudoislets expressing cAMP biosensor, cADDis (**Figure 37**); donor summary in **Table 3**). **Figure 37B** shows the reaggregation of the transduced human islet cells over time, with fully formed pseudoislets observed after 6 days of culture. Cells begin to show visible cADDis fluorescence within 48 hours, with high expression of the biosensor in transduced cells by the end of the culture period. Using this protocol, we were able to generate pseudoislets with an average transduction efficiency of 60% in α cells and 95% of β cells (**Figure 37C**; see **Table 6-7** for immunohistochemistry details). GCaMP transduction efficiencies were similar to cADDis transduction (**Figure 37E-F**).

Live-cell microperifusion set-up

Our integrated microfluidic and live-cell imaging platform is highlighted in **Figure 38**. After harvesting the cADDis-expressing pseudoislets and allowing them to incubate in fresh media overnight, pseudoislets are loaded into the center of a prewetted well on the microchip. The microchip is then clamped in a holder and placed on the microscope stage. Inside the environmental chamber attached to the microscope and maintained at 37 ^{o}C, pseudoislets are perifused with media containing α and β cells secretagogues, which are pumped through a de-bubbler to prevent the introduction of air bubbles into the system. pseudoislets in the microchip are perifused at the flow rate of 100 µL/min, with the effluent being collected at 2-minute intervals via a fraction collector (**Figure 38A-B**). The glass bottom of the microchip well allows to capture the cADDis fluorescence intensity of multiple pseudoislets in a field view, which is essential for later analysis (**Figure 38C**).

Human pseudoislet cAMP and hormone secretion dynamics

Figure 39 shows representative results using our described protocol on cADDis-expressing pseudoislets generated from native islets isolated from three human donors without diabetes. We perifused cADDis-expressing pseudoislets with 2 mM glucose (G 2), 20 mM glucose, and the phosphodiesterase inhibitor isobutylmethylxanthine (IBMX; G 20 + IBMX), and 2 mM glucose plus epinephrine (G 2 + Epi). This protocol elicits known intracellular pathways that enhance cAMP within α and β cells (**Figure 39A-B**). Our microperifusion setup facilitates the synchronous collection of intracellular cAMP dynamics through cADDis fluorescence and hormone secretion (**Figure 39C-E**). To ensure experimental rigor, we performed experiments on pseudoislets from the same donor in 2-3 replicates and plotted aggregate values in **Figures 39C-E, 39D', 39E'**. With exposure to 2mM glucose, the relative cADDis intensity was low and stable, as was insulin secretion (**Figure 39C, 39D**). When pseudoislets were exposed to 20mM glucose + IBMX, there was a robust increase in intracellular cAMP concentration, as evidenced by an increase in relative cADDis intensity (**Figure 39C**). This increase was most likely from both β and α cells, as evidenced by the concomitant marked increases in insulin and glucagon secretion (**Figure 39D, 39E**)**.** Exposure of pseudoislets to G 2 + Epi increases intracellular cAMP concentration **(Figure 39C)** and this is associated with an increase in glucagon secretion (**Figure 39E**). The observation that the cAMP response to G 2 + Epi is relatively smaller compared to the IBMX response is likely due to a combination of the lower transduction efficiency of cADDis adenoviral construct in α cells vs β cells **(Figure 39D)** plus α cell-specificity of this signal **(Figure 39E**). Therefore, based on known cAMP-mediated signaling pathways in primary human β and α cells, we successfully demonstrated the utility of our integrated platform to co-register relative fluorescence intensity of cADDis biosensor and β and α cell hormone secretory profiles across technical and biological replicates.

Human pseudoislet GCaMP and hormone secretion dynamics

Figure 40 demonstrates a disease-relevant utilization of our biosensor pseudoislet system. We utilized fluorescence-activated cell sorting (FACS) to control the proportion of β and α cells in addition to choosing which cell type was transduced with GcAMP. We perifused GcAMP-expressing pseudoislets with 2 mM glucose (G 2), 16.7 mM glucose (G 16.7) and 2 mM glucose plus epinephrine (G 2 + Epi). This protocol elicits known intracellular pathways that enhance intracellular Ca^{2+} levels within α and β cells (**Figure 40A**). We purified human β and α cells prior to recombining these cell populations to form pseudoislets that were 50% β cells (GCaMP transduced) and 50% α cells (untransduced; **Figure 40B**). When pseudoislets with 50% β-GCaMP and 50% α-untransduced are exposed to G 16.7, there is an increase in intracellular Ca^{2+} concentration, as evidenced by an increase in relative GCaMP intensity and insulin secretion (**Figure 40B**). Exposure of pseudoislets to G 2 + Epi increases glucagon secretion but there was very little change in GCaMP intensity presumably due to α cells not being transduced (**Figure 40B**). To mimic islets devoid of β cells and enriched with α cells similar to the type 1 diabetes setting, we purified α cells from dispersed human pancreatic islets with FACS to generate α cell-only pseudoislets transduced with GCaMP (**Figure 39C**). When α cell only-GCaMP pseudoislets were exposed to G 2, G 16.7 or G 2 + Epi, there is no intracellular Ca^{2+} concentration or insulin secretion, but glucagon secretion occurs when these pseudoislets are exposed to low glucose (**Figure 40C**). This highlights the utility of our system to directly manipulate the cellular makeup of pseudoislets and subsequently monitor their intracellular signaling dynamics.

Discussion

The integration of a microperifusion system, biosensor-expressing pseudoislets, and laser-scanning confocal microscopy allows for synchronous assessment of intracellular signaling events and dynamic hormone secretory profiles. The dynamic microperifusion system can deliver a series of different stimuli to the pseudoislets and provides for the collection of the effluent, in which insulin and glucagon concentration can be measured by commercially available ELISA. Concurrently, live cell imaging of biosensor-expressing pseudoislets is performed using a confocal microscopy platform with a real-time recording of intracellular signaling events in response to various stimuli. Plotting the biosensor signal and hormone profile over time allows a direct comparison of intracellular events and their influence islet hormone secretion.

Multiple considerations are key to the success of the presented protocol. These include generating biosensor-expressing pseudoislets and constant flow rate during each experiment without pseudoislet movement. At a flow rate of 100μL/min and 2-minute

fraction collection, the perifusate volume of each fraction is 200 µL and should not fluctuate more than 10 µL/fraction. In addition, while the cellSens software can adjust to a minor pseudoislet movement in the XY plane within the field of view, pseudoislets that move out of the field of view in the course of microperifusion experiment cannot be analyzed. Thus, it is important to catch any leaks and movements early on during the experiment such that attempts can be made to fix the issue. A summary of potential challenges, their common causes, solutions, and tips to prevent them from occurring are summarized in **Table 10**. Nevertheless, this protocol includes multiple opportunities to anticipate issues, such as performing a "test experiment" prior to loading the chip and monitoring pseudoislets via the microscope for significant movement during the 30-minute wash period prior to image acquisition and microperifusion fraction collection.

One limitation is that the field of view on the current confocal microscopy platform doesn't allow to capture all pseudoislets within the microchip at once. While a minimum of 30 pseudoislets are required to reliably detect insulin and glucagon in the microperifusates, only a subset can be imaged at a 20x magnification. Loading the pseudoislets into the center of the well maximizes the number that can be captured in the field of view. In addition, while the microchip is equipped with three wells, the integration with confocal microscopy limits measurements to one well at a time, requiring technical replicates to be done in series rather than in parallel. Lastly, in our current approach, we did not use a cell-specific biosensor delivery and thus collected the whole pseudoislet fluorescence which was compared to α and β cell secretory outputs using stimuli that elicit a robust insulin (20 mM glucose + IBMX) or glucagon (2 mM glucose + Epi) secretion.

The described platform allows for a novel strategy to synchronize interrogation of intracellular signaling events using biosensor and hormone secretion. This system can be further adapted to interrogate functional perturbations introduced by RNA interference (siRNA or shRNA) or CRISPR-mediated gene targeting strategies. These methods can be used to determine the biological effect of pathways of interest on a multitude of intracellular or extracellular events. Additionally, selective transduction of a particular cell type and/or exposure to cell-specific stimuli would allow for targeted interrogation of intracellular events of a specific cell type within the context of the human islet. This is opposed to more conventional techniques, where intracellular molecules such as Ca^{2+} are measured in the single-cell state via dyes, and the impact of paracrine signaling within the islet on cell function is lost. For example, α cells within human pancreatic islets could be purified using cell surface markers and subsequently transduced with the commonly used genetically encoded calcium biosensor GCaMP to assess intracellular calcium dynamics. These virally transduced cells could be re-combined with other untransduced islet cells to form pseudoislets or left to re-aggregate on their own to generate α cell-only pseudoislets that compositionally resemble islets in type 1 diabetes. Thus, our live cell

imaging with a microperifusion system overcomes previous challenges in islet biology while broadening our knowledge of integral cellular processes.

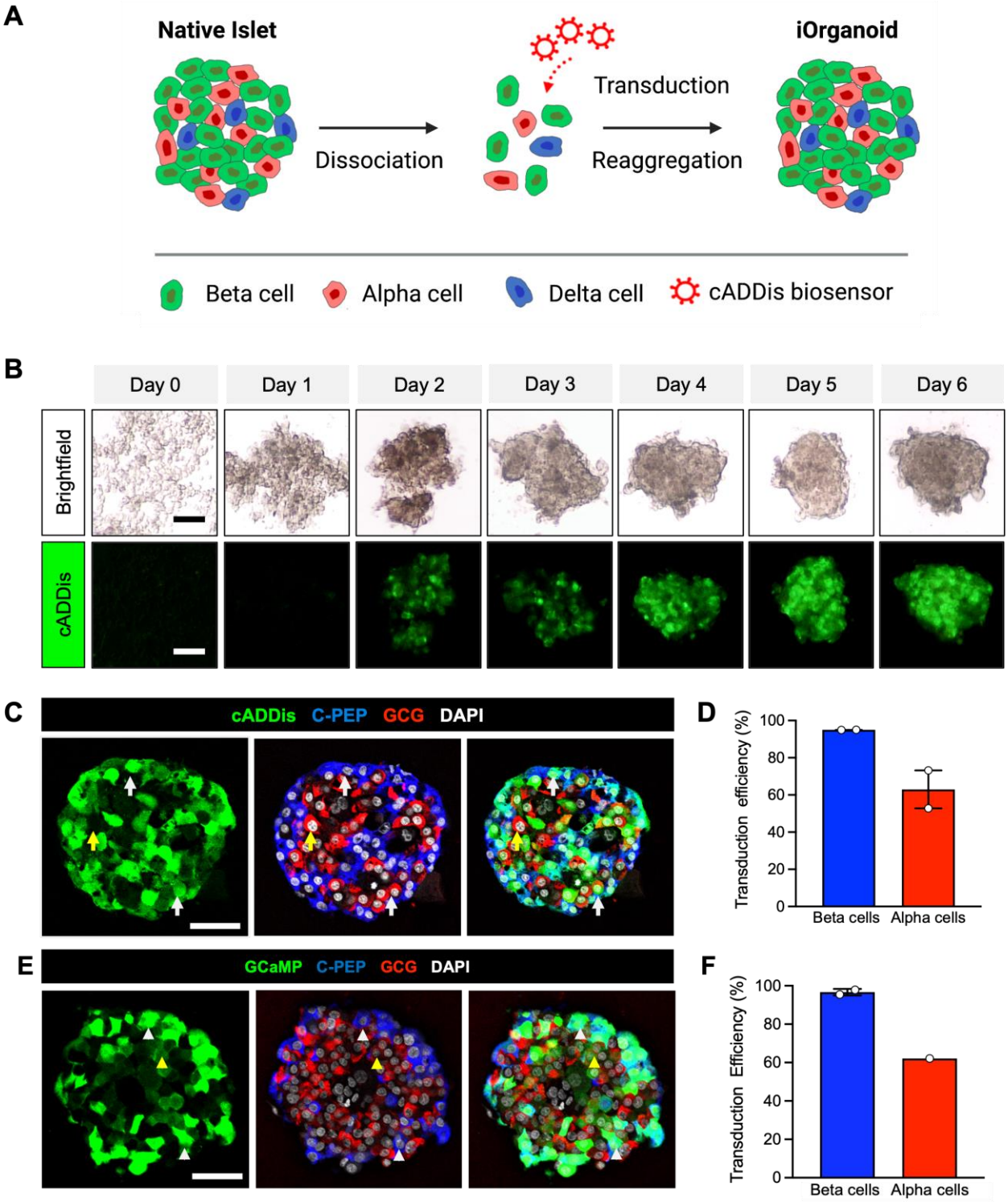

Figure 37. Formation of biosensor-expressing human pseudoislets.

Figure 37. Formation of biosensor-expressing human pseudoislets.
(A) Schematic showing primary human islet dissociation, transduction with biosensor construct in a single cell state, and reaggregation. Following reaggregation, pseudoislets are harvested and undergo synchronous live-cell imaging and microperifusion. Protocol steps are indicated throughout the schematic. (B) Representative images capturing the formation of a cADDis-expressing pseudoislet during a 6-day reaggregation period; top: brightfield with contrast, bottom: cADDis fluorescence. Scale bar = 50 μm. (C) Representative images of a cADDis-expressing pseudoislet (green) with α and β cells visualized by C-peptide (CPEP, blue) and glucagon (GCG, red) labeling, respectively. DAPI (white) was used as nuclear counterstain. White arrows highlight transduced α and β cells. The yellow arrow points to an untransduced α cell. Scale bar = 100 μm. (D) Quantification of transduction efficiency at MOI 1000 in β and α cells by a HALO cytonuclear algorithm (N = 2 donors).

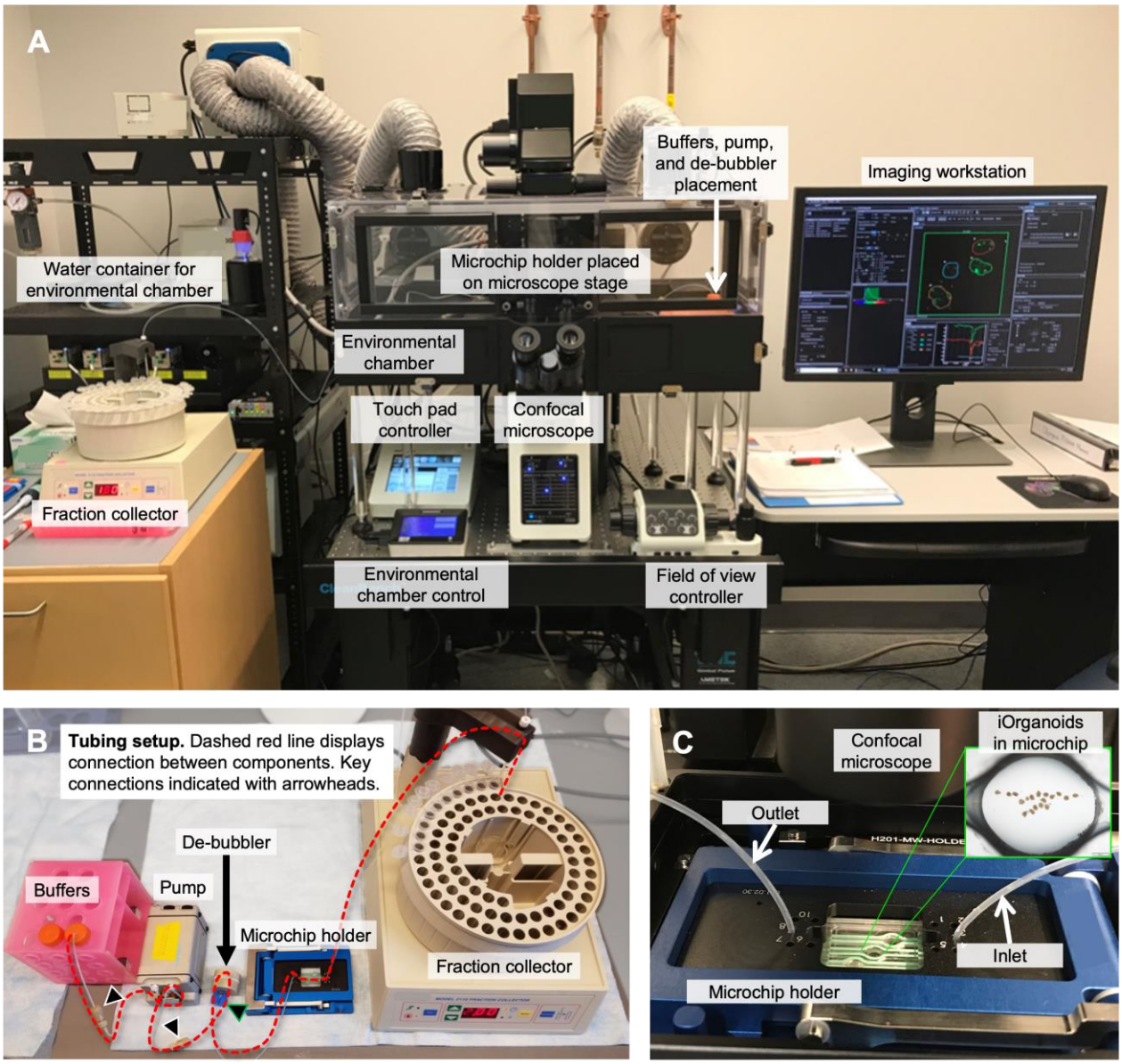

Figure 38. Integrated live cell imaging with microperifusion system.

Figure 38. Integrated live cell imaging and microperifusion system.
(A) Overview of live cell imaging and microperifusion system components. Pseudoislets in a microfluidic device (microchip) are placed on the stage of confocal laser-scanning microscope enclosed within environmental chamber. This configuration allows to temporally resolve intracellular changes in biosensor fluorescence during dynamic response to a series of well-defined secretagogues while collecting pseudoislet perifusate fractions for synchronous measurement of insulin and glucagon secretion and further integration with intracellular signaling events. (B) Components of the microfluidic platform outside of the environmental chamber. Fluid directionality is as follows: 1. Secretagogue-containing tubes → 2. 0.01” tubing → 3. Peristaltic pump tubing (0.02” inner diameter) → 4. 0.01” tubing → 5. De-bubbler → 6. Microchip inlet (0.01” tubing) → 7. Microchip holder/ microchip → 8. Microchip outlet (0.01” tubing). Note: 0.01” tubing is joined to the peristaltic pump tubing with conical adapters (white arrowheads). The tubing is plugged into the de-bubbler via a nut and ferrule (green arrowhead). The dashed red line displays the connectivity between components. (C) Close-up view of the microchip and holder within the environmental camber mounted on the confocal microscope stage.

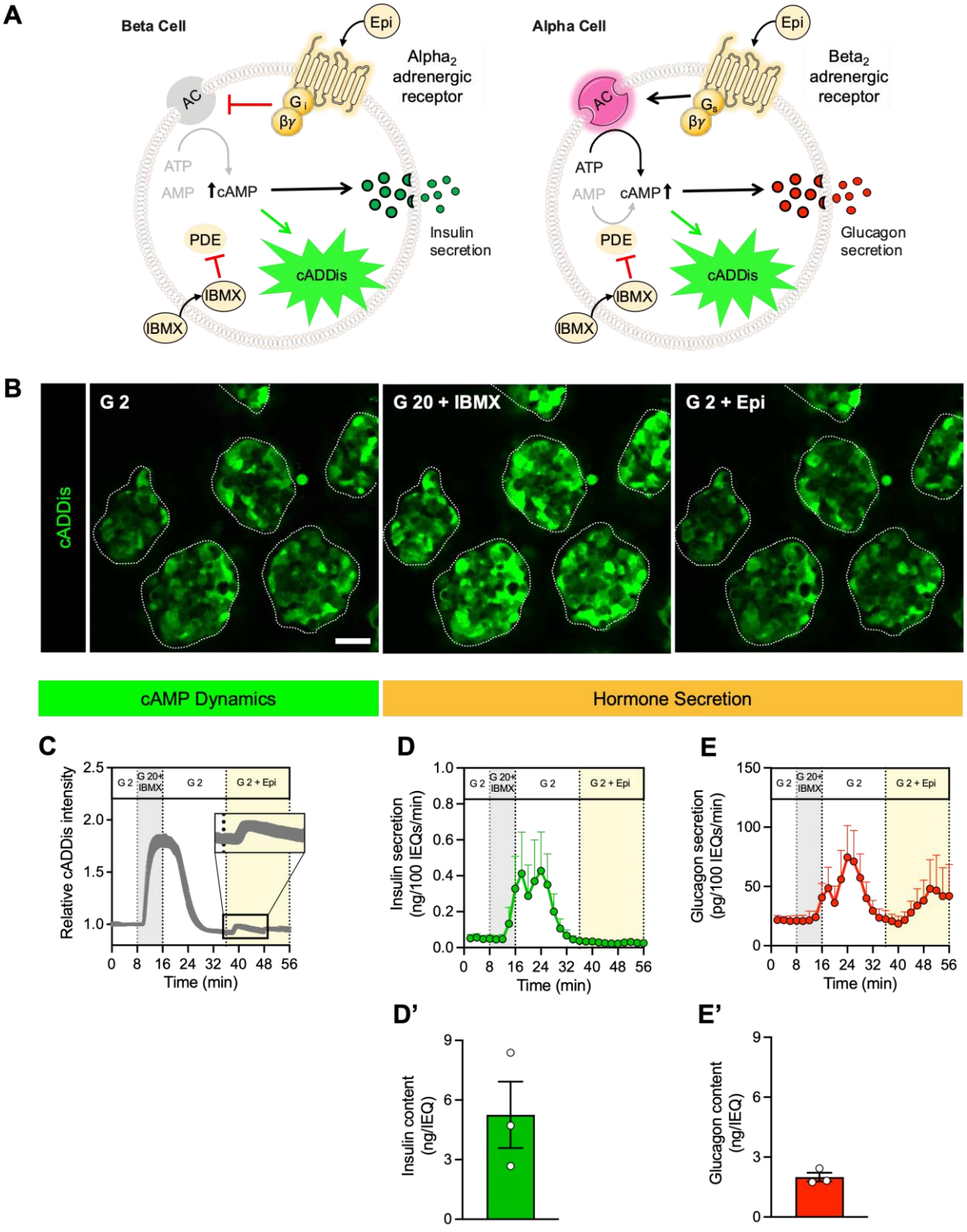

Figure 39. Human pseudoislet cAMP & hormone secretion dynamics.

Figure 39. Human pseudoislet cAMP & hormone secretion dynamics.
(A) Schematics of secretagogue-induced cADDis fluorescence and hormone secretion in β and α cells. In β cells, epinephrine (Epi) binds Gi-coupled α_2-adrenergic receptors, which leads to the inhibition of AC, decreased cAMP, and reduced insulin secretion. In α cells, Epi stimulates Gs-coupled β_2-adrenergic receptors, leading to the activation of adenyl cyclase (AC) and an increase in intracellular cAMP. In both cell types, IBMX, a phosphodiesterase (PDE) inhibitor, prevents the degradation of intracellular cAMP and promotes hormone secretion. The binding of free intracellular cAMP causes conformational changes in the cADDis protein, causing an increase in fluorescence intensity. (B) Representative images of cADDis-expressing pseudoislets during live cell imaging in response to G 2 (2 mM glucose), G 20 + IBMX (20 mM glucose + IBMX), and G 2 + Epi (2 mM glucose + Epi). Pseudoislets are outlined in white and the secretagogue type is indicated in the top left corner. Scale bar = 50 μm. (C) Relative cADDis fluorescence over time averaged across cADDis-expressing pseudoislets made from human islets of three organ donor preparations. (D) Aggregate insulin and (E) glucagon secretion in response to indicated secretagogues. Data is normalized to islet volume expressed in islet equivalents (IEQs). pseudoislets were prepared from 3 human islet donors and analyzed using 2-3 technical replicates/donor. Islet cells were transduced with cADDis adenoviral construct at MOI 500 (N = 1) or 1000 (N = 2). (D', E') pseudoislet hormone content.

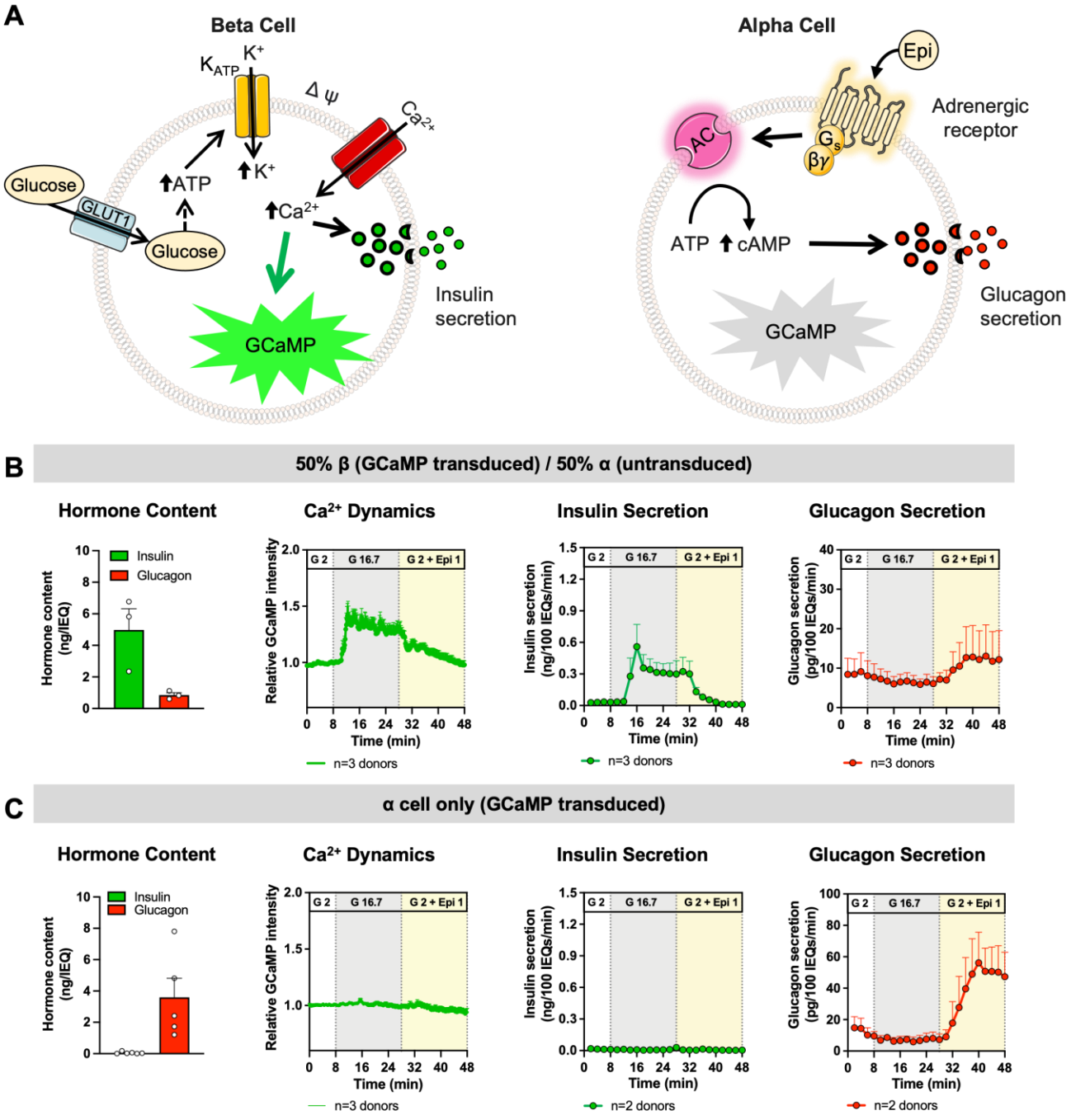

Figure 40. Human pseudoislet GCaMP & hormone secretion dynamics.

Figure 40. Human pseudoislet GCaMP & hormone secretion dynamics.
(A) Schematics of secretagogue-induced GCaMP fluorescence and hormone secretion in β and α cells. In β cells, glucose stimulates insulin secretion through the increase of intracellular ATP and the closure of K-ATP channels leading to membrane depolarization (ΔΨ) and causing the influx of calcium. In α cells, Epi stimulates Gs-coupled β_2-adrenergic receptors, leading to the activation of adenyl cyclase (AC) and an increase in intracellular cAMP. In β cells, epinephrine (Epi) binds Gi-coupled α2-adrenergic receptors, which leads to the inhibition of AC, decreased cAMP, and reduced insulin secretion. The binding of free intracellular Ca^{2+} causes conformational changes in the GCaMP protein, causing an increase in fluorescence intensity. (B-C) pseudoislets were generated from FACS-sorted islets cells recombined to make pseudoislets with (B) 50% β cells transduced with GCaMP and 50% untransduced α cells or (C) only untransduced α cells. (Left) pseudoislet hormone content. (Middle) Relative GcAMP fluorescence over time in response to low glucose (G 2), high glucose (G 16.7), and low glucose + Epi (G 2 + Epi) averaged across GcAMP-expressing pseudoislets. (Right) Aggregate insulin and glucagon secretion in response to indicated secretagogues. Data is normalized to islet volume expressed in islet equivalents (IEQs). pseudoislets were prepared from 2-3 human islet donors and analyzed using 2-3 technical replicates/donor. Islet cells were transduced with GcAMP adenoviral construct at MOI 500.

Table 10. Troubleshooting Guide.

Observation	Potential Causes	Solutions	Prevention
Poor pseudoislet formation	a. Primary islets not picked to high purity b. Low cell viability and counts c. Non-nutrient enriched media	d. High primary islet quality e. Handpicking primary islets to intentionally exclude exocrine tissue f. Vanderbilt Pseudoislet Media (VPM) improves pseudoislet survival and formation (see Walker, Haliyur, et. al. 2020)	Consider the attributes of the donor such as age, BMI, HbA1C, islet morphology, and culture time (< 2days). Also, perform quality control assays to ensure health of islets such as DTZ and FDA/PI staining. Use care when handpicking primary islets and repeatedly pass over picked plates to exclude any remaining exocrine tissue.
Decreased perifusate flow during run (fraction volume < 200 µL)	a. Tubing Leak b. Chip Leak c. Clog d. Pump Malfunction e. Deteriorating de-bubbler filter f. Crack in chip g. Broken gaskets	h. Ensure all tubing connections around leak are properly sealed i. Ensure chip is properly sealed and free of cracks; replace gaskets j. Identify location of fluid back-up and replace tubing k. Replace pump batteries; increase pump speed l. Replace filter	Performing a test run using an empty microchip prior to the experiment helps anticipate developing issues. Filtering secretagogues prevents clogs during the run.
Significant pseudoislet	a. Turbulent flow	c. See “Clog” and “Pump	A 30 min wash in baseline media prior to beginning the

movement during run	b. Potential leak (see above)	Malfunction" above d. Catch leaks and movement early on during a run	run helps settle pseudoislets.
Few pseudoislets imaged concurrently	a. Pseudoislets dispersed throughout the well	b. Load pseudoislets into the center of the well c. Once dispensed into the well, maneuver the pseudoislets into the center with a gel loading tip.	Stabilizing the pipette tip with the non-dominant hand and slowly dispensing pseudoislets into the well greatly improves loading accuracy.

CHAPTER V: ELUCIDATING THE ROLE OF NTPDASE3 AND PURINERGIC SIGNALING IN HUMAN ISLET HORMONE SECRETION

Text and data in this chapter are part of a manuscript under preparation (Richardson, et al., 2023).

Introduction

A central theme of this Dissertation is to better understand the role of the pancreatic microenvironment in insulin and glucagon secretion. Autocrine and paracrine signals such as insulin, glucagon, somatostatin, neurotransmitters, nucleotides (e.g., ATP, ADP, AMP), and nucleotide derivatives (e.g., adenosine) directly affect hormone secretion[95,294–296]. ATP is co-secreted with insulin, further implicating this molecule and its derivatives in modulating islet hormone secretion[135,297]. Abnormal insulin and glucagon secretion is observed in individuals with both type 1 diabetes (T1D) and type 2 diabetes (T2D)[223,255,298]. A better understanding of factors that control islet hormone secretion is fundamentally important for understanding islet physiology and advancing diabetes therapies.

In **Chapter III**, I examined the neurovascular architecture in islets and whether it was altered in T1D[76]. In this chapter, I will focus on one aspect of regulated insulin secretion, namely the purinergic system. The role of the purinergic system in islet physiology is incompletely defined and will be the subject of this Dissertation. First, I provide an overview of the purinergic system before detailing studies mapping the pancreatic purinergic system. Then I describe the functional studies performed in a novel mouse model and human pseudoislets to elucidate the role of a β cell-specific purinergic ecto-enzyme, NTPDase3, in modulating insulin secretion.

Purinergic receptors bind extracellular nucleotides and impact signal transmission

Extracellular nucleotides engage intracellular signaling cascades thru the activation of two purinergic receptor subtypes (**Table 11** & **Figure 41**): ionotropic (P2X) and metabotropic (P2Y and P1).

Table 11. Purinergic Receptors

Receptor Family	Receptor Names	Ligand(s)
P2X (ion channels)	P2RX1, P2RX2, P2RX3, P2RX4, P2RX5, P2RX6, P2RX7	ATP
P2Y (GPCRs)	P2RY1, P2RY2, P2RY4, P2RY6, P2RY11, P2RY12, P2RY13, P2RY14	ATP, ADP, UTP, UDP
P1 (GPCRs)	A1, A2A, A2B, A3	Adenosine

- P2X receptors are ion channels that open once ATP, their primary agonist, binds. There are seven members of the P2X receptor family, P2X1-7[240]. The tissue distribution, ion permeability, sensitivity to ATP, and rate of desensitization differ between receptors[240]. A well-characterized downstream mechanism of action for P2X receptors is the influx of Ca^{2+} ions which can cause membrane depolarization and exocytosis[240].

- P2Y receptors are GPCRs that activate various intracellular pathways through second messengers. Eight P2Y receptor subtypes bind purine and pyrimidine nucleotides with differing affinities:

    - P2Y1 (ATP > ADP), P2Y2 (ATP), P2Y4 (UTP), P2Y6 (UDP), P2Y11 (ATP), P2Y12 (ADP), P2Y13 (ADP > ATP), and P2Y14 (UDP and UDP-glucose)[240]. Due to their metabolic signaling cascade, P2Y receptors act slower than their P2X counterparts[240].

    - Similar to other GPCRs, P2Y receptors have seven transmembrane domains with three extracellular and two intracellular loops[240]. P2Y1, P2Y2, P2Y4, P2Y6, and P2Y11 are G_q-coupled and activate phospholipase C (PLC). P2Y12, P2Y13, and P2Y14 are G_i-coupled and inhibit adenylyl cyclase (AC)[240].

- P1 receptors are also GPCRs and are sensitive to adenosine. There are four P1 receptors: A1, A2A, A2B, and A3. A1 and A3 receptors are G_i-coupled, whereas A2A and A2B are G_s-coupled, G_q-coupled, or G_q-coupled[136]. G_s-coupled receptors activate AC leading to intracellular accumulations of cAMP.

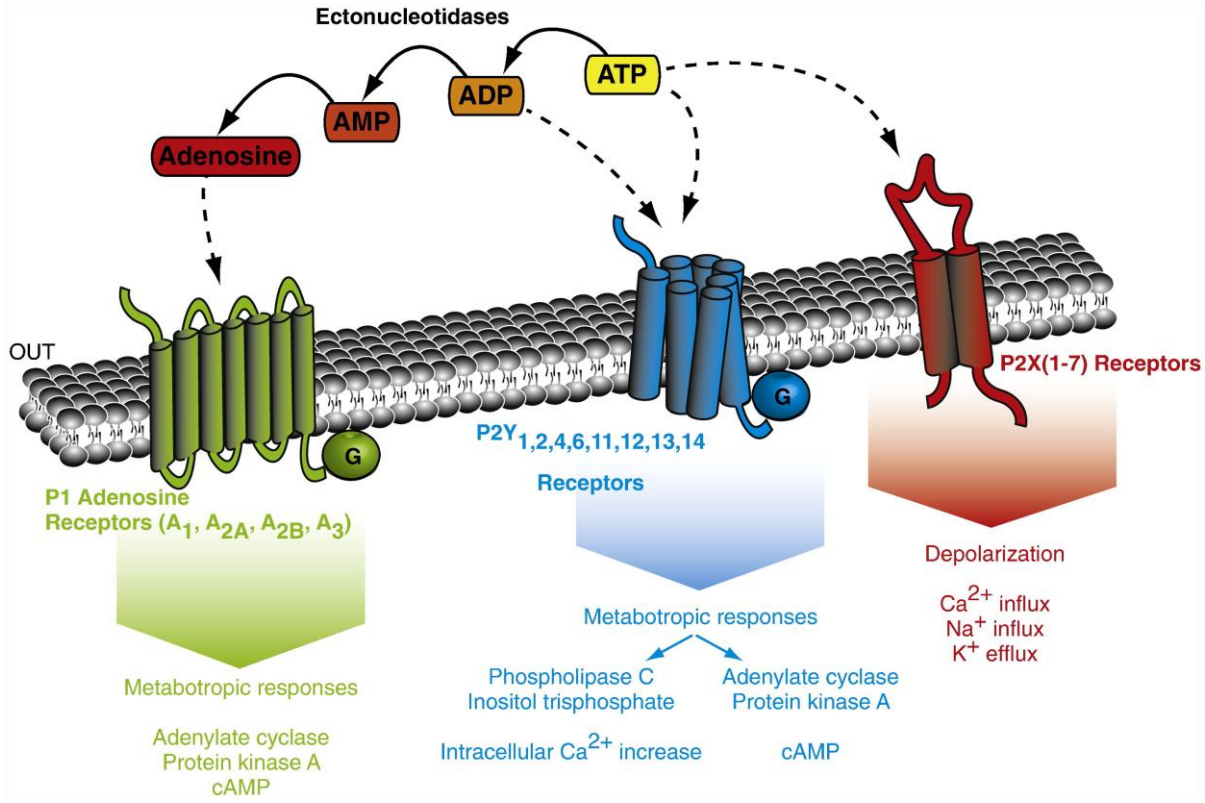

Figure 41. Purinergic receptor signaling mechanisms.
Extracellular ATP derivatives are enzymatic metabolized by ectonucleotidases. These derivatives can signal onto purinergic receptors that are comprised of three categories: P1 – adenosine receptors, P2Y – ADP & ATP receptors, P2X – ATP receptors. Both P1 and P2Y purinergic receptors are G-protein-coupled. Metabotropic (P1 and P2Y) responses and membrane depolarization (P2X) are mediated by the activation of these receptors. Figure adapted from Baroja-Mazo et al., 2013.

Ectoenzymes control extracellular nucleotide concentrations

Because of the strong impact that extracellular nucleotides have on cellular signaling, their concentration must be tightly controlled (**Table 12** & **Figure 42**). Ecto-enzyme classification is dependent upon these characteristics: 1) possess a highly active nucleotide hydrolysis site on the exterior of the cell, 2) possess a glycosylated catalytic subunit, 3) dependent on divalent cations for activity, 4) insensitive to P-/F-/V-type ATPase inhibitors, and 5) able to hydrolyze a wide range of purine and pyrimidine nucleoside tri- and diphosphates[140,141,299].

Table 12. Nucleotide Enzymes

Nucleotide Enzyme Family	Ecto-enzyme Names	Known Ligand Preference
Nucleoside triphosphate diphosphohydrolase (NTPDase)	NTPDase1	ATP ~ ATP
	NTPDase2	ATP > ADP
	NTPDase3	ATP > ADP
	NTPDase8	ATP > ADP
Ecto-nucleotide pyrophosphatase/phosphodiesterase (E-NPP)	E-NPP1	ATP, ADP, AMP
	E-NPP2	ATP, ADP, AMP
	E-NPP3	ATP
Ecto-5'-nucleotidase (Ecto-5'-NT)	Ecto-5'-NT	AMP
Adenosine deaminase (ADA)	ADA	Adenosine
Purine nucleoside phosphorylase (PNP)	PNP	Uridine, Cytidine, Adenosine, Guanosine, Deoxythymidine, Deoxycytidine, Deoxyadenosine, Deoxyguanosine

Nucleoside triphosphate diphosphohydrolases: NTPDases hydrolyze these nucleotides to rapidly terminate purinergic signaling before downstream cascades initiate harmful reactions such as immune infiltration[300–302]. There are eight different NTPDases in this family: NTPDase1-8 (**Table 12** & **Figure 42**). A subset of these NTPDases, E-NTPDases, face the extracellular space and hydrolyze ATP or ADP with varying affinities. These ectonucleotidases (E-NTPDases) are NTPDase1 (ATP ~ ADP), NTPDase2 (ATP > ADP), NTPDase3 (ATP > ADP), and NTPDase8 (ATP > ADP)[140,303,304].

The non-ectoenzyme NTPDases, NTPDase4-7, are expressed on intracellular organelles to hydrolyze intra-organelle nucleotides or are packaged into vesicles not yet defined and secreted into the circulation for longer-range effects[140,305]. Rodent NTPDases have about

84% sequence homology to human NTPDases suggesting an important role for these enzymes across species[299].

Other nucleotide metabolizing enzymes: ecto-5'-nucleotidase, adenosine deaminase, ecto-nucleotide pyrophosphatase/phosphodiesterase (E-NPPs), and purine nucleoside phosphorylase (PNP) (**Table 12** & **Figure 42**)[241]. E-NPPs metabolize ATP directly into AMP[241]. Ecto-5'-nucleotidases convert AMP into adenosine which adenosine deaminase can then convert into inosine. PNPs convert inosine into hypoxanthine[241].

These ectoenzymes are expressed in a variety of cell types. The expression pattern of these different ecto-enzymes is essential for understanding how they operate to modulate purinergic signaling in a cellular complex. For example, NTPDase1 and ecto-5'-nucleotidases are expressed on endothelial cells and lymphocytes, respectively[241]. NTPDase1 is implicated in the termination of prothrombotic and proinflammatory effects of ATP and ADP to prevent excessive clot formation that would block vessel blood flow[140,241].

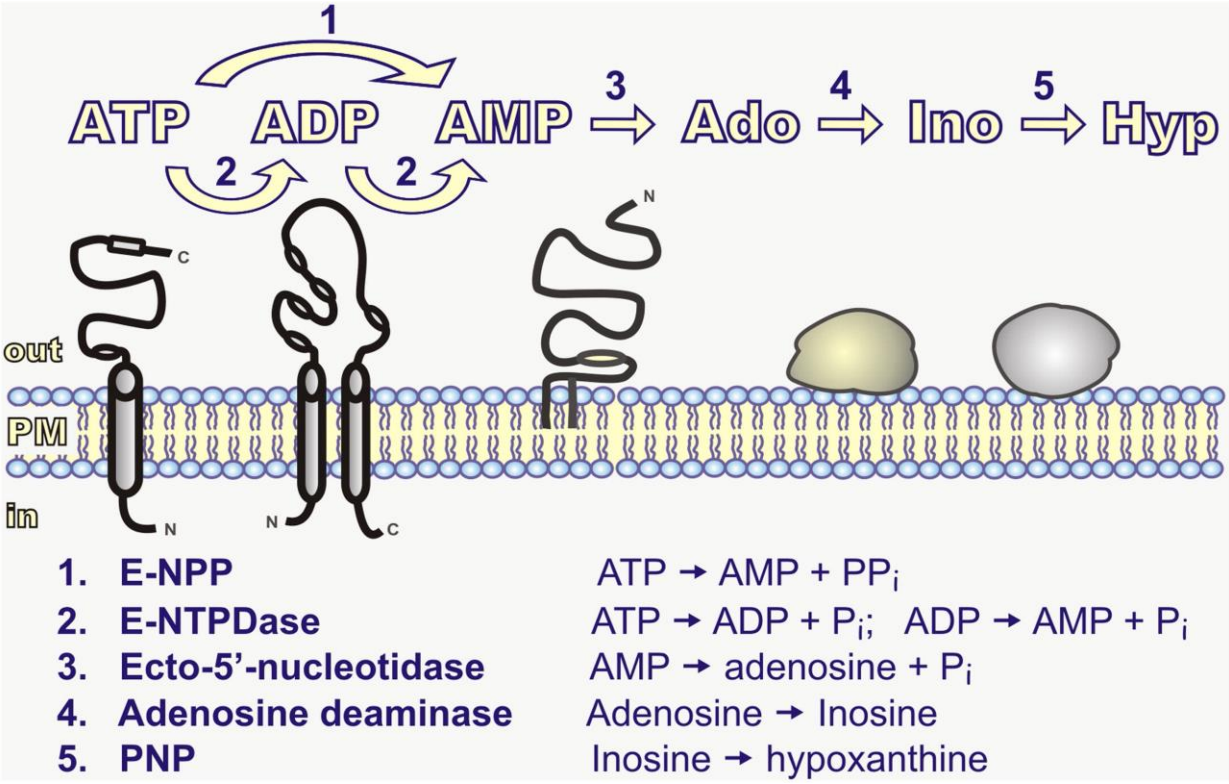

Figure 42. Ectonucleotidases hydrolyze extracellular nucleotides.
E-NPPs (1), E-NTPDases (2), and ecto-5'-nucleotidases (3) metabolize ATP (1,2) and ADP (2) into purine derivatives. AMP can be hydrolyzed into adenosine by ecto-5'-nucleotidase (3). Adenosine can be broken down into inosine and hypoxanthine by sequential adenosine deaminase (4) and PNP reactions (5). Figure adapted from Yegutkin, 2008.

NTPDase3 and pancreatic function

As early as 1978, biochemical studies found ATPase activity in rat pancreata, first implicating these enzymes in pancreatic function[306–309]. ATPase activity was demonstrated in both endocrine and exocrine cells[310]. NTPDase3, in particular, is found to localize to pancreatic endocrine cells, first in rodents and most recently in human tissue[145,154,311]. NTPDase3 is the most highly expressed NTPDase in β cells and is utilized as a β cell-specific marker for antibody-mediated cell sorting techniques[145,151,154]. Other NTPDases are expressed within the islet, such as NTPDase1 on the pancreatic endothelium and NTPDase2 on islet capillaries[154].

Interestingly, NTPDase3 also has a dynamic developmental expression in humans. NTPDase3 expression begins on acinar cells during gestational development but transitions to β cell expression postnatally between three months and five years[151]. This developmental transition coincides with the window that postnatal islet hormone secretion maturation occurs (**Figure 43**). NTPDase3 also marks mature β-like stem cells[152]. The developmental transition of NTPDase3 expression and its β cell-specific expression strongly suggests a role of NTPDase3 in functional β cell maturation and tuning islet hormone secretion.

NTPDase3 preferentially converts ATP into ADP in the extracellular space, presumably to negatively regulate the autocrine feedback loop of ATP. Studies performed in rodents show a positive correlation between NTPDase3 activity and GSIS[145,154]. ATP can also modulate vascular constriction *in vivo* and can modulate macrophage function, illuminating a purinergic system in encompassing endocrine and other islet cell types understudied in health and disease[312–316].

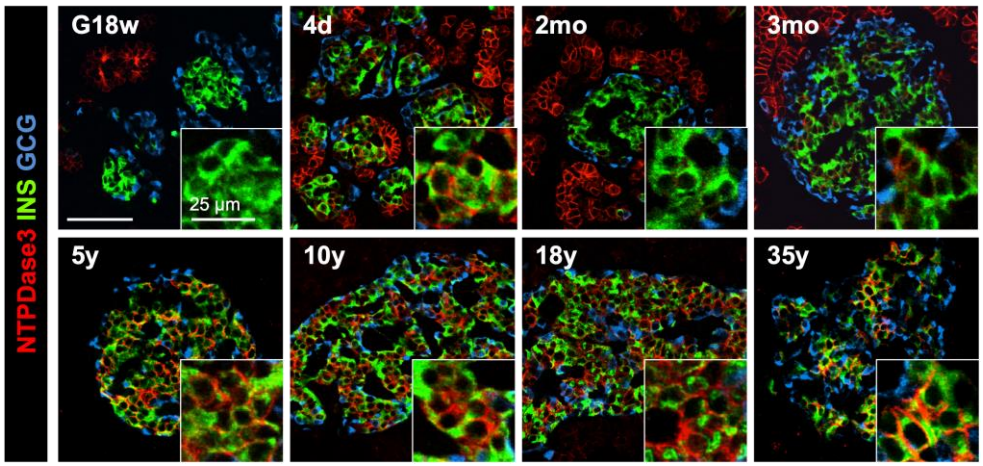

Figure 43. NTPDase3 expression in human pancreas and islets is dynamic. NTPDase3 protein expression transitions from acinar cells to β cells postnatally between 3 months and 5 years of age correlating to β cell functional maturation. Scale bar, 100 µm unless otherwise stated. Abbreviations – gestational (G), month (mo), year (y). Figure adapted from Saunders et al., 2019.

Extracellular nucleotides and pancreatic function

Because ATP is co-secreted with insulin, it can serve as a potential autocrine amplifier of insulin secretion through P2X and P2Y receptors (**Table 13**). ATP is loaded into insulin secretory granules through the vesicular nucleotide transporter (VNUT) located on the surface of granules[317]. Suppressing VNUT with small hairpin RNA (shRNA) knockdown or via a pharmacological antagonist reduces basal- and GSIS[317]. ATP is thought to be released either simultaneously with insulin or through "kiss-and-run" exocytosis such that insulin peptides can be retained as ATP is released[318]. Local intra-islet ATP concentrations as assessed with ATP biosensors are thought to reach up to 25 μM[135,319]. Measurement of local extracellular concentrations from single rodent β cells further supports the phenomenon of ATP release from insulin secretory granules[135,318,320,321]. α cells may also release nucleotides in their secretory granules due to high concentrations of phosphorus after glucagon stimulation but which sub-type of nucleotide(s) is not currently known[322].

In isolated rodent islets, extracellular ATP levels increase with insulin secretion after glucose perifusion[134]. The extracellular ATP pool and downstream nucleotide products can, in turn, bind purinergic receptors expressed on islet endocrine cells to modulate secretion (**Table 13**). Agonism of β cell P2Y receptors leads to an increase of intracellular calcium (Ca^{2+}) and subsequent insulin secretion[148,160,323–326]. Other receptors such as P2X1, P2X3, and P2X7 are also implicated in this ATP-mediated potentiation of insulin secretion from studies in rodents and human islets[149,158,159]. P2X and/or P2Y receptors expressed on α and δ cells may have paracrine responses to β cell-derived ATP[327]. ATP has been shown to either increase or have no effect on glucagon secretion under low glucose concentrations[326,328]. Somatostatin secretion in particular can be stimulated and inhibited by P2 receptor agonists and antagonists, respectively[327,329].

ATP can be broken down into its derivatives, ADP, AMP, and adenosine, by islet ecto-ATPases[330]. ATP is the most potent of these nucleotides to induce GSIS, whereas adenosine has been shown to increase glucagon secretion under low glucose concentrations[313,331,332] and decrease insulin secretion in perfused rat pancreata under high glucose concentrations[333]. Adenosine receptors expressed within the islet may mediate these adenosine effects on glucagon secretion. Adenosine receptor, ADORA2A, agonism stimulates glucagon secretion[334]. ADORAA1 receptor knockout mice have prolonged glucagon and somatostatin secretion suggesting a role of adenosine in the control of α and δ cell secretion duration[335]. Nucleotides can also act on vascular cells within the islet such as endothelial cells and pericytes. Adenosine acts as a vasodilator whereas, ATP treatment causes vasoconstriction in blood vessels[336]. Adenosine has also

been shown to decrease pericyte function via reducing intracellular Ca^{2+} resulting in pericyte relaxation and subsequent vasodilation of islet blood vessels[47,182].

Table 13. Purinergic function in pancreatic islets

Nucleotide	Related Islet Function	Effect	Receptor(s)
ATP	Insulin secretion	↑	P2X1, P2X3, P2X7
	Insulin secretion	↑	P2Y1
	Glucagon secretion	↑or ↓	Unknown
	Somatostatin secretion	↑	P2 receptors
	Vasoconstriction	↑	Unknown
Adenosine	Glucagon & somatostatin secretion	↓	ADORA1
	Glucagon secretion	↑	ADORA2A
	Insulin secretion	↓	Unknown
	Vasodilation	↑	Unknown
	Pericyte function	↓	Unknown

NTPDase3 and the purinergic receptors it indirectly modulates by controlling the extracellular ATP concentration may significantly impact pancreatic islet development and hormone secretion. There are contradictory reports from mouse and human studies, possibly due to many factors like differing purinergic system component expression between the species, dependence on glucose concentrations, and specificity of the pharmacological modulators utilized. **A better understanding of the purinergic system and purinergic cascade in human islets is assessed in this Dissertation.**

Results

We hypothesize that NTPDase3 plays an important role in the regulation of insulin secretion by modulating intra-islet nucleotide levels and thus, signaling through purinergic receptors expressed on islet cells.

Pancreatic purinergic gene expression profiling demonstrates a system for extracellular nucleotide metabolism and signaling

Ecto-nucleotidases function to quickly metabolize extracellular nucleotides and in that way modulate the signaling effects of nucleotides (**Figure 44A**). To define the purinergic expression profile of human pancreatic islets, we utilized our established single-cell RNA-sequencing dataset that identified subpopulations of α and β cells dependent upon transcription factor expression profiles[337]. We first validated that NTPDase3 (ENTPD3) is the primary ecto-NTPDase expressed in human islets (**Figure 44B**). NTPDase2 is also expressed in γ and ϵ cells which have a much lower abundance in islets. We also determined that NTPDase1 is expressed in accessory cells such as immune, endothelial, and stellate cells. Other ecto-enzymes also contribute to the enzymatic breakdown of ATP. E-NPP1, which can convert ATP to AMP, is expressed in α, γ, and ϵ cells. E-NPP2, which can convert AMP into adenosine, is expressed in α and ϵ cells. Ecto-5'-nucleotidase (NT5E) and adenosine deaminase (ADA) are expressed in endothelial and stellate cells. NT5E converts AMP into adenosine, and adenosine deaminase can reduce extracellular adenosine by converting it into inosine. Based on this gene expression data summarized in **Table 14**, we hypothesize that enzymes expressed on islet endocrine and accessory cells can lead to the production of downstream nucleotides such as ATP, ADP, AMP, and adenosine to signal onto β and α cells to modulate insulin and glucagon secretion, respectively.

We also determined the expression profile of the purinergic receptors that these nucleotide derivatives activate (**Figure 44B**). Of the ion channel P2X receptors, we found that P2RX4, an ion channel that binds ATP, is expressed in α, ductal, and immune cells. P2RX7 is also expressed in immune cells. In assessing P2Y receptor expression, we found that P2RY1 is expressed in β and immune cells. P2RY1 is a G alpha-coupled GPCR with a binding affinity for ATP. And lastly, the adenosine receptor ADORA2A, a Gs-coupled GPCR, and ADORA3, a Gi-coupled GPCR, were found to be expressed in α and immune cells, respectively. Thus, the purinergic receptor expression profile of human islets consists of multiple nucleotide-metabolizing enzymes and receptor subtypes.

Table 14. Purinergic Ecto-enzyme & Receptor Expression in Pancreatic Islets

	Ecto-enzyme or Receptor	Species	Expression
Ecto-enzyme	NTPDase1	Human	Immune, endothelial, and stellate cells
	NTPDase2	Human	γ & ϵ cells
	NTPDase3	Human & Mouse	β cells
	E-NPP1	Human	α, γ, and ϵ cells
	E-NPP2	Human	α and ϵ cells
		Mouse	α cells
	NT5E	Human	Endothelial and stellate cells
	ADA	Human	Endothelial and stellate cells
Receptor	P2X4	Human	α, ductal, and immune cells
		Mouse	α cells
	P2X7	Human	Immune cells
	P2Y1	Human	β and immune cells
		Mouse	β cells
	ADORA2A	Human	α cells
	ADORA3	Human	Immune cells

Developmental expression of purinergic components in mice and human pancreas

Previously, we determined that NTPDase3 has a dynamic expression within the human pancreas transitioning from the exocrine to the endocrine compartment postnatally[151]. To understand the expression patterns of purinergic components more broadly within the islet, we assessed the expression of nucleotide ecto-enzymes and purinergic receptors in both mouse and human α and β cells throughout development. In assessing fetal and adult human islet expression patterns from an existing bulk RNA-seq dataset, we found that E-NPP1, E-NPP2, and P2RX4 are expressed in fetal and adult α cells with ADORA2A and P2X4 increasing in expression in adult α cells (**Figure 44C**)[245]. Fetal β cells express E-NPP2, ENTPD1, P2X1, P2Y1, and P2Y13 (**Figure 44C**). Adult β cells express E-NPP2, ENTPD3, ENTPD4, P2X4, and P2Y1, with ENTPD3 and P2X4 expression increasing in

adulthood (**Figure 44C**). For expression studies in mice, we utilized an existing scRNA-seq dataset from embryonic (E17.5), neonatal (P0), juvenile (P3, P9, P15, P18), and adult (P60) mouse pancreata[247]. In mice, we found that α cell expression of E-NPP2, ENTPD3, and P2X4 are highly expressed embryonically and diminish postnatally (**Figure 44D**). In β cells, E-NPP2, ENTPD3, and P2Y1 are highly expressed embryonically with more moderate expression postnatally (**Figure 44D**). ENTPD3 and P2Y1 are β cell-specific in their expression in both mice and human (**Figure 44D**).

Immunofluorescence analysis of NTPDase3 in pancreatic tissue sections across different time points confirmed species-specific differences in NTPDase3 islet expression throughout development (**Figure 44E-L**). In human tissue, NTPDase3 is initially expressed in acinar cells during fetal development and early after birth and then becomes restricted to β cells during childhood (**Figure 44E-H, Table 4** for donor summary)[151]. Alternatively, in mice, NTPDase3 was expressed in β cells at all embryonic time points and maintained in β cells after birth and into adulthood (**Figure 44E-L,** see **Table 6-7** for immunohistochemistry information). NTPDase3 was not expressed in acinar cells of mouse pancreatic tissue at any developmental time points studied. These findings highlight purinergic expression differences between mouse and human pancreata further emphasizing the need to characterize purinergic functioning in human islets, specifically.

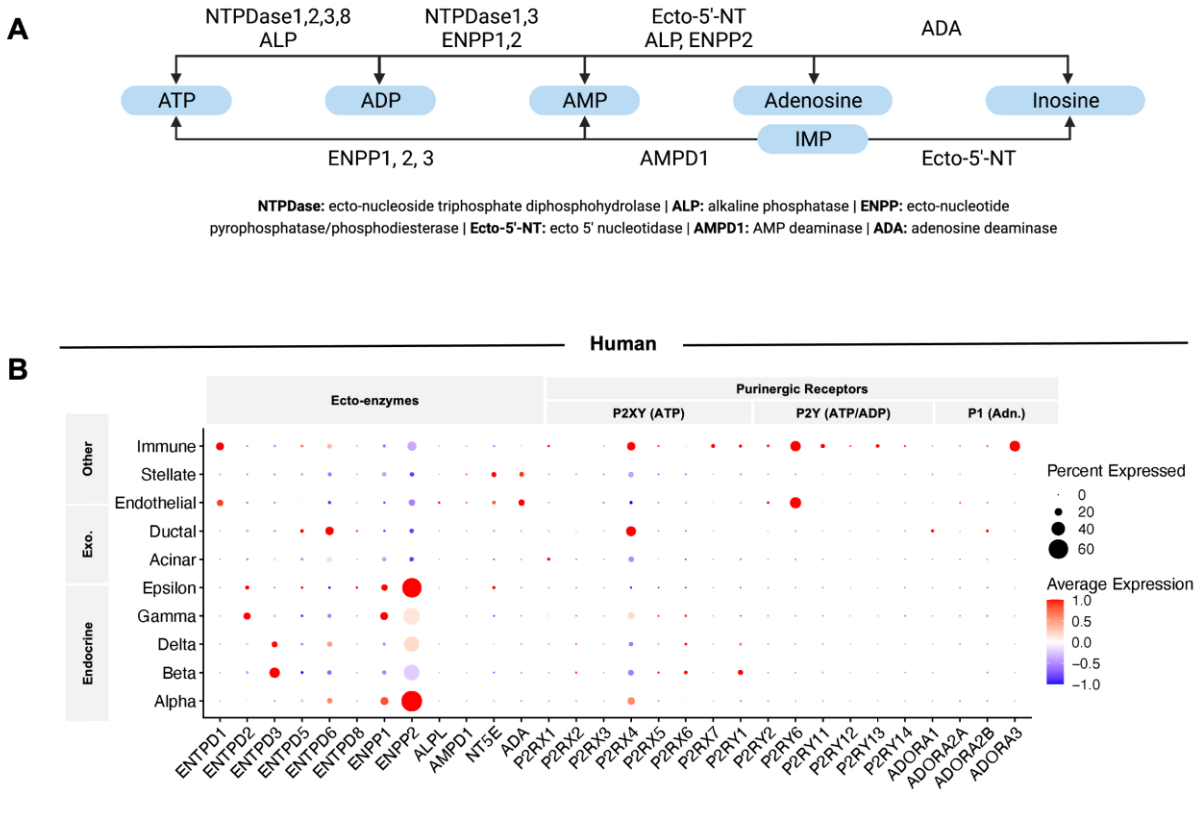

Figure 44. Pancreatic purinergic gene expression profiling demonstrates a system for extracellular nucleotide metabolism and signaling.
(A) Schematic illustrating the enzymatic conversion of extracellular ATP into ADP, AMP, IMP, Adenosine, and Inosine by major ecto-enzymes within the pancreatic islet. Abbreviations for each enzyme are denoted below the schematic. (B) Dot plot from single-cell (sc) RNA-sequencing showing the relative expression of islet ecto-enzymes and purinergic receptors detected in endocrine (α, β, δ, γ, and ϵ), exocrine (Acinar and Ductal), and accessory (Endothelial, Stellate, and Immune) cells. Ligands for the three purinergic receptor categories are stated in parentheses. Dot size is proportional to the percentage of cells with detectable transcripts and the dot color indicates the mean expression z score of a given gene (Shrestha 2021). Abbreviations: Exo, Exocrine; Adn, Adenosine; E, embryonic; P, postnatal.

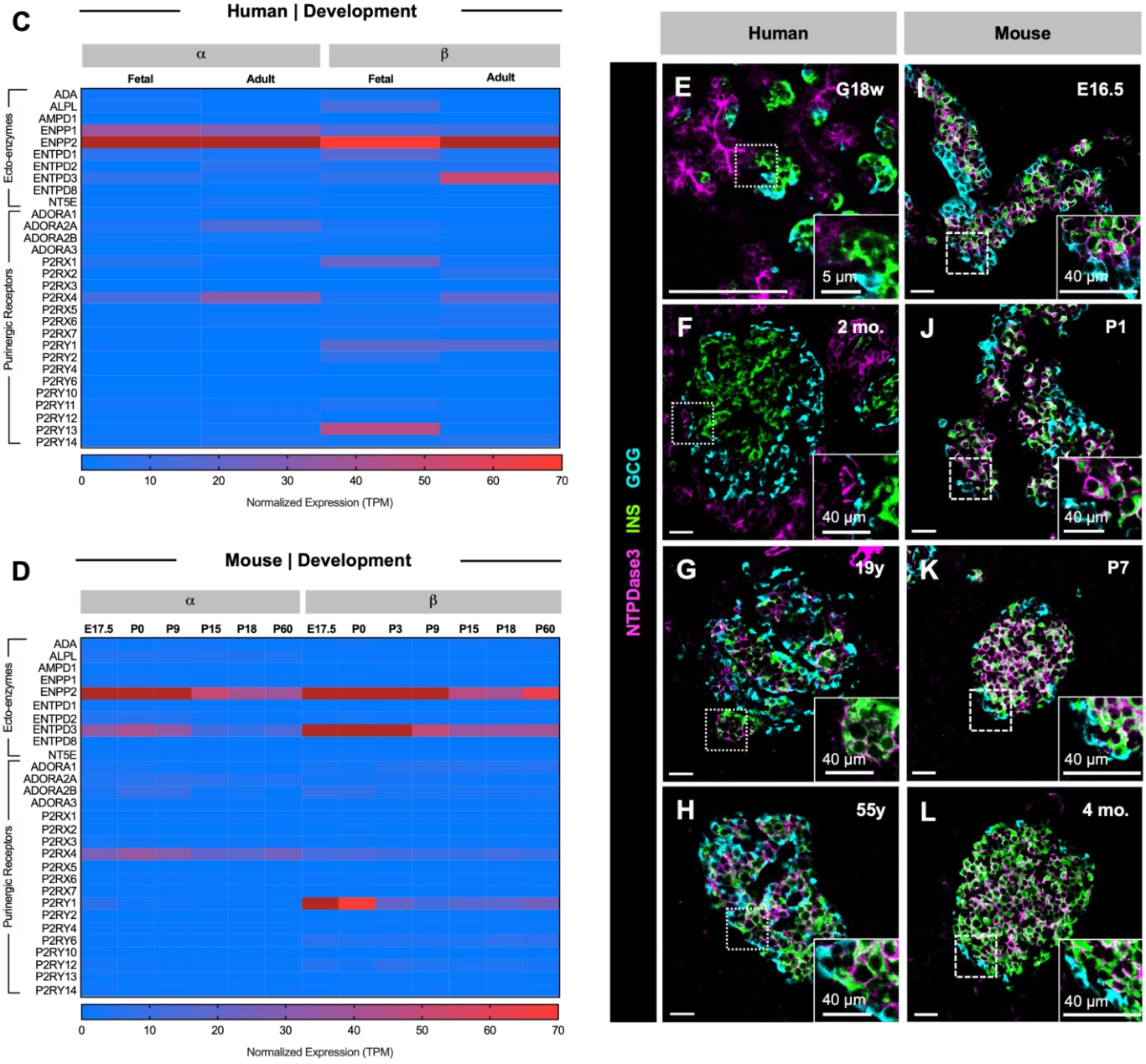

Figure 44. Pancreatic purinergic gene expression profiling demonstrates a system for extracellular nucleotide metabolism and signaling.
(C-D) Normalized expression (transcript per million, TPM) of purinergic ecto-enzymes and receptors throughout human (C) and mouse (D) Alpha (α) and Beta (β) cells at various developmental timepoints. (Human: Blodgett 2015; Mouse: Qiu 2017). (E-L) The developmental protein expression of NTPDase3 differs between mouse and human. Representative immunofluorescent images show a dynamic expression of NTPDase3 from epithelial to β cells in human pancreatic tissue postnatally (E-H) (Saunders 2018) but NTPDase is expressed from E16.5 into adulthood in mouse β cells (I-L). Human pancreatic donor information can be found in Table 4. Scale bars are 100 μm unless otherwise indicated. Abbreviations: Exo, Exocrine; Adn, Adenosine; E, embryonic; P, postnatal.

β cell-specific deletion of Entpd3 in mice blunted insulin secretion of isolated islets

Because NTPDase3 is the predominately expressed NTPDase in pancreatic islets, we next investigated the effect of NTPDase3 on islet function *in vivo*. We generated a β cell-specific NTPDase3 knockout mouse model by breeding *Entpd3*$^{fl/fl}$ female mice and MIP-CreERT male mice (*MIP-CreER; Entpd3*$^{fl/fl}$) (**Figure 45A-B**)[226,227]. Breeding and growth curves were similar between groups (**Figure 45C**). βΔENTPD3 mice displayed similar amounts of β and α cells compared to tamoxifen-treated (TMX) controls (**Figure 45D-G**). Importantly, NTPDase3 was specifically deleted from β cells of adult βΔENTPD3 mice with a small subset (3%) still expressing NTPDase3 (**Figure 45H**). Prior to TMX treatment, both groups exhibited similar insulin secretion and glucose homeostasis following a glucose tolerance test (GTT; **Figure 45I-K**).

After TMX treatment, there was no alteration of whole-body glucose homeostasis as assessed by glucose tolerance tests (GTT; **Figure 46A-F**). Challenging βΔENTPD3 mice with glucose + arginine to induce a greater insulin secretory response from β cells did not reveal a change in glucose homeostasis (**Figure 46A-F**). We did observe decreased GSIS by male βΔENTPD3 mice compared to littermate controls following a glucose + arginine challenge (**Figure 46D**). Isolated islets from the same control and βΔENTPD3 mice then underwent *in vitro* dynamic macroperifusion studies. TMX-treated male βΔENTPD3 mice showed reduced glucose-mediated and cAMP-mediated insulin secretion compared to littermate controls as assessed by (**Figure 46G-J**). Therefore, β cell-specific deletion of NTPDase3 in mice diminished insulin secretion *in vitro* but did not have a dramatic effect on whole-body glucose homeostasis.

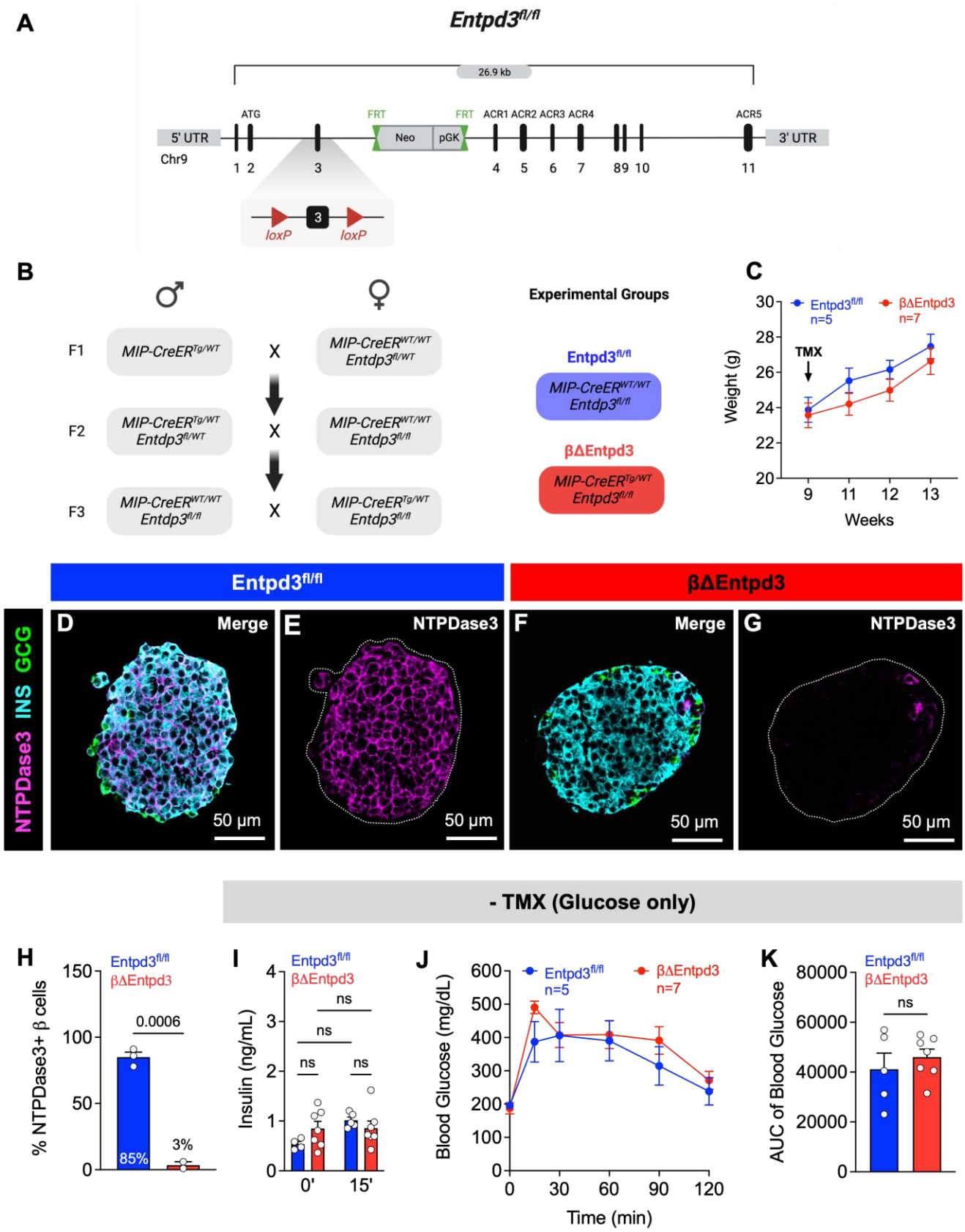

Figure 45. Characterization of βΔEntpd3 mouse model.

Figure 45. Characterization of βΔEntpd3 mouse model.
(A) Schematic of the *Enptd3* floxed gene locus with exons denoted with dark vertical bars. *LoxP* sites flank exon 3. Abbreviations: UTR, untranslated region; ATG, start site; ACR, apyrase-conserved region. (B) Breeding scheme for the generation of the tamoxifen (TMX)-inducible Entpd3 knockout mouse model (βΔENTPD3). Experimental (red) and control groups (dark and light blue) are denoted. (C) Body weight of control and Entpd3 knockout mice (blue = $Entpd3^{fl/fl}$; red = βΔEntpd3). (D-G) Representative immunofluorescence images of pancreatic islets to show the reduction of NTPDase3 (magenta) expression specifically in pancreatic β cells (blue) after TMX treatment. α cells are shown in green. (H-J) *In vivo* glucose-stimulated insulin secretion (H) and intraperitoneal glucose tolerance tests (IPGTTs; I) were done prior to TMX treatment. (J) IPGTT area under the curve analysis (AUC). The following statistical tests were performed: unpaired two-tailed t-test for panel H; one-way ANOVA with Tukey's multiple comparisons tests for I; unaired two-tailed t-test was performed for panel K. A p-value < 0.05 was significant**.**

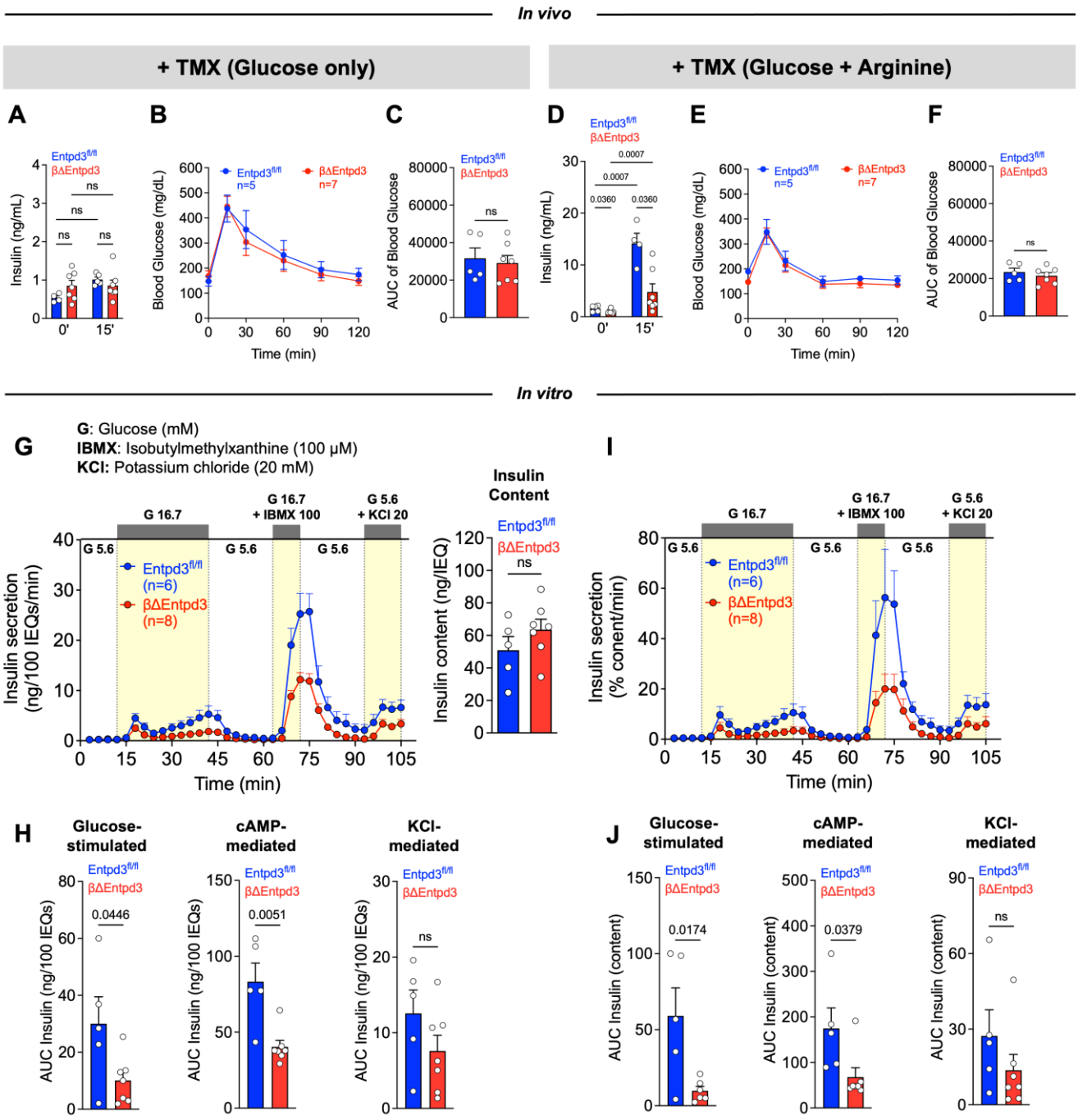

Figure 46. Tamoxifen-induced deletion of *Entpd3* in β cells blunted insulin secretion from isolated mouse islets.

(A-D) *In vivo* glucose-stimulated insulin secretion (A, D), intraperitoneal glucose tolerance tests (IPGTTs; B, E), and IPGTT area under the curve analyses (AUC; C, F). (G-J) Macroperifusion of isolated mouse islets to assess *in vitro* hormone secretion following *Entpd3* deletion normalized to islet volume expressed in islet equivalents (IEQ; G-H) or to insulin content (I-J). AUC analyses for macroperifusion experiments are shown in H & J. N = 5-7 male mice/group were used for each functional assessment in D-K. The following statistical tests were performed: one-way ANOVA with Tukey's multiple comparisons tests for A & D; paired two-tailed t-test for panels C, F, H, J. A p-value < 0.05 was significant.

NTPDase3 knockdown potentiates human pseudoislet insulin secretion

Next, we assessed the functional role of NTPDase3 and β cell-derived ATP in modulating hormone secretion in human islets. We first determined the dynamics of extracellular ATP in primary human islets. Static incubation of primary human islets with high glucose and 3-isobutyl-1-methylxanthine (16.7 mM glucose + IBMX) resulted in an increase of insulin secretion (**Figure 47A-B**). There was also an increase of extracellular ATP after exposure to high glucose and IBMX, presumably due to the release of ATP from β cells (**Figure 47A-B**). Inhibition of NTPDases with a non-specific nucleotide analog had no significant effect on insulin or ATP secretion (**Figure 47C-D**).

To specifically manipulate NTPDase3 and determine the role of NTPDase3 in human β cell function, we utilized shRNA knockdown in a primary human pseudoislet system to generate scramble shRNA ('control') and ENTPD3 shRNA ('shENTPD3') (**Figure 48A**)[32]. High β cell transduction efficiencies resulted in a 64% knockdown of ENTPD3 as assessed by RNA levels (**Figure 48B-E**). Control and shENTPD3 pseudoislets had a similar size, morphology, and β or α cell transduction efficiency, and β or α endocrine proportions (**Figure 48B-E**). In both groups, there was greater transduction efficiency in β cells compared to α cells (**Figure 48D**). After ENTPD3 knockdown, dynamic insulin secretion was increased in shENTPD3 pseudoislets in the presence of three secretagogues (high glucose, high glucose + IBMX, or KCl) when normalized to islet equivalents (IEQs; **Figure 48F-G**). We did not observe a difference in insulin secretion when normalized by content possibly due to a slightly higher but not statistically significant insulin content in shENTPD3 pseudoislets. These findings in human pseudoislets highlight a direct effect of NTPDase3 on human islet insulin secretion.

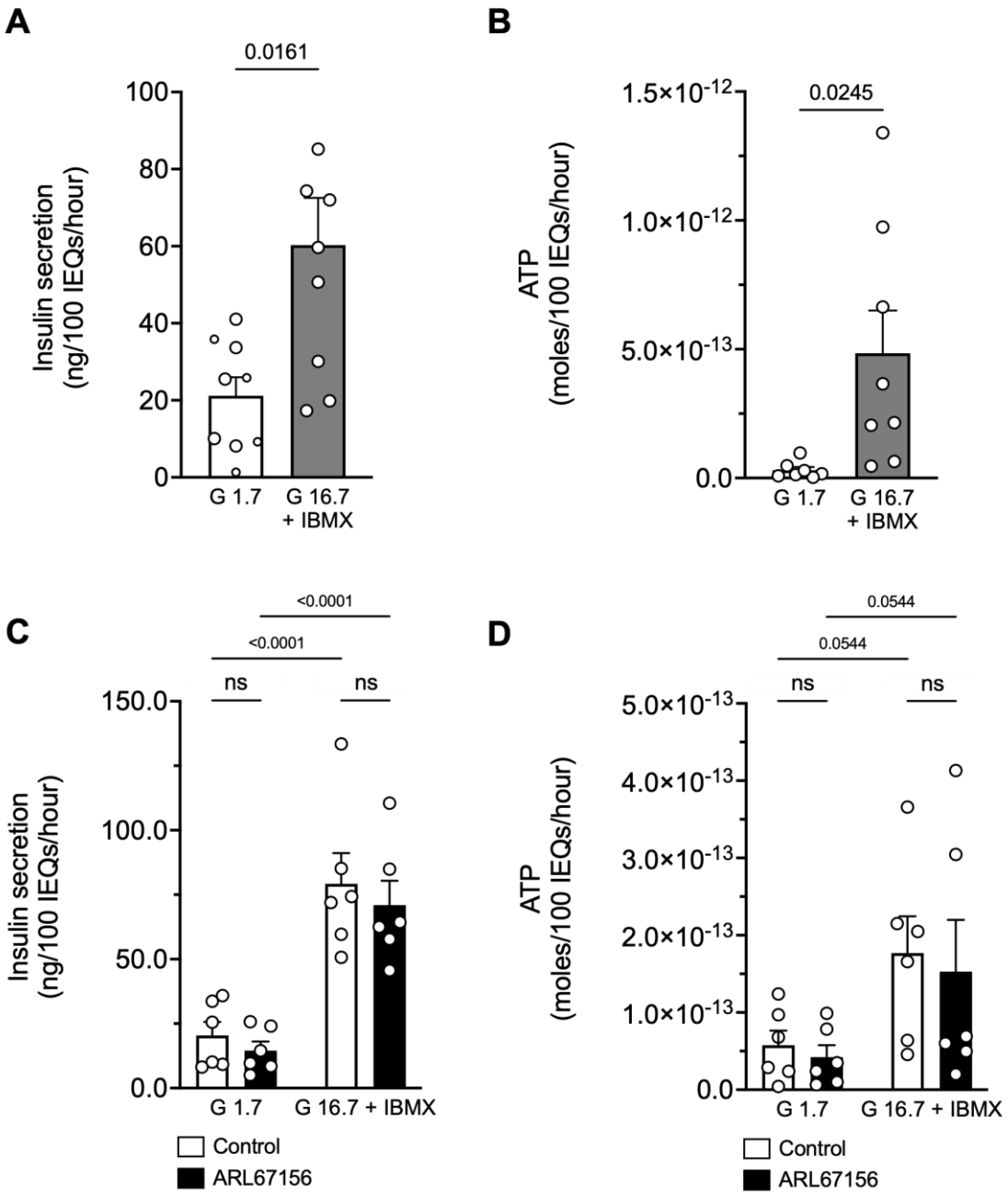

Figure 47. Extracellular ATP dynamics in primary human pancreatic islets. (A-C) Static incubation of human islets under 1.7 mM glucose (G) then 16.7 mM glucose (G) and isobutylmethylxanthine (IBMX, uM) to assess insulin (A) and extracellular ATP levels (B). N = 9 donors. (C-D) Non-specific inhibition of islet NTPDases with ARL67156 did not affect insulin secretion (C) or extracellular ATP levels (D). N = 6 donors per group. Human pancreatic donor information can be found in Table 4. The following statistical tests were performed: paired two-tailed t-test for panels A-B; one-way ANOVA with Tukey's multiple comparisons tests for C-D. A p-value < 0.05 was significant.

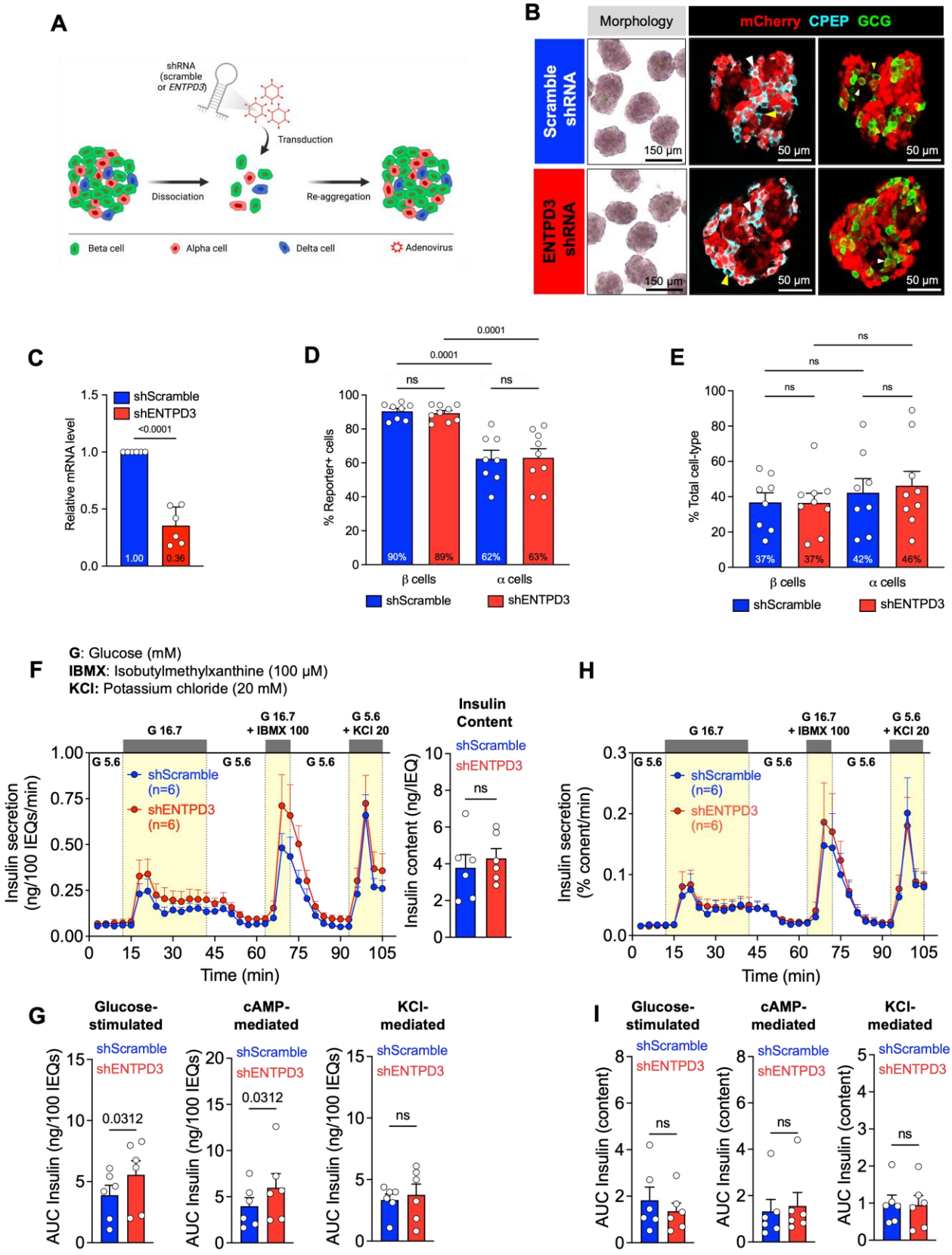

Figure 48. Human islet insulin secretion is increased following NTPDase3 knockdown.

Figure 48. Human islet insulin secretion is increased following NTPDase3 knockdown. (A) Schematic of adenoviral shRNA transduction and formation of human pseudoislets. (B) Representative images of morphology and immunofluorescent staining of shScramble (blue) and shENTPD3 (red) transduced pseudoislets. Transduced cells marked are marked by mCherry. CPEP = C-Peptide (β cells) and GCG = glucagon (α cells). White arrows indicate transduced β or α cells and yellow arrows indicate untransduced β or α cells. (C) Relative ENTPD3 mRNA levels in pseudoislets treated with scramble or ENTPD3 shRNA. N = 6 donors per group. (D) Percentage of β and α cells positive for shRNA reporter fluorescence. N = 8 donors per group. (E) Distribution of β (CPEP, blue) and α (GCG, green) cells in shScramble and shENTPD3 pseudoislets. (F) Percentage of total β and α cells within shScramble and shENTPD3 pseudoislets. N = 9 donors per group. (F-I) Pseudoislet insulin secretion was assessed by macroperifusion normalized to islet volume expressed in islet equivalents (IEQ; F-G) or to total insulin content (H-I). Insulin content for both groups in shown in F. N = 6 donors per group). Area under the curve (AUC) analyses for secretory response to each stimulus in (G,I). Scale bar sizes are denoted. Human pancreatic donor information can be found in Table 4. The following statistical tests were performed: paired two-tailed t-tests were performed for panels C, G, and I; one-way ANOVA with Tukey's multiple comparisons tests were performed for panels D & E. A p-value < 0.05 was significant.

P2Y1 receptor signaling mediates NTPDase3-dependent potentiation of insulin secretion in human islets

Purinergic receptors identified by our expression profiling may mediate these NTPDase3-dependent alterations in islet hormone secretion. In particular, we found that P2Y1 is highly and specifically expressed in human β cells (**Figure 44B-C**). P2Y1 is a Gq-coupled receptor that can bind ATP leading to an increase in intracellular Ca^{2+} levels. shRNA-mediated knockdown of ENTPD3 and co-transduction with a Ca^{2+} biosensor (GCaMP6f) in human pseudoislets resulted in ~60% GCaMP+/mCherry+ β cells and 23% ENTPD3 knockdown with similar cell-type proportions as pseudoislet preparations utilized in our macroperifusion experiments (**Figure 49A-F**).

We then simultaneously assessed intracellular Ca^{2+} dynamics and insulin secretion in a live cell microperifusion system developed by our laboratory[32]. In our preliminary studies (N = 1), exposure of shENTPD3 pseudoislets to high glucose (G 16.7) and high glucose + IBMX resulted in a greater and prolonged Ca^{2+} response (**Figure 49H-J**). Interestingly, we observed an additional surge of intracellular Ca^{2+} that subsided once glucose concentrations within the pseudoislet chamber fell back to 2 mM after changing secretagogues at Time = 30 minutes (**Figure 49H**). Furthermore, we did not see a potentiation of insulin secretion in shENTPD3 pseudoislets exposed to G 16.7 + IBMX compared to shScramble pseudoislets most likely due to lower knockdown efficiencies compared to our macroperifusion studies (23% vs. 64%; **Figure 49K-L**).

A pharmacological antagonist specific for P2Y1, MRS2500, significantly blunted Ca^{2+} and insulin responses seen in shScramble and shENTPD3 pseudoislets. shENTPD3 Ca^{2+} responses were similar to shScramble after MRS2500 treatment implicating P2Y1 in the NTPDase3-mediated potentiation of insulin secretion (**Figure 49H-K**). Together, these data suggest that the functional purinergic system within pancreatic islets plays an important role in modulating hormone secretion through nucleotide metabolizing ecto-enzyme, NTPDase3, and P2Y1.

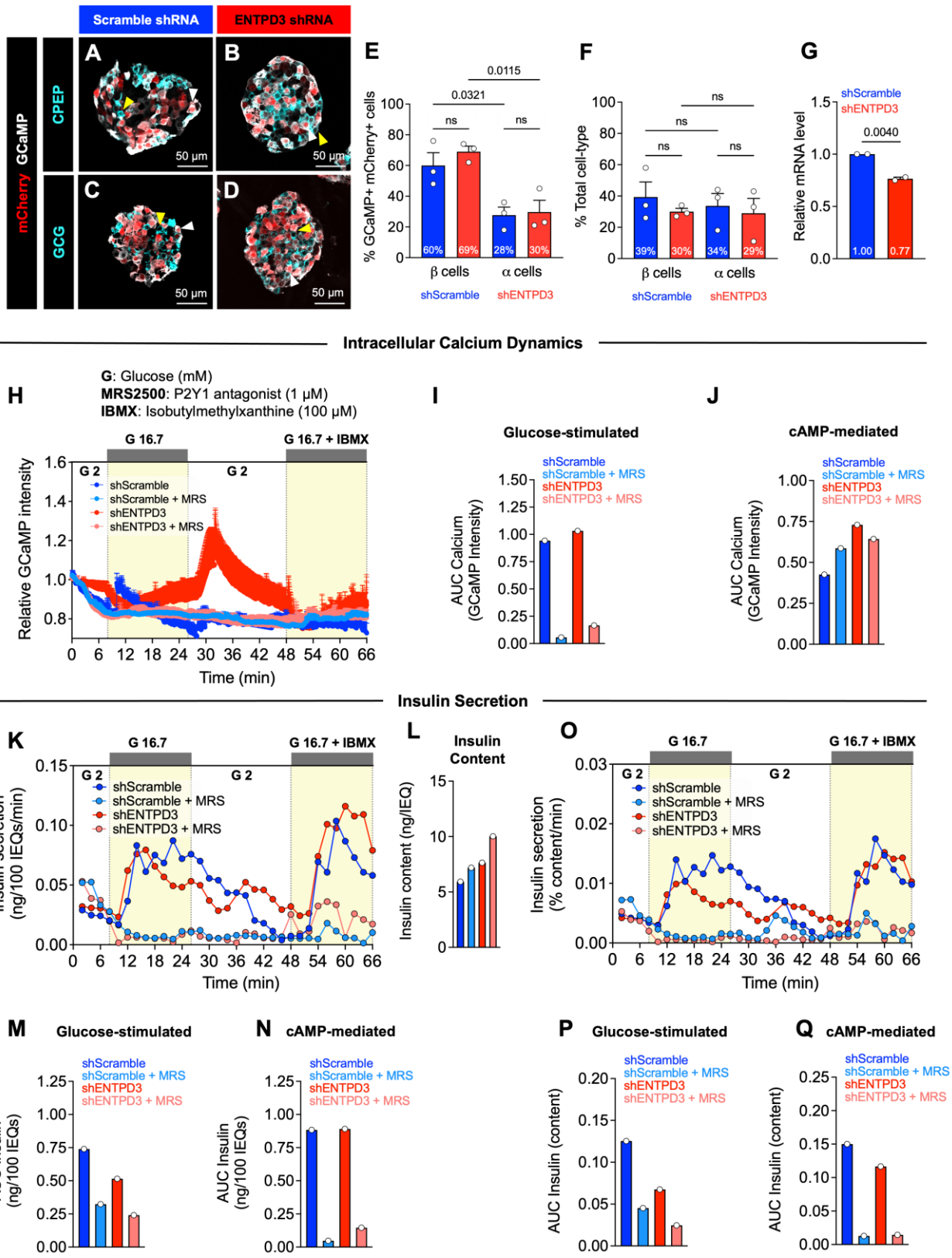

Figure 49. P2Y1 mediates NTPDase3-dependent potentiation of insulin secretion.

Figure 49. P2Y1 mediates NTPDase3-dependent potentiation of insulin secretion. (A-D) Transduced β (A-B) and α (C-D) cells marked by mCherry and GCaMP in shScramble and shENTPD3 pseudoislets. White arrows indicate mCherry+ GCaMP+ cells and yellow arrows indicate untransduced β and α cells. (E) Percentage of β or α cells positive for shRNA reporter and GCaMP fluorescence (N = 3 donors per group). (F) Distribution of β (CPEP) and α (GCG) cells in shScramble and shENTPD3 pseudoislets (N = 3 donors per group). (G) Relative ENTPD3 mRNA in pseudoislets treated with scramble or ENTPD3 shRNA (N = 2 donors per group). (H-Q) Dynamic changes in intracellular calcium as assessed by GCaMPf relative intensity (H-J) and insulin secretion (K-Q) during live cell microperifusion in response to high glucose (G 16.7), high glucose + IBMX (G16.7 + IBMX), or MRS2500 (P2Y1 antagonist) (N = 1). (I-J) Calcium signals were integrated by calculating the area under the curve (AUC) for response to each stimuli. Baseline for calcium signal normalization was set to the average value of each trace from 0 to 6 minutes before exposure to G 16.7. Insulin secretion data is normalized to islet volume expressed in islet equivalents (IEQs; L-N) or content (M-O). (J-L, N-O) Insulin content (J) and area under the curve (AUC; K—L, P-Q) for secretory response to each stimulus. Scale bar sizes are denoted. The following statistical tests were performed: one-way ANOVA with Tukey's multiple comparisons tests for panels E-F; paired two-tailed t-tests for G. P-values are denoted on each graph and a p-value < 0.05 was considered statistically significant. Human pancreatic donor information can be found in Table 4.

Discussion

The islet purinergic system is complex and involves multiple ecto-enzymes, receptors, and cell types. Nucleotide sources within the islet include β, immune, and endothelial cells, with endothelial cells also contributing to the extracellular adenosine pool (**Figure 50**). Our analysis of the islet purinergic system revealed that there are ecto-enzymes present within islets that could hydrolyze this ATP extracellular pool into its downstream derivatives that bind purinergic receptors within the islet. We also show differences between the developmental expression of purinergic system components in α and β cells of mouse and human islets. Additionally, the specific deletion of NTPDase3 in β cells resulted in a blunting of insulin secretion in mice (*in vivo* and *in vitro*). The knockdown of NTPDase3 in human islets resulted in a potentiation of insulin secretion potentially mediated through the β cell-specific P2 receptor, P2Y1. Overall, we defined a functional purinergic system in mouse and human pancreatic islets implicating NTPDase3 in controlling insulin secretion.

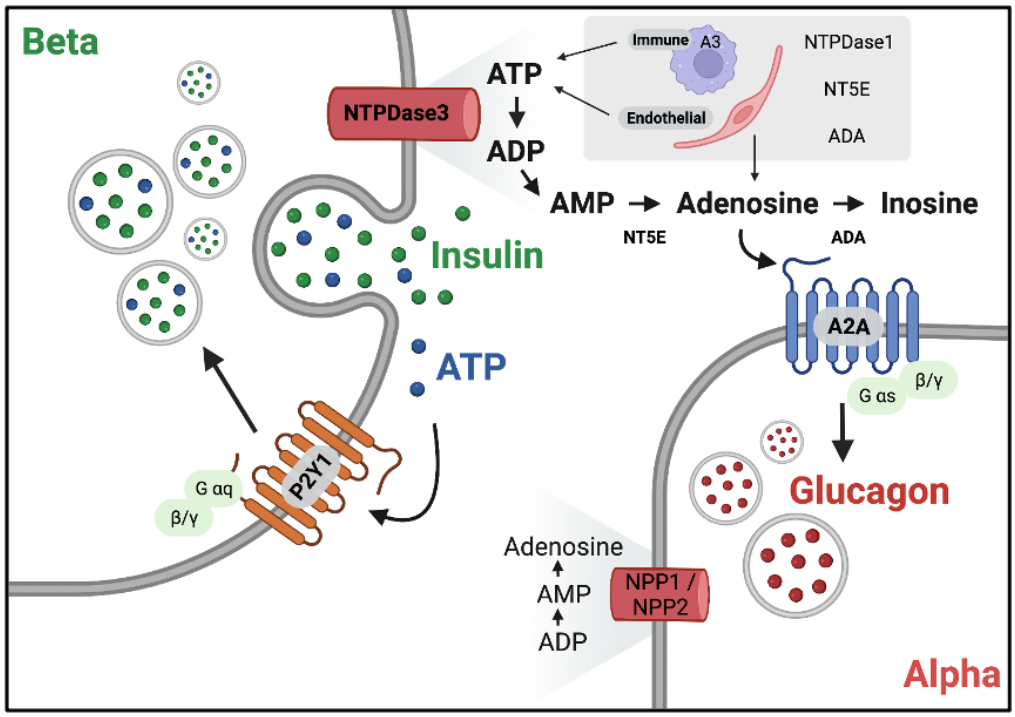

Figure 50. Functional purinergic system in human pancreatic islets. Expression profiling of purinergic genes demonstrates a system for extracellular nucleotide metabolism and signaling as exemplified by the expression of NTPDase3 in β cells, ecto-enzymes NPP1 and NPP2 in α and ϵ cells, and NT5E and ADA expression in endothelial and stellate cells. We found that the ATP receptor, P2RY1, was enriched in β cells, and an adenosine receptor, ADORA2A, was expressed in α cells by both bulk and scRNA-seq. NTPDase3 can directly modulate insulin secretion through activation of P2Y1 receptor expressed on β cells.

Mouse and human islets are similar but have important differences in the cellular composition of endocrine cell types, vasculature, innervation, and magnitude of basal and stimulated hormone secretion[75,161–163,338]. We assessed both mouse and human expression profiles and purinergic function independently to identify any species-specific differences and study two important diabetes research model systems. The dynamic developmental expression of purinergic ecto-enzymes and receptors within the human and mouse pancreas highlights a potential role for the purinergic system in islet functional maturation shared between species. Previous investigations of NTPDase3 expression within the pancreas have only studied adult rodents after islets have fully matured in architecture and hormone secretory profiles masking any developmental role for NTPDase3 and other purinergic components[145,154,155,226,339]. Perturbation of purinergic signaling within pancreatic islets may negatively affect islet development and hormone secretion. The purinergic landscape we comprehensively define in both mice and human emphasizes an intricate mixture of ecto-enzymes and receptors within pancreatic islets.

Our assessment of ATP dynamics and the effect of NTPDase3 on hormone secretion further elucidates nucleotide autocrine and paracrine mechanisms within the islet. In our assessment of NTPDase3 function in mice, we found a decrease in insulin secretion via *in vitro* macroperifusion studies and *in vivo* stimulated insulin secretion after glucose + arginine stimulation. There are contrasting findings on the effects of ATP on insulin secretion from mouse islets. A prior study showed ATP- and ADP-mediated inhibition of insulin secretion and intracellular Ca^{2+} efflux from perifused mouse β cells[340]. Additionally, high concentrations of ATP can inhibit insulin secretion from mouse islets which may underly the results from our βΔENTPD3 mice[341]. Another report showed that treatment with NTPDase inhibitor ARL67156 increased insulin secretion in mouse and human islets under similar concentrations of glucose utilized in our studies[145]. Studies utilizing ARL67156 support our human pseudoislet studies but not our mouse islet studies. ARL67156 can target multiple NTPDases and may impact other mediators of purinergic signaling[342]. In particular, our studies exposing human islets to ARL67156 *in vitro* had no effect on insulin secretion. Therefore, our utilization of an acute β cell-specific deletion of NTPDase3 served to circumvent adverse non-specific pharmacological effects. Interestingly, our *in vitro* human islet studies were in contrast with our mouse islet studies which may be due to the lower proportion of homotypic β cell interactions in human islets compared to mouse islets, species-specific differences in the potency of nucleotide receptors stimulation within islets, the differential degree of NTPDase3 knockdown between species, and/or redundancy of other islet ecto-enzymes. Future assessment of NTPDase3 function following CRISPR-mediated deletion of NTPDase3 in human islets instead of knockdown may help to reconcile our differing mouse versus human islet results.

Genetic manipulation of NTPDase3 *in vivo* has only been done via global deletion in mice until our spatiotemporal model was used in our studies[226]. Global deletion of NTPDase3 in mice did not have any basal effects on glucose homeostasis or insulin tolerance similar to our findings in βΔENTPD3 mice[226]. Female NTPDase3 global deletion mice were resistant to diet-induced obesity and obesity-associated glucose intolerance due to increased metabolic rates, brown adipose tissue activation, white adipose tissue browning, and improved adipocyte thermogenesis[226]. NTPDase3 expression in adipose autonomic nerves coupled with protective thermogenic effects seen in global deletion mice suggests an important role for NTPDase3 in regulating ATP signaling at sympathetic nerve terminals in adipose tissue.

The β cell-specific knockout mouse model that we generated maintains NTPDase3 expression in other organ systems such as the hypothalamus, peripheral nervous system, or adipose tissue, which also contribute to energy homeostasis[155,226]. We did not see a drastic effect on whole-body glucose homeostasis because our β cell-specific knockout of NTPDase3 may not have altered circulating insulin levels and subsequent glucose tolerance compared to drastic adipose tissue thermogenetic effects in global deletion settings. The addition of a metabolic stressor in the future such as a high-fat diet, obesity, and/or insulin resistance may unmask NTPDase3-dependent effects on glucose homeostasis. Furthermore, NTPDase3 perturbation in either mouse or human islets may lead to compensation by other NTPDases or ecto-enzymes convoluting our results.

The impact of NTPDase in human pseudoislets emphasizes the importance of NTPDase3 in controlling human insulin secretion. We hypothesized that the P2 purinergic receptor we found highly expressed in human β cells, P2Y1, mediated NTPDase3-dependent potentiation of insulin secretion. P2Y1 antagonism reduced insulin secretion and intracellular Ca^{2+} levels in our studies, suggesting a P2Y1-mediated role in the NTPDase3-dependent potentiation of insulin secretion. In support of these findings, prior studies have shown that exogenous ATP and P2Y1 agonist treatment in rodent and human islets increased intracellular Ca^{2+} and subsequent triggering of insulin exocytosis[147,148,160,343]. These findings align with global P2Y1 deletion mice which show increased glycemia, insulinemia, and *in vitro* insulin secretion[344]. A small-molecule screen of mouse islets identified P2Y1 as a druggable target involved in β cell function and a potential diabetes therapeutic target[345]. Furthermore, the percent P2Y1 antagonism of insulin secretion was also positively correlated with body mass index (BMI) suggesting the potential for P2Y1 antagonists to treat hyperglycemia in obesity settings[148]. Other purinergic receptors may also play a role in potentiating intra-islet insulin secretion thru extracellular ATP such as P2X3[149], P2X4[341], and P2X7[158] of which we found P2X4 to be expressed in islet endocrine cells. Our preliminary intracellular Ca^{2+} studies investigated a limited number of human islet preparations, so additional experiments assessing the

role of P2Y1 are needed better to understand its effect on insulin secretion and glucose homeostasis.

Certain experimental limitations exist for this study. MIP-CreERT mice have been reported to have high specificity of TMX-induced Cre-recombination in islets and no impairments in glucose tolerance but were also shown to have increased insulin content and transgene expression of human growth hormone (hGH) which may impact prolactin signaling within islets[346]. Utilization of our pseudoislet system may also disrupt inter-islet junctions important for cell-to-cell purinergic signaling. Generally, we are unsure of the minute effects of spontaneous islet cell reaggregation, particularly those related to architectural differences between primary islets and pseudoislets. We have previously confirmed that functional outputs between primary islets and pseudoislets are similar, underscoring the unique utility of this methodology, but intra-granule ATP may be altered following dispersion and pseudoislet formation. Due to experimental constraints, extracellular ATP levels from pseudoislets and isolated mouse islets were below assay detection levels precluding our measurement of extracellular ATP from these islets.

We also focused on the measurement of human islet extracellular ATP instead of other nucleotides such as ADP, AMP, or adenosine that also have ecto-enzymes and cognate receptors that may be acted upon within the islet. We chose to focus on ATP due to the affinity of NTPDase3 towards this molecule, but future studies warrant the exploration of these other nucleotides and NTPDase3 enzymatic activity *in vitro*. Additionally, we did not measure NTPDase3 enzymatic activity or protein levels after shRNA treatment or genetic elimination. Antibodies specific to human NTPDase3 are not currently amenable to western blot procedures further precluding our assessment of primary islet and pseudoislet protein levels. And lastly, our *in vitro* human islet may not directly translate to *in vivo* effects of NTPDase3 in humans due to the lack of other islet cell types and physiological processes governing glucose homeostasis in our *in vitro* pseudoislet model. Of note, β cell-derived ATP may affect intra-islet accessory cells that express purinergic receptors, such as macrophages and endothelial cells[300,316,347,348]. These accessory cells are required for appropriate islet patterning, postnatal functional maturation, and regulating hormone secretion[84,230,349].

Our data establish an important role of NTPDase3 in modulating insulin secretion in mouse and human islets. Additional studies are needed to determine the broader functions of the pancreatic islet purinergic system described here and if these ecto-enzymes and/or receptors could serve as pharmacological targets to treat obesity and/or diabetes. Such studies must consider the autocrine and paracrine effects of purinergic modulation and focus on improving the specificity of pharmacological agents given the ubiquitous expression of many purinergic components in other systems, such as within

immune and vascular cell types. Certain purinergic components may play a role in diabetes pathogenesis and prevention, requiring further investigation.

CHAPTER VI: SIMILARITIES BETWEEN BACTERIAL GAD AND HUMAN GAD65: IMPLICATIONS IN GUT-MEDIATED AUTOIMMUNE TYPE 1 DIABETES

Text and data in this chapter have been published in
Bedi*, Richardson*, Jia* et al. (2022). PLOS ONE.
(* = co-first authors)

Introduction

Glutamic acid decarboxylase (GAD65) is a prominent autoantibody in type 1 diabetes (T1D). For those diagnosed as a teen, in addition to having an HLA DR3/DR2 signature, it is likely to be the first autoantibody clinically detected in the blood. GAD65 antibodies are prevalent in most T1D cases, occurring in over 70% of patients[188]. Autoantibodies directed against GAD65 recognize linear and conformational epitopes throughout the protein. The functional region of GAD65 contains a catalytic group involving several residues that are distantly located in the primary amino acid sequence of the protein. The enzymatic function of GAD65 and subsequent regulation of GABA production is dependent on a key residue within the catalytic loop, Lys396[350]. This residue covalently binds pyridoxal 5'-phosphate (PLP), a co-factor essential for GABA production by GAD65. The pyridoxal-dependent decarboxylase (PDD) domain in GAD65 is necessary for the enzymatic generation of GABA. A reduction in PLP levels through deficiencies in its precursor, vitamin B6, may be implicated in GAD65 initiated autoimmunity and subsequent T1D onset[351]. Thus, T1D-related immune recognition of GAD65 is highly dependent on the exposure of these regions to autoreactive antigen-presenting cells (APCs). These activated APCs can then attack GAD65-expressing pancreatic β cells leading to their destruction and eventual T1D diagnosis.

In addition to β cells, many bacteria within the gut express GAD (bacterial nomenclature for human GAD65). While there is great diversity within the gut microbiota, more than 95% of gut bacterial species fall into four major microbial phyla: Firmicutes, Bacteroidetes, Actinobacteria, and Protecteobacteria[352]. Bifidobacterium adolescentis, in particular, is an important gut bacterial GABA producer and has the highest prevalence of gad genes in their genomes[353]. These bacterial species provide a homeostatic environment that fosters and facilitates gut epithelial integrity and immunity. Varied literature supports a decrease in microbial diversity and an increase in a “leaky gut” phenotype throughout T1D[189–191]. GABA producing Bifidobacterium bacterial counts drop as the Firmicutes/Bacteroides (F/B) ratios decrease in T1D[354]. There is also a reduction in the abundance of Clostridium clusters IV and XIVa and mucin-degrading bacteria such as Prevotella and Akkermansia. Butyrate is an important metabolite produced by these symbiotic bacterial populations.

Butyrate supports gut integrity and has β cell-specific anti-inflammatory effects[355–357]. Reducing these microbes and their byproducts may contribute to why children at risk for T1D have higher intestinal permeability and T1D-associated gut dysbiosis.

One hypothesis for the interrelationship between dysbiosis and T1D is that as these bacterial populations die, they release GAD65 mimetics that trigger the immune system. Presumably, as GABA-producing bacteria like B. adolescentis die from antibiotic misuse or other pathology, immune cells located in Peyer's patches and deep in the enterocyte border detect the inappropriate presence of GAD. Thus, APCs can further inform CD8+ T cells in nearby lymph nodes. The lymphatic pathways between the intestinal submucosa and pancreatic lymph nodes may provide a route for these “miseducated” CD8+ T cells to access GAD65+ β cells. GAD65 may also originate from β cells leading to an increase in epitope spreading and a misguided immune attack on these insulin-producing cells.

To initiate the exploration of this hypothesis, we utilized *in silico* methodologies to compare gut microbial species that decline at the onset of T1D and express GAD with GAD65 sequences in human pancreatic β cells. We show notable sequence similarity, including relevant motif and T cell epitope overlaps between several bacterial species and β cells, particularly in the functionally important pyridoxal-dependent decarboxylase (PDD) domain of GAD65. Our *in silico* exercise suggests that further investigation is warranted of the relationship between microbial disappearance and the appearance of GAD65 autoantibodies during the prodrome and presentation of T1D.

Results

Multiple sequence alignment highlights several conserved residues between human and bacterial GAD

A total of 25 GAD protein sequences, including three mammalian GAD65 (human, chimpanzee, and mouse) and 22 bacterial GAD, were aligned (**Table 15 & Figure 51**). The three mammalian GAD65 sequences exhibited high conservation, while 20 out of the 22 bacteria GAD sequences exhibited high similarity to one another. Two bacteria, Bdellobibrio sp. Qaytius and Sediminibacterium spp., did not exhibit any protein conservation, which may be due to a misannotation within the RefSeq genome. We also found interesting similarities and differences between the mammalian and bacterial GAD sequences. There were two regions of interest: AA389-397 and AA418-425. AA389-397 contained several charged residues interspaced with hydrophobic residues, potentially a conserved α-helix structure. AA418-AA425 contains conserved HK residues. These two residues represent a known pyridoxal phosphate-binding site in E.coli GAD (H275 and

K276) that is likely conserved in mammalian GAD65. Mammalian GAD65 was ~120 amino acids longer than bacterial GAD. Based on our alignment, this difference is mainly centered around the N-terminus, which suggests adaptations and inclusions of signal peptides required for complex cellular trafficking in mammalian cells. Also, we identified a few small gaps within the core regions of GAD between species, and these gaps are unlikely of any biological significance.

Motif analysis uncovers regional similarities of human and bacterial GAD enzymatic regions

Our motif analysis found 10 ungapped motifs, with each motif present in at least 10 of the sequences under consideration (**Figure 52**). Even though multiple common motifs between human GAD65 and bacterial GAD can be observed, it is noteworthy that 2 motif blocks (motifs 4 and 7) are conserved all across the organisms considered, which is indicative of the sequence similarity observed in the multiple sequence alignment. In addition, except for Streptococcus pneumoniae, motif 3 was consistently present in all sequences. The motifs were also grouped based on the phylogenetic tree constructed from the Multiple Sequence Alignment of GAD sequences. Six motif blocks (motifs 2, 3, 4, 7, 8, and 10) were conserved across three mammalian species, 6 environmental bacterial species, and 2 gut bacterial species. In addition, with exception of Streptococcus pneumoniae, 7 motif blocks were conserved across 4 T1D related bacterial species and 6 gut bacterial species. Furthermore, these motifs were queried on the Pfam and the CDD databases. All 10 motifs were identified as matches to the pyridoxal-dependent decarboxylase (PDD) conserved domain, which is instrumental in GABA biosynthesis from glutamate. Therefore, we show that human GAD65 and bacterial GAD share sequence similarities in a functional region of GAD.

Overlap exists between T cell receptor epitopes of GAD65 and bacterial GAD

To compare the overlap between T cell receptor epitopes, human GAD65, and bacterial GAD, a logo plot of the multiple sequence alignment was made using three representative bacterial GAD and three animal GAD65 proteins. Motif positions for each sequence were manually annotated using the motif coordinates obtained in motif discovery and enrichment analysis. Thereafter, the logo plot was annotated with T cell receptor epitopes, and the overlapping regions were observed. The fine lines indicate the motif coordinates, while the red blocks indicate the CD8+ epitopes and blue blocks indicate the CD4+ epitopes. Three regions overlapped with a motif, which hit the PDD domain as stated in the motif analysis result description (**Figure 53**), confirmed by a CDD search. Of the amino acids in which both CD4 and CD8 receptor epitopes overlap, at least one amino acid residue is conserved across bacterial GAD and GAD65 (**Figure 54**). Our overlap findings between bacterial GAD and human GAD65 emphasize a possible mechanism for how T cells could recognize both bacterial and human GAD65 (**Figure 55**).

Discussion

This study explored the sequence similarities between GAD in twenty GABA-producing bacteria and human GAD65. We found that human and bacterial GAD have similar motifs and conserved residues. We identified notable conservation centered around the pyridoxal-dependent decarboxylase (PDD) domain of GAD65 found in pancreatic β cells, particularly around two key substrate-binding residues. Moreover, some conserved sequences in bacterial GAD overlap with known human GAD65 T cell receptor epitopes. For example, GAD65-specific HLA-DR4 (DRB1*0401)–restricted murine T cell hybridoma line T33.1 recognizes the GAD65 274-286 epitope, and this epitope was conserved across bacteria and human samples examined here. Our *in silico* proof-of-concept suggests a possible relationship between the disappearance of GAD containing GABA-producing bacteria in the human gut microbiome and the appearance of GAD65 autoantibodies during the onset of T1D that needs to be further elucidated.

Our study investigates the genomic and residue similarities in the GAD gene of 29 bacteria, 12 of which have changed abundances in the gut microbiome of those with T1D (**Table 11**). Phylogenetically, the GAD65 sequences are separated into three distinct groups: eukaryotic GAD65, environmental bacterial GAD, and human-related bacterial GAD. Interestingly, we found that environmental bacterial GAD is closer to humans phylogenetically than gut and T1D-associated bacterial GAD. The “hygiene” hypothesis postulates that exposure to environmental bacteria and/or infectious diseases may ward off autoimmune diseases like T1D, highlighting another potential mechanism for immune recognition of GAD[358]. Nevertheless, gut and T1D bacterial species shared 3 motif blocks with mammalian GAD, suggesting an appreciable amount of sequence and motif conservation.

Additionally, we found that a residue within the GAD65 catalytic loop, Lys396, aligned across both bacteria GAD and human GAD65. Lys396 covalently binds PDP, a GAD/GAD65 co-factor essential for GABA production. When GAD65 is devoid of the PLP co-factor, it shows higher antigenicity than GAD65 bound by PDP[359]. Therefore, PLP reduction through decreased levels of its precursor, vitamin B6, may provoke β cell destruction mediated by miseducated GAD-activated T cells. Furthermore, β cell-derived GABA may provide inhibitory signals for autoimmunity such that reduced GAD65 activity may cause an exacerbation of T1D immune pathology against β cells[360].

The elimination of GABA-producing bacteria and emergence of GAD65 autoantibodies in T1D pathogenesis is explored here through *in silico* analyses. Healthy individuals have a greater gut bacterial diversity with GABA-producing pathways activated in several bacterial species compared to T1D donor stool samples[361]. Previous studies show that Bifidobacterium species are especially vulnerable to antibiotics, leading to investigations

of how antibiotic treatments influence this major GABA producer[362]. The TEDDY study cohort of children with T1D found a decrease in the abundance of multiple Bifidobacterium bacterial species in participants following treatments with antibiotics[363]. Therefore, our findings of sequence and epitope similarities further support our paradigm that eliminating GAD-producing bacterial species in humans could correlate with the emergence of GAD65 autoimmunity and subsequent development of T1D.

Thus, we propose that bacterial GAD found in GABA-producing bacteria may act as an antigen to activate submucosal T cells due to gut microbiome bacterial destruction, either through viral- or antibiotic-mediated mechanisms[364]. Further, we posit that primed bacterial GAD T cells bind GAD65 in the islet environment due to the GAD and GAD65 epitope similarity. That leaves us to explore how GAD65, an intracellular enzyme found in β cells, might get recognized by bacterial-derived anti-GAD T cells. Pre-clinical studies demonstrated that GAD65 could associate with the plasma membrane and enter the extracellular space[365,366]. In this scenario, “deputized” β cells that present GAD65 might have an opportunity to interact with GAD-sensitized T cells[367,368]. Therefore, one can imagine a scenario in which GAD-primed T cells from the gut become initially alerted to the islet environment as GAD65 is presented via these deputized β cells. Once alerted, GAD-primed T cells could destroy β cells that display GAD65 at the plasma membrane leading to the development of T1D.

It is important to note a few limitations within our analyses. Many gut microbial genomes and genome annotations were incomplete, particularly for some GABA-producing bacterial species of importance that significantly changed in T1D. We did not include several species due to missing GAD genome annotations. Together, only 20 bacterial sequences were analyzed for their homology, with many environmental organisms. A larger cohort would further strengthen our sequence analyses and hypotheses. Furthermore, we hypothesized that the change in anti-GAD65 is partly due to the changes in the gut microbiome. Additional studies are needed to determine what insult(s) would cause such a disturbance and what cellular mechanisms are involved in the miseducation of immune cells due to the release of GAD in the gut. The window for the disappearance of the GAD-containing bacterial species needs to be identified to determine if it precedes or follows the appearance of autoantibodies to GAD65 in humans. Lastly, the analysis relied on known and curated T cell epitopes of GAD65 from a literature review, in which we demonstrated similarity to bacterial GAD. Whether or not the bacterial peptides bind to human T cell receptors must be further verified *in vitro*. Taken together, our in silico analyses of genome sequences and motifs from bacterial, human, and T cell epitopes identified several homologies that may inform further experimentation and inquiry into the relationship between T1D pathogenesis and microbiome dysbiosis.

Table 15. GABA-producing bacterial species and their respective GAD gene.

Category	Organism	Gene ID
Human	Homo sapiens	2572
Primate	Pan troglodytes	466026
Mouse	Mus musculus	14417
T1D	Streptococcus pneumoniae	Z49109.1
T1D	Bifidobacterium moukalabense	61040350
T1D	Bifidobacterium adolescentis	56675515
T1D	Bacteroides fragilis	61595025
T1D	Ruminococcus	Genome not found
T1D	Veillonella	Genome not found
T1D	Blautia	Genome not found
T1D	Lachnospira	Genome not found
T1D	Alistipes obesi	Genome not found
T1D	Clostridium spp.	29570578
T1D	Prevotella	Genome not found
T1D	Parabacteroides distasonis	CP040468
Gut	Escherichia coli	946058
Gut	Listeria monocytogenes	985123
Gut	Salmonella enterica	13913147
Gut	Streptomyces sp. NRRL B-24085	6211654
Gut	Carnobacterium maltaromaticum	56848084
Gut	Nocardia brasiliensis	13733698
Gut	Lactobacillaceae	56991876
Pathogen	Gammaproteobacteria	QNEL01000191.1

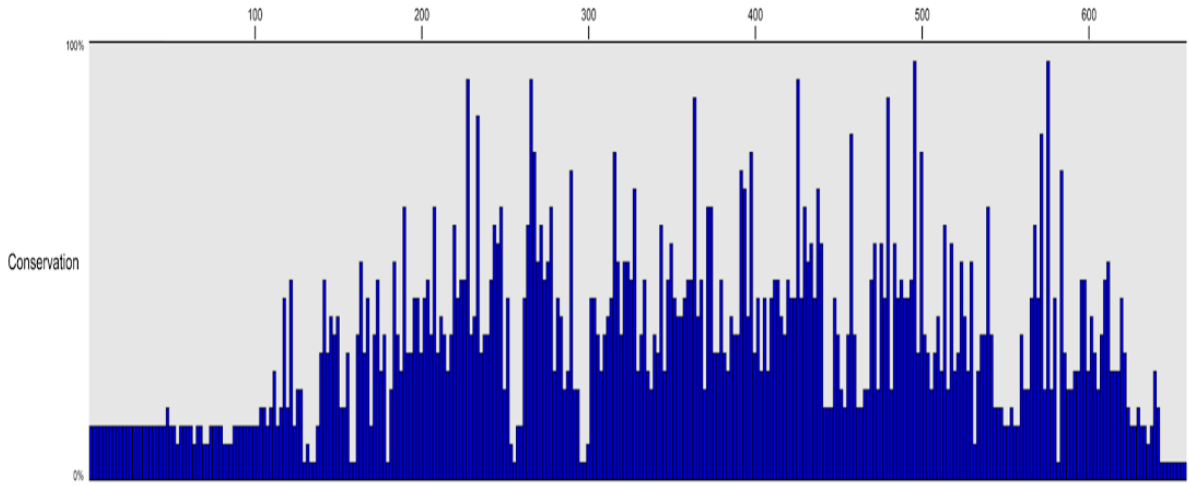

Figure 51. Multiple sequence alignment of twenty bacterial GAD proteins and three animal GAD65 proteins highlights conserved residues.
Using a conservation histogram, across a diverse number of bacterial species and 3 animal species, 12 amino acids were found to be 100% conserved. Amino acids 1-110 are likely signal peptides required for eukaryotic protein translation and cellular transport not needed in bacteria. H275 and K276 are key residues required for PDD binding and are conserved in human GAD65 and bacterial GAD.

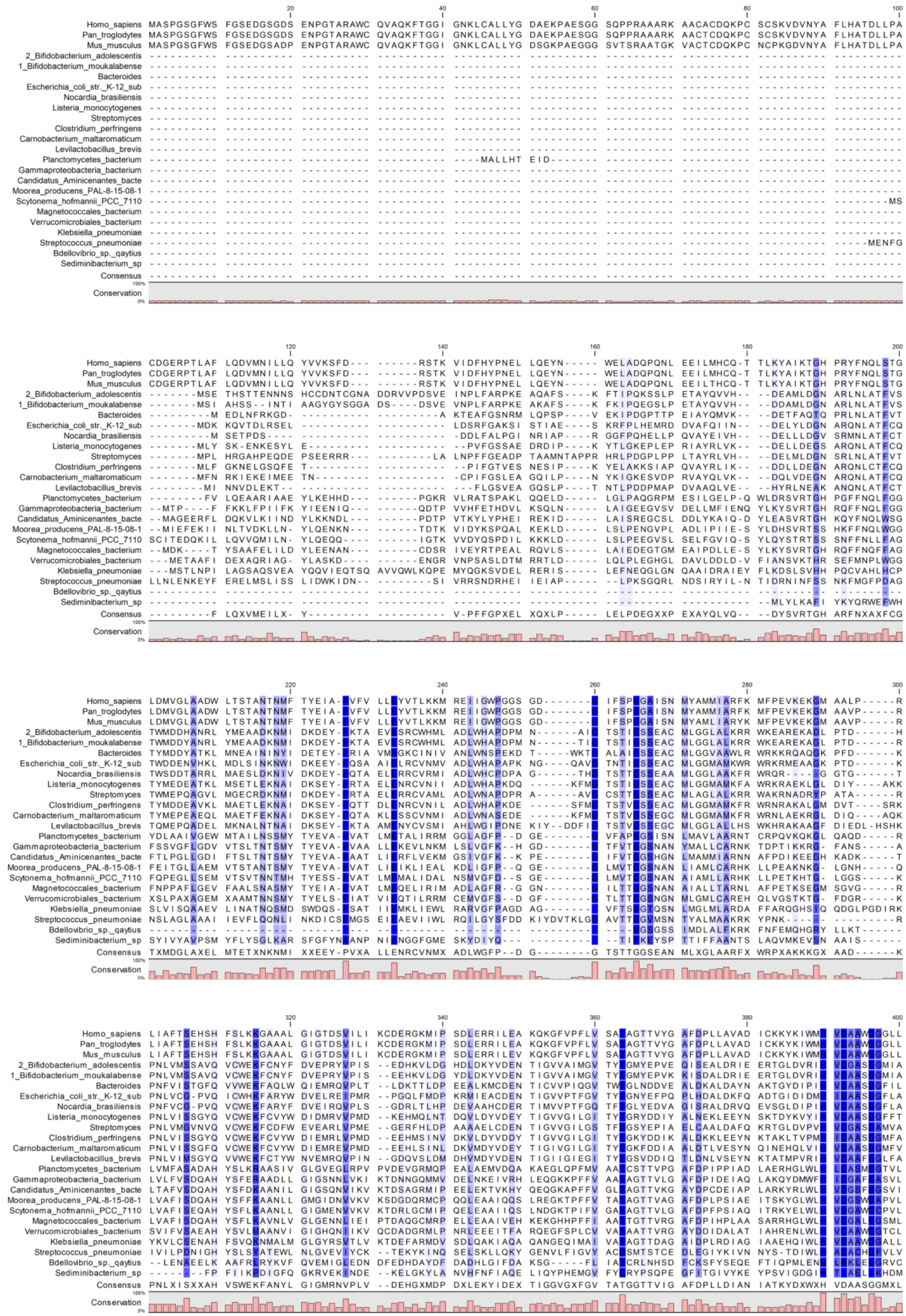
Homo_sapiens
Pan_troglodytes
Mus_musculus
2_Bifidobacterium_adolescentis
1_Bifidobacterium_moukalabense
Bacteroides
Escherichia_coli_str._K-12_sub
Nocardia_brasiliensis
Listeria_monocytogenes
Streptomyces
Clostridium_perfringens
Carnobacterium_maltaromaticum
Levilactobacillus_brevis
Planctomycetes_bacterium
Gammaproteobacteria_bacterium
Candidatus_Aminicenantes_bacte
Moorea_producens_PAL-8-15-08-1
Scytonema_hofmannii_PCC_7110
Magnetococcales_bacterium
Verrucomicrobiales_bacterium
Klebsiella_pneumoniae
Streptococcus_pneumoniae
Bdellovibrio_sp._qaytius
Sediminibacterium_sp
Consensus
Conservation

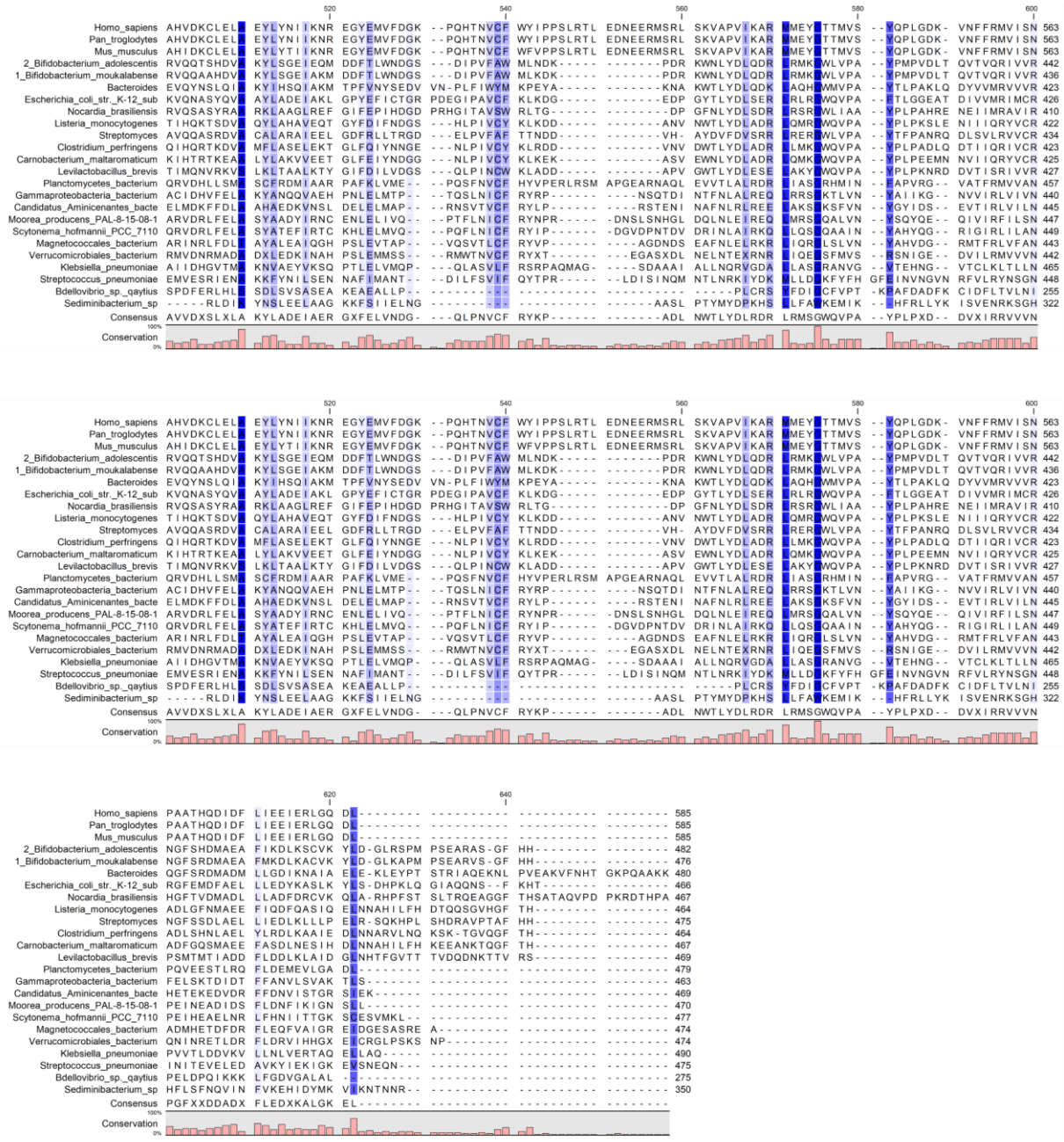

Figure 52. Multiple sequence alignment of twenty bacterial GAD proteins and three animal GAD65 proteins highlights conserved residues.

Across a diverse number of bacterial species and 3 animal species, 12 amino acids were found to be 100% conserved. Amino acids 1-110 are likely signal peptides required for eukaryotic protein translation and cellular transport not needed.in bacteria. H275 and K276 are key residues required for PDD binding and are conserved in human GAD65 and bacterial GAD.

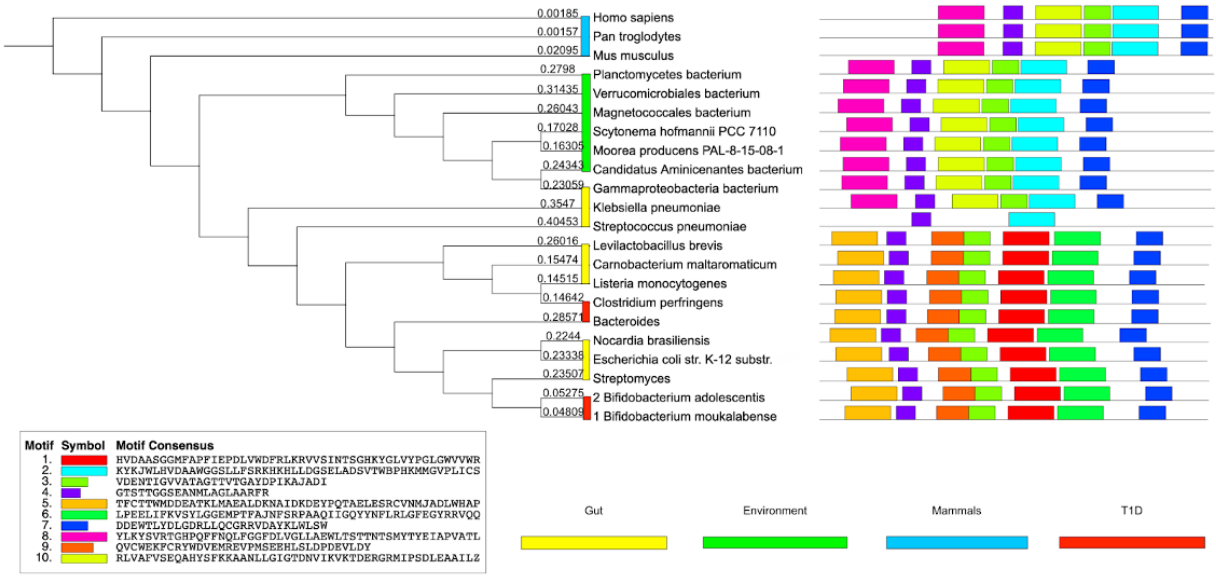

Figure 53. Motif Discovery Analysis of 19 bacterial GAD proteins and 3 animal GAD65 proteins to identify motifs conserved across various species and their functional relevance with GAD protein.

Across all 22 GAD sequences under consideration, 10 motifs were each found in at least 10 of the sequences used for motif discovery. Each motif appears in a separate color below with the individual sequences described as well. Furthermore, the GAD sequences have been grouped based on the organism category from Table 1 and the respective categories have been represented as colored bars next to the organism name. In addition, 2 of the 10 motifs were found in all of the sequences. Each motif was then queried for, using Pfam and CDD searches and it was found that all 10 of the motifs, hit the PDD domain in the GAD65 protein. All motifs match the pyridoxal-dependent decarboxylase (PDD) conserved domain.

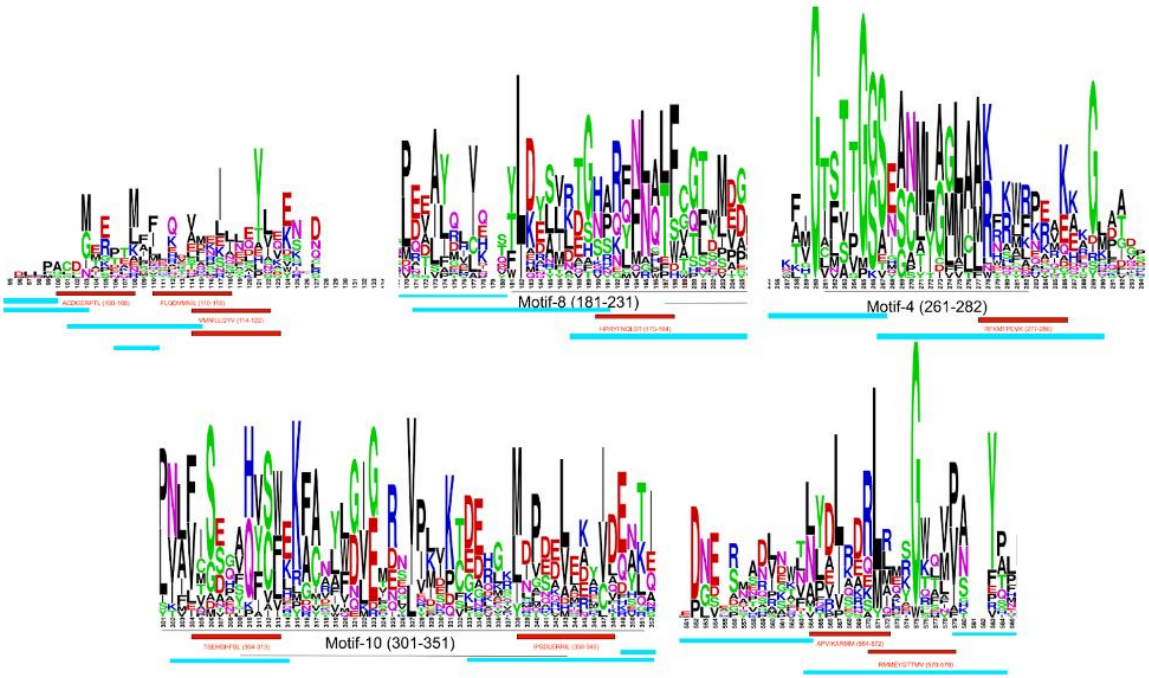

Figure 54. Conserved regions of GAD share common CD8+ and CD4+ T cell receptor epitopes.

A total of 5 regions of interest were identified by overlapping T cell receptor epitopes to the sequence logo of 3 representative bacterial GAD and 3 animal GAD65 proteins. Three regions contained a motif match to Group II pyridoxal-dependent decarboxylases. The red and blue bars correspond to CD8+ and CD4+ T cell receptor epitopes respectively. The black bars correspond to motif blocks with the motif numbers present in Figure 2. The first and last regions did not have any functional motifs but they overlap with receptor epitopes. Of the amino acids in which both CD4+ and CD8+ receptor epitopes overlap, there is at least 1 amino acid residue that is conserved across bacterial GAD and GAD65. Red is CD8+ epitopes and Blue is CD4+ epitopes.

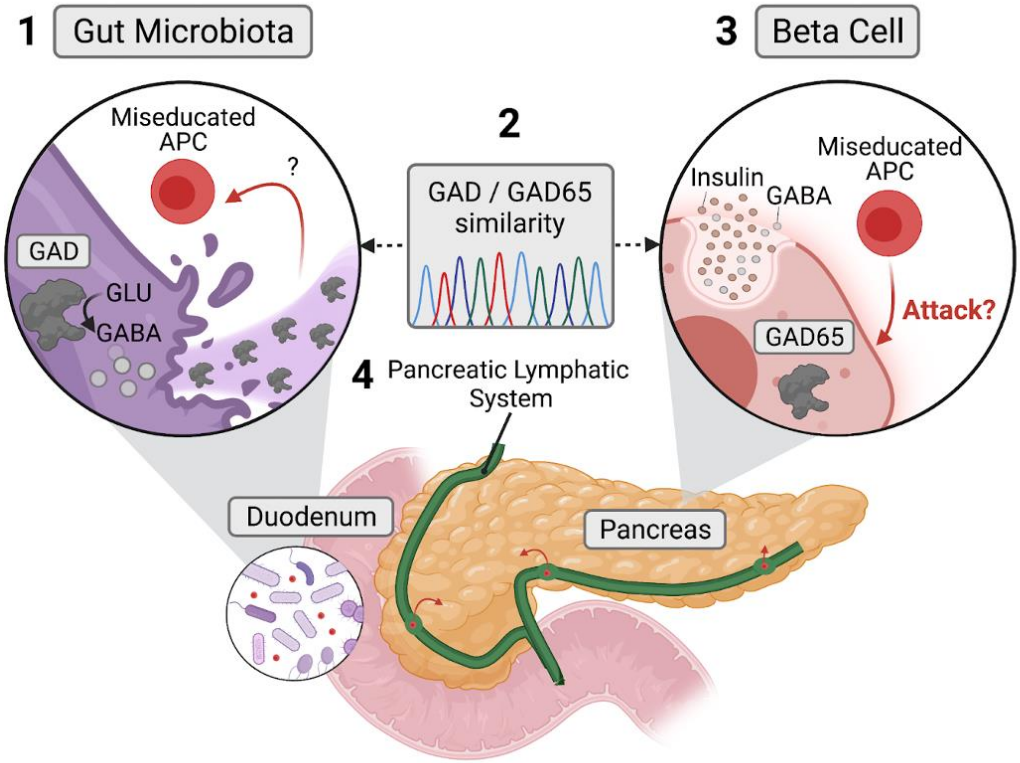

Figure 55. Miseducation of antigen-presenting cells (APCs) by bacterial GAD may contribute to pancreatic β cell immune-mediated destruction.
1) The death of GABA-producing bacteria at the onset of T1D may release bacterial GAD leading to the miseducation of APCs due to the similarity between bacterial GAD and human GAD65 (2). Therefore, this miseducation could provoke the immune system to attack and produce antibodies targeting human GAD65 expressing β cells (3). The pancreatic lymphatic system could provide a pathway for these miseducated APCs to traverse from the duodenum into pancreatic islets (4).

CHAPTER VII: SIGNIFICANCE AND FUTURE DIRECTIONS

A primary regulator of glucose homeostasis is the pancreatic islet due to its secretion of insulin and glucagon. The secretion of these potent hormones by pancreatic islet cells must be precisely regulated and this is done by the complex microenvironment of the pancreatic islet, an innervated, vascularized mini-organ. Multiple cell types within the islet sense and integrate extra- and intra-islet signals such as blood glucose and amino acids during fasting or feeding and exercise.

Summary of findings

The work detailed in this Dissertation elucidated extra- and intra-islet communication mechanisms within the pancreatic islet microenvironment, their regulation of islet hormone secretion, and their contribution to diabetes pathophysiology. This Dissertation examined a variety of topics utilizing multiple experimental paradigms ranging from *in vitro, in vivo*, and *in silico* modalities. Following a brief summary of the findings in this Dissertation, I discuss the implications, unanswered questions, and future directions of this Dissertation.

Chapter III: Human pancreatic neurovascular architecture

The first project, detailed in **Chapter III**, studied human pancreatic neurovascular architecture in healthy and T1D donors. Based on findings in rodent models of T1D, I hypothesized that there would be fewer nerve fibers and capillaries within the islet as an explanation for the reduced glucagon secretion responses seen in T1D. I found stark differences between mouse and human capillary and nerve fiber densities. Surprisingly, I did not detect a loss of capillaries or nerve fibers in T1D tissue utilizing the largest T1D donor pancreatic neurovascular cohort. I found interesting differences in capillary density throughout T1D disease duration. These studies refuted prior assumptions while clarifying and providing new insight into the understanding of the human pancreatic neurovascular landscape with a unique focus on T1D donor pancreata. Our findings suggest that alpha cell secretory changes may be decoupled from neurovascular components.

Chapter IV: Development of a live cell imaging microperifusion platform

The second project, detailed in **Chapter IV**, described the development and utilization of a platform for the synchronous acquisition of intracellular signaling events and hormone secretion in pseudoislets made from primary human islet cells using adenoviral expression of cAMP (cADDis) or Ca^{2+} (GCaMP) biosensors, and a microperifusion system. This approach allowed for the co-registration of cAMP and GCaMP dynamics by

live cell imaging with insulin and glucagon secretion. I achieved high transduction efficiency of each biosensor in pseudoislets and used our microfluidic device to pair intracellular signaling of cAMP or Ca^{2+} with hormone secretion after exposure to low glucose, high glucose, and IBMX. Elaboration of intracellular signaling in human islets will allow studies to examine the physiology and pathophysiology in new ways.

Chapter V: Role of NTPDase3 islet purinergic signaling and hormone secretion

The third project, detailed in **Chapter V**, assessed the islet purinergic system and the role of NTPDase3 in regulating hormone secretion. I comprehensively assessed the transcriptional expression profile of purinergic components in human and mouse islets and found that NTPDase3, NPP1, and NPP2 are the major ecto-enzymes expressed in human islets with NTPDase3 and NPP2 predominating in mouse islets. The action of these enzymes leads to the generation of ADP, AMP, or adenosine, all of which are ligands for the purinergic receptors I found to predominate in both mouse and human islets: P2X4, P2Y1, and ADORA2A. I also found that NTPDase1, Ecto-5'-NT, and ADA are expressed in immune and endothelial cells. I then specifically targeted NTPDase3 because of its islet-specific expression and functional control of extracellular ATP. Reduction of NTPDase3 in mouse islets led to decreased insulin secretion *in vitro* and *in vivo*. Whereas, in human pseudoislets, I saw a potentiation of insulin secretion mediated by the purinergic receptor, P2Y1. These findings highlight the important role of NTPDase3 in islet hormone secretion.

Chapter VI: Human GAD65 and bacterial GAD sequence homology implications for T1D pathogenesis

And finally, the fourth project, detailed in **Chapter VI**, evaluated a potential new mechanism by which bacteria in the gut can induce β cell GAD65 autoimmunity in T1D. Utilizing *in silico* comparisons between bacterial and human β cell GAD65 sequences, I found similarities between important GAD65 enzymatic regions and residues with an overlap in human GAD65 T cell epitopes. I suggest a paradigm in which sequence similarities between GAD65 expression in gut bacteria and β cells may result in β cell-directed autoimmunity leading to the development of T1D.

Implications, unanswered questions, and future directions

To synthesize the work described in this thesis elucidating communications systems within the islet microenvironment and to integrate my work with existing scientific knowledge, this concluding section will focus on four, interrelated themes:

- Pancreatic neurovascular architecture in health and diabetes
- Role of the purinergic system in pancreatic islet function
- Role of NTPDase3 in islet formation, functional maturation, and diabetes
- Selected aspects of T1D pathogenesis

For each, this section will first discuss the scientific implications of my work and how it supports, expands, or refutes current thinking. I then highlight important scientific questions that should be addressed and propose future scientific directions based on my work. Because part of my work developed a new integrated system to examine intracellular islet cell signaling and hormone secretion, this section concludes with a discussion of new possibilities and approaches for studying human islets.

Pancreatic neurovascular architecture in health and diabetes

Implications

Previous investigations revealed that mice pancreata are highly vascularized and innervated[60,263,271]. I compared mouse and human pancreatic tissue and highlighted significant neurovascular differences between these two species. Human pancreata have both capillary and nerve fiber inputs, but not to the extent of their murine counterparts. In both mouse and human pancreata, the endocrine portion of the pancreas is more vascularized but less innervated than the acinar compartment. Species-specific differences in autonomic neurotransmission and vascular function may be a result of this differing neurovascular architecture between species[369]. Furthermore, my findings in the human T1D donor pancreas are in sharp contrast to those reported in mouse models of T1D in which sympathetic nerve fibers are selectively lost. In NOD mice this loss is proportional to the amount of insulitis suggesting immune-mediated destruction of islets nerve fibers. My findings do not support the hypothesis that the reduction in islet sympathetic nerve fiber density seen in rodent models of T1D is the mechanism underlying dysregulated glucagon secretion in human T1D. The rodent models of T1D are imperfect with a much greater T cell infiltrate. Thus, the most straightforward explanation is that the disease course in T1D rodent models does not reflect the human T1D pathologic impacts on neurovascular architecture due to the persistence of nerve

terminals in islets. My findings indicate that other hypotheses such as those discussed below should be pursued to explain the impaired glucagon secretion in T1D.

Unanswered questions and future directions

Intrinsic α cell defect: One alternative hypothesis for the impaired glucagon secretion in T1D is an intrinsic α cell defect. T1D-related hyperglycemia causes metabolic stress on islet cells and may play a significant role in islet dysfunction. Isolated islets from T1D donors secrete less glucagon but rare residual β cells function normally compared to non-diabetic islets[223]. These studies found reduced expression of α cell-specific transcription factors, *ARX* and *MAFB*, with increased expression of β cell-specific transcription factors, NKX6.1, in α cells from T1D tissue[223]. Downstream targets of these transcription factors like ion channel components necessary for appropriate glucagon secretion also showed lower transcript levels of expression[223]. Similarly, single autoantibody-positive individuals with similar endocrine cell proportions to non-diabetic controls had preserved insulin secretion but dysregulated glucagon responses prior to disease onset[223]. Gene expression of these α cells revealed disruptions in glycolysis and oxidative phosphorylation. These findings support the hypothesis of an intrinsic α cell deficiency resulting in glucagon secretion dysfunction seen in T1D[224]. In the future, it would be beneficial to know whether β or α cell-specific transcription factor expression is altered in human islet cells to aid in our understanding of how these transcription factors and their downstream targets control signaling pathways vital to cell function and cell identity.

CNS glucose-sensing defect: Dysfunctions in CNS glucose sensing may be an alternative hypothesis for impaired glucagon secretion in T1D. Hypoglycemia is sensed in the brain to initiate counterregulatory responses via peripheral nervous system inputs to pancreatic α cells and the adrenal gland[209]. Glucose-sensing neurons in the hypothalamus elicit the counterregulatory response as evidenced by increased hypothalamic noradrenergic activity in response to local neuroglycopenia and systemic hypoglycemia. Furthermore, local administration of norepinephrine into the hypothalamus increases blood glucose levels and food intake in rodents[370–374]. Therefore, nerve fiber density in T1D islets could be unchanged while hypoglycemia may not be properly sensed in the CNS due to a variety of mechanisms such as decreased neuronal activity[375], perturbed intracellular activity before neurotransmitter release[376], and impaired cerebral blood flow[377] among other hypotheses. Disruption of CNS glucose-sensing could subsequently lead to impaired downstream counterregulatory responses such as sympathetic nerve fiber activation in the islet and dysregulated glucagon secretion. Moving forward, we must better understand the contributions that systemic hypo- and hyperglycemia have on CNS glucose sensing and neurovascular architecture utilizing islet transplantation and diabetes rodent models.

Capillary and/or nerve fiber functional defect: Another alternative hypothesis for the impaired glucagon secretion in T1D is that there my abnormal perfusion and/or nerve fiber responsiveness *in vivo* of T1D islets. Recent characterization of pancreatic capillaries and pericytes in non-diabetic pancreatic tissue provides a new understanding of vascular functioning in healthy pancreas and needs to be extended to disease settings such as T1D[182,284]. Furthermore, the ECM surrounding nerve fibers and capillaries may be perturbed in T1D further affecting the function of these inputs. Changes in the relative amounts of ECM proteins surrounding islet capillaries may lead to reduced nerve fiber and/or capillary function.

We must also study whether there are changes in other nerve fiber subtypes in T1D not studied in this Dissertation that may affect glucagon secretion such as sensory or parasympathetic nerve fibers. At this point, the field has not comprehensively assessed if T1D pancreatic islets have differential neurotransmitter receptor expression and/or neurotransmitter sensitivities compared to non-diabetic islets. Additionally, one could assess the pancreatic neurovascular architecture from autoantibody-positive donors (Stage 1 & Stage 2 T1D) before significant β cell loss and T1D islets lacking β cells with those containing residual β cells. Further, we must understand whether functional changes in the pancreatic nerve fibers or capillaries exist in T1D. To study unanswered questions surrounding vascular function, one could utilize pancreatic slice physiology to understand defects in T1D.

Role of the purinergic system in pancreatic islet function

Implications

Extracellular nucleotides, metabolized by a variety of ecto-enzymes, can activate several purinergic receptors. The ecto-enzymes and purinergic receptors are widely expressed with their expression profile differing between tissues. The combinatorial expression of ecto-enzymes and purinergic receptors in the pancreatic islet will directly affect the functional impacts these proteins have on cellular responses to extracellular nucleotides. Ecto-enzymes expressed on accessory cells such as immune and endothelial cells could also contribute to the extracellular metabolism of ATP into its derivatives ADP, adenosine, and inosine highlighting an understudied role for these cells in islet purinergic signaling and function.

To probe the function of the islet purinergic system, I focused on NTPDase3 because it is the most highly expressed NTPDase in both mouse and human pancreatic islets (see **Chapter V**). I found a difference in both NTPDase3 expression dynamics and function in mouse and human emphasizing the need to study islet physiology in model organisms

and human tissue. The functional differences we found between mice and human may be due to fewer homotypic cell interactions than do mouse islets, varying potency of nucleotides in stimulating purinergic receptors, gene deletion versus RNA knockdown in our model systems, and/or ecto-enzyme redundancy differing between species. Nonetheless, these findings highlight an important role of NTPDase3 in regulating insulin secretion while also underscoring yet another interspecies difference between mice and human.

Unanswered questions and future directions

Profiling the spatiotemporal localization of the islet purinergic system

To complement our gene expression profiling, multiplexed imaging of pancreatic tissue sections could spatially resolve the proteins of the human islet purinome[378]. These imaging techniques can visualize up to 60 markers while also providing image processing software to determine the relationships between purinergic expression and cell type localization. Additionally, high-resolution imaging of optically cleared pancreatic tissue could shed new light on structure-function interactions with ecto-enzymes, receptors, and islet and exocrine cell types[379,380]. Mapping the relative locations of purinergic components would enrich our limited understanding of the pancreatic purinome and could be utilized in the development of pharmaceutical agents to manipulate pancreatic function and treat diseases such as diabetes.

Purinergic function in pancreatic islets

Currently, there is no *in vivo* method to specifically inhibit pancreatic NTPDase3, and previous reports have only studied NTPDase3 inhibition *in* vitro with pharmacological modulators. The variable specificity of the inhibitors used by other groups may affect the function of intra-islet NTPDases and even purinergic receptors expressed in accessory cells[145,154,381]. We hypothesize that NTPDase3 deletion in mice led to a reduction of *in vitro* insulin secretion due to the following scenarios:

- Do β cells of βΔENTPD3 mice have reduced glycolytic and/or mitochondrial activity generating less intracellular ATP in response to glucose resulting in decreased insulin secretion?
- Is excess extracellular ATP in βΔENTPD3 mice activating inhibitory GPCR P2X or P2Y receptors expressed on mouse islets and/or leading to purinergic receptor desensitization resulting in an inhibitory effect of ATP?
- What is the somatostatin secretion profile of βΔENTPD3 mice? Because somatostatin serves as a negative regulator of insulin secretion, its secretion may be increased due

to the activation of δ cell-expressed P2 receptors by increased extracellular ATP in βΔENTPD3 mice.

- Is NTPDase1 which I found expressed by immune, endothelial, and stellate cells over-compensating for NTPDase3 deletion leading to too little extracellular ATP or too much of an inhibitory ATP-derivative such as adenosine abrogating proper autocrine stimulation of insulin secretion?

The function of other nucleotides and purinergic receptors within the islet is needed to understand the impact of the purinergic system on islet hormone secretion. We must understand which are the most impactful nucleotides on islet cell function and what are the extracellular nucleotide dynamics in mouse islets. To improve the resolution and nucleotide sub-type diversity of our nucleotide measurements, one could:

- Measure ADP, AMP, and adenosine to provide a more exhaustive understanding of the extracellular nucleotide pool
- Utilize pericellular or membrane-bound fluorescent biosensors for assessing nucleotide concentrations in real-time
- Combine extracellular nucleotide sensors with intracellular signaling biosensors in our live cell imaging platform to directly synchronize purinergic function and islet hormone secretion
- Develop innovative tools to spatially and temporally measure intracellular and extracellular purinergic signaling dynamics

Additionally, further assessment of the set of extracellular nucleotides and purinergic receptors underlying the potentiation of insulin secretion in NTPDase3 knockdown human pseudoislets. Also, an assessment of the effect of NTPDase3 perturbation on glucagon and somatostatin secretion as a proxy for α or δ cell function in islets from mice or human donors can also be performed. Understanding the *in vitro* purinergic system within the microenvironment and relating these processes to the *in vivo* microenvironment where islets are receiving inputs from accessory cells such as nerve fibers, vasculature, and immune cells will be important as well.

Role of NTPDase3 in islet formation, functional maturation, and diabetes

Implications

Functional islet maturity: Previous work in our laboratory identified NTPDase3 as a marker for mature adult β cells establishing its utility for sorting dispersed islet cells into single-cell populations of islet cell types[151]. In this Dissertation, I also found that the dynamic shift in gene and protein expression NTPDase3 in human islets correlates with

the maturation of GSIS postnatally (**Chapter V**)[151]. Additionally, a recent report found that clusters of stem cell-derived β-like cells that are insulin+/NTPDase3+ have better GSIS dynamics and differing transcriptional profiles than their insulin+/NTPDase3- counterparts[152]. The findings in this Dissertation paired with other reports on NTPDase3 marking functionally mature β cells suggest a role for NTPDase3 in islet maturation.

Purinergic signaling and islet immune processes: Immunoregulation by nucleotides during key developmental periods may also be controlled by purinergic ecto-enzymes and receptors[300]. ATP is a proinflammatory molecule while its derivative adenosine is an immunosuppressive signal. Intra-islet macrophages express purinergic receptors that are sensitive to β cell-derived ATP to sense islet hormone secretion and health[312,347]. Additionally, mice lacking pancreatic macrophages have impaired islet morphogenesis[349,382]. Therefore, the activity of local ecto-enzymes may be integral to the control of macrophage immune responses that affect islet function and possible islet development.

Diabetes pathology: Insulitis seen in T1D and chronic low-grade inflammation seen in T2D may also be mediated by purinergic receptors given the inflammatory signaling and apoptotic effects that extracellular ATP can illicit[185,198]. Therefore, hyperglycemia in T1D and T2D may activate intra-islet purinergic receptors initiating the release of proinflammatory cytokines and subsequent β cell dysfunction and/or death.

Unanswered questions and future directions

Going forward, we must understand whether the dynamic shift of NTPDase3 expression postnatally corresponds to the functional maturation of insulin secretion in human islets. Further, to extend upon the findings within the field that mature stem-cell-derived β cells are NTPDase3 positive, I would like to understand 1) if there are stem cell-derived NTPDase3+ β cell subsets that dictate GSIS responsiveness of the entire islet similar to β cell leader and pacemaker cells and 2) if stem cell-derived NTPDase3+ β cell subsets have a greater electrophysiological function? To address these questions, one could isolate and assess the transcriptional profiles of stem cell-derived NTPDase3+ and NTPDase3- β cells to highlight a unique subset of β cells that have enhanced GSIS. Additionally, one could employ Patch-Seq technology on stem cell-derived NTPDase3+ β cell subsets to associate measurements of exocytosis and ion channel activity with RNA-seq transcriptomic data. Furthermore, to assess the effect of NTPDase3 on islet morphogenesis, functional maturation, and immune infiltration at time points throughout pancreatic development and islet morphogenesis, one could utilize our inducible β cell-specific *Entpd3* knockout mouse model I generated in **Chapter V**.

Selected aspects of T1D pathogenesis

Implications

The gut microbiome has recently received attention as a potential disease modifier due to its influence on the immune response, intestinal permeability, and metabolite composition in T1D patients[189–191]. Interestingly, bacterial populations within the human gut also express GAD and produce GABA-like islet β cells[353]. Evidence suggests that dysbiosis of the microbiome such as reductions in GABA-producing bacteria and their respective metabolites may correlate with T1D pathogenesis and physiology[189–191]. In **Chapter VI**, the similarities I found between bacterial and human GAD65 sequences led us to postulate that GAD-primed T cells from the gut become initially alerted to the islet environment thru GAD65 presentation by α, β, endothelial cells, or some combination of the three. Once alerted, GAD-primed T cells may destroy β or α cells that display GAD65 at the plasma membrane, reducing the overall GABA levels in the islets with resulting consequences on hyperglycemia which further impacts β cell function.

Unanswered questions and future directions

The theory of molecular mimicry states that a virus carrying an epitope that closely resembles specific structures on β cells may cause auto-aggressive T cells to become activated in people with T1D[383]. Viral infection, therefore, may trigger a cross-reactive autoimmune response against GAD65 following the death of gut microbes that subsequently destroys both the cells infected with the virus and other cells expressing these activating epitopes such as β cells. We are unsure if the reduction in gut microbes in T1D trigger a cross-reactive autoimmune response against GAD65. Additionally, β cells and/or islet endothelial cells “deputized” may act as antigen-presenting cells (APCs) by interacting with GAD-sensitized T cells.

Studies comparing sequences from the gut microbiome of large T1D cohort studies such as the Environmental Determinants of Diabetes in the Young (TEDDY) cohort with bacterial GAD sequence modifications in NOD mouse models could be utilized to further explore the causal link between GAD65/GAD molecular mimicry and T1D pathogenesis proposed in our studies[384]. Additionally, one could determine the effect of microbiome-derived GAD65 and its elimination on 1) immunomodulation processes in T cells of T1D rodent models, 2) the effect of β cell-derived GAD65-generated GABA on intra-islet hormone secretion and GABA signaling in T1D pancreatic slices, and 3) T1D development. Elucidating the possible interaction of GAD65-mediated autoimmunity could contribute to the development of therapeutically effective GAD-based treatments such as vaccines in the prevention of T1D.

Integrated system to examine intracellular islet cell signaling and hormone secretion

Implications

Many important questions remain regarding signaling mechanisms that regulate islet function under physiological and pathological conditions. Microfluidic systems paired with biosensors to measure intracellular or extracellular circumvent limitations of traditional perifusion-based methods routinely used in islet studies. Manipulation of cell type proportions and/or exposure of cells to immune cells could recapitulate disease states seen in T1D. A major limitation of our microfluidic system is that it lacks blood flow and nerve fiber inputs that are important for islet function. Formats are being developed that co-culture pseudoislets with endothelial cells to form functional blood vessels to mitigate this complication[385,386]. Therefore, perfusion instead of perifusion could be achieved to better mimic *in vivo* function of human islets.

Unanswered questions and future directions

Our microfluidic platform affords the opportunity to understand how external stimuli correlate with the intracellular signaling of human islet cells in addition to if signaling molecules secreted by islets and subsequent intracellular signaling cascades change under pathophysiologic conditions such as diabetes. Moving forward a multitude of avenues can be pursued:

- Pseudoislet reaggregation:
  - Live cell imaging to monitor pseudoislets formation over time could help to further elucidate specific mechanisms dictating islet reaggregation following dissociation

- Manipulation of cell-type proportions:
  - T1D-like α cell-only or β cell-depleted pseudoislets can be made to assess the T1D islet microenvironment following the autoimmune destruction of β cells.
  - Transplant T1D-like pseudoislets into mice with normoglycemia or hyperglycemia to better understand how altering the islet microenvironment and glycemia affects islet function

- Monitoring the islet microenvironment with biosensors:
  - Measure extracellular molecules via the introduction of specific biosensors to the cytoplasm or direct them to the plasma membrane
  - Express “Sniffer” biosensor cells as a proxy to assess paracrine signaling within the islet

- Express cell-type specific intracellular signaling biosensors to evaluate cell-specific responses to physiological and disease-associated stimuli.

- Knockdown, knockout, or overexpress genes identified via transcriptional profiling of T1D or T2D islets to provide functional implications for genes implicated in diabetes pathophysiology

- Screen therapeutics with pseudoislets to provide novel ways to understand and correct islet pathophysiology.

Closing Remarks

The studies detailed in this Dissertation explore a vignette of molecular communication networks dictating islet function and dysfunction. We combine morphometric and molecular analysis on clinically relevant materials and novel models to study human and mouse islets. We integrate a variety of topics to produce significant discoveries about the physiology and pathophysiology of pancreatic islets. These findings offer a fresh understanding of the subtleties of cell-to-cell communication systems, particularly in terms of neurovascular architecture, purinergic signaling, and T1D pathogenesis. Overall, a greater understanding of these communication systems governing pancreatic function lays the groundwork for the development of more specific and effective therapeutic targets for diabetes care.

REFERENCES

1. Aronoff, S. L., Berkowitz, K., Shreiner, B. & Want, L. Glucose Metabolism and Regulation: Beyond Insulin and Glucagon. Diabetes Spectrum 3, 183–190 (2004).

2. Faber, C. L., Deem, J. D., Campos, C. A., Taborsky, G. J. & Morton, G. J. CNS control of the endocrine pancreas. Diabetologia 63, 2086–2094 (2020).

3. Unger, R. H. & Cherrington, A. D. Glucagonocentric restructuring of diabetes: a pathophysiologic and therapeutic makeover. J Clin Invest 122, 4–12 (2012).

4. Suda, K., Nobukawa, B., Takase, M. & Hayashi, T. Pancreatic segmentation on an embryological and anatomical basis. J Hepato-biliary-pan 13, 146–148 (2006).

5. Atkinson, M. A., Campbell-Thompson, M., Kusmartseva, I. & Kaestner, K. H. Organisation of the human pancreas in health and in diabetes. Diabetologia 63, 1966–1973 (2020).

6. Chen, N., I, R. U., Anjana, R. M., Mohan, V. & Pitchumoni, C. S. The complex exocrine-endocrine relationship and secondary diabetes in exocrine pancreatic disorders. J Clin Gastroenterol 45, 850–861 (2011).

7. SJ., P. The Exocrine Pancreas. San Rafael (CA): Morgan & Claypool Life Sciences (2010).

8. Slack, J. M. Developmental biology of the pancreas. Dev Camb Engl 121, 1569–80 (1995).

9. Pandiri, A. R. Overview of Exocrine Pancreatic Pathobiology. Toxicol Pathol 42, 207–216 (2014).

10. Veld, P. I. & Marichal, M. Microscopic anatomy of the human islet of Langerhans. Adv Exp Med Biol 654, 1–19 (2010).

11. Marshall, S. M. The pancreas in health and in diabetes. Diabetologia 63, 1962–1965 (2020).

12. Lacy, P. E. & Hartroft, W. S. Electron microscopy of the islets of Langerhans. Ann Ny Acad Sci 82, 287–300 (1959).

13. Baum, J., Simons, B. E., Unger, R. H. & Madison, L. L. Localization of glucagon in the alpha cells in the pancreatic islet by immunofluorescent technics. Diabetes 11, 371–4 (1962).

14. Luft, R., Efendic, S., Hökfelt, T., Johansson, O. & Arimura, A. Immunohistochemical evidence for the localization of somatostatin--like immunoreactivity in a cell population of the pancreatic islets. Med Biol 52, 428–30 (1974).

15. Larsson, L. I., Sundler, F., Håkanson, R., Pollock, H. G. & Kimmel, J. R. Localization of APP, a postulated new hormone, to a pancreatic endocrine cell type. Histochemistry 42, 377–382 (1974).

16. Wierup, N., Svensson, H., Mulder, H. & Sundler, F. The ghrelin cell: a novel developmentally regulated islet cell in the human pancreas. Regul Peptides 107, 63–69 (2002).

17. Olehnik, S. K., Fowler, J. L., Avramovich, G. & Hara, M. Quantitative analysis of intra- and inter-individual variability of human beta-cell mass. Sci Rep 7, 16398 (2017).

18. Dybala, M. P. & Hara, M. Heterogeneity of the Human Pancreatic Islet. Diabetes 68, 1230–1239 (2019).

19. Orci, L., Malaisse-Lagae, F., Baetens, D. & Perrelet, A. Pancreatic-polypeptide-rich regions in human pancreas. Lancet 312, 1200–1201 (1978).

20. Pan, F. C. & Wright, C. Pancreas organogenesis: From bud to plexus to gland. Dev Dynam 240, 530–565 (2011).

21. Jeon, J., Correa-Medina, M., Ricordi, C., Edlund, H. & Diez, J. A. Endocrine Cell Clustering During Human Pancreas Development. J Histochem Cytochem 57, 811–824 (2009).

22. Riopel, M., Li, J., Fellows, G. F., Goodyer, C. G. & Wang, R. Ultrastructural and immunohistochemical analysis of the 8-20 week human fetal pancreas. Islets 6, e982949 (2014).

23. Nair, G. & Hebrok, M. Islet formation in mice and men: lessons for the generation of functional insulin-producing β-cells from human pluripotent stem cells. Curr Opin Genet Dev 32, 171–180 (2015).

24. Jennings, R. E., Berry, A. A., Strutt, J. P., Gerrard, D. T. & Hanley, N. A. Human pancreas development. Development 142, 3126–3137 (2015).

25. Villani, V. et al. SOX9+/PTF1A+ Cells Define the Tip Progenitor Cells of the Human Fetal Pancreas of the Second Trimester. Stem Cell Transl Med 8, 1249–1264 (2019).

26. Meier, J. J. et al. β-cell development and turnover during prenatal life in humans. Eur J Endocrinol 162, 559–568 (2010).

27. Otonkoski, T., Andersson, S., Knip, M. & Simell, O. Maturation of insulin response to glucose during human fetal and neonatal development. Studies with perifusion of pancreatic isletlike cell clusters. Diabetes 37, 286–291 (1988).

28. Pan, F. C. & Brissova, M. Pancreas development in humans. Curr Opin Endocrinol Diabetes Obes 21, 77–82 (2014).

29. Lammert, E. & Thorn, P. The role of the islet niche on beta cell structure and function. J Mol Biol 432, 1407–1418 (2019).

30. Benninger, R. K. P. et al. Fluorescence-Lifetime Imaging of DNA–Dye Interactions within Continuous-Flow Microfluidic Systems. Angew. Chem. Int. Ed. 46, 2228–2231 (2007).

31. Rocheleau, J. V., Walker, G. M., Head, W. S., McGuinness, O. P. & Piston, D. W. Microfluidic glucose stimulation reveals limited coordination of intracellular Ca2+ activity oscillations in pancreatic islets. Proc National Acad Sci 101, 12899–12903 (2004).

32. Walker, J. T. et al. Integrated human pseudoislet system and microfluidic platform demonstrate differences in GPCR signaling in islet cells. JCI Insight 5, (2020).

33. Speier, S. & Rupnik, M. A novel approach to in situ characterization of pancreatic β-cells. Pflügers Archiv 446, 553–558 (2003).

34. Qadir, M. M. F. et al. Long-term culture of human pancreatic slices as a model to study real-time islet regeneration. Nat Commun 11, 3265 (2020).

35. Speier, S. et al. Noninvasive in vivo imaging of pancreatic islet cell biology. Nat Med 14, 574–578 (2008).

36. Rodriguez-Diaz, R. et al. Noninvasive in vivo model demonstrating the effects of autonomic innervation on pancreatic islet function. Proc National Acad Sci 109, 21456–21461 (2012).

37. Janjuha, S., Singh, S. P. & Ninov, N. Analysis of Beta-cell Function Using Single-cell Resolution Calcium Imaging in Zebrafish Islets. J Vis Exp Jove 57851 (2018).

38. Nyman, L. R. et al. Real-time, multidimensional in vivo imaging used to investigate blood flow in mouse pancreatic islets. J Clin Invest 118, 3790–3797 (2008).

39. Wharton, G. K. The blood supply of the pancreas, with special reference to that of the islands of Langerhans. Anatomical Rec 53, 55–81 (1932).

40. Bonner-Weir, S. & Orci, L. New perspectives on the microvasculature of the islets of Langerhans. Diabetes 31, 883–889 (1982).

41. Cleaver, O. & Melton, D. A. Endothelial signaling during development. Nat Med 9, 661–668 (2003).

42. Brissova, M. et al. Pancreatic Islet Production of Vascular Endothelial Growth Factor-A Is Essential for Islet Vascularization, Revascularization, and Function. Diabetes 55, 2974–2985 (2006).

43. Brunicardi, F. C. et al. Microcirculation of the Islets of Langerhans: Long Beach Veterans Administration Regional Medical Education Center Symposium. Diabetes 45, 385–392 (1996).

44. Dybala, M. P. et al. Integrated Pancreatic Blood Flow: Bi-Directional Microcirculation Between Endocrine and Exocrine Pancreas. Diabetes db191034 (2020).

45. Radziuk, J., Barron, P., Najm, H. & Davies, J. The effect of systemic venous drainage of the pancreas on insulin sensitivity in dogs. J Clin Invest 92, 1713–1721 (1993).

46. Tokarz, V. L., MacDonald, P. E. & Klip, A. The cell biology of systemic insulin function. J Cell Biol 217, jcb.201802095 (2018).

47. Hamilton, N. B., Attwell, D. & Hall, C. N. Pericyte-Mediated Regulation of Capillary Diameter: A Component of Neurovascular Coupling in Health and Disease. Frontiers Neuroenergetics 2, 5 (2010).

48. Atef, N., Ktorza, A., Picon, L. & Penicaud, L. Increased islet blood flow in obese rats: role of the autonomic nervous system. Am J Physiol Endocrinol Metab 262, E736–40 (1992).

49. Nyman, L. R., Ford, E., Powers, A. C. & Piston, D. W. Glucose-dependent blood flow dynamics in murine pancreatic islets in vivo. Am J Physiol Endocrinol Metab 298, E807--E814 (2010).

50. Reinert, R. B. et al. Vascular endothelial growth factor-a and islet vascularization are necessary in developing, but not adult, pancreatic islets. Diabetes 62, 4154–4164 (2013).

51. Kragl, M. & Lammert, E. The Islets of Langerhans. Adv Exp Med Biol 654, 217–234 (2010).

52. Nikolova, G. et al. The Vascular Basement Membrane: A Niche for Insulin Gene Expression and β Cell Proliferation. Dev Cell 10, 397–405 (2006).

53. Deijnen, J. H. M. van, Hulstaert, C. E., Wolters, G. H. J. & Schilfgaarde, R. van. Significance of the peri-insular extracellular matrix for islet isolation from the pancreas of rat, dog, pig, and man. Cell Tissue Res 267, 139–146 (1992).

54. Otonkoski, T., Banerjee, M., Korsgren, O., Thornell, L. -E. & Virtanen, I. Unique basement membrane structure of human pancreatic islets: implications for β-cell growth and differentiation. Diabetes Obes Metabolism 10, 119–127 (2008).

55. Richins, C. A. The innervation of the pancreas. J Comp Neurol 83, 223–236 (1945).

56. Kiba, T. et al. Ventromedial hypothalamic lesion-induced vagal hyperactivity stimulates rat pancreatic cell proliferation. Gastroenterology 110, 885–893 (1996).

57. Li, W., Yu, G., Liu, Y. & Sha, L. Intrapancreatic Ganglia and Neural Regulation of Pancreatic Endocrine Secretion. Front Neurosci 13, 21 (2019).

58. Ahrén, B. Autonomic regulation of islet hormone secretion--implications for health and disease. Diabetologia 43, 393–410 (2000).

59. Kirchgessner, A. & Gershon, M. Innervation of the pancreas by neurons in the gut. J Neurosci 10, 1626–1642 (1990).

60. Tang, S.-C., Jessup, C. F. & Campbell-Thompson, M. The Role of Accessory Cells in Islet Homeostasis. Curr Diabetes Rep 18, 117 (2018).

61. Kobayashi, S. & Fujita, T. Fine structure of mammalian and avian pancreatic islets with special reference to D cells and nervous elements. Zeitschrift Für Zellforschung Und Mikroskopische Anatomie 100, 340–363 (1969).

62. Makhmutova, M. & Caicedo, A. Optical Imaging of Pancreatic Innervation. Front Endocrinol 12, 663022 (2021).

63. Serizawa, Y., Kobayashi, S. & Fujita, T. Neuro-Insular Complex Type I in the Mouse. Arch Histol Japon 42, 389–394 (1979).

64. Nilsson, C., Zoucas, E., Lundquist, I. & Ihse, I. Effect of Selective Denervation of the Rat Pancreas on Pancreatic Endocrine Function. Eur Surg Res 33, 86–91 (2001).

65. Tamura, K., Sutherland, D. E. R. & Kaneko, G. Exocrine Function of the Heterotopic Transplanted Pancreas Segment. Pancreas 3, 324–331 (1988).

66. Schwartz, T. W. et al. Vagal, cholinergic regulation of pancreatic polypeptide secretion. J Clin Invest 61, 781–789 (1978).

67. Ahrén, B. & Holst, J. J. The cephalic insulin response to meal ingestion in humans is dependent on both cholinergic and noncholinergic mechanisms and is important for postprandial glycemia. Diabetes 50, 1030–1038 (2001).

68. Konturek, S. J., Zabielski, R., Konturek, J. W. & Czarnecki, J. Neuroendocrinology of the pancreas; role of brain-gut axis in pancreatic secretion. Eur J Pharmacol 481, 1–14 (2003).

69. Rodriguez-Diaz, R. & Caicedo, A. Neural control of the endocrine pancreas. Best Pract Res Clin Endocrinol Metab 28, 745–756 (2014).

70. Makhmutova, M. et al. Pancreatic β-Cells Communicate With Vagal Sensory Neurons. Gastroenterology 160, 875-888.e11 (2021).

71. Li, Q. & Peng, J. Sensory nerves and pancreatitis. Gland Surg 3, 284–92 (2014).

72. Juang, J.-H., Peng, S.-J., Kuo, C.-H. & Tang, S.-C. Three-dimensional islet graft histology: panoramic imaging of neural plasticity in sympathetic reinnervation of transplanted islets under the kidney capsule. Am J Physiol-endoc M 306, E559–E570 (2014).

73. Larsen, J. L. Pancreas Transplantation: Indications and Consequences. Endocr Rev 25, 919–946 (2004).

74. Rodriguez-Diaz, R. et al. Innervation patterns of autonomic axons in the human endocrine pancreas. Cell Metab 45–54 (2011).

75. Brissova, M. et al. Human Islets Have Fewer Blood Vessels than Mouse Islets and the Density of Islet Vascular Structures Is Increased in Type 2 Diabetes. J Histochem Cytochem 63, 637–645 (2015).

76. Richardson, T. M. et al. Human pancreatic capillaries and nerve fibers persist in type 1 diabetes despite beta cell loss. Am J Physiol Endocrinol Metab (2023).

77. Chien, H.-J. et al. Human pancreatic afferent and efferent nerves: mapping and 3-D illustration of exocrine, endocrine, and adipose innervation. Am J Physiology Gastrointest Liver Physiology (2019).

78. Havel, P. J. & Ahren, B. Activation of Autonomic Nerves and the Adrenal Medulla Contributes to Increased Glucagon Secretion During Moderate Insulin-Induced Hypoglycemia in Women. Diabetes 46, 801–807 (1997).

79. Lammert, E., Cleaver, O. & Melton, D. Induction of Pancreatic Differentiation by Signals from Blood Vessels. Science 294, 564–567 (2001).

80. Yoshitomi, H. & Zaret, K. S. Endothelial cell interactions initiate dorsal pancreas development by selectively inducing the transcription factor Ptf1a. Development 131, 807–817 (2004).

81. Shah, S. R. et al. Embryonic mouse blood flow and oxygen correlate with early pancreatic differentiation. Dev Biol 349, 342–349 (2011).

82. Glebova, N. O. & Ginty, D. D. Growth and survival signals controlling sympathetic nervous system development. Annu Rev Neurosci 28, 191–222 (2005).

83. Burris, R. E. & Hebrok, M. Pancreatic innervation in mouse development and β-cell regeneration. Neuroscience 150, 592–602 (2007).

84. Reinert, R. B. et al. Vascular endothelial growth factor coordinates islet innervation via vascular scaffolding. Development 141, 1480–1491 (2014).

85. Borden, P., Houtz, J., Leach, S. D. & Kuruvilla, R. Sympathetic Innervation during Development Is Necessary for Pancreatic Islet Architecture and Functional Maturation. Cell Reports 4, 287–301 (2013).

86. Proshchina, A. E., Krivova, Y. S., Leonova, O. G., Barabanov, V. M. & Saveliev, S. V. Development of Human Pancreatic Innervation. in Autonomic Nervous System (IntechOpen, 2018).

87. Johansson, Å. et al. Endothelial cell signalling supports pancreatic beta cell function in the rat. Diabetologia 52, 2385–2394 (2009).

88. Riopel, M. & Wang, R. Collagen matrix support of pancreatic islet survival and function. Frontiers Biosci Landmark Ed 19, 77–90 (2014).

89. Vlahos, A. E. et al. Endothelialized collagen based pseudo-islets enables tuneable subcutaneous diabetes therapy. Biomaterials 232, 119710 (2019).

90. Myers, J. P., Santiago-Medina, M. & Gomez, T. M. Regulation of axonal outgrowth and pathfinding by integrin-ECM interactions. Dev Neurobiol 71, 901–923 (2011).

91. Cai, Q. et al. Enhanced expression of VEGF-A in β cells increases endothelial cell number but impairs islet morphogenesis and β cell proliferation. Dev Biol 367, 40–54 (2012).

92. Brissova, M. et al. Islet microenvironment, modulated by vascular endothelial growth factor-A signaling, promotes β cell regeneration. Cell Metab 19, 498--511 (2014).

93. Rosenbaum, T., Vidaltamayo, R., Sánchez-Soto, Ma. C., Zentella, A. & Hiriart, M. Pancreatic β cells synthesize and secrete nerve growth factor. Proc National Acad Sci 95, 7784–7788 (1998).

94. Vidaltamayo, R., Sánchez-Soto, Ma. C., Rosenbaum, T., Martínez-Merlos, T. & Hiriart, M. Neuron-like phenotypic changes in pancreatic β-cells induced by NGF, FGF, and dbcAMP. Endocrine 4, 19–26 (1996).

95. Unger, R. H. & Orci, L. Paracrinology of islets and the paracrinopathy of diabetes. Proc National Acad Sci 107, 16009–16012 (2010).

96. Halban, P. A. et al. The Possible Importance of Contact between Pancreatic Islet Cells for the Control of Insulin Release. Endocrinology 111, 86–94 (1982).

97. Pipeleers, D., Veld, P. I. in't, Maes, E. & Winkel, M. V. D. Glucose-induced insulin release depends on functional cooperation between islet cells. Proc National Acad Sci 79, 7322–7325 (1982).

98. Vos, A. D. et al. Human and rat beta cells differ in glucose transporter but not in glucokinase gene expression. J Clin Invest 96, 2489–2495 (1995).

99. McCulloch, L. J. et al. GLUT2 (SLC2A2) is not the principal glucose transporter in human pancreatic beta cells: Implications for understanding genetic association signals at this locus. Mol Genet Metab 104, 648–653 (2011).

100. Patterson, J. N. et al. Mitochondrial Metabolism of Pyruvate Is Essential for Regulating Glucose-stimulated Insulin Secretion. J Biol Chem 289, 13335–13346 (2014).

101. Misler, S., Gillis, K. & Tabcharani, J. Modulation of gating of a metabolically regulated, ATP-dependent K+ channel by intracellular pH in β cells of the pancreatic islet. J Membr Biology 109, 135–143 (1989).

102. Misler, S., Barnett, D. W., Gillis, K. D. & Pressel, D. M. Electrophysiology of Stimulus-Secretion Coupling in Human β-Cells. Diabetes 41, 1221–1228 (1992).

103. Rorsman, P. & Braun, M. Regulation of Insulin Secretion in Human Pancreatic Islets. Physiology 75, 155–179 (2013).

104. Rorsman, P., Braun, M. & Zhang, Q. Regulation of calcium in pancreatic α- and β-cells in health and disease. Cell Calcium 51, 300–308 (2012).

105. Zarkovic, M. & Henquin, J.-C. Synchronization and entrainment of cytoplasmic Ca2+ oscillations in cell clusters prepared from single or multiple mouse pancreatic islets. Am J Physiol Endocrinol Metab 287, E340–E347 (2004).

106. Johnston, N. R. et al. Beta Cell Hubs Dictate Pancreatic Islet Responses to Glucose. Cell Metab 24, 389–401 (2016).

107. Salem, V. et al. Leader β-cells coordinate Ca2+ dynamics across pancreatic islets in vivo. Nat Metabolism 1, 615–629 (2019).

108. Rutter, G. A. et al. Local and regional control of calcium dynamics in the pancreatic islet. Diabetes Obes Metabolism 19, 30–41 (2017).

109. Sutherland, E. W. & Duve, C. D. Origin and distribution of the hyperglycemic-glycogenolytic factor of the pancreas. J Biological Chem 175, 663–74 (1948).

110. Gylfe, E. & Gilon, P. Glucose regulation of glucagon secretion. Diabetes Res Clin Pr 103, 1–10 (2014).

111. Walker, J. N. et al. Regulation of glucagon secretion by glucose: paracrine, intrinsic or both? Diabetes Obes Metabolism 13, 95–105 (2011).

112. Gromada, J., Franklin, I. & Wollheim, C. B. α-Cells of the Endocrine Pancreas: 35 Years of Research but the Enigma Remains. Endocr Rev 28, 84–116 (2007).

113. Marchand, S. J. L. & Piston, D. W. Glucose suppression of glucagon secretion: metabolic and calcium responses from alpha-cells in intact mouse pancreatic islets. J Biol Chem 285, 14389–14398 (2010).

114. Liu, Y.-J., Vieira, E. & Gylfe, E. A store-operated mechanism determines the activity of the electrically excitable glucagon-secreting pancreatic α-cell. Cell Calcium 35, 357–365 (2004).

115. Briant, L., Salehi, A., Vergari, E., Zhang, Q. & Rorsman, P. Glucagon secretion from pancreatic α-cells. Upsala J Med Sci 121, 113–119 (2016).

116. Kalwat, M. A. & Cobb, M. H. Mechanisms of the amplifying pathway of insulin secretion in the β cell. Pharmacol Therapeut 179, 17–30 (2017).

117. Franklin, I., Gromada, J., Gjinovci, A., Theander, S. & Wollheim, C. B. β-Cell Secretory Products Activate α-Cell ATP-Dependent Potassium Channels to Inhibit Glucagon Release. Diabetes 54, 1808–1815 (2005).

118. Ravier, M. A. & Rutter, G. A. Glucose or Insulin, but not Zinc Ions, Inhibit Glucagon Secretion From Mouse Pancreatic α-Cells. Diabetes 54, 1789–1797 (2005).

119. Diao, J., Asghar, Z., Chan, C. B. & Wheeler, M. B. Glucose-regulated Glucagon Secretion Requires Insulin Receptor Expression in Pancreatic α-Cells. J Biol Chem 280, 33487–33496 (2005).

120. Xu, E. et al. Intra-islet insulin suppresses glucagon release via GABA-GABAA receptor system. Cell Metab 3, 47–58 (2006).

121. Elliott, A. D., Ustione, A. & Piston, D. W. Somatostatin and insulin mediate glucose-inhibited glucagon secretion in the pancreatic α-cell by lowering cAMP. Am J Physiol Endocrinol Metab 308, E130–E143 (2015).

122. Müller, W. A., Faloona, G. R. & Unger, R. H. The effect of experimental insulin deficiency on glucagon secretion. J Clin Invest 50, 1992–1999 (1971).

123. Salehi, P. et al. Human Islet Isolation Outcomes From Pancreata Preserved with Histidine-Tryptophan Ketoglutarate versus University of Wisconsin Solution. Transplantation 82, 983–985 (2006).

124. Drucker, D. J. Mechanisms of Action and Therapeutic Application of Glucagon-like Peptide-1. Cell Metab 27, 740–756 (2018).

125. Reichlin, S. Somatostatin. New Engl J Medicine 309, 1495–1501 (1983).

126. Kailey, B. et al. SSTR2 is the functionally dominant somatostatin receptor in human pancreatic β- and α-cells. Am J Physiol Endocrinol Metab 303, E1107–E1116 (2012).

127. Zhang, Y. et al. GLP-1 Receptor in Pancreatic α-Cells Regulates Glucagon Secretion in a Glucose-Dependent Bidirectional Manner. Diabetes 68, 34–44 (2019).

128. Rutter, G. A. Regulating Glucagon Secretion: Somatostatin in the Spotlight. Diabetes 58, 299–301 (2009).

129. Khakh, B. S. & Burnstock, G. The Double Life of ATP. Sci Am 301, 84–92 (2009).

130. Drury, A. N. & Szent-Györgyi, A. The physiological activity of adenine compounds with especial reference to their action upon the mammalian heart1. J Physiology 68, 213–237 (1929).

131. Burnstock, G. Purinergic signalling: Its unpopular beginning, its acceptance and its exciting future. Bioessays 34, 218–225 (2012).

132. Volonté, C. & D'Ambrosi, N. Membrane compartments and purinergic signalling: the purinome, a complex interplay among ligands, degrading enzymes, receptors and transporters: The purinome. Febs J 276, 318–329 (2008).

133. Suckale, J. & Solimena, M. The insulin secretory granule as a signaling hub. Trends Endocrinol Metabolism 21, 599–609 (2010).

134. Leitner, J. W., Sussman, K. E., Vatter, A. E. & Schneider, F. H. Adenine nucleotides in the secretory granule fraction of rat islets. Endocrinology 96, 662–677 (1975).

135. Hazama, A., Hayashi, S. & Okada, Y. Cell surface measurements of ATP release from single pancreatic β cells using a novel biosensor technique. Pflügers Archiv 437, 31–35 (1998).

136. Baroja-Mazo, A., Barberà-Cremades, M. & Pelegrín, P. The participation of plasma membrane hemichannels to purinergic signaling. Biochim Biophys Acta 1828, 79–93 (2013).

137. Farnsworth, N. L. & Benninger, R. K. P. New insights into the role of connexins in pancreatic islet function and diabetes. Febs Lett 588, 1278–1287 (2014).

138. Jain, S. & Jacobson, K. A. Purinergic signaling in diabetes and metabolism. Biochem Pharmacol 187, 114393 (2020).

139. Novak, I. Purinergic receptors in the endocrine and exocrine pancreas. Purinerg Signal 4, 237–253 (2008).

140. Robson, S. C., Sévigny, J. & Zimmermann, H. The E-NTPDase family of ectonucleotidases: Structure function relationships and pathophysiological significance. Purinerg Signal 2, 409--430 (2006).

141. Zimmermann, H., Zebisch, M. & Strater, N. Cellular function and molecular structure of ecto-nucleotidases. Purinerg Signal 8, 437–502 (2012).

142. Kittel, A. et al. Localization of Nucleoside Triphosphate Diphosphohydrolase-1 (NTPDase1) and NTPDase2 in Pancreas and Salivary Gland. J Histochem Cytochem 52, 861–871 (2003).

143. Yu, W., Robson, S. C. & Hill, W. G. Expression and Distribution of Ectonucleotidases in Mouse Urinary Bladder. Plos One 6, e18704 (2011).

144. Martín-Satué, M. et al. Localization of plasma membrane bound NTPDases in the murine reproductive tract. Histochem Cell Biol 131, 615–628 (2009).

145. Syed, S. K. et al. Ectonucleotidase NTPDase3 is abundant in pancreatic β-cells and regulates glucose-induced insulin secretion. Am J Physiol Endocrinol Metab 305, E1319–E1326 (2013).

146. Coutinho-Silva, R., Parsons, M., Robson, T. & Burnstock, G. Changes in expression of P2 receptors in rat and mouse pancreas during development and ageing. Cell Tissue Res 306, 373–383 (2001).

147. Wuttke, A., Idevall-Hagren, O. & Tengholm, A. P2Y1 receptor-dependent diacylglycerol signaling microdomains in β cells promote insulin secretion. Faseb J 27, 1610–1620 (2013).

148. Khan, S. et al. A role for PKD1 in insulin secretion downstream of P2Y 1 receptor activation in mouse and human islets. Physiological Reports 7, e14250 (2019).

149. Jacques-Silva, M. C. et al. ATP-gated P2X3 receptors constitute a positive autocrine signal for insulin release in the human pancreatic β cell. Proc National Acad Sci 107, 6465–6470 (2010).

150. Tozzi, M. et al. The P2X7 receptor and pannexin-1 are involved in glucose-induced autocrine regulation in β-cells. Sci Rep 8, 8926 (2018).

151. Saunders, D. C. et al. Ectonucleoside Triphosphate Diphosphohydrolase-3 Antibody Targets Adult Human Pancreatic Beta Cells for In Vitro and In Vivo Analysis. Cell Metab 29, 1–10 (2018).

152. Docherty, F. M. et al. ENTPD3 Marks Mature Stem Cell Derived Beta Cells Formed by Self-Aggregation in Vitro. Diabetes db200873 (2021).

153. Belcher, S. M., Zsarnovszky, A. & Crawford, P. A. Immunolocalization of ecto-nucleoside triphosphate diphosphohydrolase 3 in rat brain: Implications for modulation of multiple homeostatic systems including feeding and sleep–wake behaviors. Neuroscience 137, 1331–1346 (2006).

154. Lavoie, E. G. et al. Identification of the ectonucleotidases expressed in mouse, rat, and human Langerhans islets: potential role of NTPDase3 in insulin secretion. Am J Physiol-endoc M 299, E647–E656 (2010).

155. McCoy, E. et al. Deletion of ENTPD3 does not impair nucleotide hydrolysis in primary somatosensory neurons or spinal cord. F1000research 3, 1–22 (2014).

156. Lavoie, E. G. et al. Identification of the ectonucleotidases expressed in mouse, rat, and human Langerhans islets : potential role of NTPDase3 in insulin secretion. Am J Physiol Endocrinol Metab 300, G608–G620 (2011).

157. Antonioli, L., Blandizzi, C., Csóka, B., Pacher, P. & Haskó, G. Adenosine signalling in diabetes mellitus—pathophysiology and therapeutic considerations. Nat Rev Endocrinol 11, 228–241 (2015).

158. Glas, R. et al. Purinergic P2X7 receptors regulate secretion of interleukin-1 receptor antagonist and beta cell function and survival. Diabetologia 52, 1579–1588 (2009).

159. Silva, A. M. et al. Electrophysiological and immunocytochemical evidence for P2X purinergic receptors in pancreatic β cells. Pancreas 36, 279–283 (2008).

160. Khan, S. et al. Autocrine activation of P2Y1 receptors couples Ca (2+) influx to Ca (2+) release in human pancreatic beta cells. Diabetologia 57, 2535–2545 (2014).

161. Cabrera, O. et al. The unique cytoarchitecture of human pancreatic islets has implications for islet cell function. P Natl Acad Sci Usa 103, 2334–2339 (2006).

162. Brissova, M. et al. Assessment of human pancreatic islet architecture and composition by laser scanning confocal microscopy. J Histochem Cytochem 53, 1087–1097 (2005).

163. Dai, C. et al. Islet-enriched gene expression and glucose-induced insulin secretion in human and mouse islets. Diabetologia 55, 707–718 (2012).

164. Dai, C. et al. Stress-Impaired Transcription Factor Expression and Insulin Secretion in Human Islets. Journal of Clinical Investigation 126, 1–14 (2016).

165. Saunders, D. & Powers, A. C. Replicative capacity of β-cells and type 1 diabetes. Journal of Autoimmunity 59–68 (2016).

166. Control, C. for D. National Diabetes Statistics Report 2020: Estimates of Diabetes and Its Burden in the United States. Preprint at (2020).

167. Banting, F. G., Best, C. H., Collip, J. B., Campbell, W. R. & Fletcher, A. A. Pancreatic Extracts in the Treatment of Diabetes Mellitus. Can Med Assoc J 12, 141–6 (1922).

168. Vaxillaire, M. & Froguel, P. Monogenic Diabetes in the Young, Pharmacogenetics and Relevance to Multifactorial Forms of Type 2 Diabetes. Endocr Rev 29, 254–264 (2008).

169. Aguilar-Bryan, L. & Bryan, J. Neonatal Diabetes Mellitus. Endocr Rev 29, 265–291 (2008).

170. Association, A. D. 2. Classification and Diagnosis of Diabetes | Diabetes Care | American Diabetes Association. Diabetes Care Suppl 1, S11–S24 (2017).

171. DeFronzo, R. A. From the Triumvirate to the Ominous Octet: A New Paradigm for the Treatment of Type 2 Diabetes Mellitus. Diabetes 58, 773–795 (2009).

172. Stumvoll, M., Goldstein, B. J. & Haeften, T. W. van. Type 2 diabetes: principles of pathogenesis and therapy. Lancet 365, 1333–1346 (2005).

173. Tahrani, A. A., Barnett, A. H. & Bailey, C. J. Pharmacology and therapeutic implications of current drugs for type 2 diabetes mellitus. Nat Rev Endocrinol 12, 566–592 (2016).

174. Chaudhury, A. et al. Clinical Review of Antidiabetic Drugs: Implications for Type 2 Diabetes Mellitus Management. Front Endocrinol 8, 6 (2017).

175. Herold, K. C. et al. An Anti-CD3 Antibody, Teplizumab, in Relatives at Risk for Type 1 Diabetes. New Engl J Med 381, 603–613 (2019).

176. Davis, H. A. et al. Hypoglycemia During Therapy of Diabetes. Endotext [Internet] (2021).

177. Nolan, C. J., Damm, P. & Prentki, M. Type 2 diabetes across generations: from pathophysiology to prevention and management. Lancet 378, 169–181 (2011).

178. Kahn, S. E., Hull, R. L. & Utzschneider, K. M. Mechanisms linking obesity to insulin resistance and type 2 diabetes. Nature 444, 840–846 (2006).

179. Kahn, S. E., Cooper, M. E. & Prato, S. D. Pathophysiology and treatment of type 2 diabetes: perspectives on the past, present, and future. Lancet 383, 1068–1083 (2014).

180. Esser, N., Utzschneider, K. M. & Kahn, S. E. Early beta cell dysfunction vs insulin hypersecretion as the primary event in the pathogenesis of dysglycaemia. Diabetologia 63, 2007–2021 (2020).

181. Albrechtsen, N. J. W. et al. The Liver–α-Cell Axis and Type 2 Diabetes. Endocr Rev 40, 1353–1366 (2019).

182. Almaça, J., Weitz, J., Rodriguez-diaz, R., Pereira, E. & Caicedo, A. The Pericyte of the Pancreatic Islet Regulates Capillary Diameter and Local Blood Flow Article. Cell Metab 27, 1–15 (2018).

183. Hogan, M. F. & Hull, R. L. The islet endothelial cell: a novel contributor to beta cell secretory dysfunction in diabetes. Diabetologia 60, 952–959 (2017).

184. Kraakman, M. J., Murphy, A. J., Jandeleit-Dahm, K. & Kammoun, H. L. Macrophage Polarization in Obesity and Type 2 Diabetes: Weighing Down Our Understanding of Macrophage Function? Front Immunol 5, 470 (2014).

185. Eguchi, K. & Nagai, R. Islet inflammation in type 2 diabetes and physiology. J Clin Invest 127, 14–23 (2017).

186. Powers, A. C. & Eisenbarth, G. S. Autoimmunity to Islet Cells in Diabetes Mellitus. Annu Rev Med 36, 533–544 (1985).

187. Ziegler, A. G. et al. Seroconversion to Multiple Islet Autoantibodies and Risk of Progression to Diabetes in Children. Jama 309, 2473–2479 (2013).

188. Petersen, J. S. et al. Detection of GAD65 Antibodies in Diabetes and Other Autoimmune Diseases Using a Simple Radioligand Assay. Diabetes 43, 459–467 (1994).

189. Murri, M. et al. Gut microbiota in children with type 1 diabetes differs from that in healthy children: a case-control study. Bmc Med 11, 46 (2013).

190. Goffau, M. C. de et al. Aberrant gut microbiota composition at the onset of type 1 diabetes in young children. Diabetologia 57, 1569–1577 (2014).

191. Zhou, H. et al. Evaluating the Causal Role of Gut Microbiota in Type 1 Diabetes and Its Possible Pathogenic Mechanisms. Front Endocrinol 11, 125 (2020).

192. Keskinen, P. et al. First-phase insulin response in young healthy children at genetic and immunological risk for Type I diabetes. Diabetologia 45, 1639–1648 (2002).

193. Siljander, H. T. et al. Insulin secretion and sensitivity in the prediction of type 1 diabetes in children with advanced β-cell autoimmunity. Eur J Endocrinol 169, 479–485 (2013).

194. Evans-Molina, C. et al. β Cell dysfunction exists more than 5 years before type 1 diabetes diagnosis. JCI Insight 3, 1–10 (2018).

195. Oram, R. A., Sims, E. K. & Evans-Molina, C. Beta cells in type 1 diabetes: mass and function; sleeping or dead? Diabetologia 62, 567–577 (2019).

196. Mathieu, C., Lahesmaa, R., Bonifacio, E., Achenbach, P. & Tree, T. Immunological biomarkers for the development and progression of type 1 diabetes. Diabetologia 61, 2252–2258 (2018).

197. Vecchio, F. et al. Abnormal neutrophil signature in the blood and pancreas of presymptomatic and symptomatic type 1 diabetes. JCI Insight 3, 1--17 (2018).

198. Campbell-Thompson, M. et al. Insulitis and β-Cell Mass in the Natural History of Type 1 Diabetes. Diabetes 65, 719–731 (2016).

199. Graham, K. L. et al. Autoreactive Cytotoxic T Lymphocytes Acquire Higher Expression of Cytotoxic Effector Markers in the Islets of NOD Mice after Priming in Pancreatic Lymph Nodes. Am J Pathology 178, 2716–2725 (2011).

200. Roep, B. O. & Atkinson, M. Animal models have little to teach us about Type 1 diabetes: 1. In support of this proposal. Diabetologia 47, 1650–1656 (2004).

201. Leiter, E. H. & Herrath, M. von. Animal models have little to teach us about Type 1 diabetes: 2. In opposition to this proposal. Diabetologia 47, 1657–1660 (2004).

202. Veld, P. I. Insulitis in human type 1 diabetes: a comparison between patients and animal models. Semin Immunopathol 36, 569–579 (2014).

203. Staeva, T. P., Chatenoud, L., Insel, R. & Atkinson, M. A. Recent Lessons Learned From Prevention and Recent-Onset Type 1 Diabetes Immunotherapy Trials. Diabetes 62, 9–17 (2013).

204. Kaddis, J. S. et al. Human Pancreatic Islets and Diabetes Research. Jama 301, 1580–1587 (2009).

205. Hart, N. J. & Powers, A. C. Use of human islets to understand islet biology and diabetes: progress, challenges and suggestions. Diabetologia 62, 1–11 (2018).

206. Walker, J. T., Saunders, D. C., Brissova, M. & Powers, A. C. The Human Islet: Mini-Organ With Mega-Impact. Endocr Rev 42, bnab010- (2021).

207. Gloyn, A. L. et al. Every islet matters: improving the impact of human islet research. Nat Metabolism 1–8 (2022).

208. Cryer, P. E. Minireview: Glucagon in the Pathogenesis of Hypoglycemia and Hyperglycemia in Diabetes. Endocrinology 153, 1039–1048 (2012).

209. Cryer, P. E. Mechanisms of Hypoglycemia-Associated Autonomic Failure and Its Component Syndromes in Diabetes. Diabetes 54, 3592–3601 (2005).

210. Bolli, G. et al. Abnormal Glucose Counterregulation in Insulin-dependent Diabetes Mellitus: Interaction of Anti-Insulin Antibodies and Impaired Glucagon and Epinephrine Secretion. Diabetes 32, 134–141 (1983).

211. Siafarikas, A. et al. Early Loss of the Glucagon Response to Hypoglycemia in Adolescents With Type 1 Diabetes. Diabetes Care 35, 1757–1762 (2012).

212. Arbelaez, A. M. et al. Blunted glucagon but not epinephrine responses to hypoglycemia occurs in youth with less than 1 yr duration of type 1 diabetes mellitus. Pediatr Diabetes 15, 127–134 (2014).

213. Dagogo-Jack, S. E., Craft, S. & Cryer, P. E. Hypoglycemia-associated autonomic failure in insulin-dependent diabetes mellitus. Recent antecedent hypoglycemia reduces autonomic responses to, symptoms of, and defense against subsequent hypoglycemia. J Clin Invest 91, 819–828 (1993).

214. Sperling, M. A., Aleck, K. & Voina, S. Suppressibility of glucagon secretion by glucose in juvenile diabetes. J Pediatrics 90, 543–547 (1977).

215. Unger, R. H., Aguilar-Parada, E., Müller, W. A. & Eisentraut, A. M. Studies of pancreatic alpha cell function in normal and diabetic subjects. J Clin Invest 49, 837–848 (1970).

216. Gerich, J. E., Mokan, M., Veneman, T., Korytkowski, M. & Mitrakou, A. Hypoglycemia Unawareness. Endocr Rev 12, 356–371 (1991).

217. Saravia, F. & Homo-Delarche, F. Is innervation an early target in autoimmune diabetes? Trends Immunol 24, 574–579 (2003).

218. Taborsky, G. J. et al. Loss of islet sympathetic nerves and impairment of glucagon secretion in the NOD mouse: Relationship to invasive insulitis. Diabetologia 52, 2602–2611 (2009).

219. Seemayer, T. A., Oligny, L. L., Tannenbaum, G. S., Goldman, H. & Colle, E. Animal model of human disease. Diabetes mellitus. Am J Pathology 101, 485–8 (1980).

220. Mei, Q., Mundinger, T. O., Lernmark, A. & Taborsky, G. J. Early, selective, and marked loss of sympathetic nerves from the islets of BioBreeder diabetic rats. Diabetes 51, 2997--3002 (2002).

221. Mundinger, T. O., Mei, Q., Figlewicz, D. P., Lernmark, Aa. & Taborsky, G. J. Impaired glucagon response to sympathetic nerve stimulation in the BB diabetic rat: effect of early sympathetic islet neuropathy. Am J Physiol Endocrinol Metab 285, E1047–E1054 (2003).

222. Canzano, J. S. et al. Islet Microvasculature Alterations With Loss of Beta-cells in Patients With Type 1 Diabetes. J Histochem Cytochem 67, 41--52 (2018).

223. Brissova, M. et al. α Cell Function and Gene Expression Are Compromised in Type 1 Diabetes. Cell Reports 22, 2601–2614 (2018).

224. Doliba, N. M. et al. α Cell dysfunction in islets from nondiabetic, glutamic acid decarboxylase autoantibody–positive individuals. J Clin Investigation 132, e156243 (2022).

225. Bedi, S. et al. Similarities between bacterial GAD and human GAD65: Implications in gut mediated autoimmune type 1 diabetes. Plos One 17, e0261103 (2022).

226. Sandhu, B. et al. Global deletion of NTPDase3 protects against diet-induced obesity by increasing basal energy metabolism. Metabolism 154731 (2021).

227. Wicksteed, B. et al. Conditional Gene Targeting in Mouse Pancreatic β-Cells. Diabetes 59, 3090–3098 (2010).

228. Balamurugan, A. N., Chang, Y., Fung, J. J., Trucco, M. & Bottino, R. Flexible Management of Enzymatic Digestion Improves Human Islet Isolation Outcome from Sub-Optimal Donor Pancreata. Am J Transplant 3, 1135–1142 (2003).

229. Dai, C. et al. Age-dependent human β cell proliferation induced by glucagon-like peptide 1 and calcineurin signaling. J Clin Invest 127, 3835–3844 (2017).

230. Saunders, D. C. et al. Coordinated interactions between endothelial cells and macrophages in the islet microenvironment promote β cell regeneration. Npj Regen Medicine 6, 22 (2021).

231. Reinert, R. B. et al. Tamoxifen-Induced Cre-loxP Recombination Is Prolonged in Pancreatic Islets of Adult Mice. Plos One 7, e33529 (2012).

232. Brissova, M. et al. Reduction in pancreatic transcription factor PDX-1 impairs glucose-stimulated insulin secretion. J Biol Chem 277, 11225–11232 (2002).

233. Aamodt, K. I. et al. Development of a reliable automated screening system to identify small molecules and biologics that promote human β-cell regeneration. Am J Physiol Endocrinol Metab 311, E859–E868 (2016).

234. Dorrell, C. et al. Transcriptomes of the major human pancreatic cell types. Diabetologia 54, 2832 (2011).

235. Souza, A. H. de et al. Intra-islet GLP-1, but not CCK, is necessary for β-cell function in mouse and human islets. Sci Rep 10, 2823 (2020).

236. Daniel, S., Noda, M., Straub, S. G. & Sharp, G. W. Identification of the docked granule pool responsible for the first phase of glucose-stimulated insulin secretion. Diabetes 48, 1686–1690 (1999).

237. Kayton, N. S. et al. Human islet preparations distributed for research exhibit a variety of insulin-secretory profiles. Am J Physiol Endocrinol Metab 308, E592–E602 (2015).

238. Lenguito, G. et al. Resealable, optically accessible, PDMS-free fluidic platform for ex vivo interrogation of pancreatic islets. Lab Chip 17, 772–781 (2017).

239. Haliyur, R. et al. Human islets expressing HNF1A variant have defective β cell transcriptional regulatory networks. J Clin Invest 129, 246–251 (2018).

240. Puchałowicz, K., Tarnowski, M., Baranowska-Bosiacka, I., Chlubek, D. & Dziedziejko, V. P2X and P2Y Receptors—Role in the Pathophysiology of the Nervous System. Int J Mol Sci 15, 23672–23704 (2014).

241. Yegutkin, G. G. Nucleotide- and nucleoside-converting ectoenzymes: Important modulators of purinergic signalling cascade. Biochimica Et Biophysica Acta Bba - Mol Cell Res 1783, 673–694 (2008).

242. Tweedie, S. et al. Genenames.org: the HGNC and VGNC resources in 2021. Nucleic Acids Res 49, gkaa980- (2020).

243. Jonsson, A., Hedin, A., Müller, M., Skog, O. & Korsgren, O. Transcriptional profiles of human islet and exocrine endothelial cells in subjects with or without impaired glucose metabolism. Sci Rep-uk 10, 22315 (2020).

244. Walker, J. T. et al. RFX6-mediated dysregulation defines human β cell dysfunction in early type 2 diabetes. Biorxiv 2021.12.16.466282 (2021).

245. Blodgett, D. M. et al. Novel Observations From Next-Generation RNA Sequencing of Highly Purified Human Adult and Fetal Islet Cell Subsets. Diabetes 64, 3172–3181 (2015).

246. Erener, S. et al. Deletion of pancreas-specific miR-216a reduces beta-cell mass and inhibits pancreatic cancer progression in mice. Cell Reports Medicine 2, 100434 (2021).

247. Qiu, W.-L. et al. Deciphering Pancreatic Islet β Cell and α Cell Maturation Pathways and Characteristic Features at the Single-Cell Level. Cell Metab 25, 1194-1205.e4 (2017).

248. Shrestha, S. et al. Combinatorial transcription factor profiles predict mature and functional human islet α and β cells. JCI Insight 6, e151621 (2021).

249. Hao, Y. et al. Integrated analysis of multimodal single-cell data. Cell 184, 3573-3587.e29 (2021).

250. James, E. A., Mallone, R., Kent, S. C. & DiLorenzo, T. P. T-Cell Epitopes and Neo-epitopes in Type 1 Diabetes: A Comprehensive Update and Reappraisal. Diabetes 69, 1311–1335 (2020).

251. Thompson, J. D., Higgins, D. G. & Gibson, T. J. CLUSTAL W: improving the sensitivity of progressive multiple sequence alignment through sequence weighting, position-specific gap penalties and weight matrix choice. Nucleic Acids Res 22, 4673–4680 (1994).

252. Bailey, T. L., Johnson, J., Grant, C. E. & Noble, W. S. The MEME Suite. Nucleic Acids Res 43, W39–W49 (2015).

253. Crooks, G. E., Hon, G., Chandonia, J.-M. & Brenner, S. E. WebLogo: A Sequence Logo Generator. Genome Res 14, 1188–1190 (2004).

254. Hampton, R. F., Jimenez-Gonzalez, M. & Stanley, S. A. Unravelling innervation of pancreatic islets. Diabetologia 65, 1069–1084 (2022).

255. Gerich, J. E., Langlois, M., Noacco, C., Karam, J. H. & Forsham, P. H. Lack of Glucagon Response to Hypoglycemia in Diabetes: Evidence for an Intrinsic Pancreatic Alpha Cell Defect. Science 182, 171–173 (1973).

256. Brown, R. J., Sinaii, N. & Rother, K. I. Too much glucagon, too little insulin: time course of pancreatic islet dysfunction in new-onset type 1 diabetes. Diabetes Care 31, 1403–4 (2008).

257. Sherr, J. et al. Evolution of Abnormal Plasma Glucagon Responses to Mixed-Meal Feedings in Youth With Type 1 Diabetes During the First 2 Years After Diagnosis. Diabetes Care 37, 1741–1744 (2014).

258. Longo, D. L. & Cryer, P. E. Mechanisms of Hypoglycemia-Associated Autonomic Failure in Diabetes. New Engl J Medicine 369, 362–372 (2013).

259. Taborsky, G. J., Ahrén, B. & Havel, P. J. Autonomic mediation of glucagon secretion during hypoglycemia: implications for impaired alpha-cell responses in type 1 diabetes. Diabetes 47, 995–1005 (1998).

260. Tominaga, M. et al. Morphologic and Functional Changes in Sympathetic Nerve Relationships With Pancreatic α-Cells After Destruction of β-Cells in Rats. Diabetes 36, 365–373 (1987).

261. Persson-Sjögren, S., Holmberg, D. & Forsgren, S. Remodeling of the innervation of pancreatic islets accompanies insulitis preceding onset of diabetes in the NOD mouse. J Neuroimmunol 158, 128–137 (2005).

262. Alvarsson, A. et al. A 3D atlas of the dynamic and regional variation of pancreatic innervation in diabetes. Sci Adv 6, eaaz9124 (2020).

263. Tang, S.-C. et al. Pancreatic neuro-insular network in young mice revealed by 3D panoramic histology. Diabetologia 61, 158–167 (2018).

264. Mundinger, T. O. et al. Human Type 1 Diabetes Is Characterized by an Early, Marked, Sustained, and Islet-Selective Loss of Sympathetic Nerves. Diabetes 65, 2322–2330 (2016).

265. Campbell-Thompson, M. et al. Islet sympathetic innervation and islet neuropathology in patients with type 1 diabetes. Sci Rep 11, 6562 (2021).

266. Lundberg, M. et al. The density of parasympathetic axons is reduced in the exocrine pancreas of individuals recently diagnosed with type 1 diabetes. Plos One 12, e0179911 (2017).

267. Plank, J. L. et al. Influence and timing of arrival of murine neural crest on pancreatic beta cell development and maturation. Dev Biol 349, 321–330 (2011).

268. Campbell-Thompson, M. L. et al. Relative Pancreas Volume Is Reduced in First-Degree Relatives of Patients With Type 1 Diabetes. Diabetes Care 42, 281–287 (2018).

269. Wright, J. J. et al. Decreased pancreatic acinar cell number in type 1 diabetes. Diabetologia 1–6 (2020).

270. Damond, N. et al. A Map of Human Type 1 Diabetes Progression by Imaging Mass Cytometry. Cell Metab 29, 755-768.e5 (2019).

271. Chiu, Y. C., Hua, T. E., Fu, Y. Y., Pasricha, P. J. & Tang, S. C. 3-D imaging and illustration of the perfusive mouse islet sympathetic innervation and its remodelling in injury. Diabetologia 55, 3252–3261 (2012).

272. Carmeliet, P. & Tessier-Lavigne, M. Common mechanisms of nerve and blood vessel wiring. Nature 436, 193–200 (2005).

273. Adams, R. H. & Eichmann, A. Axon Guidance Molecules in Vascular Patterning. Csh Perspect Biol 2, a001875 (2010).

274. Dolenšek, J., Rupnik, M. S. & Stožer, A. Structural similarities and differences between the human and the mouse pancreas. Islets 7, e1024405 (2015).

275. Korpos, E. et al. The Peri-islet Basement Membrane, a Barrier to Infiltrating Leukocytes in Type 1 Diabetes in Mouse and Human. Diabetes 62, 531–542 (2012).

276. Otonkoski, T., Banerjee, M., Korsgren, O., Thornell, L. -E. & Virtanen, I. Unique basement membrane structure of human pancreatic islets: implications for β-cell growth and differentiation. Diabetes Obes Metabolism 10, 119–127 (2008).

277. Hajizadeh-Saffar, E. et al. Inducible VEGF expression by human embryonic stem cell-derived mesenchymal stromal cells reduces the minimal islet mass required to reverse diabetes. Sci Rep 5, 9322 (2015).

278. Ghezelayagh, Z. et al. Recapitulating pancreatic cell–cell interactions through bioengineering approaches: the momentous role of non-epithelial cells for diabetes cell therapy. Cell Mol Life Sci 78, 7107–7132 (2021).

279. Virtanen, I. et al. Blood vessels of human islets of Langerhans are surrounded by a double basement membrane. Diabetologia 51, 1181–1191 (2008).

280. Belfort-DeAguiar, R. et al. Noradrenergic Activity in the Human Brain: A Mechanism Supporting the Defense Against Hypoglycemia. J Clin Endocrinol Metabolism 103, 2244–2252 (2018).

281. Tang, S.-C. et al. Human pancreatic neuro-insular network in health and fatty infiltration. Diabetologia 61, 168–181 (2018).

282. Chakravarthy, H. et al. Converting Adult Pancreatic Islet α Cells into β Cells by Targeting Both Dnmt1 and Arx. Cell Metab 25, 622–634 (2017).

283. Campanucci, V., Krishnaswamy, A. & Cooper, E. Diabetes Depresses Synaptic Transmission in Sympathetic Ganglia by Inactivating nAChRs through a Conserved Intracellular Cysteine Residue. Neuron 66, 827–834 (2010).

284. Gonçalves, L. M. & Almaça, J. Functional Characterization of the Human Islet Microvasculature Using Living Pancreas Slices. Front Endocrinol 11, 602519 (2021).

285. Glieberman, A. L. et al. Synchronized stimulation and continuous insulin sensing in a microfluidic human Islet on a Chip designed for scalable manufacturing. Lab Chip 19, 2993–3010 (2019).

286. Morini, S. et al. Revascularization and remodelling of pancreatic islets grafted under the kidney capsule. J Anat 210, 565–577 (2007).

287. Yu, Q., Shuai, H., Ahooghalandari, P., Gylfe, E. & Tengholm, A. Glucose controls glucagon secretion by directly modulating cAMP in alpha cells. Diabetologia 62, 1212–1224 (2019).

288. Hughes, J. W., Ustione, A., Lavagnino, Z. & Piston, D. W. Regulation of islet glucagon secretion: Beyond calcium. Diabetes Obes Metabolism 20, 127–136 (2018).

289. Chen, C., Cohrs, C. M., Stertmann, J., Bozsak, R. & Speier, S. Human beta cell mass and function in diabetes: Recent advances in knowledge and technologies to understand disease pathogenesis. Mol Metab 6, 943–957 (2017).

290. Halban, P. A. et al. β-Cell Failure in Type 2 Diabetes: Postulated Mechanisms and Prospects for Prevention and Treatment. Diabetes Care 37, 1751–1758 (2014).

291. Tewson, P. H., Martinka, S., Shaner, N. C., Hughes, T. E. & Quinn, A. M. New DAG and cAMP Sensors Optimized for Live-Cell Assays in Automated Laboratories. J Biomol Screen 21, 298–305 (2015).

292. Chen, T.-W. et al. Ultra-sensitive fluorescent proteins for imaging neuronal activity. Nature 499, 295–300 (2013).

293. Seino, S. Cell signalling in insulin secretion: the molecular targets of ATP, cAMP and sulfonylurea. Diabetologia 55, 2096–2108 (2012).

294. Braun, M., Ramracheya, R. & Rorsman, P. Autocrine regulation of insulin secretion. Diabetes Obes Metabolism 14, 143–151 (2012).

295. Caicedo, A. Paracrine and autocrine interactions in the human islet: More than meets the eye. Semin Cell Dev Biol 24, 11–21 (2013).

296. Rodriguez-Diaz, R. et al. Paracrine Interactions within the Pancreatic Islet Determine the Glycemic Set Point. Cell Metab 27, 549-558.e4 (2018).

297. Obermüller, S. et al. Selective nucleotide-release from dense-core granules in insulin-secreting cells. J Cell Sci 118, 4271–4282 (2005).

298. Hædersdal, S., Lund, A., Knop, F. K. & Vilsbøll, T. The Role of Glucagon in the Pathophysiology and Treatment of Type 2 Diabetes. Mayo Clin Proc 93, 217–239 (2018).

299. Smith, T. M. & Kirley, T. L. Cloning, sequencing, and expression of a human brain ecto-apyrase related to both the ecto-ATPases and CD39 ecto-apyrases1. Biochim Biophys Acta 1386, 65–78 (1998).

300. Vitiello, L., Gorini, S., Rosano, G. & Sala, A. la. Immunoregulation through extracellular nucleotides. Blood 120, 511–518 (2012).

301. Szabo, C. & Pacher, P. The Outsiders: Emerging Roles of Ectonucleotidases in Inflammation. Sci Transl Med 4, 146ps14-146ps14 (2012).

302. Antonioli, L., Pacher, P., Vizi, E. S. & Haskó, G. CD39 and CD73 in immunity and inflammation. Trends Mol Med 19, 355–367 (2013).

303. Zimmermann, H. Two novel families of ectonucleotidases: molecular structures, catalytic properties and a search for function. Trends Pharmacol Sci 20, 231–236 (1999).

304. Kukulski, F. et al. Comparative hydrolysis of P2 receptor agonists by NTPDases 1, 2, 3 and 8. Purinerg Signal 1, 193–204 (2005).

305. Zimmermann, H. Ectonucleoside triphosphate diphosphohydrolases and ecto-5′-nucleotidase in purinergic signaling: how the field developed and where we are now. Purinerg Signal 17, 117–125 (2021).

306. Harper, F., Lamy, F. & Calvert, R. Some properties of a Ca2+- and (or) Mg2+-requiring nucleoside di- and tri-phosphatase(s) associated with the membranes of rat pancreatic zymogen granules. Can J Biochem Cell B 56, 565–576 (1978).

307. Lambert, M. & Christophe, J. Characterization of (Mg,Ca)-ATPase Activity in Rat Pancreatic Plasma Membranes. Febs J 91, 485–492 (1978).

308. Martin, S. S. & Senior, A. E. Membrane adenosine triphosphatase activities in rat pancreas. Biochim Biophys Acta . 602, 401–418 (1980).

309. Hamlyn, J. M. & Senior, A. E. Evidence that Mg2+- or Ca2+-activated adenosine triphosphatase in rat pancreas is a plasma-membrane ecto-enzyme. Biochem J 214, 59–68 (1983).

310. Burnstock, G. & Novak, I. Purinergic signalling in the pancreas in health and disease. J Endocrinol 213, 123–141 (2012).

311. Munkonda, M. N. et al. Characterization of a monoclonal antibody as the first specific inhibitor of human NTP diphosphohydrolase-3. Febs J 276, 479–496 (2009).

312. Weitz, J. R. et al. Secretory Functions of Macrophages in the Human Pancreatic Islet are Regulated by Endogenous Purinergic Signaling. Diabetes db190687 (2020).

313. Loubatières-Mariani, M. M., Chapal, J. & Roye, M. Effects of adenosine on the secretions of glucagon and insulin of isolated ad perfused pancreas of the rat. C R Seances Soc Biol Fil 176, 663–9 (1982).

314. Bertrand, G., Chapal, J., Loubatières-Mariani, M. M. & Roye, M. Evidence for two different P2-purinoceptors on β cell and pancreatic vascular bed. Brit J Pharmacol 91, 783–787 (1987).

315. Hillaire-Buys, D., Chapal, J., Petit, P. & Loubatières-Mariani, M.-M. Dual regulation of pancreatic vascular tone by P2X and P2Y purinoceptor subtypes. Eur J Pharmacol 199, 309–314 (1991).

316. Zhou, R., Dang, X., Sprague, R. S., Mustafa, S. J. & Zhou, Z. Alteration of purinergic signaling in diabetes: Focus on vascular function. J Mol Cell Cardiol 140, 1–9 (2020).

317. Geisler, J. C. et al. Vesicular Nucleotide Transporter-Mediated ATP Release Regulates Insulin Secretion. Endocrinology 154, 675–684 (2013).

318. MacDonald, P. E., Braun, M., Galvanovskis, J. & Rorsman, P. Release of small transmitters through kiss-and-run fusion pores in rat pancreatic β cells. Cell Metab 4, 283–290 (2006).

319. Karanauskaite, J., Hoppa, M. B., Braun, M., Galvanovskis, J. & Rorsman, P. Quantal ATP release in rat β-cells by exocytosis of insulin-containing LDCVs. Pflügers Archiv - European J Physiology 458, 389 (2008).

320. Detimary, P., Jonas, J. C. & Henquin, J. C. Stable and diffusible pools of nucleotides in pancreatic islet cells. Endocrinology 137, 4671–4676 (1996).

321. Braun, M. et al. Corelease and Differential Exit via the Fusion Pore of GABA, Serotonin, and ATP from LDCV in Rat Pancreatic β Cells. J Gen Physiology 129, 221–231 (2007).

322. Foster, M. C., Leapman, R. D., Li, M. X. & Atwater, I. Elemental composition of secretory granules in pancreatic islets of Langerhans. Biophys J 64, 525–532 (1993).

323. Chevassus, H. et al. P2Y receptor activation enhances insulin release from pancreatic β-cells by triggering the cyclic AMP/protein kinase A pathway. Naunyn-schmiedeberg's Archives Pharmacol 366, 464–469 (2002).

324. Chapal, J. & Loubatieres-Mariani, M.-M. Attempt to antagonize the stimulatory effect of ATP on insulin secretion. Eur J Pharmacol 74, 127–134 (1981).

325. Kindmark, H. et al. Measurements of cytoplasmic free Ca2+ concentration in human pancreatic islets and insulinoma cells. Febs Lett 291, 310–314 (1991).

326. Loubatières-Mariani, M. M., Loubatières, A. L., Chapal, J. & Valette, G. Adenosine triphosphate (ATP) and glucose. Action on insulin and glucagon secretion. C R Seances Soc Biol Fil 170, 833–6 (1976).

327. Bertrand, G., Gross, R., Ribes, G. & Loubatières-Mariani, M.-M. P2 purinoceptor agonists stimulate somatostatin secretion from dog pancreas. Eur J Pharmacol 182, 369–373 (1990).

328. Weir, G. C., Knowlton, S. D. & Martin, D. B. Nucleotide and Nucleoside Stimulation of Glucagon Secretion. Endocrinology 97, 932–936 (1975).

329. Salehi, A., Qader, S. S., Grapengiesser, E. & Hellman, B. Pulses of somatostatin release are slightly delayed compared with insulin and antisynchronous to glucagon. Regul Peptides 144, 43–49 (2007).

330. Levin, S. R., Kasson, B. G. & Driessen, J. F. Adenosine Triphosphatases of Rat Pancreatic Islets. J Clin Invest 62, 692–701 (1978).

331. Loubatieres-Mariani, M.-M., Chapal, J., Lignon, F. & Valette, G. Structural specificity of nucleotides for insulin secretory action from the isolated perfused rat pancreas. Eur J Pharmacol 59, 277–286 (1979).

332. Rüsing, D., Müller, C. E. & Verspohl, E. J. The impact of adenosine and A2B receptors on glucose homoeostasis. J Pharm Pharmacol 58, 1639–1645 (2006).

333. Ismail, N. A., Denshary, E. E. S. M. E. & Montague, W. Adenosine and the regulation of insulin secretion by isolated rat islets of Langerhans. Biochem J 164, 409–413 (1977).

334. Gross, R., Bertrand, G., Ribes, G. & Loubatières-Mariani, M. M. α2 -Adrenergic Potentiation of Adenosine-Stimulating Effect on Glucagon Secretion. Endocrinology 121, 765–769 (1987).

335. Salehi, A., Parandeh, F., Fredholm, B. B., Grapengiesser, E. & Hellman, B. Absence of adenosine A1 receptors unmasks pulses of insulin release and prolongs those of glucagon and somatostatin. Life Sci 85, 470–476 (2009).

336. Burnstock, G. & Ralevic, V. Purinergic Signaling and Blood Vessels in Health and Disease. Pharmacol Rev 66, 102–192 (2014).

337. Shrestha, S. et al. Combinatorial transcription factor profiles predict mature and functional human islet α and β cells. JCI Insight 6, e151621 (2021).

338. Rodriguez-Diaz, R. et al. Autonomic Axons in the Human Endocrine Pancreas Show Unique Innervation Patterns. Cell Metabolism 14, 45–54 (2012).

339. Lavoie, É. G., Kukulski, F., Lévesque, S. A., Lecka, J. & Sévigny, J. Cloning and characterization of mouse nucleoside triphosphate diphosphohydrolase-3. Biochem Pharmacol 67, 1917–1926 (2004).

340. Petit, P., Bertrand, G., Schmeer, W. & Henquin, J. C. Effects of extracellular adenine nucleotides on the electrical, ionic and secretory events in mouse pancreatic β-cells. Brit J Pharmacol 98, 875–882 (1989).

341. Ohtani, M., Ohura, K. & Oka, T. Involvement of P2X Receptors in the Regulation of Insulin Secretion, Proliferation and Survival in Mouse Pancreatic β-Cells. Cell Physiol Biochem 28, 355–366 (2011).

342. Crack, B. E. et al. Pharmacological and biochemical analysis of FPL 67156, a novel, selective inhibitor of ecto-ATPase. Brit J Pharmacol 114, 475–481 (1995).

343. Hauke, S., Rada, J., Tihanyi, G., Schilling, D. & Schultz, C. ATP is an essential autocrine factor for pancreatic β-cell signaling and insulin secretion. Physiological Reports 10, e15159 (2022).

344. Léon, C. et al. The P2Y1 receptor is involved in the maintenance of glucose homeostasis and in insulin secretion in mice. Purinerg Signal 1, 145–151 (2005).

345. Marcheva, B. et al. P2Y1 purinergic receptor identified as a diabetes target in a small-molecule screen to reverse circadian β-cell failure. Elife 11, e75132 (2022).

346. Oropeza, D. et al. Phenotypic Characterization of MIP-CreERT1Lphi Mice With Transgene-Driven Islet Expression of Human Growth Hormone. Diabetes 64, 3798–3807 (2015).

347. Weitz, J. R. et al. Mouse pancreatic islet macrophages use locally released ATP to monitor beta cell activity. Diabetologia 61, 182–192 (2018).

348. Bours, M. J. L., Swennen, E. L. R., Virgilio, F. D., Cronstein, B. N. & Dagnelie, P. C. Adenosine 5′-triphosphate and adenosine as endogenous signaling molecules in immunity and inflammation. Pharmacol Therapeut 112, 358–404 (2006).

349. Banaei-Bouchareb, L. et al. Insulin cell mass is altered in Csf1op/Csf1op macrophage-deficient mice. J Leukocyte Biol 76, 359–367 (2004).

350. Fenalti, G. et al. GABA production by glutamic acid decarboxylase is regulated by a dynamic catalytic loop. Nat Struct Mol Biol 14, 280–286 (2007).

351. Rubí, B. Pyridoxal 5'-phosphate (PLP) deficiency might contribute to the onset of type I diabetes. Med Hypotheses 78, 179–182 (2012).

352. Sommer, F. & Bäckhed, F. The gut microbiota — masters of host development and physiology. Nat Rev Microbiol 11, 227–238 (2013).

353. Duranti, S. et al. Bifidobacterium adolescentis as a key member of the human gut microbiota in the production of GABA. Sci Rep-uk 10, 14112 (2020).

354. Leiva-Gea, I. et al. Gut Microbiota Differs in Composition and Functionality Between Children With Type 1 Diabetes and MODY2 and Healthy Control Subjects: A Case-Control Study. Diabetes Care 41, 2385–2395 (2018).

355. Prause, M., Pedersen, S. S., Tsonkova, V., Qiao, M. & Billestrup, N. Butyrate Protects Pancreatic Beta Cells from Cytokine-Induced Dysfunction. Int J Mol Sci 22, 10427 (2021).

356. Harbison, J. E. et al. Gut microbiome dysbiosis and increased intestinal permeability in children with islet autoimmunity and type 1 diabetes: A prospective cohort study. Pediatr Diabetes 20, 574–583 (2019).

357. Soyucen, E. et al. Differences in the gut microbiota of healthy children and those with type 1 diabetes. Pediatr Int 56, 336–343 (2014).

358. Mishra, S. et al. Probiotics and Prebiotics for the Amelioration of Type 1 Diabetes: Present and Future Perspectives. Microorg 7, 67 (2019).

359. Towns, R. & Pietropaolo, M. GAD-65 autoantibodies and their role as biomarkers of type 1 diabetes and latent autoimmune diabetes in adults (LADA). Drug Future 36, 847 (2011).

360. Bhat, R. et al. Inhibitory role for GABA in autoimmune inflammation. Proc National Acad Sci 107, 2580–2585 (2010).

361. Strandwitz, P. et al. GABA-modulating bacteria of the human gut microbiota. Nat Microbiol 4, 396–403 (2019).

362. Pokusaeva, K. et al. GABA-producing Bifidobacterium dentium modulates visceral sensitivity in the intestine. Neurogastroent Motil 29, e12904 (2017).

363. Vatanen, T. et al. The human gut microbiome in early-onset type 1 diabetes from the TEDDY study. Nature 562, 589–594 (2018).

364. Pereira, M. S., Redanz, S. & Kriegel, M. A. Skin Deep: The Role of the Microbiota in Cutaneous Autoimmunity. J Invest Dermatol (2022).

365. Jin, H. et al. Demonstration of functional coupling between γ-aminobutyric acid (GABA) synthesis and vesicular GABA transport into synaptic vesicles. Proc National Acad Sci 100, 4293–4298 (2003).

366. Christgau, S. et al. Membrane anchoring of the autoantigen GAD65 to microvesicles in pancreatic beta-cells by palmitoylation in the NH2-terminal domain. J Cell Biology 118, 309–320 (1992).

367. Li, Y. et al. Revisiting the Antigen-Presenting Function of β Cells in T1D Pathogenesis. Front Immunol 12, 690783 (2021).

368. Cianciaruso, C. et al. Primary Human and Rat β-Cells Release the Intracellular Autoantigens GAD65, IA-2, and Proinsulin in Exosomes Together With Cytokine-Induced Enhancers of Immunity. Diabetes 66, 460–473 (2016).

369. Lundberg, J. M. Pharmacology of cotransmission in the autonomic nervous system: integrative aspects on amines, neuropeptides, adenosine triphosphate, amino acids and nitric oxide. Pharmacol Rev 48, 113–78 (1996).

370. Beverly, J. L., Vries, M. G. D., Bouman, S. D. & Arseneau, L. M. Noradrenergic and GABAergic systems in the medial hypothalamus are activated during hypoglycemia. Am J Physiology-regulatory Integr Comp Physiology 280, R563–R569 (2001).

371. Beverly, J. L., Vries, M. G. de, Beverly, M. F. & Arseneau, L. M. Norepinephrine mediates glucoprivic-induced increase in GABA in the ventromedial hypothalamus of rats. Am J Physiology-regulatory Integr Comp Physiology 279, R990–R996 (2000).

372. Vries, M. G. de, Lawson, M. A. & Beverly, J. L. Hypoglycemia-induced noradrenergic activation in the VMH is a result of decreased ambient glucose. Am J Physiology-regulatory Integr Comp Physiology 289, R977–R981 (2005).

373. Chafetz, M. D., Parko, K., Diaz, S. & Leibowitz, S. F. Relationship between medial hypothalamic α2-receptor binding, norepinephrine, and circulating glucose. Brain Res 384, 404–408 (1986).

374. Page, K. A. et al. Small Decrements in Systemic Glucose Provoke Increases in Hypothalamic Blood Flow Prior to the Release of Counterregulatory Hormones. Diabetes 58, 448–452 (2009).

375. Evans, S. B. et al. Inactivation of the PVN during hypoglycemia partially simulates hypoglycemia-associated autonomic failure. Am J Physiology-regulatory Integr Comp Physiology 284, R57–R65 (2003).

376. McCrimmon, R. J. et al. Potential Role for AMP-Activated Protein Kinase in Hypoglycemia Sensing in the Ventromedial Hypothalamus. Diabetes 53, 1953–1958 (2004).

377. Thomas, M., Sherwin, R. S., Murphy, J. & Kerr, D. Importance of cerebral blood flow to the recognition of and physiological responses to hypoglycemia. Diabetes 46, 829–833 (1997).

378. Black, S. et al. CODEX multiplexed tissue imaging with DNA-conjugated antibodies. Nat Protoc 16, 3802–3835 (2021).

379. Fu, Y.-Y. et al. Three-dimensional optical method for integrated visualization of mouse islet microstructure and vascular network with subcellular-level resolution. J Biomed Opt 15, 046018-046018–9 (2010).

380. Campbell-Thompson, M. & Tang, S.-C. Pancreas Optical Clearing and 3-D Microscopy in Health and Diabetes. Front Endocrinol 12, 644826 (2021).

381. L'evesque, S. A., Lavoie, 'E G. , Lecka, J., Bigonnesse, F. & S'evigny, J. Specificity of the ecto-ATPase inhibitor ARL 67156 on human and mouse ectonucleotidases. Brit J Pharmacol 152, 141--150 (2007).

382. Geutskens, S. B., Otonkoski, T., Pulkkinen, M., Drexhage, H. A. & Leenen, P. J. M. Macrophages in the murine pancreas and their involvement in fetal endocrine development in vitro. J Leukocyte Biol 78, 845–852 (2005).

383. Coppieters, K. T., Wiberg, A. & Herrath, M. G. Viral infections and molecular mimicry in type 1 diabetes. Apmis 120, 941–949 (2012).

384. Group, T. S. The Environmental Determinants of Diabetes in the Young (TEDDY) Study. Ann Ny Acad Sci 1150, 1–13 (2008).

385. Palikuqi, B. et al. Adaptable haemodynamic endothelial cells for organogenesis and tumorigenesis. Nature 585, 426–432 (2020).

386. Penko, D. et al. Incorporation of endothelial progenitor cells into mosaic pseudoislets. Islets 3, 73–79 (2011).